INSTYTUT INFORMATYKI TEORETYCZNEJ I STOSOWANEJ
POLSKIEJ AKADEMII NAUK

OPARTY NA IOT SYSTEM PODEJMOWANIA DECYZJI I KIEROWANIA PASAŻERAMI PODCZAS EWAKUACJI AWARYJNEJ STATKÓW WYCIECZKOWYCH

ROZPRAWA DOKTORSKA

dr Yuting Ma
Promotor:
dr Erol Gelenbe, prof. IITiS PAN

Gliwice, 2025

INSTITUTE OF THEORETICAL AND APPLIED INFORMATICS, POLISH ACADEMY OF SCIENCES

IOT-BASED DECISION MAKING AND PASSENGER ROUTING FOR THE EMERGENCY EVACUATION OF CRUISE SHIPS

DOCTORAL DISSERTATION

Yuting Ma, PhD
Supervisor:
Erol Gelenbe, PhD

Gliwice, 2025

Abstract

The management of major emergencies is a well-established area of research that aims to minimize loss of life and maximize human well-being, also reducing loss of property and economic damage. Examples of such emergencies, which unfortunately occur frequently, include the summer fires around the Mediterranean that require a rapid response to avoid the loss of dwellings and agricultural property, or the annual hurricane season events in the United States, which can require the evacuation of millions of people. Within this broad scope, this doctoral dissertation focuses on accidents with cruise ships that carry large numbers of passengers. In these emergencies, physical space is highly constrained, and one needs to have pre-defined methods for evacuating the passengers and crew members within delays that have been defined by specialized international standards agencies. Facing this challenge requires the use of special-purpose decision aids, including Internet of Things (IoT) infrastructure that can sense the location of evacuees within the ship and help them reach the evacuation exits rapidly with the help of sophisticated routing algorithms and algorithmic methods. A key issue in this area is to understand the performance of the methods that are used to address such emergencies, such as the actual exit times for evacuees who may have different physical capabilities based on age or health condition. After reviewing the main technical challenges in this area, this document summarizes our doctoral dissertation and the related publications, which focus on the evacuation of Cruise Ships, and develop simulation and analytical methods to optimize the evacuation through routing techniques that may apply to each individual evacuee. Our simulations and analytical models show that the IoT can substantially assist in accelerating the evacuation process and reducing the evacuation delays to meet the safety standards in this area.

Streszczenie

Zarządzanie poważnymi sytuacjami awaryjnymi jest dobrze ugruntowaną dziedziną badań, której celem jest minimalizacja strat w ludziach oraz maksymalizacja dobrostanu ludzi, przy jednoczesnym ograniczaniu strat majątkowych i szkód ekonomicznych. Takie sytuacje awaryjne występują często i obejmują na przykład letnie pożary na obszarze Morza Śródziemnego, które wymagają szybkiej reakcji w celu ochrony domów i zasobów rolniczych, oraz coroczny sezon huraganów w Stanach Zjednoczonych, który może wymagać ewakuacji milionów ludzi. W tym szerokim kontekście, niniejsza rozprawa doktorska koncentruje się szczególnie na wypadkach z udziałem statków wycieczkowych przewożących dużą liczbę pasażerów. W takich sytuacjach przestrzeń fizyczna jest bardzo ograniczona, a opracowane wcześniej metody ewakuacji są niezbędne, aby zapewnić pasażerom i załodze możliwość dotarcia do miejsc bezpiecznych w wyznaczonych ramach czasowych określonych przez wyspecjalizowane międzynarodowe agencje normatywne. Rozwiązanie tego wyzwania wymaga wykorzystania specjalistycznych narzędzi wspomagania decyzji, w tym infrastruktury Internetu Rzeczy (IoT), która może śledzić położenie ewakuowanych na pokładzie i kierować ich do wyjść ewakuacyjnych w sposób efektywny, korzystając z zaawansowanych algorytmów trasowania oraz metod obliczeniowych. Kluczową kwestią w tym obszarze jest zrozumienie skuteczności stosowanych metod, w tym rzeczywistego czasu opuszczania statku przez ewakuowanych, którzy mogą mieć różne zdolności fizyczne w zależności od wieku lub stanu zdrowia. Po przeglądzie głównych wyzwań technicznych związanych z ewakuacją statków wycieczkowych, rozprawa podsumowuje przeprowadzone badania doktorskie oraz powiązane publikacje. Badania te koncentrują się na optymalizacji procedur ewakuacyjnych poprzez modele symulacyjne i analityczne, stosując techniki trasowania dostosowane do każdego ewakuowanego. Wyniki pokazują, że podejścia oparte na IoT mogą znacząco przyspieszyć ewakuację, skrócić opóźnienia i pomóc w zapewnieniu zgodności ze standardami bezpieczeństwa.

Contents

Acknowledgements

I would like to begin by expressing my deepest gratitude to my supervisor, Prof. Erol Gelenbe, not only for his invaluable support in the research presented in this thesis, but also for his continuous motivation, guidance, and assistance in many other aspects, all of which have greatly contributed to my academic and personal development. This thesis would not have been possible without his advice and assistance. During my studies at the Institute of Theoretical and Applied Informatics (IITIS-PAN), Polish Academy of Sciences, Prof. Gelenbe provided me with expert insights and consistently devoted his time to carefully and patiently discussing my work, helping me to correct mistakes and further refine my research. I will always cherish the guidance and suggestions I have received from him, wherever my career may lead me.

I am also grateful to my colleagues, Dr. Mert NAKIP and the PhD candidates Mohammed Nasereddin and Qixian Ren, for their ongoing support and encouragement. During moments of adversity and doubt, they lifted my spirits and helped me adapt to both the academic and everyday life at IITIS-PAN.

Next, I wish to thank my family, especially my grandparents, for their unwavering support of my decisions. They have always been my greatest source of strength, allowing me to pursue my dreams without worry.

Furthermore, I would like to give a special thanks to the funding organization, IITiS-PAN, for making this thesis possible. It has provided me with the opportunity and financial support to pursue this research and has been of great assistance with administrative matters and daily life. I sincerely appreciate the support of all members at our institute. Additionally, my former funding organization, Wuhan University of Technology, China, enabled me to conduct part of the research included in this thesis, for which I am deeply grateful.

I am also indebted to all the friends and colleagues I have had the chance to collaborate with over these years, as I split my time between IITiS-PAN and Wuhan University of Technology. Thanks to their support, I have the possibility to do so. In addition, I would like to extend my gratitude to all of my co-authors for their valuable contributions.

I truly appreciate all the support, advice, discussions, and collaborations I have had the opportunity to experience. I also acknowledge and appreciate my own efforts and dedication throughout this journey.

1 Introduction

The management of major emergencies, to minimize loss of life and maximize human well-being, minimize loss of property and economic damage, is an active and well-established area of research. Such emergencies frequently occur in peacetime, and tragically also occur during warfare as we see today [VSTH$^+$25, Sun25]. Commonly occurring recent examples of emergencies that require rescue and evacuation include:

- The frequent fires that occur around the Mediterranean coast, in particular during the summer period [New25].
- The annual hurricane season in the southeastern United States, including Florida, that can require the evacuation of millions of people along congested roads [Reu24b].
- Seasonal floodings that occur regularly in various parts of the world, including in Europe, such as the floods in northeastern Spain in 2024 [Reu24a].
- Accidents or malevolent events that have occurred over recent years in theaters, sports arenas, large hotels, and during cultural or sports events [New24b, Tim24].
- Accidents with cruise ships, as discussed in Section 1.3.
- Industrial accidents in factories, building sites, and underground or overground mines [Con23, New24a].

Though each event is distinct and different, all these events are characterized by a few common characteristics:

- Physical space is constrained, either because it is a built environment with buildings and roadways, some of which become blocked during the emergency.
- Civilians have to be evacuated rapidly, while emergency personnel such as ambulances, police, firemen, expert volunteers, have to enter the area rapidly.
- The civilian evacuees include both able-bodied people, and others who have to be helped or carried out, due to young or old age, or injuries.
- Part of the area contains health hazards, such as fires, smoke, or high levels of pollution or noxious materials or gases.

Thus, addressing these challenges has often required the use of specialized and complex cyber-physical systems [GGW12, GW13], and substantial work has been conducted on algorithmic methods to address them [BG19]. A key issue in this area is to understand the performance of the methods that are used to address such emergencies, such as exit times for civilians, expected survival rates, speed with which emergency staff and equipment arrive at the scene, and several others [Gel00, GM10] which can require sophisticated modelling techniques [Gel94].

The need to address these challenges in a comprehensive modelling approach, that attempts to encompass all the significant aspects of an emergency, has lead to a long line of simulation studies [ÖNU$^+$00, BGLM09], and several special purpose simulation tools have been developed [DFG10, GW12].

The highly distributed structure of such events with a large number of autonomous human, and possibly robotic, agents interacting with each other and affecting the outcome, has given rise to both agent-based simulators [FGG$^+$12] and analytical modelling studies [DG13a].

1.1 Technical Challenges

In addition to the need for realistic simulations, emergency evacuations have several common technical challenges that are worth mentioning. They all require emergency personnel to be able to search the relevant areas so as to find hazards and victims; thus some work has sought inspiration from the efficiency with which some animal species are able to search for food, for other animals of the same species, or for safe areas for their activities [GSSR97], and from other techniques such as foraging and the behavior of physical systems when they identify and locate targets for physical or chemical interactions [Gel10].

Another common aspect is the need to make "good" decisions, but not necessarily optimal decisions, in a very short time. This requires software-based decision aids [FG09] and fast and accurate decision algorithms [GTN10]. Since these decisions are embodied in physical space and time, computational models that explicitly represent and exploit space would be particularly useful [FGG13].

Since evacuees should be able to move (or be moved) rapidly and efficiently to exit areas, or other areas where they an be safe and receive adequate care, emergency management needs efficient routing algorithms, while we know that many such algorithms are computationally intensive [GLL06], and may not be adequate for providing decisions in real time with partial and incomplete information [GFG12]. Thus, fast machine learning based algorithms have been suggested using Reinforcement Learning [BDG13, BG14b] inspired by smart network packet routing. Because of the possible lack of information and coordination between different parts of the system, emergency evacuation can also lead to excessive congestion caused by evacuees or their vehicles using common paths [DG13b], so that approaches that use shared Cloud Computing for common decision making have also been suggested [BG14a].

Many of the above considerations underline the need of communications for emergency evacuation systems, where public mobile networks may be "down" due to physical events or lack of sources of electricity

[GC15, Gel23]. In such cases, one must seek communication technologies which are self-aware and self-organize [Gel06, DDF+06], and which also adapt to possible congestion in the network [GN10]. Thus disruption tolerant communications systems [GG13a] and opportunistic delay tolerant communication systems have been suggested [GG12, GG13b].

As soon as communications are discussed in the context of emergency management, one must also consider the issues of cybersecurity [DGC+18, GDC+18], as well as about how smart cyberattack detection can be carried out without prior knowledge of the cyberattacks that an emergency situation may encounter [GY16, BYG+18]. In addition, such cyberattacks can aim at the security of the end users, but also aim directly at the signalling schemes that allow the network to establish and maintain the communications [GAPG15].

While all these aspects are important to emergency management systems, in the next Section we will turn more specifically to the evacuation of Cruise Ships, which is the subject of this dissertation.

1.2 The Cruise Industry

The cruise industry is a vital component of the global tourism sector, having experienced the fastest growth prior to the COVID-19 pandemic, and contributing significantly to the global economy, job creation, and cultural exchange [Kiz20, LY20]. According to the State of the Cruise Industry Report 2025 published by Cruise Lines International Association (CLIA), the ocean cruise industry experienced a compound annual growth rate of 6.3% in passenger amounts from 1990 to 2025 [(CL25]. As shown in Fig. 1, while the ocean cruise industry was brought to a standstill for nearly two years by the COVID-19 pandemic, it has demonstrated a rapid rebound. By 2023, cruise travel had already reached 106% of the pre-COVID levels of 2019, with 29.1 million passengers sailing, indicating the strong resilience of cruise tourism in the face of global downturns.

Simultaneously, fifteen new cruise ships, with a combined passenger capacity of $38,629$, are expected to be completed by 2025 (see Table 1). This influx will increase the global ocean cruise passenger capacity to $704,200$ across 370 vessels [Wat25]. We can also see from Table 1 that large cruise ships, offering a wide array of onboard activities and amenities, have indeed become a dominant force in the cruise industry. Such vessels typically feature highly complex internal layouts, comprising multiple decks with restaurants, theaters, shopping areas, pools, and other entertainment venues, as well as hundreds of passenger cabins (see Fig. 2), and are considered one of the safest ways to travel. Although the frequency of large cruise ship accidents has decreased significantly over the last decade owing to the introduction of new safety regulations and guidelines, improved crew training schemes, and technological innovations, the consequences of such accidents remain catastrophic.

The next section collates and analyzes ship accidents that have occurred during this century, with particular focus on the role of evacuation in these accidents, in order to highlight the importance of effective evacuation and to identify key factors to consider when designing emergency evacuation approaches for passengers on vessels.

1.3 A Survey of Marine Casualties and Incidents

Grounding (or stranding), contact, collision, and fire constitute the predominant categories of accidents for passenger ships of all subtypes, including cruise ships, pure passenger ships, and passenger Ro-Ro cargo vessels [EAP23]. Such events generally pose a serious threat to the viability of the ship, crew, passengers, and cargo. According to the Annual Overview of marine casualties and incidents 2024 published by the European Maritime Safety Agency (EMSA), there are a total of 6370 passenger ships involved in marine casualties and incidents in the territorial seas of European Union (EU) member states during the period from 2014 to 2023, resulting in 2149 injuries and 54 fatalities [Eur24]. Among these marine casualties and incidents, 53.4% are classified as less serious, 28.4% as serious, 2.7% as very serious, and 15.5% as marine incidents (see Fig. 3). In addition to passenger ship accidents in the territorial seas of EU member states, accidents also occur from time to time in other seas. In 2002, the MV Le Joola RO-RO ferry capsized

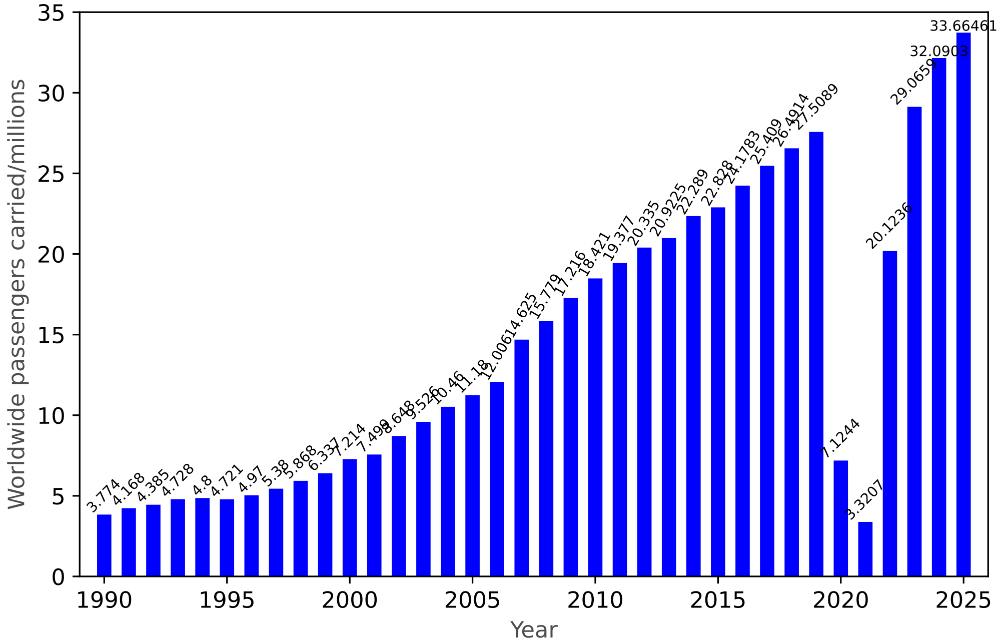

Figure 1: Number of global cruise ship passengers from 1990 to 2025.

Table 1: New ocean cruise ships scheduled for completion in 2025.

Cruise company	Cruise ship	Estimated completion data	Passenger capacity
TUI Cruises	Mein Schiff Relax	Q1	4,000
MSC Cruises	World America	Q1	5,400
Norwegian	Aqua	Q1	3,571
Asuka/NYK	Asuka III	Spring	744
Royal Caribbean	Star of the Seas	Q2	5,610
Oceania	Allura	Q2	1,200
Viking Ocean	Viking Vesta	Q2	998
Ritz-Carlton	Luminara	Q3	456
Princess	Star Princess	Q3	4,300
SunStone (Aurora Expeditions)	Douglas Mawson	Q3	186
Four Seasons	Four Seasons I	Q4	180
Celebrity	Xcel	Q4	3,260
Windstar	Star Seeker	Q4	224
Disney	Adventure	Q4	6,000
Disney	Destiny	Q4	2,500

Figure 2: Schematic view of the cruise ship *Monster of the deep*.

off the coast of The Gambia, resulting in $1,863$ fatalities and 64 survivors, ranking as the third-worst peacetime disaster in maritime history [RMM06]. There are several immediate factors playing a role in this disaster, including poor cargo stowage, severe passenger overloading, engine failure, adverse weather, and improper evacuation. With regard to the evacuation process, the excess passengers concentrated on the upper decks, making the ship highly unstable. Moreover, to take cover from the storm, they rushed en masse to one side, which further aggravated the hull tilt and significantly accelerated the capsizing. In 2006, the MS al-Salam Boccaccio 98, a RO-RO passenger ferry, sank in the Red Sea, resulting in over 1,000 deaths [Sol13]. The immediate cause of the sinking was identified as the buildup of seawater in the hull during firefighting operations in the engine room, which induced a severe listing and ultimately led to the ship capsizing. According to the Panama Maritime Authority Preliminary Investigation Report, at $19:09$, the fire alarm on MS al-Salam Boccaccio 98 was activated, providing visual and audible alerts on the control panel at the bridge, but orders to evacuate the vessel were never given or carried out as per established procedures. The majority of passengers remained waiting for evacuation instructions from the master until the vessel sank. In 2014, the ferry MV Sewol foundered while en route from Incheon to Jeju in South Korea under calm sea conditions [JS17]. Out of 476 passengers and crew, only 172 people survived this disaster. The primary cause of the sinking was an unreasonably sudden turn to starboard, which triggered a shift of cargo to port and, in turn, induced a heavy listing and the eventual capsizing. The captain ordered passengers to stay in their cabins rather than mobilizing an evacuation of passengers while the Sewol ferry was listing. Therefore, this accident is considered to be a man-made disaster, since all passengers could have survived if adequate evacuation procedures had been implemented. In 2021, the passenger ferry MV Avijan-10 caught fire on the Sugandha River [con21]. This accident resulted in more than 40 deaths and more than 100 injuries. Most of the victims either died from the fire or drowned during their escape. Analysis of the aforementioned ship accidents indicates that the complete elimination of maritime accidents is practically unrealistic, and that inappropriate post-accident evacuation is one of the major factors contributing to the associated catastrophic consequences.

Conversely, the implementation of effective evacuation procedures can substantially mitigate maritime accidents in terms of a reduction in resultant fatalities and injuries. In 2013, the MV Grandeur of the Seas, carrying 2,224 passengers and a crew complement of 796, was on fire [Aut14]. Once the emergency situation was declared, the crew was first sent to their emergency stations, and passengers were directed to their muster stations. Therefore, despite the serious and large conflagration causing significant structural damage, no personal injuries were reported among passengers or crew members, thanks to the timely and effective emergency evacuation. Similarly, all individuals aboard the Yangtze Grand View No. 7 cruise ship were safely evacuated to shore within 29 minutes, with no reported injuries.

In summary, the evacuation decision plays a crucial role in protecting the lives of those on board when a passenger ship is involved in a serious accident. Evacuation planning for passengers on a damaged ship is a highly complex transshipment problem, affected by factors such as the propagation of hazards, the spatial and temporal distribution of evacuees and life-saving appliances, the dynamic inclinations of the ship, the capacity of muster stations, and the survival time of the vessel. In addition, the design of evacuation strategies is influenced by the underlying support infrastructure available on board a ship. All cruise ships are required by the International Convention for the Safety of Life at Sea (SOLAS) to have pre-deployed static evacuation plans to direct evacuees to muster stations in the event of an emergency. These plans must indicate the current area or cabin of passengers, the designated assembly area, the locations of lifeboats and liferafts, and the escape routes. Static evacuation plans are designed to provide paths with the shortest distance to muster stations, but they neglect other essential factors influencing evacuation efficiency and passenger safety. In recent years, intelligent ships equipped with advanced technologies such as the Internet of Things (IoT) have gradually become the norm in the cruise industry. Various IoT-based evacuation systems have been proposed to provide dynamic evacuation plans that can react to changing conditions on board and can adapt guidance using real-time data collected from IoT infrastructures.

Based on the above motivation, the main objective of this thesis is to develop IoT-based emergency evacuation systems tailored for evacuees on cruise ships under conditions of dynamic inclination and capsizing risk.

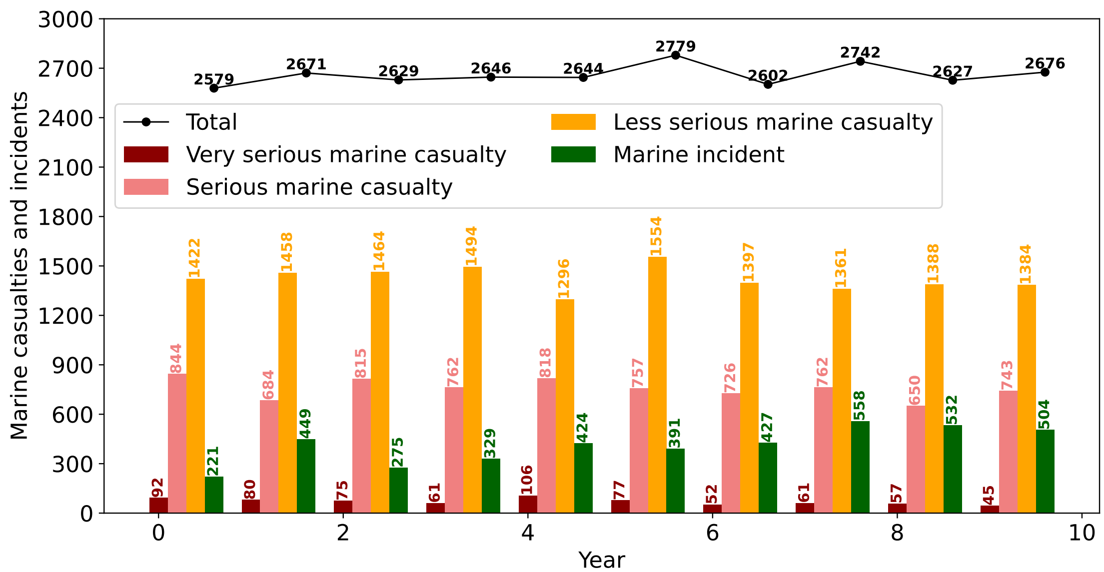

Figure 3: Evolution of the number of marine casualties and incidents, organized by severity.

1.4 Literature Review

This chapter is divided into five main parts: the first part reviews current approaches to constructing navigable networks in ship indoor environments. The second part presents a comprehensive review of existing evacuation route planning algorithms for passengers on board. The third part introduces models and tools available to simulate and assess ship evacuations. The fourth part summarizes research on emergency evacuation systems, including signage-based, leader-based, and mobile equipment-based systems. The final part discusses gaps in the research on the four above-mentioned aspects of ship evacuation.

1.4.1 Navigable Network Construction in Ship Interiors

Navigable networks model the indoor structure as graphs composed of nodes (locations) and edges (paths between locations), which are then utilized to incorporate the knowledge about locations as well as the dynamic evolution of hazards, accessibility, and path quality to support the optimization of evacuation routes during emergencies. The construction of a navigable network within the interior of a cruise ship is fundamental to identifying egress paths for passengers on board. Currently, there are three main types of methods for navigable network construction: Poincaré duality-based methods, grid-based methods, and Voronoi diagram-based methods. Each represents a different measure taken to generate a graph model for subsequent evacuation route planning.

Poincaré duality-based methods represent a volume object as a dual node, and a facet as a dual edge bounded by dual nodes denoting adjacent volume objects. Therefore, the dual structure can be viewed as a graph of connections among 3D objects. In practice, 3D objects can be employed to delineate distinct subspaces within the cruise ship indoor space environment, which collectively constitute the overall spatial configuration of the vessel. [Gon22] partitions the ship interior into multiple sub-regions based on the general arrangement plan using specific rules. For instance, each cabin or staircase is treated as an individual sub-region; long corridors are subdivided into several sub-regions; and compartments with a large number of evacuees, who need to be divided into different evacuation groups, are similarly partitioned into multiple sub-regions. Each sub-region is projected to a dual node, and the connections between adjacent dual nodes are represented as edges. In [PVSW08], nodes correspond to compartments, closures (e.g., doors, hatches), and intersections, while links represent various types of passageways. [Łoz06] models rooms as nodes of the navigable graph, and connections between them are represented by edges of the graph. [Li11, LC19] views compartments, muster stations, corridors, and staircases as nodes, with doors regarded as arcs that connect these nodes. Each link or node is characterized by attributes such as capacity, distance (or time) cost, degree of risk, and type, which can be defined as either static or dynamic depending on whether they remain constant or vary over time. [Gon22, PVSW08] calculate traversal delays across passageways by taking the flow quantities and their physical lengths into consideration. In [Łoz06], the travel time experienced along a link is estimated using the link length, clear width, mean walking speed of a person, and the flow quantity. [Li11] adopts walking speeds corresponding to different crowd densities, as specified in MSC.1/Circ.1238, to predict the passing time along passages. In citeyuan2015passengers, crowd density, as well as ship rolling and pitching, are regarded as key factors impacting passenger movement speed. [LC19] employs a two-stage genetic algorithm to optimize the service levels of nodes and edges to calculate the network parameters such as node and edge capacities, as well as the passing time across edges. Poincaré duality-based methods tend to excessively simplify and abstract the complex sub-regions within a ship interior. Therefore, although navigable networks constructed using such methods can effectively capture the topological relations among these sub-regions, they inherently sacrifice the geometric details of the sub-units, which in turn limits their ability to support fine-grained path-planning for emergency evacuation.

Grid-based methods discretize the interior floor of a ship into uniform grids, each with the same size and shape. The center of each grid is viewed as a node of the navigable graph, while connections between neighboring grid centers are edges. [WZX20] replaces the traditional quadrilateral cells with hexagonal cells to equalize the movement distance between grids, and thus establishes a basis for the unified time coordinate for implementing the cellular ant algorithm to plan emergency evacuation paths. Without sufficient consideration of the dynamics of walking conditions on cruise ships, [WZX20] estimates the time of each move to the next grid using a constant movement speed and the grid length. Because of the requirement for uniform grids, grid-based methods face challenges in accurately representing the complex and diverse sub-regions in a ship indoor environment.

Voronoi diagram (VD)-based methods use vertices and edges of the VD to represent nodes and links in the navigable network, respectively. [Wal04] generates a generalized Voronoi graph (GVG) with the vertices placed at the locations of the corresponding meet points of the generalized Voronoi Diagram (GVD). The edges of the GVG connect vertices that denote adjacent meet points in the GVD. GVD is a retraction of a free space onto one-dimensional curves, constructed from a complete geometric description of the boundaries of obstacles within an indoor environment. [ZLMC23] extracts a set of feature nodes containing structure information to sparsify the GVG and improve search efficiency for optimal emergency evacuation routes. Existing VD-based methods for generating navigable networks in ship interiors typically select nodes that maximize the distance from all obstacles. However, networks constructed in this manner often struggle to provide alternative egress routes, which is critical considering the dynamic conditions of ship evacuation.

1.4.2 Emergency Evacuation Planning Approaches

The objective of evacuation planning is to ensure that evacuees leave hazardous environments safely and efficiently by optimizing evacuation routes, the timing of evacuation orders, and other factors affecting evacuation performance. Compared with the relatively mature research on land-based evacuation planning, studies on ship evacuation planning started lately and primarily focused on evacuation path planning. Previous evacuation planning algorithms designated for cruise ship passengers can be categorized into two types: static algorithms and dynamic algorithms. Static algorithms concentrate on optimizing either the distance to muster stations or the total clearance time for all evacuees prior to an accident. In addition, some static algorithms focus on the design of ship interior layouts, including corridor widths and the capacities of muster stations. On the other hand, dynamic algorithms have the ability to respond to varying conditions on board and adjust the evacuation routes of passengers as needed. A detailed literature review of these two categories of planning algorithms is presented as follows.

1.4.2.1 Static Emergency Evacuation Planning Approaches

On the one hand, static emergency evacuation planning algorithms have been developed to optimize the evacuation layout to improve personnel safety. [WLL$^+$22] uses the FDS + EVAC software package to establish a passenger ship evacuation simulation model that considers the influence of passenger population composition and ship familiarity. The model is applied to explore congestion points within ship interiors, which in turn can aid in the optimization of staircase layouts to improve the evacuation process. Additionally, the optimization of the timing of evacuation orders has drawn considerable attention. [XZW$^+$20] adopts the Legendre polynomial chaos expansion method to construct the surrogate model of passenger assembly time with respect to response time parameters, which depend on the issuance of evacuation orders. The optimal response time parameters are then calculated using a Genetic Algorithm (GA).

On the other hand, static emergency evacuation planning algorithms have been proposed to optimize evacuation routes. However, these planned routes are typically based solely on the original interior layout of passenger ships and/or the initial distribution of passengers. That is to say, they cannot adapt to environmental changes and crowd dynamics in a real time manner. [NLZL17] plans the shortest path from the initial position of a passenger to the target position using the Dijkstra algorithm. [NCLK21] focuses on minimizing the time to save all passengers from the ship to the nearest safe point using various evacuation tools (e.g., lifeboats, salvage ship, sea robots, and helicopters), while also minimizing the cost of the solution. This problem is formulated as a non-preemptive scheduling problem of n independent jobs (evacuee groups) on m uniform parallel machines (evacuation tools). An iterative utilization of a modified Leung-Ng algorithm is introduced to efficiently find the optimal solution [LN17]. Some studies employ swarm intelligence algorithms, such as the ant colony algorithm, to search for the optimal static evacuation path. For example, [WZX20] combines the ant colony algorithm with the cellular automata model to develop a cellular ant algorithm that identifies evacuation paths with the minimum total number of path cells on the basis of a grid map. The layouts and evacuation plans optimized using static emergency evacuation planning algorithms are fixed and cannot adapt to real-time changes, such as crowd and environmental dynamics, and thus may perform poorly, especially in dynamic ship evacuation scenarios.

1.4.2.2 Dynamic Emergency Evacuation Planning Approaches

Dynamic emergency evacuation planning algorithms concentrate on combining planning algorithms with underlying sensing and communication systems to guide evacuees out of hazardous environments in real time, while considering crowd and environmental dynamics. Various dynamic emergency evacuation planning algorithms have been proposed, such as potential field-based algorithms, swarm intelligence algorithms, network flow-based algorithms, geometric algorithms, game-theory-based algorithms, temporally ordered routing algorithms (TORA), and reinforcement learning (RL) algorithms.

Social Potential Field (PF)-based algorithms assign potential values to nodes, normally combining attractive potentials originating from exits with repulsive potentials generated by hazards and obstacles. Evacuees are able to navigate toward exits while avoiding hazards and obstacles by following the constructed artificial potential field. For instance, [LR05, LDRR03] develops a distributed algorithm for sensor networks that directs evacuees out of hazardous environments. In this protocol, the artificial potential field is computed according to the current state relative to hazards and the information about the goal of an evacuee. By combining dynamic programming and the artificial potential field to find the safe and short paths, evacuees can avoid getting stuck in local minima. [PTT06] considers the structures of 3D buildings and extends the distributed protocol proposed in [LR05] for evacuation in 3D built environments with multiple emergency events and exits coexisting. The protocol designates the roles of nodes (e.g., exit nodes, stair nodes, and normal nodes) based on the 3D building structure at the deployment stage. Users located in hazardous and non-hazardous areas are treated differently to look for safer and shorter escape paths. To handle the local optimum problem, the partial link reversal mechanism in TORA is adopted in this protocol. [WLJ15] presents a congestion-adaptive and small stretch emergency navigation algorithm with WSNs to achieve mild congestion at slight detours near hazardous areas, while avoiding unnecessary detours for individuals distant from hazards. In this algorithm, a compound map of the network, including a potential map and a hazard level map, is constructed for emergency navigation. The hazard level map is created by enforcing nodes around hazards to form bands with different hazard level weights so that evacuees are dispersed along paths in different bands to alleviate congestion near hazards. To address the emergency dynamics, a local status update mechanism is incorporated in this algorithm. [WLZJ16] further considers both the hazard levels of emergencies and the evacuation capabilities of exits and proposes a situation-aware emergency navigation algorithm with WSNs to keep evacuees farther away from emergencies with higher hazard levels while easing potential congestion at exits with lower evacuation capabilities. In this algorithm, a hazard potential field is established to model the hazard levels of emergencies and the evacuation capacities of exits as positive and negative hazard potentials, respectively. Evacuees can achieve navigation success and optimal safety by following the descent gradient of the hazard potential field.

Swarm Intelligence algorithms mimic the collective behavior of decentralized and self-organized systems to solve complex problems, particularly in crowd evacuation optimization. For instance, [LZXZ21] proposes an improved ant colony algorithm to solve the multipath evacuation planning of crowds on cruise ships by considering the crowd density and speed. The speed of passengers during an emergency on a cruise ship is influenced by crowd density as well as individual age. To improve the computational efficiency, an increasing flow method is introduced into the proposed algorithm. [GGR15] proposes an ant colony optimization-based algorithm to generate near-optimal escape plans for every evacuee, considering both mobility impairments caused by dynamic hazards and data unreliability in realistic environments. [Wan13] formulates ship evacuation as a multi-objective problem, considering evacuation time, passenger conflicts, and congestion levels. A grey theory-based multi-objective ant colony optimization algorithm is employed to solve this problem. In this approach, an external archive is used to store Pareto optimal solutions based on grey relational analysis. [TRK16] focuses on the search and rescue problem in indoor environments. In order to find the best search and rescue plan, including the number of responders required and their individual routes, which minimizes the overall time to cover the search area, an ant colony-based algorithm is presented by this study. In this proposed algorithm, each ant in colony represents a complete tour of all rescuer paths. Besides the ant colony algorithm, some studies use particle swarm optimization (PSO) to optimize ship evacuation. For instance, [YZLW14] proposes a neighborhood PSO, where each particle determines the next position based on individual cognition, social behavior, and the behavior of its neighborhood. Compared with the basic PSO, which merely takes into account individual cognition and social behavior when determining the next position of a particle, the proposed neighbor PSO can sufficiently address staff conflicts caused by all particles moving toward the best goal position. The artificial fish swarm algorithm (AFSA) has also been applied to optimize evacuation routes on cruise ships. [LZZ+22] proposes an improved AFSA to solve a multi-route planning problem for cruise ship evacuation. In this algorithm, the entire fish swarm is used to simulate all evacuees, who work cooperatively to form a set of evacuation routes. The crowding problem is tackled by considering the impact of crowding on movement speed and by introducing waiting and distribution mechanisms into this algorithm. The genetic algorithm is also another typical swarm intelligence algorithm used to optimize crowd evacuation. [LCZ15] combines the genetic algorithm with a road segment travel time prediction method to determine the optimal evacuation plan by taking into consideration the interactions among passengers. [ZDZ+19] pays attention to the role of passenger leaders and proposes a hybrid bi-level model to optimize both the initial placement of leaders and their routes during evacuations. In the lower model, a co-simulation heuristic approach that integrates the genetic algorithm with an improved A^* algorithm is developed to determine the evacuation routes of leaders by considering the coordination mechanism. The genetic algorithm is used to search for the optimal exit assignment by evaluating candidate evacuation strategies based on the solution generated using the improved A^* algorithm.

In some studies, ship evacuation is modeled as a network flow problem [AA09, HT01], where evacuees are conceptualized as fluid flowing through a network that represents the interior layout of a ship. Each edge in the network has a capacity, which denotes the maximum number of people that can traverse it at any given time. By managing the flows through the network, specific evacuation objectives such as minimizing the overall evacuation time can be achieved. [CT24] models evacuation optimization problems either as a maximum flow problem, which aims to evacuate the largest possible number of people within a limited time, considering link capacity constraints, or as a minimum cost problem, which seeks to minimize the total evacuation cost. Algorithms such as the Edmond-Karp method for the maximum flow problem and the iteration method proposed by Busacker and Gowan for the minimum cost problem are applied to solve these problems. [LXG+24] formulates ship evacuation as a multi-criteria optimization problem, grounded in a hydraulic network, which considers the allocation framework, counterflow prevention, and plan feasibility. A two-stage simulated annealing algorithm is developed to efficiently optimize the allocation of passengers from their initial locations to assembly stations. [VW25] considers the varying mobility levels of evacuee groups and classifies them into three types: Young adults, Elders and children, and Wheelchair users. The assignment of these groups of evacuees is formulated as a multi-commodity flow problem. The resulting solution is then transformed into explicit individual evacuation routes using flow decomposition approaches. [LZW+11] takes both pedestrian congestion and the flexibility of rescue forces into account, and models the movement of evacuees as network flows on a directed graph that represents the whole emergency scene. By calculating the maximum flow and minimum cut on the directed graph, rescue commands that identify critical danger areas and optimized navigation routes are provided to firefighters to eliminate these key hazards so as to reduce congestion during evacuation. Given the dynamic nature of the evacuation optimization problem, some studies construct a time-expanded network by duplicating the original static network for each discrete time step within the planning horizon. After that, various algorithms are utilized to compute the optimal evacuation plan. For example, [LZBA12] developed an Evacuation Scheduling Algorithm that integrates the Dijkstra algorithm to determine evacuation routes with a greedy algorithm to find the maximum flow of each path and the schedule to execute the flow at each time step. This developed algorithm maximizes the total number of evacuees for short-notice evacuation planning through a fast solution process, owing to its low computational complexity, even for the extremely large evacuation networks generated by the expansion operation. In order to deal with complex and evolving fire situations during emergencies, [DHZ+22] enhances the Ford-Fulkerson algorithm based on real-time sensor data on temperature and toxic gas concentration to achieve optimal dynamic path planning for emergency evacuation, ensuring that all persons are evacuated within the safe evacuation time.

Geometric algorithms commonly construct a global topological structure to represent the hazardous environment, which then serves as the public infrastructure for crowd evacuation. All evacuees are guided to the exits through this structure, without the need for individual path planning. For instance, [LWYD08, WLL+12] builds a road map embedded in the sensor network to provide navigation routes with guaranteed safety to evacuees. To handle the dynamics (shrinkage, expansion, and disappearance) of hazards, an efficient updating mechanism is designed to rebuild the road map. The road map backbone is constructed by concatenating the medial axis of the hazardous environment, which captures the topological and geometric features of the environment. Each point on the medial axis is closest to at least two distinct points on the boundaries of hazardous areas. The exit is then connected to the road map backbone following the most descending direction of the virtual power field generated around the hazardous area within the cell containing the exit. Each segment of the road map backbone is assigned a direction to maximize the distance from hazardous areas. All evacuees are guided from the inside of their cells to the road map backbone along routes calculated in the same manner as those connecting the exit to the backbone.

Common graph search algorithms used in evacuation planning include the Breadth-First-Search (BFS) algorithm, Dijkstra algorithm, and the A^* algorithm. [BAS05] carries out a BFS algorithm on the communication network by flooding the whole network with packets to calculate the shortest feasible navigation path that minimizes path length while staying outside hazardous zones. To reduce the communication overhead caused by flooding, a skeleton graph which is a sparse subset of the full sensor network is constructed to find approximate safe paths. [CLL15] modifies the standard Dijkstra algorithm by adding a virtual node connected to all exit nodes and reversing the start and virtual end nodes so as to calculate the shortest path from any unknown point in a building to the closest exit. Dangerous nodes are excluded from the network to ensure the safety of the computed paths. [MHZ22] proposes an improved A^* algorithm to identify the route with the minimum cost, considering the influence of personnel density and obstacles. In order to prevent severe congestion during evacuation, the personnel density at each node is collected in real time. Nodes with extremely high density are excluded, and quadratic planning is executed to determine the optimal evacuation route. In order to enhance the efficiency of searching evacuation routes in multi-destination scenarios, [ZLJ+20] devises a variant of the classic A^* algorithm that accounts for the real-time population density and can obtain the optimal solution in a single pass. Instead of searching individual exits through multiple passes, the modified A^* algorithm chooses the most time-efficient path among all candidate exits in a single pass. In addition, due to the bounded cost, the modified algorithm only explores the direction with the minimum F-score at each iteration.

The TORA assigns a temporally ordered sequence number expressed as a quintuple to each node to facilitate multipath routing from a source to a destination. [TPT06] modified the standard TORA to look for safer, but not necessarily shorter, escape routes. Each node is assigned an initial altitude according to its hop count to the nearest exit, with nodes closer to exits given lower altitudes and those farther away assigned higher altitudes. Once an emergency is detected, nodes located within a hazardous region recalculate their altitudes based on their hop count to both the emergency location and the nearest exit. Additionally, to address the local minima problem, the partial-reversal method is used to adjust the altitudes of nodes with local minima. Evacuees in hazardous and non-hazardous regions are guided according to different escape rules to ensure their safety during evacuation. Considering the high communication overhead caused by frequent or periodic flooding for planning and replanning emergency navigation paths, [CMMV12] proposes a distributed path planning algorithm for emergency navigation with sensor networks. This algorithm builds a directed navigation graph in a localized manner, based on the coordinates of the sensors. Nodes in dangerous and safe zones are assigned a quadruple according to distinct rules. Directed links between neighboring nodes are then configured locally based on the quadruples associated with these nodes. The partial reversal method is employed to ensure that each sensor maintains at least one outgoing edge. When the hazardous environment changes due to the dynamic nature of hazards, only the edges affected by the change are reconfigured, which also drastically reduces communication expense. [CCT15a] considers the influence of interactions among evacuees, corridor capacity and length, as well as exit capacity on total evacuation time, and develops a load-balancing guiding scheme to minimize overall evacuation time of people in a building. The proposed scheme is designed by constructing load-balancing guiding trees rooted at each exit, based on the TORA combined with an analytical model that estimates the evacuation time of each evacuee.

Some studies have applied game theory to address decision-making problems during emergency evacuations. Game theory-based approaches consider the interactive decision-making and strategy adaptation among evacuees. For instance, [LYD12] determines optimal exit choices for each passenger during an emergency evacuation using Nash equilibrium, taking into account the strategies of other passengers, the distance to each exit, exit capacity, and the real-time crowd density near the exits.

Reinforcement Learning has been applied to emergency evacuation in buildings, with a key focus on constructing realistic environments to train RL agents for effective evacuation planning. For instance, [SAGG20] proposes the first fire evacuation environment used to train RL agents to plan evacuation in dynamic hazardous conditions. This environment is graph-based, accurately modeling the building structure. In addition, it incorporates many keys features such as fire spread, crowd behavior uncertainty, and bottlenecks in rooms. Another primary challenge in RL-based evacuation is designing effective RL approaches that enable agents to make decisions in highly dynamic emergency situations with numerous changing variables and complex constraints. [SAGG20] proposes a deep Q-learning model with Q-matrix transfer learning, which introduces a pretraining module to incorporate the knowledge of the shortest path to the exit into a DQN-based agent. The pretraining module is achieved by applying Q-learning on the building model graph to learn the shortest path from each room to the exit, which is represented as a Q-matrix. The learned information is then transferred to the DQN model by pretraining it to replicate the Q-matrix. Finally, the pretrained DQN agent is trained on the complete fire evacuation environment to execute the optimal evacuation planning. Due to the challenge of obtaining complete information about the entire environment, fully observable RL settings are often impractical. Therefore, some studies focus on learning path planning policies in partially observable environments. For instance, [SKS$^+$19] combines the asynchronous advantage actor-critic (A3C) algorithm with imitation learning to enable multiple agents to learn a common policy in a shared environment based on the high-dimensional partial observations from each agent. Given the reliance on imitation learning from a centralized planner, [MLM21] proposes a distributed heuristic multi-agent path finding approach with communication. This approach combines deep Q-learning with graph convolutional communication to facilitate log-horizon and cooperative path planning for multiple agents. The potential choices of single-agent shortest paths are embedded into the input to the Q-network as heuristic guidance. Each agent is trained independently in a distributed manner using a curriculum learning strategy.

1.4.3 Ship Evacuation Simulation Models and Tools

This section reviews the evacuation simulation models and software currently available for modeling the evacuation process of passengers on board. Given that on-site evacuation drills can be very costly and realistically difficult, evacuation simulation has received extensive attention in recent years. Evacuation simulation not only enables advanced evacuation analysis but also aids in assessing and comparing the performance of different evacuation planning strategies. Existing evacuation models can be divided into two types: discrete models and continuous models. In discrete models, time, space, and state variables are all discrete. Specifically, floor plans are partitioned into distinct grids, and continuous time is discretized into discrete time steps. Movement of individuals is governed by predefined rules. Continuous models describe individual behaviors using differential equations, in which variables can take on any real number value. The literature review for these two categories of models is detailed below, along with an overview of the evacuation software developed based on them.

1.4.3.1 Discrete Evacuation Models

Cellular Automata (CA) and the Lattice Gas Model (LGM) are commonly employed as discrete models to simulate ship evacuation. CA consists of a regular lattice of cells, each occupying one of a finite set of discrete states. The state of each cell evolves over time according to rules that consider its own state and the states of its neighboring cells. [HKRL12] utilizes a CA-based simulation model to analyze human evacuation behavior on a passenger ship. In this model, individual behavior (i.e., the basic movement direction of a passenger), crowd behavior (e.g., separation, alignment, and cohesion), and counterflow-avoiding behavior are jointly taken into account to determine the local rules for each cell. [Xia10] proposes a sub-space network flow model based on CA, where the ship interior is divided into sub-spaces with different safety levels according to their distance to muster stations, and passengers transfer from lower to higher safety levels. CA is applied for the simulation of the evacuation transition of passengers within each sub-space. [Du21] combines a fire smoke diffusion model with CA to simulate passenger evacuation in passenger ship fire scenarios and further optimizes interior layouts based on the smoke toxicity index. In CA, a static field, constructed based on the distance to muster stations, and a dynamic field, influenced by the psychological state of individuals, are introduced to guide movement decisions. The aforementioned models for ship evacuation simulation consider the influence of real-world ship interior layouts on the evacuation process, while they fail to account for the impact of ship inclination on passenger evacuation. Given the different tasks undertaken by crew members and passengers during emergencies, [Xie12, Xie10] establishes a hierarchical microscopic ship evacuation model based on CA and the social force model. The force situation of passengers on an inclined ship deck is analyzed and incorporated into the social force model. However, the estimation of grid occupancy probabilities does not take into account the impact of the ship inclination state. [MC14] comprehensively integrates individual attributes, including gender, age, walking speed, response time, and location, into CA model to simulate passenger evacuation. Moreover, factors such as the locations and capacities of muster stations, the distribution of other passengers and obstacles, the ship inclination angle, and social relationships among passengers are all considered when making movement decisions.

In order to more veritably model passenger evacuation behavior, some studies extend the traditional CA into a multi-grid model. In this model, each grid element can be subdivided into smaller elements until the desired level of granularity is achieved, and a passenger is allowed to occupy multiple basic elements to simulate the staggered arrangements observed in real-world crowd evacuation scenarios. [Wu11] integrates interval estimation theory with a multi-grid model to simulate the evacuation of stairs on passenger ships under floating states. [CHZ11] simultaneously considers the interaction forces among passengers as well as between passengers and structural elements to build cabin and exit static floor fields within the multi-grid model for enhancing the authenticity and accuracy of passenger evacuation simulations on ships with multi-level exits. Aiming to simulate passenger evacuation on ships under heel or trim states, [ZZJ18] incorporates a speed reduction factor into the multi-grid model. [HCZ25] proposes a moving neighbor-based multi-grid model for modeling passenger evacuation. The shape of the moving neighborhood is adapted to reflect the attenuation of passenger movement in all directions, which is caused by the hull motion on water.

The lattice gas model (LGM) is another extension of CA. In this model, individuals are regarded as particles without volume but with mass, which can only occupy grid points and move along the grid lines. In order to simulate evacuation on cruise ship staircases, [HC20] analyzes both the structural features of the staircases and the movement rules of passengers on them. Based on the analysis, a modified lattice gas model is proposed to model cruise staircase evacuation. [HZJ21] put forwards a distance accumulation lattice gas model to realize the evacuation simulation in respect of walking, bent-over walking, and crawling, the latter two arising due to deck tilting.

Discrete models face challenges in accurately representing interactions among passengers, as well as between passengers and ship interior facilities, due to the discretization of space, time, and passenger movement in the evacuation system.

1.4.3.2 Continuous Evacuation Models

The Social Force (SF) model is a representative continuous model commonly used to analyze the dynamic behavior of crowds during evacuation. This model relies on specific forces to represent how environmental factors influence individual behavior. It gives the underlying rationale for passenger movement and enables more realistic simulation of crowd evacuations. [CXM+20] incorporates the attractive force from exits, the anisotropy of passenger motion, the effect of relative velocity, and the repulsive contact force to prevent overlapping into the traditional SF model proposed by Helbing to simulate ship passenger evacuation. [ZZHQ19] leverages on the SF model together with specific torque models to reproduce both the translational and rotational movement behavior of passengers. Moreover, [ZZHQ19] pays attention to individual differences and the speed reduction caused by ship rolling, and models the evacuation of a heterogeneous crowd on a rolling ship. [Sho10] derives an expression for passenger evacuation speed on a ship in a stable inclined state, based on the analysis of crowd dynamics aboard inclined ships. [LC19] comes up with a route selection model that accounts for passenger familiarity with ship interior layouts and social relationships among passengers, based on a mark point-based discrete selection framework. The model is further incorporated into the SF model to enable a more authentic simulation of passenger evacuation. [BKRB15, BKSB16] evaluates evacuation times under specific wave intensities, ship velocities, and relative wave direction angles using a modified SF model that combines with the possibility of collisions with obstacles and other passengers. [NLL18] proposes a modified SF model that accounts for the collection of life jackets, counterflow avoidance, and following behavior. The model is further extended for simulating evacuations on large multi-deck cruise ships by integrating a hierarchical path planning model. [FLZ+23] considers the crew guidance during emergencies as well as the real-time occupancy of exits to enhance the SF model tailored for evacuation simulation on inclined ships.

1.4.3.3 Software for Evacuation Simulation

Based on these discrete and continuous models, several mature commercial software tools, such as Pathfinder, AnyLogic, and BuildingExodus, have been developed to simulate and visualize crowd evacuations and to evaluate the effectiveness of evacuation plans. Pathfinder and BuildingExodus utilized the CA model, whereas AnyLogic is built upon the SF model. AN overview of the three software tools is provided as follows:

- BuildingExodus: The space is discretized into two-dimensional grids of size $0.5m \times 0.5m$, with pedestrians represented as two-dimensional entities. BuildingExodus includes five sub-models, i.e., OCCUPANT, MOVEMENT, BEHAVIOR, TOXICITY, and HAZARD, which enable the simulation of crowd movement under both normal and emergency conditions. In addition, psychological and behavioral differences among pedestrians from different countries can be simulated with this tool.

- Pathfinder: The space is projected to a 3D triangular mesh, and pedestrians are modeled as 3D entities. Each Pedestrian can be defined by parameters such as walking speed and shoulder breadth.

- AnyLogic: This tool can simulate pedestrian movement and reproduce phenomena such as arching at exits, congestion, and “faster-is-slower" effect through environment and behavior modeling. In addition, AnyLogic can be redeveloped using JAVA to achieve various customized functions. In this thesis, we will utilize AnyLogic to simulate, analyze, and visualize the evacuation process of passengers on cruise ships.

1.4.4 Ship Emergency Evacuation Systems

The success of an evacuation depends on the effective use of guidance technologies to direct evacuees along the planned evacuation routes. Nowadays, passengers are typically guided during emergencies by evacuation signage and crew members who serve as evacuation guides. The literature review of these two categories of technologies is detailed as follows.

In accordance with IMO resolution A.1116(30), an escape route sign must be a symbol with an additional arrow, and the texts "assembly" and "exit" should also be displayed additionally, in one or multiple languages. Attention should be given to the connection between the evacuation plan and escape signage that guides passengers to assembly stations, rather than simply installing as many signs as possible. Existing evacuation signage can be classified into two types: static signage and dynamic signage. Static signage cannot adjust guidance directions based on the spatio-temporal distribution of passengers or the dynamic evolution of hazards [ZDI+19]. In normal situations, such signage can direct passengers to a designated muster station. However, during emergencies, certain passageways may become inaccessible due to the high hazard levels or severe crowding. In such cases, following the instructions of static signage can be very dangerous for passengers. Dynamic signage can provide time-varying evacuation guidance in response to changing emergency conditions, which has attracted considerable attention in recent years. A series of studies have proved the effectiveness of dynamic signage through field experiments, questionnaires, or virtual simulation experiments [GXL14, GXD+17a, GXD+17b]. In addition, [KMMS17] investigates the preferences of people of different ages for various types of digital, situation-adaptive escape route signage under emergency conditions on titled passenger ships. The decision-making behavior of young people (20-30 years) is significantly influenced by flashing elements on signage, whereas elderly people (60-77 years) primarily base their decisions on the integrated information regarding signage updates. Evacuation signage is likely to be neglected by evacuees due to social influence observed in group situations [FCSF19]. Moreover, during emergencies, evacuees tend to experience panic stimulated by alarms, smoke, or flames, which can induce evacuees to ignore signage [DLW+22]. In addition, smoke and/or darkness may further reduce or limit the visibility of the signage [KvdWH24].

According to Chapter III, Regulation 19 of SOLAS, several crew members are assigned to key locations, such as staircases, to guide evacuees towards designated muster stations during emergencies. These crew members (also referred to as evacuation guides) convey instructions through voice or gestures, which have been demonstrated to be an effective measure of facilitating evacuation. [FLZ+23] evaluates the effect of guidance provided by evacuation guides on evacuation performance using a modified SF model. These guides balance the allocation of evacuees to different muster stations and simultaneously help passengers avoid crowded areas by monitoring the station occupancy and identifying bottlenecks in real time during emergencies. In order to address the uneven distribution of pedestrian flow among staircases, [HCZ25] proposes a staircase evacuation guidance model based on the crowd density of staircases. A guantum-inspired evolutionary algorithm is utilized to search for the optimal threshold for pedestrian transfers into and out of staircases and to determine the corresponding transfer timing. In real-life scenarios, crew members may be unable to reach their designated positions in time to guide evacuees. What's more, passengers may fail to notice evacuation guides due to their psychological or physiological status, as well as limited visibility caused by environmental factors.

Neither evacuation signage-based guidance nor crew member-based guidance can provide individualized evacuation instructions tailored to passengers with different attributes. With the increasing ubiquity of smartphones and tablets, many studies have integrated portable devices carried by evacuees into emergency evacuation systems for land-based buildings such as sports arenas and shopping centers. These portable devices can display a 2D (or 3D) floor plan, the current location of the user, feasible (or best) evacuation routes, exit locations and occupancy levels, as well as hazard locations in real time. [CCT15b] employs smartphones to periodically detect the current positions of evacuees using signal strength-based localization and transmit this location information to an evacuation server, which calculates customized escape paths and sends them back to the smartphone of each evacuee. In addition to signal strength-based localization, some studies utilize infrastructure-based positioning technologies, such as radio-frequency Identification (RFID) or iBeacon, to determine evacuees' locations [SAC+16]. In [GB14], the built-in cameras on smartphones take photos and upload them to the cloud, where image-based localization algorithms are performed to determine users' position. In addition, in situ hazard information is reported by smartphones to the cloud, where hazard prediction algorithms are applied to estimate the spatio-temporal distribution of hazards. The smartphones themselves constitute an energy-efficient *ad hoc* network to communicate with cloud server access points for two-way data exchange. Smartphone-based guidance is also often integrated with WSNs, which are inherently capable of automatically monitoring and interacting with the physical world [WHL+14]. In such evacuation systems, sensors collaboratively monitor the environment and the real-time distribution of evacuees, and compute navigation directions using embedded algorithms. Smartphones can access the WSNs and receive evacuation instructions from the nearest sensor. Most of the existing evacuation systems that integrate smartphones with WSNs provide identical navigation directions to all individuals located at the same sensor simultaneously, which is likely to cause severe congestion, especially considering the situation where a large number of evacuees gather in a small area. Another drawback of such systems is the very limited computing capacity of low-cost sensors, which severely constrains the real-time execution of complex evacuation algorithms, as well as the scalability and adaptability of the system. If the WSNs, an evacuation server, and smartphones can be integrated, then on the one hand, the intensive computations required to determine the optimal evacuation routes for a substantial amount of passengers on cruise ships in the presence of dynamic hazards and ship inclination states can be offloaded to the server. On the other hand, the use of the hazard monitoring ability of WSNs and the location sensing capability of smartphones can enhance the reliability and resilience of information collection in the system. Therefore, in this thesis, we focus on the design of an evacuation system that integrates WSNs, smartphones, and an evacuation server, enabling passengers to obtain individualized guidance from their smartphones. The guidance is generated in the evacuation server by performing navigation algorithms based on environmental dynamics (e.g., hazard and ship inclination) detected by WSNs, the spatio-temporal distribution of passengers, obtained through real-time uploads of individual locations via smartphones, as well as additional individual attribute information.

1.4.5 Research Gaps in the Literature

Based on the above literature review on evacuation research for passengers on cruise ships, the gaps in research on the construction of navigable networks in ship interiors and ship emergency evacuation algorithms:

- Existing ship navigable network modeling methods are inadequate for generating egress paths that meet the practical requirements of cruise ship evacuees, particularly given the structural complexity and diversity of interior sub-units, as well as the dynamic nature of evacuation conditions (e.g., spreading hazards and varying inclination angles).
- Compared to the relatively mature land-based evacuation research, studies on ship evacuation are scanty. Most existing ship emergency evacuation planning relies on land-based evacuation approaches, while overlooking the uniqueness of passenger ship evacuation. The key factors influencing the uniqueness of passenger ship evacuation compared to land-based building evacuation are listed as follows:
  - Evacuees on cruise ships are generally required to wear life jackets, which are typically stored in passenger cabins or muster stations. Therefore, the spatio-temporal distribution of life jackets must be taken into account when planning evacuation plans for passengers and crew members during emergencies.

- There are a limited number of muster stations on large cruise ships, each with a fixed capacity. Consequently, the real-time occupancy of multiple muster stations must be considered to achieve a balanced ship evacuation.
- A ship is typically in a dynamically tilted state after an accident. Human walking speed is significantly affected by the dynamic inclination. Thus, the dynamics of human mobility must be incorporated in ship emergency evacuation planning.
- Crowd movement, in turn, affects the state of a damaged cruise ship. Lopsided crowd distribution can exacerbate ship inclination and accelerate sinking, thereby greatly reducing the likelihood of a successful evacuation. Therefore, the spatio-temporal distribution of evacuees among passageways within the ship should be balanced during an emergency evacuation.
- According to the IMO guidelines for passenger ship evacuation (MSC.1/Circ.1238), a performance standard, i.e., a maximum allowable evacuation time, must be complied with under all circumstances.

1.5 Research Objectives

Based on the aforementioned motivation and literature review, the main objective of this thesis is to develop emergency evacuation planning approaches, along with a navigable network tailored to dynamic evacuation conditions that accounts for the complexity and diversity of interiors, for our proposed ship evacuation system integrating WSNs, an evacuation server, and individual smartphones. To achieve this goal, the following studies are carried out:

- We design four ship emergency evacuation approaches: a centralized single-evacuee emergency navigation algorithm, a two-stage hybrid single-evacuee navigation algorithm, a centralized cooperative multipath multi-evacuee evacuation planning algorithm, as well as a distributed and decentralized RL-based multi-evacuee evacuation planning method. It is worth noticing that we also propose a ship navigable network construction method based on the Voronoi diagram for building the graph model used by the first three algorithms.
- We evaluate the impact of IoT system imperfections and passenger errors on cruise ship evacuation performance using our proposed two-stage hybrid single-evacuee emergency navigation approach.
- We propose an IoT-driven scheduling for congestion avoidance in emergency evacuation based on queuing theory, which evaluates the average evacuation performance of different routing methods, including our proposed two-stage hybrid emergency navigation algorithm, under various pull policies.

1.6 Published Papers

This thesis is primarily based on the research presented in the appended papers. The papers included in this thesis have been published in scientific journals or conference proceedings, except for Paper V, which has been completed but not yet submitted, and Paper VIII, which is currently under peer review.

Paper I Liu K, **Ma Y**, Chen M, et al. Wend: An efficient wsn-assisted emergency navigation algorithm for dynamic hazardous ship indoor environments[J]. IEEE Sensors Journal, 2022, 23(1): 632-646.

Paper II **Ma Y**, Liu K, Chen M, et al. ANT: Deadline-aware adaptive emergency navigation strategy for dynamic hazardous ship evacuation with wireless sensor networks[J]. IEEE Access, 2020, 8: 135758-135769.

Paper III Liu K, **Ma Y**, Chen M, et al. A survey of crowd evacuation on passenger ships: Recent advances and future challenges[J]. Ocean Engineering, 2022, 263: 112403.

Paper IV **Ma Y**, Liu K, Chen M, et al. Rapid Crowd Evacuation for Passenger Ships Using LP-WAN[J]. IEEE Transactions on Intelligent Transportation Systems, 2023, 25(2): 1720-1735.

Paper V **Ma Y**, Liu K, Chen M, Gelenbe E. D3QTP: Distributed Decentralized Deep Q-Learning with table-driven Pretraining for Ship Evacuation.

Paper VI **Ma Y**, Gelenbe E, Liu K. Impact of IoT system imperfections and passenger errors on cruise ship evacuation delay[J]. Sensors, 2024, 24(6): 1850.

Paper VII **Ma Y**, Gelenbe E, Liu K. Iot performance for maritime passenger evacuation[C]//2024 IEEE 10th World Forum on Internet of Things (WF-IoT). IEEE, 2024: 1-6.

Paper VIII Gelenbe E, **Ma Y**. IoT-Driven Scheduling for Congestion Avoidance in Emergency Evacuation.

The author has also been involved in additional research related to ship emergency evacuation that is not included in this thesis, which has been published in scientific journals or conference proceedings, with one written in Chinese. They are listed below.

Zeng X, Liu K, **Ma Y**, et al.“ DC-HEN: A Deadline-aware and Congestion-relieved Hierarchical Emergency Navigation Algorithm for Ship Indoor Environments,” /2023 IEEE International Conference on Mobility, Operations, Services and Technologies (MOST). IEEE, 2023: 44-54.

Feng X, **Ma Y**, Chen M, et al.,“ Vision-and inertial sensor-based passenger identity recognition for evacuation in cruise ship interiors,” *Journal of Traffic Information and Safety*, 2024, 42(1): 67-75.

1.7 Summary of Appended Papers

This section provides an overview of the papers included in this thesis. Paper III is a survey and is thus not discussed here.

1.7.1 Paper I-Centralized Approximation Scheme for Path Planning in Emergency Navigation of Dynamic Hazardous Ship Indoor Environments via WSNs

Fig. 4 shows an architecture overview of the research in Paper I. In this paper, we first propose a 3-D navigable network construction method to support subsequent evacuation allocation. Specifically, subspaces within ship interiors are classified into two types: simple subspaces and complex subspaces. The former refer to cubical rooms with either a hypothetical single door or two doors on opposite walls, while the latter include spaces whose floor projections form concave polygons, spaces with two doors on the same wall or adjacent walls, and spaces with more than two doors. For simple subspaces, a method based on Poincaré duality is applied to generate the navigable networks, whereas for complex subspaces, a method based on the VD construction algorithm is employed. Doors, staircases, and concave corners in a complex subspace are used as initial Voronoi vertices, with additional nodes added to further tessellate the space. The initial Voronoi vertices and subsequently added nodes in adjacent cells are connected by links, forming a navigable network for the complex subspace. The navigable networks of all simple and complex subspaces are connected based on their topological relationships to create a complete 3D navigable network of the ship interior. Parameters such as the average traversal time across each link at ship inclinations of 0° and 30°, along with the spatiotemporal distribution of hazards predicted from WSN data, are used to characterize the navigable network.

Based on the constructed navigable network, the graph model is presented, followed by a detailed statement of the ship emergency navigation problem, including its assumptions and formal formulation. An efficient approximation scheme, based on the fully polynomial-time approximation algorithm proposed by Hassin [Has92], is developed to determine a near-optimal solution to the formulated problem. The proposed scheme builds off two fundamental techniques: *Rounding and Scaling* and *Relaxing*. We also analyzed the error bound of the solution calculated by our proposed scheme and implemented extensive simulations on the real-world cruise ship, *Yangtze Gold 7*, to assess the performance of our scheme in terms of five perspectives, i.e., average escape time, navigation success ratio, average path length, minimum distance to hazards, and algorithm runtime.

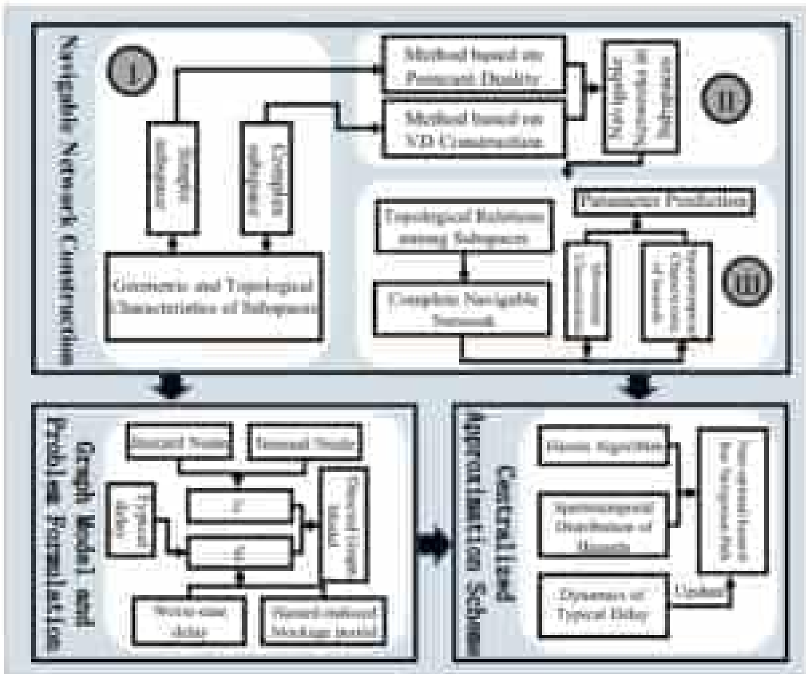

Figure 4: An overview of the research architecture of Paper I.

1.7.2 Paper II-Two-stage Adaptive Decision Making for Emergency Navigation on Dynamic Hazardous Ship Indoor Environments via WSNs

Given the risk of frequent oscillations (i.e., moving back and forth) during navigation caused by repeated recalculation of navigation directions in the previously proposed centralized approximation scheme, we designed a two-stage emergency navigation approach to reduce evacuees' oscillations and enhance the real-time capability of providing evacuation decisions. An overview of the research architecture of Paper II is shown in Fig. 5.

First, in the pre-processing phase, lookup tables are synthesized at each waypoint (i.e., staircase nodes and exit nodes) using the algorithm in [Bar18], without consideration of the spatial-temporal distribution of hazards, from which the outgoing edge can be determined, for any given remaining worst-case delay bound, to reach the exit with the minimum remaining typical delay. However, navigating solely according to these lookup tables may cause evacuees to become trapped by dynamic hazards. Therefore, we update the synthesized lookup table at a waypoint based on hazard dynamics predicted using WSN data if and only if no path exists from the waypoint to the exit that follows the neighbor specified in the lookup table, with all segments in the path unaffected by hazards. The construction and updating of lookup tables require non-trivial computations and thus are offloaded to preprocessing that is performed before an emergency. In the runtime phase, each evacuee independently makes decisions at intermediate waypoints based on their actual delays, which are affected by ship inclination dynamics, and the updated lookup tables. The run-time processing is extremely efficient and works as follows: if the remaining evacuation deadline is larger than the worst-case delay bound in a lookup table entry at the user waypoint, the evacuee takes the outgoing edge with the minimum typical delay from those entries. We evaluated the performance of the proposed two-stage hybrid emergency navigation approach across different network sizes in terms of average path length, average escape time, navigation success ratio, and minimum distance to hazards.

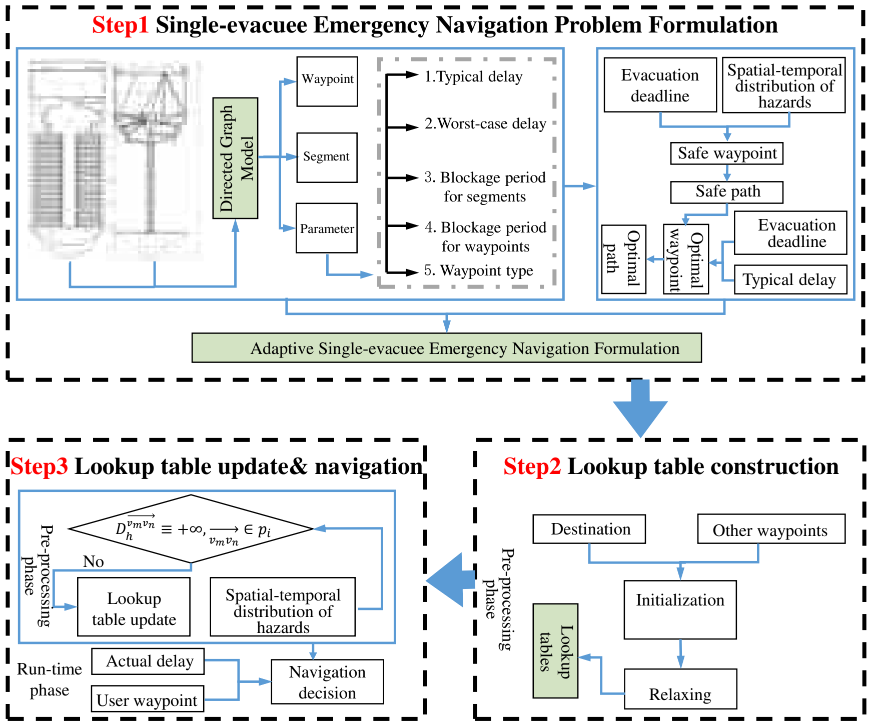

Figure 5: An overview of the research architecture of Paper II.

1.7.3 Paper IV-Centralized Cooperative Multipath Planning for Crowd Evacuation on Dynamic Ships based on IoT Technologies

The two emergency navigation methods described above do not take into account waiting times caused by evacuee queues resulting from the concurrent movement of individuals and the limited capacity of corridors or staircases. Therefore, navigation using these methods may lead to heavy congestion, and thus can prolong total evacuation time and jeopardize evacuees' chances of survival. To alleviate the congestion of passageways, we designed a cooperative multipath planning method for large-scale crowd evacuation on dynamic ships, which evenly distributes the evacuation load among corridors and staircases. Fig. 6 presents an overview of the research architecture of Paper IV.

First, we developed a loading-based scheme to determine the evacuation order of evacuees. This scheme is based on an analytical model that estimates evacuation time using typical delays across links. Then, dedicated paths for evacuees are planned according to the determined evacuation order and a lookup table-based analytical model for estimating evacuation time using both typical and worst-case delays. In addition, considering that some evacuees may not follow the provided instructions during an emergency due to panic or misunderstanding, known as behavior deviation, we also developed a partial-update scheme to adjust the evacuation order and paths for those affected by such deviation behaviors. Finally, we carried out extensive simulations to evaluate the performance of our proposed cooperative multipath planning approach from four perspectives, i.e., total evacuation time, evacuation success ratio, congestion distribution, and average escape rate, using a simulated ship indoor environment comprising the second, third, and fourth floors of the *Yangtze Gold 7* cruise. Moreover, the proposed approach was applied to the *Costa Concordia* cruise, which suffered a disaster at 21 : 45 on 13 January 2012 after colliding with a reef in the Tyrrhenian sea. Results demonstrate that it is possible to prevent the loss of lives that occurred in the *Costa Concordia* disaster by implementing our approach.

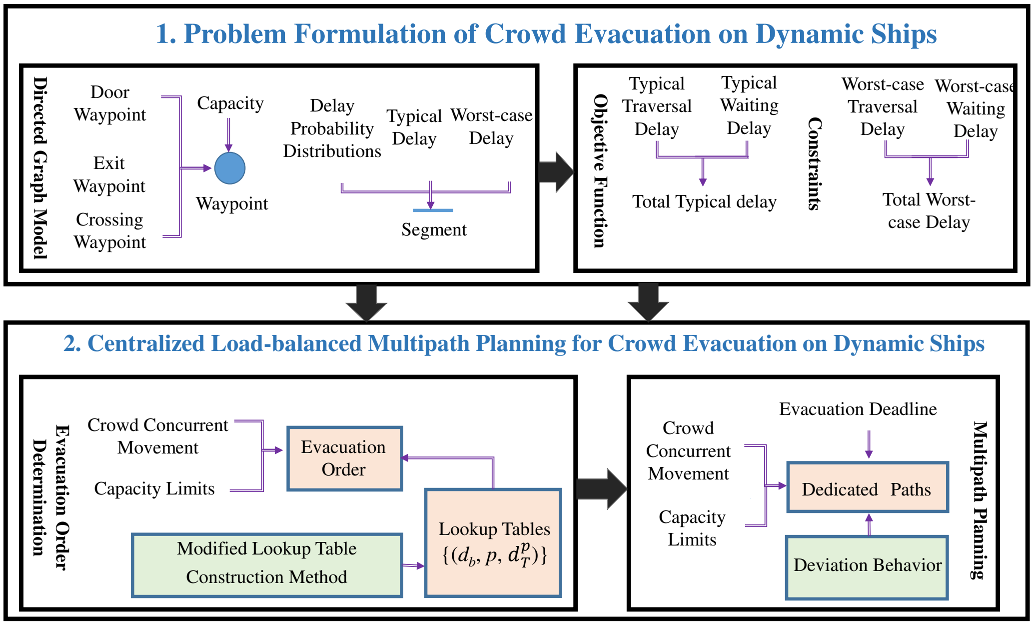

Figure 6: An overview of the research architecture of Paper IV.

1.7.4 Paper V-Distributed and Decentralized Deep RL-based Method with Table-driven Pretraining for Ship Evacuation

However, on the one hand, the computational complexity of the proposed cooperative multipath planning method grows exponentially as the number of evacuees increases, making it computationally infeasible for very large crowds. On the other hand, the proposed method relies on centralized planning in an evacuation server, which requires up-to-date global knowledge, such as the current distribution of evacuees. Therefore, due to intense activities during an emergency, computation and communication delays are likely to occur, which makes it challenging to provide real-time navigation guidance. Additionally, if the server breaks down during an emergency, none of the evacuees can receive instructions from it. The lack of guidance may cause disorientation and aimless movement, potentially increasing evacuation time and the risk of injuries or fatalities. Therefore, we devised a distributed and decentralized deep RL-based method with table-driven pretraining for emergency evacuation in dynamic hazardous ship indoor environments. An overview of the research architecture of Paper V is presented in Fig. 7.

First, we designed a ship emergency evacuation environment used to train RL agents for evacuation planning. The environment is modeled as a discrete gridworld and incorporates realistic features such as hazard spread, exit bottlenecks, spatiotemporal distribution of life-saving equipment, and dynamic ship inclination.

We also proposed a novel RL approach that integrates a lookup table-based pretraining module to provide appropriate initial network weights of a Dueling-DQN-based agent. Specifically, in the pretraining module, we generate a graph model with grid centers as nodes and passageways between neighboring grids as links, so that each node has at most four links. Each link is characterized by a probabilistic delay function. Based on the generated graph model, routing tables are established for each node using a modified optimal table-driven algorithm [ABG+20], from which, for each node, the minimum expected delay to an exit can be determined under a given worst-case delay bound when selecting a particular successor node as the navigation direction. Leveraging the routing tables, we build a Q-matrix by distinguishing between nodes in the feasible set and those in the infeasible set. The feasible set comprises all successor nodes that do not violate the evacuation deadline, even under worst-case delays. The built Q-matrix is then transferred to a Dueling DQN model by pretraining the model to reproduce the Q-matrix. Compared to directly pretraining a Dueling DQN network in the pretraining environment, which requires more time to converge, our module requires much less time. After pretraining, the agent is trained on the complete ship evacuation task. In order to simplify the learning task, the information within the agent's field of view is separated into multiple channels: six observation channels, three reference channels, and three ego-agent state channels. The observation and reference channels are processed by an encoder consisting of convolutional layers and a Gated Recurrent Unit (GRU), while the ego-agent state channels are processed through a Fully Connected (FC) layer. Each agent can perform six actions, i.e., move forward/backward/left/right, stay still, and pick up a piece of life-saving equipment. Different rewards are received by the agent to incentivize it to make optimal evacuation decisions. In addition, we employed a distributed learning framework, Ape-X, to speed up the learning procedure. Extensive simulations were conducted to examine the performance of our proposed distributed and decentralized deep RL-based method with table-driven pretraining, with respect to average reward, average evacuation time, and success ratio.

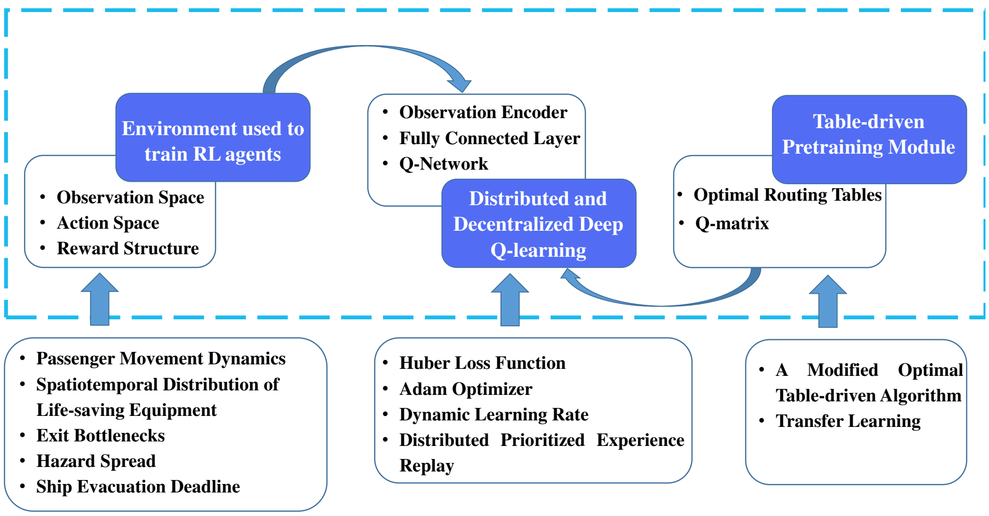

Figure 7: An overview of the research architecture of Paper V.

1.7.5 Papers VI and VII-Impact of IoT System Imperfections and Passenger Errors on Cruise Ship Evacuation Delay

As discussed above, wireless networks and computational servers that are used for decision-making are likely to experience congestion, especially considering that decisions and communications must be frequently updated in response to the dynamic nature of evacuation environments. This congestion can lead to delays in transmitting network packets, and navigation decisions may be compromised by the delayed instructions or information used in emergency navigation algorithms. In addition, passengers are likely to make mistakes in following the instructions provided by an evacuation system due to panic, misinterpretation of guidance, or limited visibility of directional indicators.

While most prior work has neglected these factors, this chapter specifically analyzes their impact on passenger evacuation time through extensive simulations. The simulations are implemented in a simulated environment of the second, third, and fourth decks of the real-world cruise ship *Yangtze Gold* 7, using a two-part simulation framework. The first part employs AnyLogic 8.8.2 to construct the evacuation simulation model, where the SF model is adopted to govern passenger movement. The second part utilizes a path-planning module written in Python to compute evacuation directions for evacuees based on the proposed two-stage hybrid emergency navigation approach. The computed directions are transferred to the AnyLogic-based evacuation simulation model at each simulation step whenever movement instructions need to be updated.

We evaluate the effect of the *Probability of Delay* (PoD), which is probabilistically assigned to each node to indicate whether the information lag is $IL = 1$ with probability PoD or $IL = 0$ with probability $1 - PoD$, on the performance of the evacuation system, in terms of the average evacuation time of passengers located in different regions. $IL = 1$ means that each node in the navigable network provides evacuees with information regarding their next moves, delayed by one step in computation and transmission, whereas $IL = 0$ means that each node receives the exact, up-to-date direction recommendation from the Information Technology System (ITS). All simulation results are obtained based on 100 independent runs, with the probability PoD drawn separately for each run and for each node. The results show that evacuation time increases with PoD, regardless of passengers' locations, whether in cabins, the restaurant, or other areas.

Additionally, we assess how non-compliance with evacuation suggestions influences the average evacuation time of passengers in various regions. Non-compliance is modeled as the choice of evacuees to miss the correct direction provided by the evacuation system and instead take an alternative direction at random. To this effect, we define the *Probability of Error* (PoE), probabilistically assigned to each passenger, to represent whether a passenger does not obey the offered navigation direction with probability PoE or follows it with probability $1 - PoE$. The simulation results indicate that the performance ratio of the average evacuation time as compared to the ideal case of $PoE = 0$ increases with PoE for passengers in different areas. Nevertheless, relative to PoD, the non-compliance behavior of passengers has a less pronounced effect on the average evacuation time across various areas.

1.7.6 Paper VIII-IoT-driven Scheduling for Congestion Avoidance in Emergency Evacuation

In many circumstances, IoT can play a crucial role in facilitating the effective and efficient management of human evacuation during emergencies. Specifically, it can be used to detect the presence of evacuees in different locations, identify hazards and crowd congestion, make navigation decisions based on this information, and dynamically guide evacuees to mitigate or eliminate congestion and enhance evacuation safety and efficiency. Therefore, in this chapter, we suggest several strategies for using IoT to direct evacuees, based on the analysis of an emergency evacuation system using an analytical queueing network approach with multiple routing rules. The IoT is employed to guide passengers in a manner that moves them forward when other passengers exit through the exit points.

We model the emergency evacuation system as a network of queues with unbounded capacity, indicating that the corridors and staircases are designed to be large enough so that they are never completely filled by people. Four different routing methods are used to select the next link. In *Selection Rule* 1, an evacuee leaving a node (except the final node) selects the successor link with equal probability. In *Selection Rule* 2, the evacuee chooses the successor link with the highest service rate. In *Selection Rule* 3, the evacuee selects a successor link with probability proportional to the ratio of its service rate to the total service rate of all successor links. In *Selection Rule* 4, the evacuee chooses the successor link that minimizes the delay to the exit while respecting the worst-case delay bound. In order to alleviate congestion in passageways, we suggest the *Pull Policy*, which exploits messages from the exit point to instruct evacuees to leave their waiting areas and proceed toward the exit. To achieve this, a sensor at the exit is utilized to detect the departure of an evacuee, and a network-based communication system relays a message to a waiting area, with the probability inversely proportional to the number of waiting areas. In the waiting area, a visual indicator, e.g., a light that turns green or red, would either restrict or encourage entrance into passageways. Note that there is also an *impatience time*, after which an evacuee is allowed to enter his/her preferred passageway even if no message is received from the exit point. Furthermore, we propose a heuristic extension of the *Pull Policy*, which sends messages simultaneously to all waiting areas with probability 1 in order to reduce the likelihood that a message from the exit node reaches waiting areas without evacuees.

We evaluate the impact of the proposed *Pull Policy* and its heuristic extension on average total time under the four routing rules described above using extensive numerical simulations in a simulated environment encompassing the second, third, and fourth decks of the *Yangtze Gold* 7 cruise ship. The average total time spent by an evacuee in the evacuation system at steady state is derived from the average of the total number of evacuees in the system using Little's Law [Lit61]. The average total number of evacuees is calculated from the steady-state probabilities of having at least one evacuee in a source node, a final node, and a passageway. Simulation results show that: (1) messages from the exit node lead to an improvement of evacuation performance, as indicated by the decreased average total time spent by evacuees; (2) an increase in the total arrival rate at source nodes has an adverse effect on the average total evacuation time across various routing rules and pull policies; (3) higher service rates at waiting areas result in a decrease in the average total evacuation time; (4) the choice of routing rule significantly influences the average total time spent in the system. It is worth noticing that the performance of a routing rule varies depending on the total arrival rate at source nodes. Additionally, the results demonstrate that the effect of the service rate at waiting areas on the average total time spent by evacuees is influenced by the total arrival rate at source nodes, and vice versa.

1.8 Chapter Summary

Section 1.1 presents several common technical challenges encountered in emergency evacuation. Section 1.2 and Section 1.3 introduce the topic of emergency evacuation for ship passengers by noting the dynamic growth of the cruise industry and the potentially catastrophic consequences of cruise ship accidents. The significance of ship passenger emergency evacuation and the primary factors affecting passenger survival are also discussed in Section 1.3. In Section 1.4, we present an overview of existing studies on emergency evacuation, including navigable network construction in ship interiors, emergency evacuation planning algorithms, ship evacuation models and tools, and ship emergency evacuation systems. This section also analyzes and summarizes the research gaps in navigable network construction in ship interiors and in emergency evacuation methods for onboard passengers, with further research objectives detailed in Section 1.5. The published papers relevant to this thesis are presented in Section 1.6. Section 1.7 offers a summary of the appended research papers included in this thesis.

References

[AA09] Hossam Abdelgawad and Baher Abdulhai. Emergency evacuation planning as a network design problem: a critical review. *Transportation Letters*, 1(1):41–58, 2009.

[ABG+20] Kunal Agrawal, Sanjoy Baruah, Zhishan Guo, Jing Li, and Sudharsan Vaidhun. Hard-real-time routing in probabilistic graphs to minimize expected delay. In *2020 IEEE Real-Time Systems Symposium (RTSS)*, pages 63–75. IEEE, 2020.

[Aut14] Bahamas Maritime Authority. Casualty investigation report: Fire onboard grandeur of the seas, 2014. Accessed: 2025-09-15.

[Bar18] Sanjoy Baruah. Rapid routing with guaranteed delay bounds. In *2018 IEEE Real-Time Systems Symposium (RTSS)*, pages 13–22. IEEE, 2018.

[BAS05] Chiranjeeb Buragohain, Divyakant Agrawal, and Subhash Suri. Distributed navigation algorithms for sensor networks. *arXiv preprint cs/0512060*, 2005.

[BDG13] Huibo Bi, Antoine Desmet, and Erol Gelenbe. Routing emergency evacuees with cognitive packet networks. In *Information Sciences and Systems 2013: Proceedings of the 28th International Symposium on Computer and Information Sciences*, pages 295–303. Springer International Publishing Cham, 2013.

[BG14a] Huibo Bi and Erol Gelenbe. A cooperative emergency navigation framework using mobile cloud computing. In *Information Sciences and Systems 2014: Proceedings of the 29th International Symposium on Computer and Information Sciences*, pages 41–48. Springer International Publishing Cham, 2014.

[BG14b] Huibo Bi and Erol Gelenbe. Routing diverse evacuees with cognitive packets. In *2014 IEEE International Conference on Pervasive Computing and Communication Workshops (PERCOM WORKSHOPS)*, pages 291–296. IEEE, 2014.

[BG19] Huibo Bi and Erol Gelenbe. A survey of algorithms and systems for evacuating people in confined spaces. *Electronics*, 8(6):711, 2019.

[BGLM09] Sandro Bologna, Erol Gelenbe, Eric HAM Luiijf, and Vincenzo Masucci. Diesis: an interoperable european federated simulation network for critical infrastructures. *proc. EURO SIW*, 2009.

[BKRB15] Marina Balakhontceva, Vladislav Karbovskii, Dmitrii Rybokonenko, and Alexander Boukhanovsky. Multi-agent simulation of passenger evacuation considering ship motions. *Procedia Computer Science*, 66:140–149, 2015.

[BKSB16] Marina Balakhontceva, Vladislav Karbovskii, Serge Sutulo, and Alexander Boukhanovsky. Multi-agent simulation of passenger evacuation from a damaged ship under storm conditions. *Procedia computer science*, 80:2455–2464, 2016.

[BYG+18] Olivier Brun, Yonghua Yin, Erol Gelenbe, Y. Murat Kadioglu, Javier Augusto-Gonzalez, and Manuel Ramos. Deep learning with dense random neural networks for detecting attacks against iot-connected home environments. In *Security in Computer and Information Sciences: First International ISCIS Security Workshop 2018, Euro-CYBERSEC 2018, London, UK, February 26-27, 2018, Revised Selected Papers, CCIS*, volume 821, pages 79–89. Springer International Publishing, 2018.

[CCT15a] Lien-Wu Chen, Jen-Hsiang Cheng, and Yu-Chee Tseng. Distributed emergency guiding with evacuation time optimization based on wireless sensor networks. *IEEE Transactions on Parallel and Distributed Systems*, 27(2):419–427, 2015.

[CCT15b] Lien-Wu Chen, Jen-Hsiang Cheng, and Yu-Chee Tseng. Optimal path planning with spatial-temporal mobility modeling for individual-based emergency guiding. *IEEE Transactions on Systems, Man, and Cybernetics: Systems*, 45(12):1491–1501, 2015.

[CHZ11] Miao Chen, Duanfeng Han, and Haipeng Zhang. Research on a multi-grid model for passenger evacuation in ships. *Journal of Marine Science and Application*, 10(3):340–346, 2011.

[(CL25] Cruise Lines International Association (CLIA). State of the cruise industry report 2025, May 18 2025. Accessed: 2025-09-15.

[CLL15] Jehyun Cho, Ghang Lee, and Seungjae Lee. An automated direction setting algorithm for a smart exit sign. *Automation in Construction*, 59:139–148, 2015.

[CMMV12] Dazhi Chen, Chilukuri K Mohan, Kishan G Mehrotra, and Pramod K Varshney. Distributed in-network path planning for sensor network navigation in dynamic hazardous environments. *Wireless Communications and Mobile Computing*, 12(8):739–754, 2012.

[con21] Wikipedia contributors. 2021 bangladesh ferry fire, 2021. Accessed: 2025-09-15.

[Con23] Wikipedia Contributors. Kostenko mine fire, October 28 2023. Accessed: 2025-09-15.

[CT24] C Che and J Tian. Maximum flow and minimum cost flow theory to solve the evacuation planning. *Advances in Engineering Innovation*, 12:60–64, 2024.

[CXM+20] Zhu Chenghua, Guo Xiang, Chen Miao, et al. Research on the personnel agent model in ship evacuation simulation. *Computer Simulation*, 37(6):328–331, 2020. In Chinese with English abstract.

[DDF+06] Simon Dobson, Spyros Denazis, Antonio Fernández, Dominique Gaïti, Erol Gelenbe, Fabio Massacci, Paddy Nixon, Fabrice Saffre, Nikita Schmidt, and Franco Zambonelli. A survey of autonomic communications. *ACM Transactions on Autonomous and Adaptive Systems (TAAS)*, 1(2):223–259, 2006.

[DFG10] Nikolaos Dimakis, Avgoustinos Filippoupolitis, and Erol Gelenbe. Distributed building evacuation simulator for smart emergency management. *The Computer Journal*, 53(9):1384–1400, 2010.

[DG13a] Antoine Desmet and Erol Gelenbe. Graph and analytical models for emergency evacuation. In *2013 IEEE International Conference on Pervasive Computing and Communications Workshops (PERCOM Workshops)*, pages 523–527. IEEE, 2013.

[DG13b] Antoine Desmet and Erol Gelenbe. Reactive and proactive congestion management for emergency building evacuation. In *38th Annual IEEE Conference on Local Computer Networks*, pages 727–730. IEEE, 2013.

[DGC+18] Joanna Domanska, Erol Gelenbe, Tadek Czachorski, Anastasis Drosou, and Dimitrios Tzovaras. Research and innovation action for the security of the internet of things: The seriot project. In *Recent Cybersecurity Research in Europe: Proceedings of the 2018 ISCIS Security Workshop, Imperial College London. Lecture Notes CCIS No. 821, Springer Verlag*, volume 821, 2018.

[DHZ$^+$22] Kunxiang Deng, Lei Hu, Qingyong Zhang, Danhong Zhang, Jiahua Chen, and Wei Fan. Emergency evacuation scheme of cruise ship under fire situation based on multi-source multi-sink maximum flow model. In *2022 37th Youth Academic Annual Conference of Chinese Association of Automation (YAC)*, pages 728–733. IEEE, 2022.

[DLW$^+$22] Kaifeng Deng, Meng Li, Guanning Wang, Xiangmin Hu, Yan Zhang, Huijie Zheng, Koukou Tian, and Tao Chen. Experimental study on panic during simulated fire evacuation using psycho-and physiological metrics. *International journal of environmental research and public health*, 19(11):6905, 2022.

[Du21] Hongli Du. Study on ship personnel fire evacuation based on cellular automata. Master's thesis, Harbin Engineering University, Harbin, China, 2021.

[EAP23] Eleftheria Eliopoulou, Aimilia Alissafaki, and Apostolos Papanikolaou. Statistical analysis of accidents and review of safety level of passenger ships. *Journal of Marine Science and Engineering*, 11(2):410, 2023.

[Eur24] European Maritime Safety Agency (EMSA). Annual overview of marine casualties and incidents 2024, November 2024. Accessed: 2025-09-15.

[FCSF19] Libi Fu, Shuchao Cao, Weiguo Song, and Jie Fang. The influence of emergency signage on building evacuation behavior: An experimental study. *Fire and materials*, 43(1):22–33, 2019.

[FG09] Avgoustinos Filippoupolitis and Erol Gelenbe. A decision support system for disaster management in buildings. In *Proceedings of the 2009 Summer Computer Simulation Conference*, pages 141–147, 2009.

[FGG$^+$12] Avgoustinos Filippoupolitis, Erol Gelenbe, Daniele Gianni, Laurence Hey, George Loukas, Stelios Timotheou, and Others. Distributed agent-based building evacuation simulator. 2012.

[FGG13] Avgoustinos Filippoupolitis, Gokce Gorbil, and Erol Gelenbe. Spatial computers for emergency support. *The Computer Journal*, 56(12):1399–1416, 2013.

[FLZ$^+$23] Siming Fang, Zhengjiang Liu, Shengquan Zhang, Xinjian Wang, Yihang Wang, and Shengke Ni. Evacuation simulation of an ro-ro passenger ship considering the effects of inclination and crew's guidance. *Proceedings of the institution of mechanical engineers, part M: journal of engineering for the maritime environment*, 237(1):192–205, 2023.

[GAPG15] Gokce Gorbil, Omer H Abdelrahman, Mihajlo Pavloski, and Erol Gelenbe. Modeling and analysis of rrc-based signalling storms in 3g networks. *IEEE Transactions on Emerging Topics in Computing*, 4(1):113–127, 2015.

[GB14] Erol Gelenbe and Huibo Bi. Emergency navigation without an infrastructure. *Sensors*, 14(8):15142–15162, 2014.

[GC15] Erol Gelenbe and Yves Caseau. The impact of information technology on energy consumption and carbon emissions. *ACM Ubiquity*, 2015(June):1–15, 2015.

[GDC$^+$18] Erol Gelenbe, Joanna Domanska, Tadeusz Czàchorski, Anastasis Drosou, and Dimitrios Tzovaras. Security for internet of things: The SerIoT project. In *2018 International Symposium on Networks, Computers and Communications (ISNCC)*, pages 1–5. IEEE, 2018.

[Gel94] Erol Gelenbe. G-networks: a unifying model for neural and queueing networks. *Annals of Operations Research*, 48(5):433–461, 1994.

[Gel00] Erol Gelenbe. System performance evaluation: methodologies and applications. 2000.

[Gel06] Erol Gelenbe. Users and services in intelligent networks. In *IEE Proceedings-Intelligent Transport Systems*, volume 153, pages 213–220. IET, 2006.

[Gel10] Erol Gelenbe. Search in unknown random environments. *Physical Review E—Statistical, Nonlinear, and Soft Matter Physics*, 82(6):061112, 2010.

[Gel23] Erol Gelenbe. Electricity consumption by ict: Facts, trends, and measurements. *ACM Ubiquity*, 2023(August):1–15, 2023.

[GFG12] Gokce Gorbil, Avgoustinos Filippoupolitis, and Erol Gelenbe. Intelligent navigation systems for building evacuation. In *Computer and Information Sciences II: 26th International Symposium on Computer and Information Sciences*, pages 339–345. Springer, 2012.

[GG12] Gokce Gorbil and Erol Gelenbe. Resilience and security of opportunistic communications for emergency evacuation. In *Proceedings of the 7th ACM workshop on Performance monitoring and measurement of heterogeneous wireless and wired networks*, pages 115–124, 2012.

[GG13a] Gokce Gorbil and Erol Gelenbe. Disruption tolerant communications for large scale emergency evacuation. In *Pervasive Computing and Communications Workshops (PERCOM Workshops), 2013 IEEE International Conference on*, pages 540–546. IEEE, 2013.

[GG13b] Gokce Gorbil and Erol Gelenbe. Resilient emergency evacuation using opportunistic communications. In *Computer and Information Sciences III*, pages 249–257. Springer, 2013.

[GGR15] Morten Goodwin, Ole-Christoffer Granmo, and Jaziar Radianti. Escape planning in realistic fire scenarios with ant colony optimisation. *Applied Intelligence*, 42(1):24–35, 2015.

[GGW12] Erol Gelenbe, Gokce Gorbil, and Fang-Jing Wu. Emergency cyber-physical-human systems. In *2012 21st International Conference on Computer Communications and Networks (ICCCN)*, pages 1–7. IEEE, 2012.

[GLL06] Erol Gelenbe, Peixiang Liu, and Jeremy Laine. Genetic algorithms for route discovery. *IEEE Transactions on Systems, Man, and Cybernetics, Part B (Cybernetics)*, 36(6):1247–1254, 2006.

[GM10] Erol Gelenbe and Isi Mitrani. *Analysis and synthesis of computer systems*, volume 4. World Scientific, 2010.

[GN10] Erol Gelenbe and Edith Ngai. Adaptive random re-routing for differentiated qos in sensor networks. *The Computer Journal*, 53(7):1052–1061, 2010.

[Gon22] Dingfei Gong. Research on ship personnel evacuation planning model based on the hungarian method and software development. Master's thesis, Huazhong University of Science and Technology, Wuhan, China, 2022.

[GSSR97] Erol Gelenbe, Nestor Schmajuk, John Staddon, and John Reif. Autonomous search by robots and animals: A survey. *Robotics and Autonomous Systems*, 22(1):23–34, 1997.

[GTN10] Erol Gelenbe, Stelios Timotheou, and David Nicholson. Fast distributed near-optimum assignment of assets to tasks. *The Computer Journal*, 53(9):1360–1369, 2010.

[GW12] Erol Gelenbe and Fang-Jing Wu. Large scale simulation for human evacuation and rescue. *Computers & Mathematics with Applications*, 64(12):3869–3880, 2012.

[GW13] Erol Gelenbe and Fang-Jing Wu. Future research on cyber-physical emergency management systems. *Future Internet*, 5(3):336–354, 2013.

[GXD+17a] Edwin R Galea, Hui Xie, Steven Deere, David Cooney, and Lazaros Filippidis. Evaluating the effectiveness of an improved active dynamic signage system using full scale evacuation trials. *Fire Safety Journal*, 91:908–917, 2017.

[GXD+17b] ER Galea, H Xie, S Deere, D Cooney, and L Filippidis. An international survey and full-scale evacuation trial demonstrating the effectiveness of the active dynamic signage system concept. *Fire and Materials*, 41(5):493–513, 2017.

[GXL14] Edwin R Galea, Hui Xie, and Peter J Lawrence. Experimental and survey studies on the effectiveness of dynamic signage systems. *Fire Safety Science*, 11:1129–1143, 2014.

[GY16] Erol Gelenbe and Yongha Yin. Deep learning with random neural networks. In *2016 International Joint Conference on Neural Networks (IJCNN)*, pages 1633–1638. IEEE, 2016.

[Has92] Refael Hassin. Approximation schemes for the restricted shortest path problem. *Mathematics of Operations research*, 17(1):36–42, 1992.

[HC20] Min Hu and Wei Cai. Evacuation simulation and layout optimization of cruise ship based on cellular automata. *International Journal of Computers and Applications*, 42(1):36–44, 2020.

[HCZ25] Min Hu, Wei Cai, and Tao Zhang. Study of behaviors of passengers on ships and evacuation simulation method based on evacuation experiments. *Journal of Transportation Safety & Security*, 17(3):227–252, 2025.

[HKRL12] Sol Ha, Nam-Kug Ku, Myung-Il Roh, and Kyu-Yeul Lee. Cell-based evacuation simulation considering human behavior in a passenger ship. *Ocean engineering*, 53:138–152, 2012.

[HT01] Horst W Hamacher and Stevanus A Tjandra. Mathematical modelling of evacuation problems: A state of art. 2001.

[HZJ21] Haoyang Han, Jundong Zhang, and Ruizheng Jiang. Application of extended lattice gas automata model in ship evacuation simulation. *Mobile Information Systems*, 2021(1):6335388, 2021.

[JS17] Jongsoon Jin and Geoboo Song. Bureaucratic accountability and disaster response: Why did the korea coast guard fail in its rescue mission during the sewol ferry accident? *Risk, Hazards & Crisis in Public Policy*, 8(3):220–243, 2017.

[Kiz20] Joanna Kizielewicz. Measuring the economic and social contribution of cruise tourism development to coastal tourist destinations. 2020.

[KMMS17] Sonja Th Kwee-Meier, Alexander Mertens, and Christopher M Schlick. Age-related differences in decision-making for digital escape route signage under strenuous emergency conditions of tilted passenger ships. *Applied ergonomics*, 59:264–273, 2017.

[KvdWH24] Erica Kinkel, C Natalie van der Wal, and Serge P Hoogendoorn. The effects of three environmental factors on building evacuation time. *Heliyon*, 10(5), 2024.

[LC19] YP Li and W Cai. Research progress on ship evacuation. *Ship Build. China*, 1:228–241, 2019.

[LCZ15] Manxia Liu, Yuansheng Cheng, and Pan Zhang. Shortest path planning of ship channels considering mutual influence among multiple people. *Shipbuilding of China*, 56(2):185–192, 2015.

[LDRR03] Qun Li, Michael De Rosa, and Daniela Rus. Distributed algorithms for guiding navigation across a sensor network. In *Proceedings of the 9th annual international conference on Mobile computing and networking*, pages 313–325, 2003.

[Li11] Na Li. Research on ship personnel evacuation methods based on dynamic network flow. Master's thesis, Harbin Engineering University, Harbin, China, 2011.

[Lit61] John DC Little. A proof for the queuing formula: L= λ w. *Operations research*, 9(3):383–387, 1961.

[LN17] Joseph YT Leung and CT Ng. Fast approximation algorithms for uniform machine scheduling with processing set restrictions. *European Journal of Operational Research*, 260(2):507–513, 2017.

[Łoz06] Dorota H Łozowicka. Problems associated with evacuation from the ship in case of an emergency situation. *International Journal of Automation and Computing*, 3(2):165–168, 2006.

[LR05] Qun Li and Daniela Rus. Navigation protocols in sensor networks. *ACM Transactions on Sensor Networks (TOSN)*, 1(1):3–35, 2005.

[LWYD08] Mo Li, Jiliang Wang, Zheng Yang, and Jingyao Dai. Sensor network navigation without locations. In *Proceedings of the 6th ACM conference on Embedded network sensor systems*, pages 391–392, 2008.

[LXG+24] Yapeng Li, Qin Xiao, Jiayang Gu, Wei Cai, and Min Hu. Modeling and solving passenger ship evacuation arrangement problem. *Reliability Engineering & System Safety*, 246:110075, 2024.

[LY20] Yui-yip Lau and Tsz Leung Yip. The asia cruise tourism industry: Current trend and future outlook. *The Asian Journal of Shipping and Logistics*, 36(4):202–213, 2020.

[LYD12] Sun Liang, Ma Yue, and Lian Dongben. Game theory based exit selection model for evacuation. *Computer Systems & Applications*, 21(1):111–114, 2012.

[LZBA12] Gino J Lim, Shabnam Zangeneh, M Reza Baharnemati, and Tiravat Assavapokee. A capacitated network flow optimization approach for short notice evacuation planning. *European Journal of Operational Research*, 223(1):234–245, 2012.

[LZW+11] Shen Li, Andong Zhan, Xiaobing Wu, Panlong Yang, and Guihai Chen. Efficient emergency rescue navigation with wireless sensor networks. *J. Inf. Sci. Eng.*, 27(1):51–64, 2011.

[LZXZ21] Linfan Liu, Huajun Zhang, Jupeng Xie, and Qin Zhao. Dynamic evacuation planning on cruise ships based on an improved ant colony system (iacs). *Journal of Marine Science and Engineering*, 9(2):220, 2021.

[LZZ+22] Linfan Liu, Huajun Zhang, Yu Zhan, Yixin Su, and Changfan Zhang. Intelligent optimization method for the evacuation routes of dense crowds on cruise ships. *Simulation Modelling Practice and Theory*, 117:102496, 2022.

[MC14] Chen Miao and Zhu Chenghua. Research on passengers' evacuation model in ships based on agent theory. In *2014 IEEE International Conference on Mechatronics and Automation*, pages 441–446. IEEE, 2014.

[MHZ22] Dun Meng, Zhuo Hu, and Huajun Zhang. Simulation of multi-layer ship evacuation system based on improved a* algorithm. *Journal of System Simulation*, 34(6):1375–1382, 2022.

[MLM21] Ziyuan Ma, Yudong Luo, and Hang Ma. Distributed heuristic multi-agent path finding with communication. In *2021 IEEE International Conference on Robotics and Automation (ICRA)*, pages 8699–8705. IEEE, 2021.

[NCLK21] Chi To Ng, TCE Cheng, Eugene Levner, and Boris Kriheli. Optimal bi-criterion planning of rescue and evacuation operations for marine accidents using an iterative scheduling algorithm. *Annals of Operations Research*, 296(1):407–420, 2021.

[New24a] AP News. Cave-in leaves 2 miners dead, 1 missing at mysłowice-wesoła coal mine in poland, May 16 2024. Accessed: 2025-09-15.

[New24b] AP News. Russia says 60 dead, 145 injured in concert hall raid; islamic state group claims responsibility, March 22 2024. Accessed: 2025-09-15.

[New25] AP News. Fires engulf turkey's mediterranean coast as government declares 2 disaster zones, July 10 2025. Accessed: 2025-09-15.

[NLL18] Baocheng Ni, Zhuang Lin, and Ping Li. Agent-based evacuation model incorporating life jacket retrieval and counterflow avoidance behavior for passenger ships. *Journal of Statistical Mechanics: Theory and Experiment*, 2018(12):123405, 2018.

[NLZL17] Baocheng Ni, Zhen Li, Pei Zhang, and Xiang Li. An evacuation model for passenger ships that includes the influence of obstacles in cabins. *Mathematical Problems in Engineering*, 2017(1):5907876, 2017.

[ÖNU+00] Tuncer I Ören, Susan K Numrich, Adelinde M Uhrmacher, Linda F Wilson, and Erol Gelenbe. Agent-directed simulation: challenges to meet defense and civilian requirements. In *Proceedings of the 32nd Winter Simuation Conference*, pages 1757–1762, 2000.

[PTT06] Meng-Shiuan Pan, Chia-Hung Tsai, and Yu-Chee Tseng. Emergency guiding and monitoring applications in indoor 3d environments by wireless sensor networks. *International Journal of Sensor Networks*, 1(1-2):2–10, 2006.

[PVSW08] Francisco Pérez-Villalonga, Javier Salmerón, and Kevin Wood. Dynamic evacuation routes for personnel on a naval ship. *Naval Research Logistics (NRL)*, 55(8):785–799, 2008.

[Reu24a] Reuters. Devastating flash floods hit northeastern spain, killing at least 95, October 29 2024. Accessed: 2025-09-15.

[Reu24b] Reuters. Thousands flee hurricane milton, causing traffic jams and fuel shortages, October 8 2024. Accessed: 2025-09-15.

[RMM06] Dawn Rothe, Stephen Muzzatti, and Christopher W Mullins. Crime on the high seas: Crimes of globalization and the sinking of the senegalese ferry le joola. *Critical Criminology*, 14(2):159–180, 2006.

[SAC+16] Stephen Statler, A Audenaert, J Coombs, T Gordon, P Hendrix, K Kolodziej, P Leddy, B Parker, M Proietti, and R Rotolo. *Beacon technologies*. Springer, 2016.

[SAGG20] Jivitesh Sharma, Per-Arne Andersen, Ole-Christoffer Granmo, and Morten Goodwin. Deep q-learning with q-matrix transfer learning for novel fire evacuation environment. *IEEE Transactions on Systems, Man, and Cybernetics: Systems*, 51(12):7363–7381, 2020.

[Sho10] Liao Shouheng. *Study on the Evacuation Model of Ship Personnel under Inclined Conditions*. PhD thesis, Dalian Maritime University, Dalian, 2010. In Chinese with English abstract.

[SKS+19] Guillaume Sartoretti, Justin Kerr, Yunfei Shi, Glenn Wagner, TK Satish Kumar, Sven Koenig, and Howie Choset. Primal: Pathfinding via reinforcement and imitation multi-agent learning. *IEEE Robotics and Automation Letters*, 4(3):2378–2385, 2019.

[Sol13] Hussein Soliman. The sinking of the al-salam boccaccio 98 ferry in the red sea: The integration of disaster support system models and emergency management experience. *International Journal of Disaster Risk Reduction*, 4:44–51, 2013.

[Sun25] The Sun. Fire at westfield stratford shopping centre leads to mass evacuation, September 7 2025. Accessed: 2025-09-15.

[Tim24] The Times. Car bomb attack in somalia kills nine during euro 2024 final, July 14 2024. Accessed: 2025-09-15.

[TPT06] Yu-Chee Tseng, Meng-Shiuan Pan, and Yuen-Yung Tsai. Wireless sensor networks for emergency navigation. *Computer*, 39(7):55–62, 2006.

[TRK16] H Tashakkori, A Rajabifard, and M Kalantari. Facilitating the 3d indoor search and rescue problem: An overview of the problem and an ant colony solution approach. *ISPRS annals of the photogrammetry, remote sensing and spatial information sciences*, 4:233–240, 2016.

[VSTH+25] Adi Vitman-Schorr, Mor Ben Tov, Liat Hagbi, Liran Freidus, Vered Shenaar-Golan, and Michal Segal. Evacuation experiences of older adults during armed conflict: Community, place attachment, and well-being. *Journal of Environmental Psychology*, page 102754, 2025.

[VW25] Andres Velez and Stein W Wallace. Active guidance systems in maritime evacuations: optimizing the lifeboat allocation for cruise ships. *Annals of Operations Research*, pages 1–27, 2025.

[Wal04] Jan Oliver Wallgrün. Autonomous construction of hierarchical voronoi-based route graph representations. In *International Conference on Spatial Cognition*, pages 413–433. Springer, 2004.

[Wan13] Kan Wang. *Research on Ship Personnel Evacuation Based on Intelligent Optimization Algorithms*. Ph.d. thesis, Harbin Engineering University, 2013. In Chinese.

[Wat25] Cruise Market Watch. Growth of the ocean cruise line industry, 2025. Accessed: 2025-09-15.

[WHL+14] Lin Wang, Yuan He, Wenyuan Liu, Nan Jing, Jiliang Wang, and Yunhao Liu. On oscillation-free emergency navigation via wireless sensor networks. *IEEE Transactions on Mobile Computing*, 14(10):2086–2100, 2014.

[WLJ15] Chen Wang, Hongzhi Lin, and Hongbo Jiang. Cans: Towards congestion-adaptive and small stretch emergency navigation with wireless sensor networks. *IEEE Transactions on Mobile Computing*, 15(5):1077–1089, 2015.

[WLL+12] Jiliang Wang, Zhenjiang Li, Mo Li, Yunhao Liu, and Zheng Yang. Sensor network navigation without locations. *IEEE Transactions on Parallel and Distributed systems*, 24(7):1436–1446, 2012.

[WLL+22] Xinjian Wang, Zhengjiang Liu, Sean Loughney, Zaili Yang, Yanfu Wang, and Jin Wang. Numerical analysis and staircase layout optimisation for a ro-ro passenger ship during emergency evacuation. *Reliability Engineering & System Safety*, 217:108056, 2022.

[WLZJ16] Chen Wang, Hongzhi Lin, Rui Zhang, and Hongbo Jiang. Send: A situation-aware emergency navigation algorithm with sensor networks. *IEEE Transactions on Mobile Computing*, 16(4):1149–1162, 2016.

[Wu11] Kanke Wu. Research on passenger evacuation models at staircases of passenger ships. Master's thesis, Dalian Maritime University, Dalian, China, 2011.

[WZX20] Peiliang Wang, Ting Zhang, and Yingjie Xiao. Emergency evacuation path planning of passenger ship based on cellular ant optimization model. *Journal of Shanghai Jiaotong University (Science)*, 25(6):721–726, 2020.

[Xia10] Haisong Xiao. Preliminary study on ship personnel evacuation simulation. Master's thesis, Harbin Engineering University, Harbin, China, 2010.

[Xie10] Moubiao Xie. Research on microscopic models for ship evacuation. Master's thesis, Harbin Engineering University, Harbin, China, 2010.

[Xie12] Moubiao Xie. Research on agent-based simulation for ship evacuation. Master's thesis, Harbin Engineering University, Harbin, China, 2012.

[XZW+20] Qimiao Xie, Shaogang Zhang, Jinhui Wang, Siuming Lo, Shuaishuai Guo, and Tao Wang. A surrogate-based optimization method for the issuance of passenger evacuation orders under ship fires. *Ocean Engineering*, 209:107456, 2020.

[YZLW14] Gan-Nan Yuan, Li-Na Zhang, Li-Qiang Liu, and Kan Wang. Passengers' evacuation in ships based on neighborhood particle swarm optimization. *Mathematical Problems in Engineering*, 2014(1):939723, 2014.

[ZDI+19] Min Zhou, Hairong Dong, Petros A Ioannou, Yanbo Zhao, and Fei-Yue Wang. Guided crowd evacuation: approaches and challenges. *IEEE/CAA Journal of Automatica Sinica*, 6(5):1081–1094, 2019.

[ZDZ+19] Min Zhou, Hairong Dong, Yanbo Zhao, Petros A Ioannou, and Fei-Yue Wang. Optimization of crowd evacuation with leaders in urban rail transit stations. *IEEE transactions on intelligent transportation systems*, 20(12):4476–4487, 2019.

[ZLJ+20] Zeyu Zhang, Hangxin Liu, Ziyuan Jiao, Yixin Zhu, and Song-Chun Zhu. Congestion-aware evacuation routing using augmented reality devices. In *2020 IEEE International Conference on Robotics and Automation (ICRA)*, pages 2798–2804. IEEE, 2020.

[ZLMC23] Xiaoling Zeng, Kezhong Liu, Yuting Ma, and Mozi Chen. Dc-hen: A deadline-aware and congestion-relieved hierarchical emergency navigation algorithm for ship indoor environments. In *2023 IEEE International Conference on Mobility, Operations, Services and Technologies (MOST)*, pages 44–54. IEEE, 2023.

[ZZHQ19] Dawei Zhang, Haitao Zhu, Simo Hostikka, and Shi Qiu. Pedestrian dynamics in a heterogeneous bidirectional flow: Overtaking behaviour and lane formation. *Physica A: Statistical Mechanics and Its Applications*, 525:72–84, 2019.

[ZZJ18] Yao Zhang, Dianye Zhang, and Jian Jin. Evacuation path optimization algorithm for inland river passenger ship in emergency situation. *Journal of Coastal Research*, (83):256–260, 2018.

Appendix A: Paper I

WEND: An Efficient WSN-Assisted Emergency Navigation Algorithm for Dynamic Hazardous Ship Indoor Environments

Kezhong Liu, *Member, IEEE*, Yuting Ma, Mozi Chen, *Member, IEEE*, Kehao Wang, Kai Zheng, and Xuming Zeng

***Abstract*—A reliable and efficient emergency evacuation of a damaged cruise ship is essential for passenger safety. Although many advanced evacuation approaches based on wireless sensor networks (WSNs) are capable of exploring dynamic environmental hazards and provide real-time navigation service, such approaches are mainly used in buildings on land, taking no account of the complex ship structure, deadline for ship survival, and dynamic ship inclination, and therefore may fail to evacuate passengers before ship capsizing. This article proposes WEND, an efficient WSN-assisted emergency navigation algorithm for dynamic hazardous ship indoor environment, which informs each passenger about a hazard-avoid route that minimizes the total dynamic typical delay with error bound guarantee while meeting the deadline for ship capsizing in a real-time manner. To achieve this aim, WEND investigates ship interior layout to construct a 3-D topological model and analyzes the time-history of the roll motion of a damaged passenger ship to evaluate ship survival time and the dynamics of pedestrian movement. Then, an efficient adaptive emergency navigation algorithm building on the ideas of Hassin's algorithm is presented to provide a hazard-avoid path from each passenger's current location to boarding stations such that the worst-case delay along this path is no greater than the specified deadline, and the total dynamic typical delay is small. We evaluate our algorithm by conducting extensive simulations. The results demonstrate that WEND improves the navigation success ratio by approximately 30% and 10% compared with the state-of-the-art navigation methods, namely the expected number of oscillations (ENO)-based oscillation-free method (OPEN) and the deadline-aware adaptive emergency navigation strategy (ANT), respectively.**

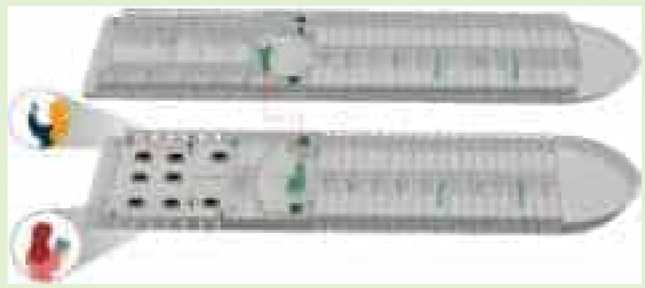

***Index Terms*— Approximation algorithm, dynamic navigation model, ship evacuation, wireless sensor networks (WSNs).**

Nomenclature

$\mathcal{V}$	Set of landmarks.
$\mathcal{E}$	Set of segments.
$\mathcal{V}_h$	Set of hazardous landmarks.
$\mathcal{V}_g$	Set of general landmarks.
v_u	User landmark.
v_e	Exit landmark.
$\overrightarrow{v_i v_j}$	Segment between landmark v_i and v_j.
$d_T^{\overrightarrow{v_i v_j}}(t)$	Typical delay of a segment at time point.
$d_W^{\overrightarrow{v_i v_j}}$	Worst-case delay of a segment.
$\mathcal{D}_h^{v_j}(t)$	Set of the shortest interval of hazardous arrival time at segments ending with v_j at time t.
$D_h^{\overrightarrow{v_i v_j}}(t)$	Shortest interval of hazardous arrival time at a segment $\overrightarrow{v_i v_j}$ at time t.
$\mathcal{E}_v$	Set of neighbor segments of a landmark.
p_{ue}	Navigation path from user landmark v_u to exit landmark v_e.
$d_T^p(\mathcal{T})$	Typical delay of p during time interval $\mathcal{T}$.
d_W^p	Worst-case delay of p.

Manuscript received 29 July 2022; revised 24 August 2022 and 14 September 2022; accepted 30 September 2022. Date of publication 10 October 2022; date of current version 29 December 2022. This work was supported in part by the National Natural Science Foundation of China (NSFC) under Grant 51979216 and in part by the Natural Science Foundation of Hubei Province, China, under Grant 2021CFA001. The associate editor coordinating the review of this article and approving it for publication was Dr. Masood Ur Rehman. *(Corresponding author: Mozi Chen.)*

Kezhong Liu is with the School of Navigation, the National Engineering Research Center for Water Transport Safety, and the Hubei Key Laboratory of Inland Shipping Technology, Wuhan University of Technology, Wuhan 430063, China (e-mail: kzliu@whut.edu.cn).

Yuting Ma, Mozi Chen, Kai Zheng, and Xuming Zeng are with the School of Navigation, Wuhan University of Technology, Wuhan 430063, China (e-mail: chenmz@whut.edu.cn).

Kehao Wang is with the School of Information Engineering, Wuhan University of Technology, Wuhan 430063, China.

Digital Object Identifier 10.1109/JSEN.2022.3211877

I. Introduction

EMERGENCY evacuation of a passenger ship becomes very important, especially considering the enormous loss of life in case of passenger ship disasters [1], [2]. Costa Concordia disaster left 32 passengers and crew dead and more than 4000 traumatized [3]. The sinking of the Al-Salam Boccaccio 98 ferry took the lives of more than 1000 people [4]. According to a safety technical investigation report submitted by the Italian Ministry of Infrastructure and Transport, inefficient emergency evacuation is considered one of the primary factors for such serious casualties [5]. Therefore, an efficient and safe ship evacuation strategy plays a critical role in protecting passengers' lives when ships encounter accidents. Ship evacuation is very complex because of the ship's complicated internal structure, the dynamic evacuation environment, and the limited ship survival time.

Most of the existing ship evacuation research focuses on developing simulation programs that can handle complex navigation scenarios, i.e., the influence of ship motion and human behaviors [6], [7], [8], [9]. However, the simulation-based approaches are high-priced and time-consuming, which has a negative performance impact on the time-critical ship evacuation service. In addition, the results from these approaches are only effective for the previously specified damage case. That is to say, they cannot provide appropriate navigation service for evacuees in a real-time manner, considering dynamic emergency scenarios.

Wireless sensor networks (WSNs), which can be widely deployed in the fields of interest, are capable of automatically exploring and interacting with the dynamic environment. Therefore, we can incorporate WSNs into emergency navigation systems to extensively monitor the ever-changing ship indoor environment and then provide real-time navigation service to users equipped with portable devices such as personal digital assistants (PDAs) and smartphones [10], [11], [12], [13], [14], [15], [16]. However, considering the complex 3-D model of ship internal structure, the dynamic ship inclination, and the deadline for ship sinking, most existing WSN-assisted emergency navigation approaches for land cannot be directly applied to ship evacuation.

According to presently valid regulations, passenger ships need sufficient hydrostatic stability to survive from certain damage cases (e.g., fire, collision, and grounding) [17], [18], [19]. However, the required damage stability does not, in all cases, guarantee the survival of a ship over an infinite period of time, especially if an accident takes place at unfavorable sea states or weather conditions. In such a case, the time available for ship evacuation is limited. That is, passengers and crew must escape from their current locations to a specified boarding point for lifeboats or Marine Evacuation Systems within a specified deadline. Otherwise, there is very little chance of surviving for them. However, to the best of our knowledge, the existing WSN-assisted navigation methods do not take the hard deadline into account, which can dramatically jeopardize users' chances of survival. Specifically, these approaches consider the impact of variations of hazards and aim to guide users to escape without oscillations while away from hazards, but they ignore navigation efficiency, leading to passengers' remaining in danger for a long period of time and thus missing the deadline for ship survival [14].

For general land-based buildings, the traversal speed of evacuees is only affected by their own properties (e.g., their age, gender, physical and psychological status) [20], [21] and the density of passageways which is related to the distribution and spatial-temporal movement of evacuees [22]. While on a passenger ship, there is a special feature for the movement speed of passengers distinguishing it from that in land-based buildings since the fact that evacuees escape on an unstable surface. That is, the walking speed on a passenger ship is not only influenced by the above-mentioned factors, but also severely influenced by the changing slope angles, which is unrelated to the passengers' personal attributes or their spatiotemporal movement [23], [24]. When the inclination angle varies over time, passengers tend to feel dizzy, and their gait alters as well, all of which results in a change in individual walking speed. We can evaluate the dynamic passengers' movement during evacuation using simulated data from the following organizations: the Korea Research Institute of Ship and Ocean Engineering, the Netherlands Organization for Applied Scientific Research (TNO), the Swiss Federal Institute of Technology, and the Monash University in Australia [25], [26]. However, the existing WSN-assisted navigation systems do not fully consider the dynamics of passenger walking speeds due to changing inclination states, which can result in the variation of transit time on the same passageway. They utilize the path length, which is considered to maintain invariable in time, to design different metrics of path planning (e.g., the shortest route, the minimum exposure route, and the oscillation-free route to navigate evacuees), and thus the paths may be time-consuming or impassable in practice [14], [27], [28], [29].

In addition, most of the existing WSN-based navigation approaches deal with only 2-D sensing fields and take no account of actual arrangement of navigation environment [30], [31]. These approaches explore physical obstacles in the environment and construct the route graph during runtime phase, which spends a significant amount of time due to the extremely complicated internal structure of a cruise ship, and thus cannot offer real-time navigation services for trapped users.

In this article, we propose WEND, an efficient WSN-assisted emergency navigation algorithm for dynamic hazardous ship indoor environments, which can, in real-time or near real-time, provide passengers with hazard-avoid navigation paths that achieve no more than $(1 + \epsilon)d_T^{p^*}(\mathcal{T})$[1] typical delay while simultaneously guaranteeing to respect the specified deadline even if the worst-case delay is encountered in traversing the path. To achieve this purpose, WEND first constructs the 3-D topological model of a real-world passenger ship and then deploys sensors based on the 3-D model to monitor dynamic hazards and serve as landmarks to guide passengers to a destination. Then, WEND analyzes the effect of dynamic ship inclination on delay and combines the impact of crowd density, flood water depth, as well as locations of segments and damages on a passenger ship

[1] ϵ is an approximation factor, $p^*(\mathcal{T})$ is the optimal path defined in Section III-B, $d_T^{p^*}(\mathcal{T})$ denotes the typical delay of path $p^*(\mathcal{T})$.

to determine the typical delay and the worst-case delay bound across each path accordingly. Based on the two delay parameters and the monitored hazard situation and movement, an adaptive emergency navigation strategy with low time complexity, motivated by a fully polynomial approximation scheme, namely, Hassin's Algorithm [32], [33], is proposed. We evaluate WEND by conducting extensive simulations. The results demonstrate that WEND improves the navigation success ratio by approximately 30% and 10% compared with the state-of-the-art navigation methods, namely the expected number of oscillations (ENO)-based oscillation-free method (OPEN) and the deadline-aware adaptive emergency navigation strategy (ANT), respectively.

The main contributions of our study are summarized as follows.

1) To the best of our knowledge, this is the first WSN-assisted navigation strategy taking 3-D topological structure of a real passenger ship into consideration. We utilize a Voronoi Diagram (VD)-based method to automatically tessellate complex rooms (i.e., rooms with more than one door in the ship), and construct a variable navigable network before the application of our path finding algorithm.
2) We synthetically consider the dynamics of both hazards and changing walking environments and construct a dynamic navigation model.
3) Given the serious threat of ship capsizing to passengers' survival, we design WEND, an efficient emergency navigation algorithm that can, in near real-time, find hazard-avoid paths with no more than $(1+\epsilon)d_T^{p^*}(\mathcal{T})$ total typical delay while guaranteeing to respect the deadline for ship capsizing under all circumstances.
4) We theoretically analyze the upper and lower bounds on the typical delay of the path provided by our approximate algorithm and evaluate WEND using extensive simulations. Experimental results demonstrate that WEND outperforms the state-of-the-art evacuation methods in terms of navigation efficiency and navigation success ratio.

The remainder of this article is organized as follows. Section II presents our motivation and preliminary. Section III presents the dynamic navigation model and problem formulation. The detail of the design of our method is introduced in Section IV. Section V presents theoretical analyses and proofs on several important issues. We evaluate the performance of our approach through extensive simulations in Section VI. Finally, Section VII concludes this work.

II. Motivation

In this section, we motivate our design by showing the three particular characteristics of ship evacuation, which are not considered in prior works.

A. Deadline-Aware Emergency Navigation

The main difference of emergency evacuation between ships and other scenarios is that there exist specific deadlines for the ship tasks, i.e., the ship sinks or is too banked to move. Our prior work, i.e., ANT for Ship Evacuation with WSNs, takes into account the two features of ship passenger evacuation and assumes a model that characterizes each passageway by a worst-case delay (i.e., a guaranteed upper bound on the delay) and a typical-case delay (i.e., an estimate of the delay that is typically encountered upon traveling a passageway) [34]. The performance objective considered in ANT is to identify the next node that minimizes the typical delay while respecting the deadline for ship capsizing and avoiding hazards under all circumstances. ANT can select different directions for different passengers based on their actual walking delay, which will be affected by dynamic ship motion. However, ANT does not consider the variation of the estimate of the typical delay of each segment. That is, the look-up tables in ANT are established only using the initial typical delays, and thus escaping along the provided guiding direction may not be optimal. If we only depend on the periodic recalculation of look-up tables, whose construction is extremely time-consuming, there will be a negative performance impact on the time-critical ship evacuation service. In addition, ANT deals with only 2-D sensing fields and takes no account of the actual arrangement of the navigation environment.

B. Effect of Dynamic Ship Inclination on Walking Time

Due to the ship's complex indoor environment, the physical distance may not represent the closeness between two landmarks corresponding to two sensor nodes. Therefore, in our design, we measure the closeness in terms of passenger walking time that, in some cases (see Fig. 1), is not proportional to the physical distance. As mentioned above, there is a deadline for ship evacuation by which passengers need to escape from their current locations to the specified boarding point. Otherwise, it denotes navigation failure for them. Therefore, except for the estimate of the delay typically encountered across a link between two nodes, each link is also characterized by an estimate of the upper bound on maximum delay on it, which is trustworthy at very high assurance levels. The calculation procedure of the two delay parameters is introduced in detail in Section IV-C.

When considering the effect of dynamic ship inclination, it becomes even more challenging to design navigation routes. Because of the inflow of water through any opening produced by damage (e.g., a collision), the mass, the center of gravity, and the moment of inertia of the ship will vary accordingly, which causes the changing slope angle and thus alters the typical delay on each link. Therefore, our algorithm needs to handle the scenario where typical delays are dynamic.

In addition, according to the investigation by TNO, the decrease in walking speed for dynamic motion conditions is less than for the static list [35]. For this reason, the effect of the ship pitching and rolling on walking time is not taken into account in this article. Specifically, typical delays on certain links are represented as a monotonically decreasing staircase function whose staircase height and width are determined by the specific evacuation scenario.

C. Effect of Complex 3-D Ship Indoor Environment

When facing the rapid increase in ship size and the more complicated topology of ship indoor environment, it becomes

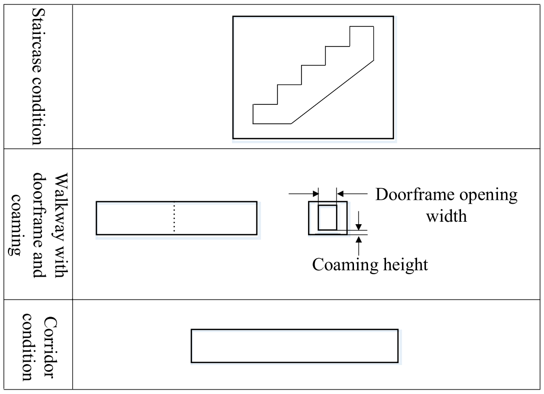

Fig. 1. Examples of walking condition on a passenger ship.

more challenging to provide real-time navigation suggestions to passengers. Large cruise and passenger ships, typically with 6 to 16 stories and having the capacity to accommodate thousands of passengers (e.g., Harmony of the Seas, a Royal Caribbean cruise ship, which can contain 6360 passengers), are packed with restaurants, entertainment venues, and accommodation categories [36]. Exploring the internal topological structure of such ships and then constructing a route graph during the run-time phase is extremely time-consuming and may cause heavy traffic overhead. Therefore, the provision of situational awareness in the preprocessing phase for emergency evacuation becomes particularly important. That is, we need to extract the 3-D topological model of a passenger ship before the run-time phase to find all feasible navigation routes containing corridors, staircases, and elevators.

In addition, due to the large-scale network configurations, exact navigation algorithms will be computationally expensive and time-consuming. Therefore, in this article, we need to design an efficient approximation scheme for ship emergency navigation.

III. Model and Problem Formulation

In this section, we first introduce the navigation model and then formulate the problem.

A. Model and Definitions

In this part, we provide an in-depth description of the navigation model, with notations presented in Nomenclature.

In order to provide real-time navigation service, a WSN is deployed in the navigation scenario according to the 3-D topological model of ship indoor environment, which is derived in the preprocessing phase. The WSN is modeled by a directed graph $\mathcal{G} = (\mathcal{V}, \mathcal{E})$, where $\mathcal{V}$ is the set of landmarks and $\mathcal{E}$ denotes the set of walking paths between two landmarks (called segments in our design). Each landmark v ($v \in \mathcal{V}$) corresponds to a sensor node. There are two types of landmark roles: hazardous landmark $\mathcal{V}_h$ and general landmark $\mathcal{V}_g$, which indicate a landmark inside or outside of hazardous regions. The hazardous region is modeled as a convex hull of the subset of hazardous landmarks. We assume that there are a finite number of hazardous regions threatening users' safety, and regarding the pattern of dynamics of hazard, we suppose that hazardous regions can only expand as time passes. Note

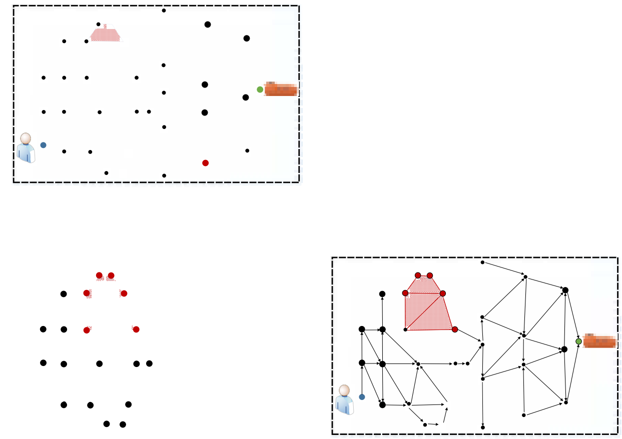

(c) (d)

Fig. 2. Scenarios of emergency navigation and corresponding navigation models. The black circles denote general landmarks, the red circles represent hazardous landmarks, the green circle indicates the exit landmark, and the blue landmark represents the user landmark (a) Scenario of emergency navigation at time t_1. (b) Model of emergency navigation at time t_1. (c) Scenario of emergency navigation at time t_2. (d) Model of emergency navigation at time t_2.

that the landmark's role may transform with the dynamics of hazards. The landmark that a user currently arrives at is defined as the user landmark ($v_u \in \mathcal{V}$), and the landmark closest to a muster station is considered as the exit landmark ($v_e \in \mathcal{V}$). Fig. 2 shows the scenarios of emergency navigation using a WSN at different times and corresponding navigation models. In our scenarios, there is an exit that users are required to lead to.

Each directed segment $\overrightarrow{v_i v_j}$ (i.e., the directed walking path between a landmark v_i and another landmark v_j) is characterized by two delay parameters: typical delay $d_T^{\overrightarrow{v_i v_j}}(t)$ ($d_T^{\overrightarrow{v_i v_j}}(t) > 0$) and worst-case delay $d_W^{\overrightarrow{v_i v_j}}$ [$d_W^{\overrightarrow{v_i v_j}} \geq d_T^{\overrightarrow{v_i v_j}}(t)$], which represent an estimate of the delay that is typically encountered, and a guaranteed upper bound on the maximum delay, across the segment $\overrightarrow{v_i v_j}$, respectively. Considering the effect of the continuously increasing heel angle of a damaged passenger ship on pedestrian movement during navigation process, the typical delay on each segment will vary dynamically. Each landmark v is presented as a three-tuple: $\langle \mathrm{ID}, \mathrm{LC}, \mathcal{D}_{\mathrm{h}}^{\mathrm{v}}(\mathrm{t}) \rangle$. ID is a unique landmark identifier, which is assigned when a sensor network is deployed, and LC denotes the location coordinate of a landmark, which is assumed to be available in our navigation scenario. $D_h^{\overrightarrow{v_i v_j}}(t)$ represents the shortest interval of time during which hazard expands from the initial location until encroaching on the neighbor segment $\overrightarrow{v_i v_j}$ of the landmark v_j. $\mathcal{D}_h^{v_j}(t)$ is defined as follows:

$$\mathcal{D}_h^{v_j}(t) \triangleq \left\{ D_h^{\overrightarrow{v_i v_j}}(t) \mid \overrightarrow{v_i v_j} \in \mathcal{E}_{v_j} \right\}.$$

$\mathcal{E}_{v_j}$ represents the set of the neighbor segments of the landmark v_j, which is defined as follows:

$$\mathcal{E}_{v_j} \triangleq \left\{ \overrightarrow{v_i v_j} \mid \overrightarrow{v_i v_j} \in \mathcal{E} \right\}.$$

The calculation procedure of $D_h^v(t)$ is introduced in detail in Section IV-C. For segment $\overrightarrow{v_i v_j}$ ($\overrightarrow{v_i v_j} \in \mathcal{E}_{v_j}$, $v_j \neq v_e$), if $D_h^{\overrightarrow{v_i v_j}}(t) \neq +\infty$, then hazard is approaching it. Otherwise, it means hazards do not influence the segment.

A navigation path p_{ue} consists of a landmark sequence, on which the user landmark v_u is the header and the exit landmark v_e is the rear

$$p_{ue}(\mathcal{T}) \triangleq \langle v_u, \ldots, v_i, v_j, \ldots, v_e \rangle$$

where $p_{ue}(\mathcal{T})$ denotes the landmark sequence which is dynamically updated according to the dynamics of typical delay and stored in every landmark between a user landmark and an exit landmark. $\mathcal{T}$ indicates the cumulative time which is the sum of Δt of the segments on $p_{ue}(\mathcal{T})$. The typical delay and the worst-case delay of a path $p(\mathcal{T})$ are defined as follows, respectively,

$$d_T^p(\mathcal{T}) \triangleq \sum_{\forall \overrightarrow{v_i v_j} \in p(\mathcal{T})} d_T^{\overrightarrow{v_i v_j}}(t)$$

and

$$d_W^p(\mathcal{T}) \triangleq \sum_{\forall \overrightarrow{v_i v_j} \in p(\mathcal{T})} d_W^{\overrightarrow{v_i v_j}}.$$

B. Problem Formulation

The objective of our emergency navigation strategy is to plan a path $p^*(\mathcal{T})$ apart from hazardous regions, through which a user can arrive at the exit landmark within a specified deadline under all circumstances, while experiencing the minimum typical delay from initial user landmark to exit landmark. Below, we formulate the properties we desire in our navigation strategy.

1) *Path Safety Guaranteed:* Let $\mathcal{P}_{je}$ denote the set of paths from v_j to v_e and $\mathcal{V}_i^s$ be the set of safe neighbor landmarks of v_i. $\mathcal{V}_i^s$ is defined as follows: if $\exists\, p_{je} \in \mathcal{P}_{je}$, $\forall v_n \in p_{je}$ $(v_n \neq v_j)$ satisfies

$$d_W^{\overrightarrow{v_i v_j}} + d_W^{p_{jn}} \leq D_h^{\overrightarrow{v_m v_n}}(t), \quad v_m \in p_{je} \wedge \overrightarrow{v_m v_n} \in \mathcal{E}_{v_n} \quad (1)$$

then v_j is regarded as a safe neighbor landmark of v_i, and all safe neighbors of v_i form the set $\mathcal{V}_i^s$. Let $\mathcal{P}_{ie}^s$ be the set of safe paths from v_i to v_e. We have the following expression for $\mathcal{P}_{ie}^s$: with respect to a path p_{ie}, if and only if for each landmark v_i that lies on p_{ie}, $v_j \in \mathcal{V}_i^s$, then p_{ie} is considered as a safe path from v_i to v_e, where $v_j \in p_{ie}$ and $\overrightarrow{v_i v_j} \in \mathcal{E}_{v_j}$, and all safe paths from v_i to v_e form the set $\mathcal{P}_{ie}^s$.

2) *Path Efficiency Guaranteed:* Let $d_T^{*p_{ie}}(t_i)$ be the minimum typical delay that can be achieved from v_i to v_e while simultaneously guaranteeing the avoidance of both dynamic hazards and exceeding a hard deadline with regard to time t_i (timestamp of arriving at the landmark v_i). $d_T^{*p_{ie}}(t_i)$ is defined as follows:

$$d_T^{*p_{ie}}(t_i) \triangleq \min\left\{ d_T^{\overrightarrow{v_i v_j}}(t) + d_T^{*p_{je}}(t_j) \right\}$$

where $v_j \in \mathcal{V}_i^s$. That is, $d_T^{*p_{ie}}(t_i)$ is the minimum value of the typical delay from v_i to v_j **plus** the minimum typical delay that can be achieved from v_j to v_e while guaranteeing the avoidance of both dynamic hazards and exceeding a hard deadline with regard to time t_j.

Then, we define π_i as the optimal neighboring landmark of v_i which determines the value of $d_T^{*p_{ie}}(t)$ $(\overrightarrow{v_i \pi_i} \in \mathcal{E})$, and thus the safe path $p_{ue} \in \mathcal{P}_{ue}^s$ can be called the optimal path $p^*(\mathcal{T})$, if and only if for each landmark v_i that lies on p_{ue}, $v_j = \pi_i$.

3) *Algorithm Efficiency Guaranteed:* An emergency navigation scheme demands a time-critical response with respect to the provision of guidance. The extensive time cost required to run the navigation strategy has a negative impact on ship evacuation service and thus is undesired.

IV. WEND Design

In this section, we propose an efficient approximation scheme, WEND, for emergency navigation in ship indoor environments, which fulfills all the goals in Section III-B. We first present an overview of WEND. The second part introduces the 3-D navigation network construction of a passenger ship. The third part describes the calculation procedure of the parameters of our dynamic navigation model. Finally, we present the process of path generation and navigation, followed by an example of our navigation scheme.

A. Design Overview

Fig. 3 shows an architecture overview of the proposed navigation scheme. There are two modules in our scheme: parameter predictor and routing predictor. These modules are integrated on a path planning server, supporting a navigation workflow consisting of several phases, namely initialization, parameter estimation, and path generation.

We considering the following: a trapped passenger equipped with a portable device is navigated toward a muster station on a ship. The portable device uses a radio frequency (RF) module to access the WSN deployed in advance. First, the parameter predictor evaluates the typical delay $d_T^v(t)$ and worst-case delay $d_W^{\overrightarrow{v_i v_j}}$ on segments, and $\mathcal{D}_h^v(t)$, the set of the shortest interval of time during which hazards encroach on segments. Based on the dynamics of both emergency and ship inclination, $d_T^{\overrightarrow{v_i v_j}}(t)$ and $\mathcal{D}_h^v(t)$ can be updated in a real-time pattern. Second, the routing predictor is triggered to calculate the path $p^*(\mathcal{T})$ for each user according to our proposed path planning algorithm. The trapped user can avoid hazardous regions and reach the exit within a specified deadline under all circumstances while experiencing a no more than $(1+\epsilon)d_T^{p^*}(\mathcal{T})$ typical delay from the initial user landmark to exit landmark in accordance with the indicators on the device.

B. 3-D Navigation Network Construction

In this part, we present the detail of generating a navigation network in a 3-D ship indoor environment, which is the first step of WEND. This network includes only connection available for pedestrian movement within a ship. That is to say, adjacent floors are connected only by vertical connection representing staircases, and spatial relationships between

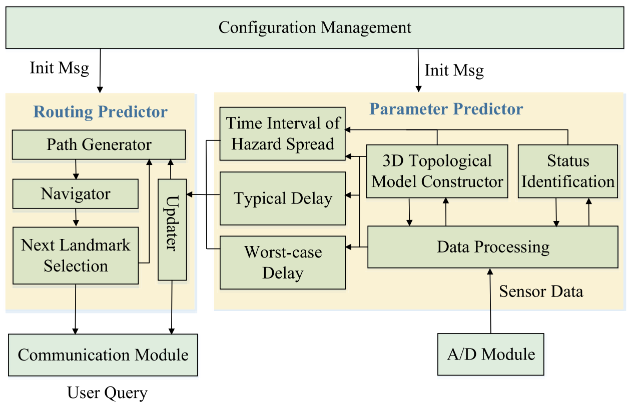

Fig. 3. Overview of our navigation architecture.

adjacent rooms sharing a wall with a door are reflected in the network.

If the navigation network in simple models, e.g., when it consists of "cubical" rooms with one door or two doors located on opposite walls, is generated based on the Poincaré duality [37]. In the network, a room is represented by a dual node (corresponding to a landmark), a wall with a door is a dual edge (corresponding to a segment) bounded by dual nodes representing adjacent rooms.

However, the above network cannot be effectively used for navigation routes when rooms have a complex shape and many doors. A method of navigation network construction in complex rooms, based on the VD, is presented in Algorithm 1.

Algorithm 1 Navigation Network Construction Algorithm

Input: Floor polygon f, $\mathrm{TL}_{\mathrm{max}}$, T_1;
Output: Tessellation f;
$\mathcal{R}_1 = f$;
$TL = 1$;
while $TL \leq \mathrm{TL}_{max}$ **do**
  for *each element* N_j *in* $\mathcal{N}$ **do**
    for *each element* R_k *in* $\mathcal{M}$ **do**
      Calculate a bisector line bl of $\overline{N_j N_k}$;
      Calculate the set $\mathcal{I}$ of the intersection points of bl with R_k;
      if $|\mathcal{I}| \geq 2$ **then**
        Create edge (j, k) and insert it into the existing tessellation of the polygon f;
        Add the cell including N_j to $\mathcal{R}$;
        Add the cells adjacent to the edges intersected by (j, k) to $\mathcal{M}$;
      end
    end
    Remove edges from inside the boundary of the newly created cell for N_j.
  end
  for *each edge* e *in the tessellation of* f **do**
    if $|e| \geq \mathrm{T}_1$, or e *is bounded by two constraint nucleation points,* or *end-points of* e *lie on noncollinear constraint edges* **then**
      Calculate the bisector point bp for e and add bp into $\mathcal{N}$;
    end
  end
  $TL = TL{+}1$;
end

$\mathrm{TL}_{\mathrm{max}}$ and TL denote the maximum tessellation level and the current tessellation level, respectively, T_1 is the threshold value for edge length; $\mathcal{N}$ represents the set of constraint nucleation points for f, which are projections of door nodes, concave corner nodes, and staircase nodes of f; $\mathcal{R}$ denotes the set of VD cells; $\mathcal{M}$ is the set of cells for testing, in which each cell is added from $\mathcal{R}$ and includes node N_j; edge (j, k) is bounded by the intersection points in $\mathcal{I}$, which divides R_k into two cells such that each cell includes one of the nodes N_j and N_k; e denotes the edge connecting nucleation points of adjacent cells in $\mathcal{R}$; constraint edges are the original polygon edges of f.

Fig. 4 illustrates a close-up of a single level, the second floor, on a real-word passenger ship,"Yangtze Gold 7." Feasible routes for passengers, generated after the first iteration of tessellation and the second iteration of tessellation, are represented in Fig. 4(b) and (c), respectively.

C. Navigation Model Parameter Estimation

1) Estimation of Worst-Case Delay and Typical Delay: Table I shows the walking speeds of an evacuee when the distance from the front evacuee is more than 0.5 m, which are regulated by MSC/Circ.1238 [38]. According to the speed data, we assume that the initial typical speed across each segment is 1.0, 0.8, or 1.2 m/s, depending on which type of facility the segment is located in. One segment includes only one type of facility. Considering the effect of the continuously increasing heel angle of a damaged ship on pedestrian movement, passengers' typical speed will dynamically updated. Based on [39], it is found that passengers' age and gender have a trivial impact on their speed at sea. Therefore, in this article, we only utilize the current slope angle of a passenger ship and the average individual walking speed to determine the dynamic typical speed. Combining this speed and segment length gives rise to the typical delay of each segment.

Considering the influence of watertight bulkheads on liquid flow in ship compartments, two different procedures are used to estimate worst-case speed across different segments: For segments which are not affected by flooding water due to watertight bulkheads, the worst-case speed across them can be calculated as follows:

$$S_W = \begin{cases} 0.55 \times R_1^{30^\circ}, & \text{Stairs (down)} \\ 0.44 \times R_1^{30^\circ}, & \text{Stairs (up)} \\ 0.67 \times R_1^{30^\circ}, & \text{Corridors} \\ 1.2 \times R_1^{30^\circ}, & \text{Open space} \end{cases} \tag{2}$$

where $R_1^{30^\circ}$ denotes the reduction factor of walking speed at heel angle 30°; for segments affected by flooding water, the worst-case speed is as followed:

$$S_W = \begin{cases} 0.55 \times R_1^{30^\circ} \times R_2^{0.8}, & \text{Stairs (down)} \\ 0.44 \times R_1^{30^\circ} \times R_2^{0.8}, & \text{Stairs (up)} \\ 0.67 \times R_1^{30^\circ} \times R_2^{0.8}, & \text{Corridors} \\ 1.2 \times R_1^{30^\circ} \times R_2^{0.8}, & \text{Open space} \end{cases} \tag{3}$$

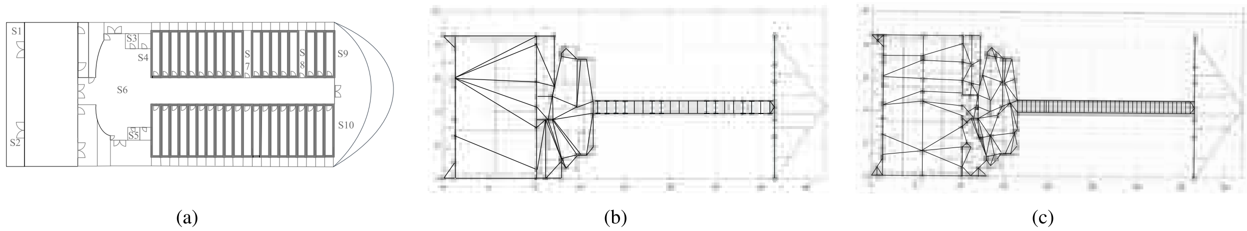

Fig. 4. Navigation network of the second floor of a passenger ship. (a) Close-up of the second floor of a passenger ship. (b) Navigation network generated after the first iteration of tessellation. (c) Navigation network generated after the second iteration of tessellation.

TABLE I
VALUES OF SPECIFIC FLOW AND SPEED

Facility Type	Flow (p/(ms))	speed of persons (m/s)
Stairs (down)	0	1.0
	0.54	1.0
	1.1	0.55
Stairs (up)	0	0.8
	0.43	0.8
	0.88	0.44
Corridors	0	1.2
	0.65	1.2
	1.3	0.67

where we take the effect of flooding water on pedestrian movement into account, $R_2^{0.8}$ represents the speed reduction factor at water depth 0.8 m [40].

2) Estimation of $\mathcal{D}_h^{v}(t)$: The default landmark role is general landmark. In the initialization phase, each element in $\mathcal{D}_h^{v}(t_0)$ is set as follows:

$$D_h^{\overrightarrow{v_iv_j}}(t_0) = \begin{cases} +\infty, & \text{if } v_j \neq v_e \\ T_c(t_0), & \text{if } v_j == v_e \end{cases} \tag{4}$$

where $T_c(t_0)$ denotes the remaining ship survival time at time t_0. The interval of time from hazardous landmarks to segments may be captured in a real-time pattern using the periodic probes. A landmark v_j receiving a probe from a hazardous landmark determines whether to update the value in $\mathcal{D}_h^{v_j}(t)$ based on [34, Algorithm 1].

D. Path Generation Algorithm

This section describes our proposed ϵ-approximation algorithm for emergency navigation in ship indoor environments. We first briefly describe two basic techniques termed *rounding and scaling* and *relaxing* used in the algorithm.

1) Rounding and Scaling: To approximate p^* in polynomial time, we perform the *rounding and scaling* operation as shown in Algorithm 2. The complexity of Algorithm 2 is $O(|\mathcal{E}|(U/L)(n/\epsilon))$, where U and L denote the upper and lower bounds for the optimal solution, respectively, n is the number of landmarks, and ϵ $(0 < \epsilon < 1)$ is an approximation factor.

$g_j(d_T)$ denotes the minimum worst-case delay of a $u - j$ path whose typical time is at most d_T.

Algorithm 2 Rounding and Scaling Algorithm

Input: $\mathcal{G}=(\mathcal{V},\mathcal{E})$, $\{d_W^{\overrightarrow{v_iv_j}}, d_T^{\overrightarrow{v_iv_j}}\}_{\overrightarrow{v_iv_j}\in\mathcal{E}}$, $T_c(t)$, L, U, ϵ;

Output: $\hat{p^*}$ and $\widehat{d_T^{\hat{p^*}}}$;

for *each* $\overrightarrow{v_iv_j} \in \mathcal{E}$ **do**
  $\widehat{d_T^{\overrightarrow{v_iv_j}}} = \lfloor \frac{d_T^{\overrightarrow{v_iv_j}}(n-1}{)} L\epsilon \rfloor+1$
end
$\hat{U} = \lfloor \frac{U(n-1}{)} L\epsilon \rfloor$+n;
for $j \neq u$ **do**
  $g_j(0) = +\infty$
end
for $\widehat{d_T} = 0, 1, 2, \ldots, \hat{U}$ **do**
  $g_u(\widehat{d_T}) = 0$;
end
for $\widehat{d_T} = 1, 2, 3, \ldots, \hat{U}$ **do**
  while $j \neq u$ **do**
    relaxing $g_j(\widehat{d_T})$
  end
  if $g_e(\widehat{d_T}) \leq T_c(t)$ **then**
    $\widehat{d_T^{\hat{p^*}}} = \widehat{d_T}$;
    return $\widehat{d_T^{\hat{p^*}}}$ and $\hat{p^*}$;
    break;
  end
end

2) Relaxing: The *relaxing* operation is as follows:

$$g_j(d_T) = \min\left\{ g_j(d_T - 1), \min_{k|d_T^{\overrightarrow{v_kv_j}} \leq d_T} \left\{ g_k\left(d_T - d_T^{\overrightarrow{v_kv_j}}\right) + d_W^{\overrightarrow{v_kv_j}} \right\} \right\}. \tag{5}$$

In the following, we present the overall structure of our approximation algorithm.

3) Top-Level Algorithm: In reality, hazardous regions and typical delay may vary in time as mentioned in Sections II-B and III-A. The effects of such dynamics on Algorithm 2 mainly reflect in two aspects. First, the path provided by Algorithm 2 may not be optimal any more due to the change of typical delay. Second, the path may be blocked because the encroachment of hazards upon segments, which inevitably results in user oscillations and thus keeps the user remaining in danger for a longer period of time and finally misses the hard deadline for ship evacuation. In order to compensate for these impacts, we design Algorithm 3 which informs each passenger about a hazard-avoid oscillation-free route to reach the exit landmark within a given deadline under all circumstances, while guaranteeing to get the passenger to experience a no more than $(1+\epsilon)d_T^{p^*}(\mathcal{T})$ typical delay. In the following, we present the details of each step of Algorithm 3.

1) Line 2, in the variable $\widehat{p^*(t)}$, computes a $T_c(t)$-path from v_u to v_e with a no more than $(1+\epsilon)d_T^{p^*}(\mathcal{T})$ typical delay.
2) In Line 3, a variable $test1$ is set equal to FALSE, thereby indicating that there are not segments in the path $\widehat{p^*(t)}$, which a user cannot cross before hazards encroach on them.
3) Line 4 constructs a set $\mathcal{E}_{\text{test}}$ to subsume segments that a user cannot cross before hazards damage them along the planned path.
4) For loop of Lines 5–10 check each segment already in path $\widehat{p^*(t)}$ to determine whether it should be subsumed into $\mathcal{E}_{\text{test}}$. In Line 7, $\widehat{p^*_{uj}(t)}$ represents a connected sequence of segments from v_u to v_j, which are components of $\widehat{p^*(t)}$.
5) Lines 11–14 remove the segments in set $\mathcal{E}_{\text{test}}$ from $\mathcal{E}$ in order to reconstruct the navigation network connectivity and call Algorithm 2 based on the current $\mathcal{G}=(\mathcal{V},\mathcal{E})$ to get path $\widehat{p^*(t)}$ and select the neighbor landmark $\hat{\pi_u}$ on path $\widehat{p^*(t)}$ as the user's next landmark. During the next iteration, $\hat{\pi_u}$ is set as the new user landmark as shown in Line 15.
6) Line 16 checks whether the typical delay has changed. According to the result, Lines 17–21 perform in the following manner.
   a) If there is a change in typical delay then we recalculate the path $\widehat{p^*(t_{\text{new}})}$ from the current user landmark to exit landmark according to the changed typical delay, where t_{new} is the timestamp of arriving at the current landmark.
   b) If the typical delay has not changed then the user moves to the neighbor landmark of the current user landmark on the path $\widehat{p^*(t_{N-1})}$, where t_{N-1} is the timestamp of departing from the previous landmark.

Algorithm 3 Top-Level Algorithm

```
  Input: G=(V, E);
  Output: p*(T);
1 while v_u ≠ v_e do
2   Call procedure Rounding and Scaling Algorithm;
3   test1 = FALSE;
4   E_test={};
5   for each segment v_i v_j ∈ p*(t) do
6     if d_W^{p*_uj(t)} > D_h^{v_i v_j}(t) then
7       test1 = TRUE;
8       insert v_i v_j into E_test
9     end
10  end
11  if E_test ≠ {} then
12    Set E=E \ E_test;
13    Go to Line 2;
14  end
15  v_u=π_u;
16  if there is a change in typical delay then
17    Go to Line 2;
18  else
19    v_u=π_u;
20    Go to Line 16;
21  end
22 end
```

E. Example of WEND

Let us now consider the path generation of the example graph of Fig. 5(a) by the algorithm of Section IV-D. The blue circle represents the user landmark, the black circles denote general landmarks, the red circle represents the hazardous landmark, and the green circle indicates the exit landmark. Each segment is characterized by two delay parameters: the typical delay $d_T^{\overrightarrow{v_iv_j}}(t)$ (see the blue numbers), and the worst-case delay $d_W^{\overrightarrow{v_iv_j}}$ (see the red numbers). The red arrow indicates the moving direction of the emergency site. Suppose that v_1 becomes a hazardous landmark at time $t=30$. In addition, it is assumed that $T_c(t_0)$ and ϵ, respectively, equal 80 and 0.25.

1) Compute Upper and Lower Bounds of the Optimal Path: According to Algorithm 4, the upper bound of the optimal path $p^*(\mathcal{T})$ is set to $5+5+14+5+14+12.5+5=60.5$. As shown in Fig. 5(b), $\mathcal{G}^7=(\mathcal{V},\mathcal{E}^7(t_0))$ has a 80-path p^7 and all segments in p^7 belong to $\mathcal{E}_s^{nh}(p^7)$, and in $\mathcal{G}^6$ [see Fig. 5(c)] all paths from v_u to v_e have worst-case delays larger than 80. Then the lower bound equals $d_T^7(t_0)=10$.

2) Call Procedure Rounding and Scaling Algorithm: Upon calling the procedure Rounding and Scaling Algorithm, $\widehat{p^*(t_0)}=\langle v_u(v_0), v_8, v_7, v_6, v_5, v_9, v_e\rangle$, an 80-path from v_u to v_e with a no more than $(1+0.25)d_T^{p^*}(t_0)$ typical delay, is obtained as shown in Fig. 5(d).

3) Check Segments of Path $\widehat{p^*(t_0)}$: According to the moving direction and speed of the emergency site, we check all segments of path $\widehat{p^*(t_0)}$ and obtain the set $\mathcal{E}_{\text{test}}=\{\}$. That is, all segments in $\widehat{p^*(t_0)}$ belong to safe segments for $\widehat{p^*(t_0)}$.

4) User Navigation Guidance and Path Replanning: We set v_8 as the next landmark. Suppose that it takes 20 to arrive at v_8. That is, the duration remaining between the current instant and the instant by which the user must reach the exit is 60. Upon reaching v_8, we assume that it checks there are changes in typical delays as shown in Fig. 5(e). Invoke the procedure Rounding and Scaling again. An updated optimal path $\widehat{p^*(t=20)}=\langle v_u(v_8), v_7, v_{10}, v_9, v_e\rangle$ is calculated, and thus v_7 is set as the next landmark. The process of user navigation guidance and path replanning is repeated until the user is guided to the exit. In this example, there are no variations in typical delays when the user gets to v_7, v_{10}, and v_9. Therefore, $\widehat{p^*(\mathcal{T})}=\langle v_0, v_8, v_7, v_{10}, v_9, v_e\rangle$.

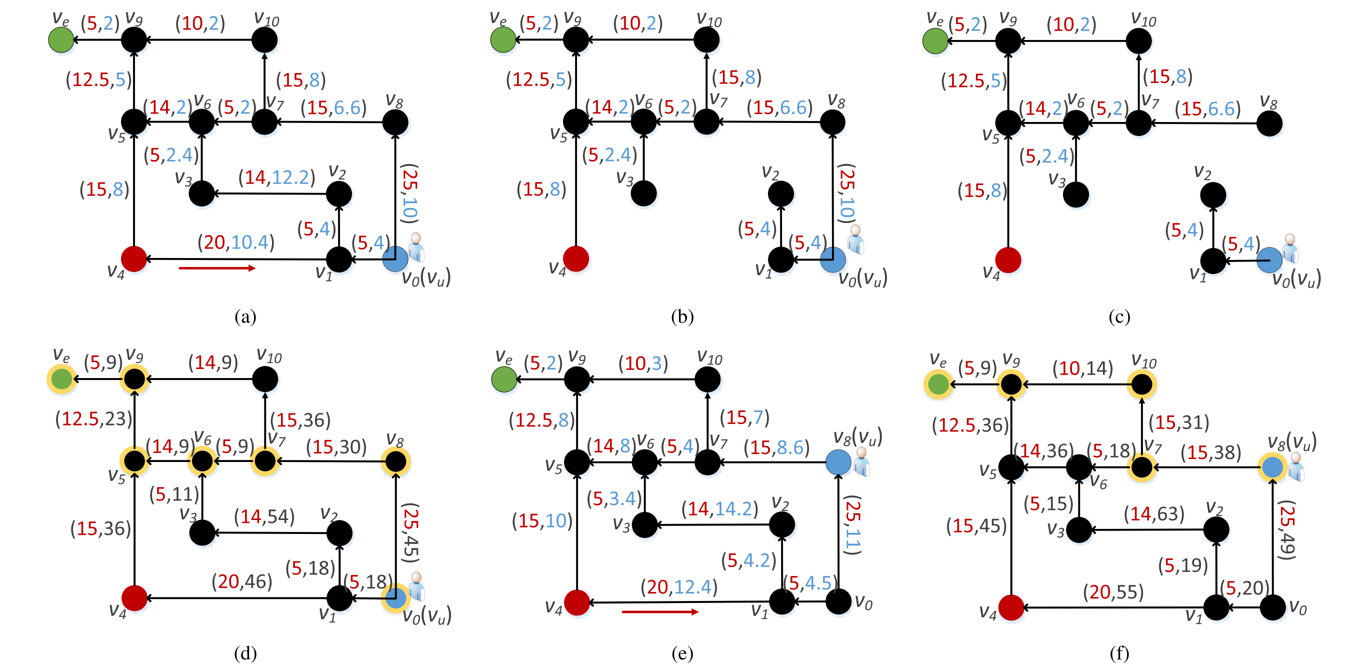

Fig. 5. Example graph. (a) Navigation model at the initial time t_0, $\mathcal{G} = (\mathcal{V}, \mathcal{E}(t_0))$. A user is located at the landmark v_0. (b) Graph $\mathcal{G}^7 = (\mathcal{V}, \mathcal{E}^7(t_0))$. (c) Graph $\mathcal{G}^6 = (\mathcal{V}, \mathcal{E}^6(t_0))$. (d) Graph after rounding and scaling each segment $\overrightarrow{v_iv_j}$ in $\mathcal{G} = (\mathcal{V}, \mathcal{E}(t_0))$, $\widehat{p^*(t_0)} = \langle v_u, v_8, v_7, v_6, v_5, v_9, v_e \rangle$. (e) Navigation model at time $t = 20$, $\mathcal{G} = (\mathcal{V}, \mathcal{E}(t = 20))$. The user moves to the landmark v_8. (f) Graph after rounding and scaling each segment $\overrightarrow{v_iv_j}$ in $\mathcal{G} = (\mathcal{V}, \mathcal{E}(t = 20))$, $\widehat{p^*(t = 20)} = \langle v_u, v_7, v_{10}, v_9, v_e \rangle$.

V. Analysis and Discussion

In this section, we compute an upper bound and a lower bound on the optimal route defined in Section III-B, and then calculate the error bound of our proposed approximate solution. Finally, the analysis of the impact of the correlation of typical delay and worst-case delay is presented.

A. Upper/Lower Bounds on Our Defined Optimal Path

Here, we present how to calculate the high-quality upper and lower bounds of the optimal path $p^*(\mathcal{T})$.

1) Upper Bound of $p^*(\mathcal{T})$: First, we calculate a route p^U with the minimum worst-case delay based on the navigation graph model without hazardous regions inserted. The minimum worst-case delay is an upper bound of the path $p^*(\mathcal{T})$. Then, we gradually insert hazardous regions one by one to update the upper bound, so that it can bound $p^*(\mathcal{T})$ more accurately. Algorithm 4 shows the pseudo code of the estimation of the upper bound of $p^*(\mathcal{T})$. $\mathcal{R}_h$ denotes the set of hazardous regions, n_h is the total number of hazardous regions, $\mathcal{G}_s^i = (\mathcal{V}, \mathcal{E}_s^i(p^U))$, $\mathcal{E}_s^i(p^U)$ denotes the safe segments for p^U after the i'th hazardous region is inserted. A segment $\overrightarrow{v_iv_j}$ can be regarded as a safe segment for p^U if and only if $d_W^{p_{uj}} \le D_h^{\overrightarrow{v_iv_j}}(t_0)$, $p_{uj} \in p^U$.

2) Lower Bound of $p^*(\mathcal{T})$: First, we start by ordering the distinct values $d_T^{\overrightarrow{v_iv_j}}(t_0)$. Let $d_T^1(t_0) < d_T^2(t_0) < \cdots < d_T^l(t_0)$ be all the distinct typical delay values of the segments. Clearly $l \le |\mathcal{E}| = m$. Define $\mathcal{E}^i(t_0)$ to be the set of segments with typical delay not greater than $d_T^i(t_0)$. That is, for $1 \le i \le l$,

Algorithm 4 Calculating Upper Bound of $p^*(\mathcal{T})$ Algorithm

Input: $\mathcal{G}$=($\mathcal{V}$, $\mathcal{E}$), $\mathcal{R}_h$;
Output: U;
Calculate U (corresponding to the minimum worst-case delay from initial user landmark to exit landmark) based on $\mathcal{G}_s^0$;
for $i \leftarrow 1$ to n_h **do**
  for *each segment* $\overrightarrow{v_iv_j} \in p^U$ **do**
    if $\overrightarrow{v_iv_j} \notin \mathcal{E}_s^i(p^U)$ **then**
      Update the path p^U based on $\mathcal{G}_s^i$;
      break;
    end
  end
end

$\mathcal{E}^i(t_0)$ is defined as follows:

$$\mathcal{E}^i(t_0) \triangleq \left\{ \overrightarrow{v_iv_j} \in \mathcal{E} \mid d_T^{\overrightarrow{v_iv_j}}(t_0) \le d_T^i(t_0) \right\}.$$

Let $\mathcal{G}^i = (\mathcal{V}, \mathcal{E}^i(t_0))$, then $\mathcal{G}^l = \mathcal{G}$. Moreover, since $\mathcal{G}^l$ must have a $T_c(t_0)$-path p^l and all segments in p^l belong to $\mathcal{E}_s^{n_h}(p^l)$, (otherwise the instance has no solution) there must exist a unique index j ($1 \le j \le l$) such that $\mathcal{G}^j$ has a $T_c(t_0)$-path p^j and all segments in p^j belong to $\mathcal{E}_s^{n_h}(p)$, and in $\mathcal{G}^{j-1}$ all paths $\mathcal{P}^{j-1}$ from initial landmark to exit landmark [for $\forall p^{j-1} \in \mathcal{P}^{j-1}, \forall \overrightarrow{v_iv_j} \in \mathcal{E}_s^{n_h}(p^{j-1})$] have worst-case delay larger than $T_c(t_0)$. Then

$$L = d_T^j(t_0) \le d_T^{p^*(\mathcal{T})}.$$

B. Error Bound of Our Proposed Approximate Solution

Here, we have discussion on the error bound caused by our approximate algorithm. First, we estimate the error bound when the typical delay is static, then based on the results in Lemma 1, we give the error bound when typical delay varies with time.

Lemma 1: For the situation where the typical delay is static: If $U \geq d_T^{p^*}$ then Algorithm 2 returns a feasible path, $\hat{p}^*$, that satisfies $d_T^{p^*} \leq d_T^{\hat{p}^*} \leq d_T^{p^*} + L\epsilon$.

Proof: By definition, $d_T^{p^*} \leq d_T^{\hat{p}^*}$. For each segment $\overrightarrow{v_i v_j} \in p^*$, $\widehat{d_T^{\overrightarrow{v_i v_j}}} \leq (d_T^{\overrightarrow{v_i v_j}}(n-1/))L\epsilon + 1$. Thus

$$\widehat{d_T^{p^*}} \triangleq \sum_{\overrightarrow{v_i v_j}\in p^*} \widehat{d_T^{\overrightarrow{v_i v_j}}} \leq \frac{(n-1)}{L\epsilon} \sum_{\overrightarrow{v_i v_j}\in p^*} d_T^{\overrightarrow{v_i v_j}} + n - 1$$
$$\leq \frac{(n-1)\,U}{L\epsilon} + n - 1 \leq \hat{U}. \tag{6}$$

Each segment $\overrightarrow{v_i v_j} \in p$ satisfies

$$\frac{d_T^{\overrightarrow{v_i v_j}}(n-1)}{L\epsilon} \leq \widehat{d_T^{\overrightarrow{v_i v_j}}} \leq \frac{d_T^{\overrightarrow{v_i v_j}}(n-1)}{L\epsilon} + 1. \tag{7}$$

Thus

$$d_T^p \triangleq \sum_{\overrightarrow{v_i v_j}\in p} d_T^{\overrightarrow{v_i v_j}} \leq \frac{L\epsilon}{n-1} \sum_{\overrightarrow{v_i v_j}\in p} \widehat{d_T^{\overrightarrow{v_i v_j}}} \triangleq \frac{L\epsilon}{n-1}\widehat{d_T^p}$$
$$\leq \sum_{\overrightarrow{v_i v_j}\in p} d_T^{\overrightarrow{v_i v_j}} + L\epsilon \triangleq d_T^p + L\epsilon. \tag{8}$$

According to (6) and (8)

$$d_T^{\hat{p}^*} \leq \frac{L\epsilon}{n-1}\widehat{d_T^{\hat{p}^*}} \leq \frac{L\epsilon}{n-1}\widehat{d_T^{p^*}} \leq d_T^{p^*} + L\epsilon. \tag{9}$$

Lemma 2: For the situation where the typical delay is dynamic: If $U \geq d_T^{p^*}(\mathcal{T})$ then Algorithm 3 returns a feasible path, $\widehat{p^*(\mathcal{T})}$, that satisfies $d_T^{p^*}(\mathcal{T}) \leq d_T^{\hat{p}^*}(\mathcal{T}) \leq d_T^{p^*}(\mathcal{T}) + L\epsilon$.

Proof: By definition, $d_T^{p^*}(\mathcal{T}) \leq d_T^{\hat{p}^*}(\mathcal{T})$. We assume that a user traverses m_1 segments after the first change on typical delay. According to (7)

$$\sum_{\overrightarrow{v_i v_j}\in p_{un_1}} d_T^{\overrightarrow{v_i v_j}} \leq \frac{L\epsilon}{n-1} \sum_{\overrightarrow{v_i v_j}\in p_{un_1}} \widehat{d_T^{\overrightarrow{v_i v_j}}}$$
$$\leq \sum_{\overrightarrow{v_i v_j}\in p_{un_1}} d_T^{\overrightarrow{v_i v_j}} + \frac{m_1 L\epsilon}{n-1} \tag{10}$$

where p_{un_1} denotes the route from v_u to v_{n_1}, which consists of m_1 segments. n_i denotes the landmark at which a user arrives after traversing m_1 segments, and m_i is the number of segments that a user travels after the i'th change **minus** the number of the already-traversed segments after the (i-1)'th change. We assume that the typical delay changes N_c times until arriving at the exit landmark v_e. The overall delay of a path thus

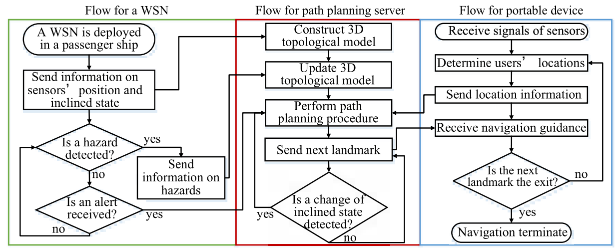

Fig. 6. Flow diagram of our navigation scheme.

$$d_T^p(\mathcal{T}) \triangleq \sum_{i=0,j=1}^{i=N_c-1,j=N_c} \sum_{\overrightarrow{v_i v_j}\in p_{n_i n_j}} d_T^{\overrightarrow{v_i v_j}}(\Delta t)$$
$$\leq \frac{L\epsilon}{n-1} \sum_{i=0,j=1}^{i=N_c-1,j=N_c} \sum_{\overrightarrow{v_i v_j}\in p_{n_i n_j}} \widehat{d_T^{\overrightarrow{v_i v_j}}}(\Delta t)$$
$$\triangleq \frac{L\epsilon}{n-1}\widehat{d_T^p}(\mathcal{T}) \leq \sum_{i=0,j=1}^{i=N_c-1,j=N_c} \sum_{\overrightarrow{v_i v_j}\in p_{n_i n_j}} d_T^{\overrightarrow{v_i v_j}}(\Delta t)$$
$$+ \frac{\left(m_1 + \cdots + m_{N_c}\right) L\epsilon}{n-1} \leq d_T^p(\mathcal{T}) + L\epsilon \tag{11}$$

where n_0 and n_{N_c} denote the user landmark v_u and the exit landmark v_e, respectively. According to (6)

$$\widehat{d_T^{p^*}} \triangleq \sum_{i=0,j=1}^{i=N_c-1,j=N_c} \sum_{\overrightarrow{v_i v_j}\in p^*_{n_i n_j}} \widehat{d_T^{\overrightarrow{v_i v_j}}}$$
$$\leq \frac{(n-1)}{L\epsilon} \sum_{i=0,j=1}^{i=N_c-1,j=N_c} \sum_{\overrightarrow{v_i v_j}\in p^*_{n_i n_j}} d_T^{\overrightarrow{v_i v_j}}$$
$$+ m_1 + m_2 + \cdots + m_{N_c}$$
$$\leq \frac{(n-1)\,U}{L\epsilon} + n - 1 \leq \hat{U}. \tag{12}$$

According to (11) and (12)

$$d_T^{\hat{p}^*}(\mathcal{T}) \leq \frac{L\epsilon}{n-1}\widehat{d_T^{\hat{p}^*}}(\mathcal{T}) \leq \frac{L\epsilon}{n-1}\widehat{d_T^{p^*}}(\mathcal{T}) \leq d_T^{p^*}(\mathcal{T}) + L\epsilon. \tag{13}$$

C. Impact of the Correlation of Typical Delay and Worst-Case Delay

In this part, we analyze the impact of the correlation of typical delay and worst-case delay on our path planning algorithm. In our scenario, the correlation between typical delay and worst-case delay is neither perfect positive nor perfect negative, and thus the algorithm needs to build off the ideas of the restricted shortest path algorithm. However, if the correlation coefficient between the two delay parameters is $+z1.0$ or -1.0, various shortest path algorithm [41] may be applied to calculate the hazard-avoid $T_c(t)$-path with the minimum typical delay only utilizing the worst-case delay on each segment. Actually, in such a case the path with the minimum worst-case delay from the initial user landmark to exit landmark is the defined optimal solution.

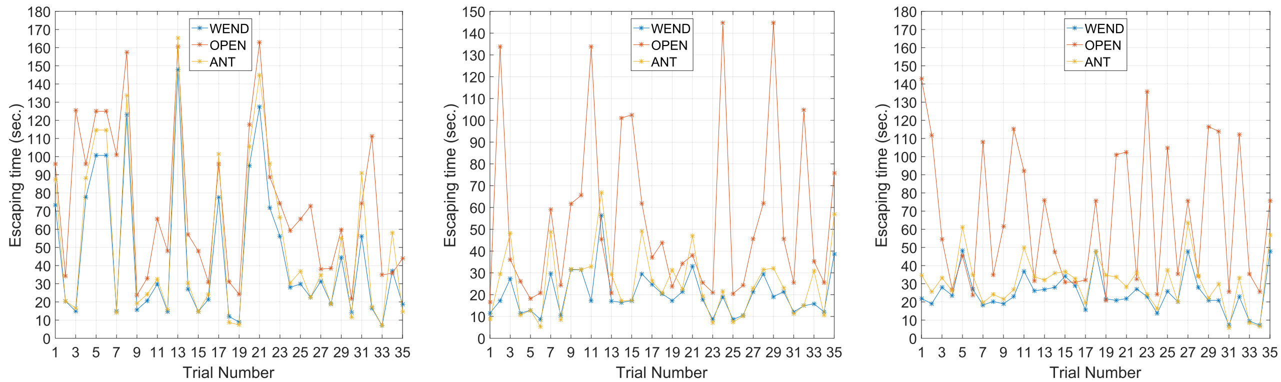

(a) (b) (c)

Fig. 7. Comparisons of average escape time for navigation scenario 1) under different values of ϵ. (a) $\epsilon = 1$. (b) $\epsilon = 0.5$. (c) $\epsilon = 0.25$.

VI. Performance Evaluation

We carry out extensive simulations to evaluate the performance of our approach. We compare this algorithm with the state-of-the-art navigation approaches, namely OPEN and ANT, from five perspectives, i.e., average escape time, navigation success ratio, average path length, minimum distance to hazards, and emergency response time.

A. Experimental Scenario and System Flowchart

Fig. 6 shows the flow diagram of the proposed navigation scheme. The current location of the passenger is detected using the received strength of wireless signals on his/her smartphone. The sensor with the strongest signal strength serves as the user node, and the user node information is transmitted to the path planning server. In addition, the location information on each sensor is also sent to the server and used to construct the 3-D topological model and predict the typical delay and worst-case delay on segments. In case of an emergency, the WSN forwards the information of hazards to the server, and the path generator is triggered to compute the route. The trapped user can be guided to the next landmark by complying with the indicator on the device. In addition, the guidance direction can be updated in a real-time pattern based on the dynamics of ship inclination.

To assess the performance of WEND on a damaged passenger ship, we conduct our proposed scheme in navigation scenarios that model the topological structure of a real-world cruise ship, namely the "Yangtze Gold 7" cruise. To examine the scalability, we vary the number of iterations of tessellation to generate navigation networks with different numbers of landmarks. We define two different navigation scenarios as shown in Fig. 4: 1) navigation network generated after the first iteration of tessellation (named SF) where 98 nodes are deployed [see Fig. 4(b)] and 2) navigation network generated after the second iteration of tessellation (named SS) where 196 nodes are deployed [see Fig. 4(c)]. "Yangtze Gold 7" passenger ship can carry 398 passengers. Therefore, the number of evacuated users ranges from 30 to 390 in our simulations. For each trial of the user count, we insert three hazardous regions into the network and allocate hazards' initial size and expansion (i.e., expanding direction and speed). Hazard is assumed to exhibit dynamics in only one pattern, i.e., expansion, in our simulation. During the simulations, the ratio of the size of each hazardous region to the total network size is maintained below 5%, the same with that assumed in [14]. The locations of emergency sites and users are randomly generated in the field for each round, and all users are required to arrive at the same exit. For each trial, we exploit the navigation scenario 1) unless explicitly stated otherwise.

Navigation model parameters including worst-case delay and initial typical delay on each segment are set using parameters of a real-world passenger ship, "Yangtze Gold 7" passenger ship. The hard deadline for ship evacuation and dynamics of typical delay are determined by the analysis of maritime accident investigation reports and case studies. In our simulations, the worst-case and initial typical moving speed of a user are set as 0.1088 m and 0.4143 m/s, respectively. We assume that the typical speed changes every 10 s and the deadline for evacuation is fixed at 100 s. The simulation results reported below are the average values after 20 runs.

We perform the simulation experiments written in MATLAB on a personal computer (Operating System: Windows 10 Education) equipped with Intel Core i5-8400 CPU @ 2.8 GHz and 8.0-GB memory.

B. Average Escape Time

This group of simulations evaluates path efficiency by comparing the user escape time of the route planned in each approach. A shorter escape time indicates a more efficient navigation path, as users are more likely to evacuate to the exit within the deadline along this route.

Fig. 7 shows the user escape time of the three approaches under different values of ϵ for navigation scenario 1) that has one user node deployed randomly. The data is collected from 35 trials. We can see that our method outperforms OPEN and ANT by yielding a shorter escape time in more than 90% and 70% of trials, respectively. The escape time provided by OPEN is much longer than that offered by our approach and ANT in some cases, such as Experiment 3 in Fig. 7(a) and Experiment 14 in Fig. 7(b). That is because the OPEN scheme aims at generating a navigation path that minimizes the probability of oscillation. It proposes a novel path metric, ENO, calculated

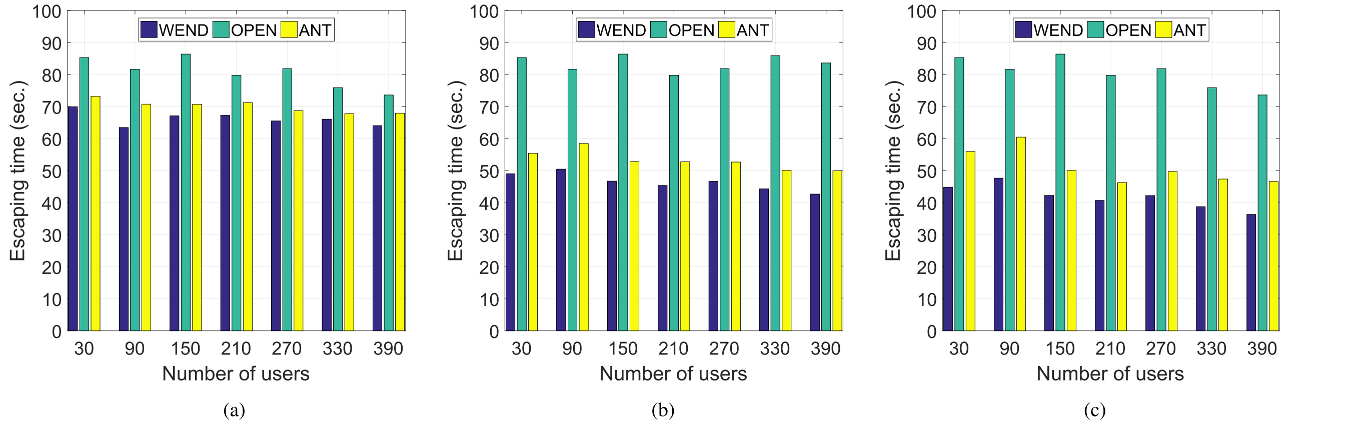

Fig. 8. Comparisons of average escape time for different values of ϵ under different numbers of users. (a) $\epsilon = 1$. (b) $\epsilon = 0.5$. (c) $\epsilon = 0.25$.

only by the spatial and temporal accumulated emergency level to achieve an oscillation-free path. Without sufficient consideration of the typical delay on each segment, OPEN is likely to result in large detours and thus long escape time, and finally missing the hard deadline for evacuation. We also notice that in rare cases, such as Experiment 12 in Fig. 7(b), it takes longer to escape along the navigation route of our approach and ANT. That is because two delay parameters are specified on each segment in the WEND scheme, and thus the provided path not only has the shortest typical time but also guarantees the user's arrival within the deadline considering worst-case delays. That is, it is not the theoretically fastest safe path. In addition, ANT shows equal or better performance compared with WEND when the escaping time of the user is less than 10 s. It is mainly because we assume that the typical speed changes every 10 s. That is to say, there is no dynamic variation when the escaping time is no greater than 10 s. In this case, ANT can provide the optimal guidance $p^*(\mathcal{T})$, and the path provided by WEND, an approximation scheme for the ship emergency navigation, can achieve a no more than $(1+\epsilon)d_T^{p^*}(\mathcal{T})$ typical delay.

Fig. 8 shows the average escape time of each approach under different numbers of users. In Fig. 8, experimental results for $\epsilon = 1$, $\epsilon = 0.5$, $\epsilon = 0.25$ are shown. We can see that in average WEND decreases the navigation time by 20%, 35%, 50% compared with OPEN, and 4%, 12%, and 20% compared with ANT, for $\epsilon = 1$, $\epsilon = 0.5$, and $\epsilon = 0.25$, respectively. This result demonstrates the superior navigation efficiency using WEND when ϵ is set as 0.5 and 1. WEND can determine a navigation path with a no more than $(1+\epsilon)d_T^{p^*}(\mathcal{T})$ typical delay while simultaneously considering the hazard motion tendency and the worst-case source-to-destination delay guarantee.

We further evaluate the scalability of WEND at larger scales. Specifically, we carry out a group of simulations, where $40, 90, \ldots, 340, 390$ users are inserted in navigation scenarios 1) and 2), respectively. Fig. 9 shows the average escape time of OPEN, ANT, and WEND. OPEN98, ANT98, and WEND98 indicate the results in scenario 1) where 98 nodes are deployed, and OPEN196, ANT196, and WEND196 denote the experiments conducted in scenario 2) with 196 nodes deployed.

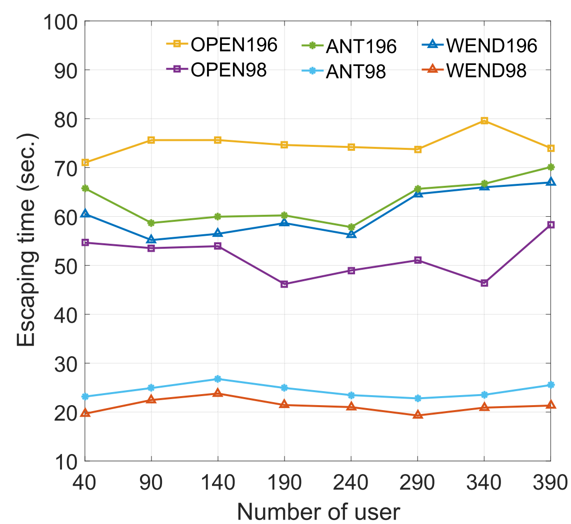

Fig. 9. Comparisons of average escape time for $\epsilon = 0.5$ under different numbers of users and navigation scenarios.

We can observe that all three methods have increased ratios as the network size is increased. That is probably because distance-based delay measurement in the two approaches becomes more accurate when more nodes are involved as the network scale increases. However, WEND outperforms both ANT and OPEN by always taking shorter to navigate users in both scenarios 1) and 2).

C. Navigation Success Ratio

We evaluate the navigation success ratio of the three methods in this group of simulations, which is measured by the average arrival possibility within the deadline for evacuation. The time available for passenger evacuation on a damaged ship is limited. Passengers must arrive at a muster station within the deadline; otherwise, their navigation fails. Therefore, we can evaluate the navigation success ratio by calculating the possibility of reaching the exit within the deadline. In our simulation, this possibility is expressed as $1-(F(d_T^p(\mathcal{T}))/T_c(t_0))$, where $F(d_T^p(\mathcal{T}))$ is computed by the

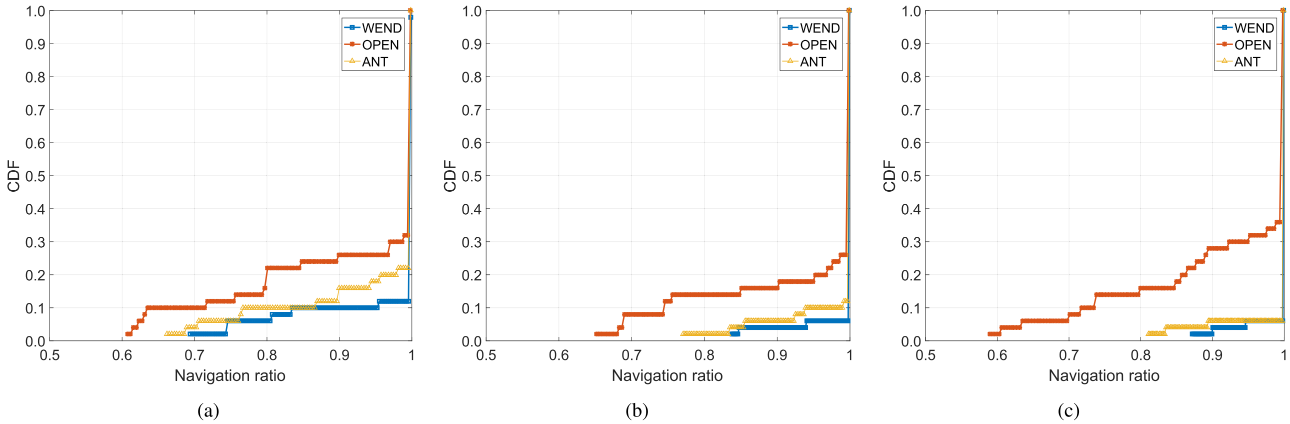

Fig. 10. Comparisons of navigation success ratio for navigation scenario 1) under different values of ϵ. (a) $\varepsilon = 1$. (b) $\varepsilon = 0.5$. (c) $\varepsilon = 0.25$.

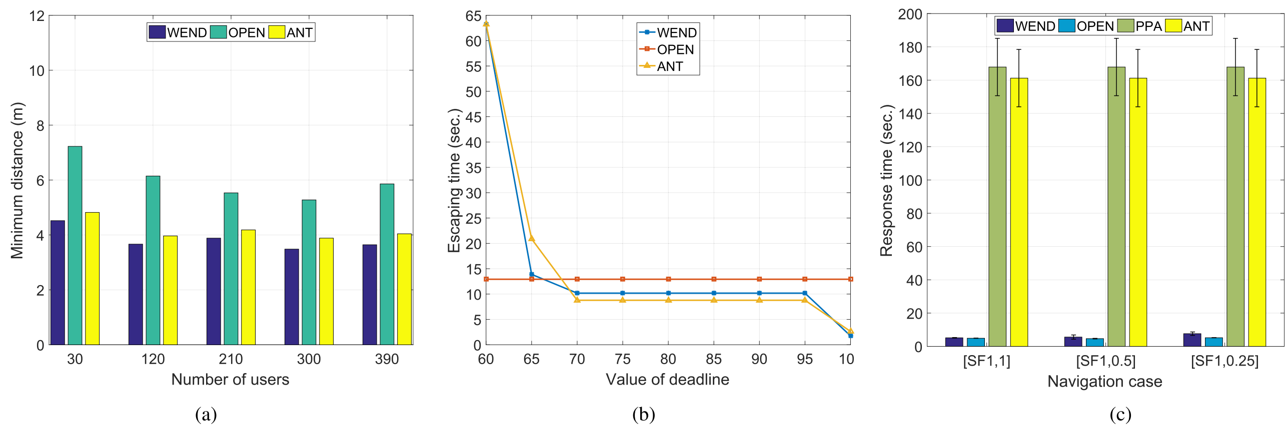

Fig. 11. Comparisons of minimum distance to hazards, average escape time, and the response time. (a) Comparisons of minimum distance to hazards for $\varepsilon = 0.5$. (b) Comparisons of average escape time $\varepsilon = 0.5$. (c) Comparisons of response time.

following equation:

$$F\left(d_T^p(\mathcal{T})\right) = \begin{cases} 0, & \text{if } d_T^p(\mathcal{T}) \le T_c(t_0) \\ d_T^p(\mathcal{T}) - T_c(t_0), & \text{if } d_T^p(\mathcal{T}) > T_c(t_0). \end{cases} \quad (14)$$

In the controlled simulation, we consider that missing the deadline is the only factor, which causes navigation failure.

We inject 150 user nodes into the navigation scenario 1). ϵ is set to 1, 0.5, and 0.25. Fig. 10 shows the cumulative distribution function (cdf) of the arrival possibility within the deadline of OPEN, ANT, and WEND. We can see that more than 70%, 80%, and 85% of users can be successfully navigated to the exit within the deadline for evacuation using WEND for $\epsilon = 1$, $\epsilon = 0.5$, and $\epsilon = 0.25$, respectively. All of them are much better than the cases with OPEN which can guarantee that around 60% of users can be successfully navigated. OPEN fails to ensure navigation success in certain scenarios because it is likely to cause detours, which increases user escape time and thus leads to navigation failure. Moreover, WEND's performance clearly outperforms ANT because ANT does not update the look-up tables according to the changing typical delay.

D. Minimum Distance to Hazards

We evaluate the effectiveness of WEND in terms of the absolute safety of the planned path, which is measured by the minimum distance from the route to hazardous regions. A larger distance to hazards indicates a better safety of the navigation route, as it provides a better chance for the guided user to safely bypass hazardous regions. Fig. 11(a) shows the minimum distance to hazards of the three approaches under different numbers of users. We can see that the OPEN approach presents the superior result with the distance more than 5 m. WEND and ANT have the distance of approximately 4 m, which is slightly lower than that of OPEN, however, which does not indicate a considerable threat to users. It is unnecessary to find a path for which the optimal result with the maximum safe distance is achieved because means the navigation decision is often over-conservative, which can increase the time spent in the navigation environment, thereby reducing the overall safety of guided users. In comparison, WEND greatly reduces the stay time of users in the hazardous environment, enhancing the opportunity to arrive at the exit within the specified deadline.

E. Impact of Deadline

We emphasize that the ability to deal with different deadlines is one of the core advantages of our method. To test the impact of different settings of the deadline, we conduct simulations on the navigation scenario 1) for $\epsilon = 0.5$ with different deadlines. As shown in Fig. 11(b), for WEND and ANT the escape time decreases as the deadline for evacuation increases. For OPEN, the escape time is independent of the deadline variation. We also notice when the deadline is set as 60 s, the escape time provided by both WEND and ANT is approximately 65 s which exceeds the specified deadline. The reason is that there is not a route satisfying the worst-case bound when the deadline is set to 60 s. In such a case, the minimum worst-case source-to-destination delay is selected as the escape time by WEND. In addition, we can see that the escaping time of ANT is close to that of WEND when the deadline ranges from 70 to 100. The main reason is the escaping time is less than 10 s, while the typical speed changes every 10 s. That is, there is no dynamic variation when the escaping time is no greater than 10 s.

F. Average Emergency Response Time

An emergency navigation system demands a time-critical response with respect to the provision of navigation decisions. In this simulation, we compare the navigation efficiency of each method in terms of response time (i.e., the running time of each algorithm). We perform the simulation experiments on a personal computer (Operating System: Windows 10 Education) equipped with Intel Core i5-8400 CPU @ 2.8 GHz and 8.0-GB memory. Fig. 11(c) shows the response time of OPEN, WEND, ANT, and PPA (a pseudo-polynomial algorithm for our problem, which does not round and scale typical delay). We can see that OPEN achieves a similar result in terms of the response time compared with WEND, while the path provided by this scheme cannot guarantee users' escape within the deadline, which extremely jeopardizes the users' chances of survival. We also notice that our approach is much superior to ANT and PPA.

VII. Conclusion and Discussion

Emergency navigation is essential for passengers on a damaged ship. Considering the deadline for ship evacuation and the dynamics of travel time on each segment caused by the changing heel angle, it is challenging to ensure passenger survival. In this study, based on graph theory, we design a Hard-Real-Time emergency navigation strategy in dynamic graphs to minimize escape time, WEND, for ship evacuation. Our method can identify a navigation path with a no more than $(1+\epsilon)d_T^{p^*}(\mathcal{T})$ typical delay while guaranteeing the avoidance of dynamic hazardous regions and respecting the specified deadline under all circumstances in scenarios where the typical delay estimations are dynamic. Extensive simulations are used to demonstrate the advantages of our method.

In this work, we do not take into account the physical and psychological factors of moving passengers and the capacity constraints of roads, which is to be addressed in our future work. In addition, the load balancing among different exits is also an important topic requiring an in-depth investigation.

References

[1] E.-G. Ryu, C.-S. Yang, and J.-W. Choi, "Fundamental research for escape guidance system development of passenger ship," *J. Navigat. Port Res.*, vol. 41, no. 2, pp. 39–46, Apr. 2017.

[2] D. Lee, H. Kim, J.-H. Park, and B.-J. Park, "The current status and future issues in human evacuation from ships," *Saf. Sci.*, vol. 41, no. 10, pp. 861–876, Dec. 2003.

[3] P. Gubian, M. Piccinelli, B. Neri, P. Neri, and F. Giurlanda, "The disaster of Costa Concordia cruise ship: An accurate reconstruction based on black box and automation system data," in *Proc. 2nd Int. Conf. Inf. Commun. Technol. Disaster Manag. (ICT-DM)*, Nov. 2015, pp. 178–185.

[4] H. Soliman, "The sinking of the Al-Salam Boccaccio 98 ferry in the Red Sea: The integration of disaster support system models and emergency management experience," *Int. J. Disaster Risk Reduction*, vol. 4, pp. 44–51, Jun. 2013.

[5] D.-G. Yoon and C.-S. Kim, "Analysis report of the elapse for Costa Concordia's disaster," *J. Korean Soc. Mar. Environ. Saf.*, vol. 18, no. 4, pp. 331–335, Aug. 2012.

[6] C. Nasso, S. Bertagna, F. Mauro, A. Marinò, and V. Bucci, "Simplified and advanced approaches for evacuation analysis of passenger ships in the early stage of design," *Brodogradnja, Teorija Praksa Brodogradnje Pomorske Tehnike*, vol. 70, no. 3, pp. 43–59, 2019.

[7] V. Bucci, A. Marinò, F. Mauro, R. Nabergoj, and C. Nasso, "On advanced ship evacuation analysis," in *Proc. 22nd Int. Conf. Eng. Mech. (IM)*, Svratka, Czech Republic, 2016, pp. 1–8.

[8] H. Kim, M.-I. Roh, and S. Han, "Passenger evacuation simulation considering the heeling angle change during sinking," *Int. J. Nav. Archit. Ocean Eng.*, vol. 11, no. 1, pp. 329–343, Jan. 2019.

[9] M. Hu, W. Cai, and H. Zhao, "Simulation of passenger evacuation process in cruise ships based on a multi-grid model," *Symmetry*, vol. 11, no. 9, p. 1166, Sep. 2019.

[10] M. Erdelj, M. Król, and E. Natalizio, "Wireless sensor networks and multi-UAV systems for natural disaster management," *Comput. Netw.*, vol. 124, pp. 72–86, Sep. 2017.

[11] M. Abdulkarem, K. Samsudin, F. Z. Rokhani, and M. F. A. Rasid, "Wireless sensor network for structural health monitoring: A contemporary review of technologies, challenges, and future direction," *Nature*, vol. 19, no. 3, pp. 693–735, Feb. 2020.

[12] C. Wang, H. Lin, R. Zhang, and H. Jiang, "SEND: A situation-aware emergency navigation algorithm with sensor networks," *IEEE Trans. Mobile Comput.*, vol. 16, no. 4, pp. 1149–1162, Apr. 2017.

[13] S. M. Kumar and L. Lakshmanan, "A situation emergency building navigation disaster system using wireless sensor networks," in *Proc. Int. Conf. Commun. Signal Process. (ICCSP)*, Apr. 2018, pp. 0378–0382.

[14] L. Wang, Y. He, W. Liu, N. Jing, J. Wang, and Y. Liu, "On oscillation-free emergency navigation via wireless sensor networks," *IEEE Trans. Mobile Comput.*, vol. 14, no. 10, pp. 2086–2100, Oct. 2015.

[15] C. Wang, H. Lin, and H. Jiang, "CANS: Towards congestion-adaptive and small stretch emergency navigation with wireless sensor networks," *IEEE Trans. Mobile Comput.*, vol. 15, no. 5, pp. 1077–1089, May 2016.

[16] A. Gunathillake and A. V. Savkin, "Mobile robot navigation for emergency source seeking using sensor network topology maps," in *Proc. 36th Chin. Control Conf. (CCC)*, Jul. 2017, pp. 6027–6030.

[17] I. Bačkalov et al., "Ship stability, dynamics and safety: Status and perspectives from a review of recent STAB conferences and ISSW events," *Ocean Eng.*, vol. 116, pp. 312–349, Apr. 2016.

[18] K. J. Rawson and E. C. Tupper, *Basic Ship Theory*, vol. 1. London, U.K.: Butterworth, 2001.

[19] H. Nowacki, "Archimedes and ship design," in *Archimedes in the 21st Century*. Springer, 2017, pp. 77–112.

[20] Y. Han and H. Liu, "Modified social force model based on information transmission toward crowd evacuation simulation," *Phys. A, Stat. Mech. Appl.*, vol. 469, pp. 499–509, Mar. 2017.

[21] R. Zhou, Y. Cui, Y. Wang, and J. Jiang, "A modified social force model with different categories of pedestrians for subway station evacuation," *Tunnelling Underground Space Technol.*, vol. 110, Apr. 2021, Art. no. 103837.

[22] L.-W. Chen and J.-X. Liu, "Time-efficient indoor navigation and evacuation with fastest path planning based on Internet of Things technologies," *IEEE Trans. Syst., Man, Cybern., Syst.*, vol. 51, no. 5, pp. 3125–3135, May 2021.

[23] T. Meyer-König, P. Valanto, and D. Povel, "Implementing ship motion in AENEAS—Model development and first results," in *Pedestrian and Evacuation Dynamics 2005*. Berlin, Germany: Springer, 2007, pp. 429–441.

[24] K. V. Kostas et al., "Motions effect for crowd modeling aboard ships," in *Pedestrian and Evacuation Dynamics 2012*. Cham, Switzerland: Springer, 2014, pp. 825–833.

[25] D. Lee, J.-H. Park, and H. Kim, "A study on experiment of human behavior for evacuation simulation," *Ocean Eng.*, vol. 31, nos. 8–9, pp. 931–941, Jun. 2004.

[26] H. Kim, J.-H. Park, D. Lee, and Y.-S. Yang, "Establishing the methodologies for human evacuation simulation in marine accidents," *Comput. Ind. Eng.*, vol. 46, no. 4, pp. 725–740, Jul. 2004.

[27] M. Li, J. Wang, Z. Yang, and Z. Yang, "Sensor network navigation without locations," in *Proc. EEE INFOCOM*, Apr. 2009, pp. 2419–2427.
[28] C. Buragohain, D. Agrawal, and S. Suri, "Distributed navigation algorithms for sensor networks," 2005, *arXiv:cs/0512060*.
[29] Q. Li, M. De Rosa, and D. Rus, "Distributed algorithms for guiding navigation across a sensor network," in *Proc. 9th Annu. Int. Conf. Mobile Comput. Netw.*, 2003, pp. 313–325.
[30] H. Li and A. V. Savkin, "An algorithm for safe navigation of mobile robots by a sensor network in dynamic cluttered industrial environments," *Robot. Comput.-Integr. Manuf.*, vol. 54, pp. 65–82, Dec. 2018.
[31] S. Allali and M. Benchaiba, "Safe route guidance of rescue robots and agents based on hazard areas dissemination," in *Proc. Int. Conf. Math. Inf. Technol. (ICMIT)*, Dec. 2017, pp. 29–37.
[32] D. H. Lorenz and D. Raz, "A simple efficient approximation scheme for the restricted shortest path problem," *Oper. Res. Lett.*, vol. 28, no. 5, pp. 213–219, 2001.
[33] R. Hassin, "Approximation schemes for the restricted shortest path problem," *Math. Oper. Res.*, vol. 17, no. 1, pp. 36–42, Feb. 1992.
[34] Y. Ma et al., "ANT: Deadline-aware adaptive emergency navigation strategy for dynamic hazardous ship evacuation with wireless sensor networks," *IEEE Access*, vol. 8, pp. 135758–135769, 2020.
[35] P. Valanto, "Time-dependent survival probability of a damaged passenger ship ii-evacuation in seaway and capsizing," Sub-Committee Stability Load Lines Fishing Vessels Saf., Hamburg, Germany, HSVA Rep. 1661, 2006, pp. 42–62.
[36] R. A. Klein, "Cruises and bruises: Safety, security and social issues on polar cruises," in *Cruise Tourism in Polar Regions*. London, U.K.: Routledge, 2010, pp. 83–100.
[37] P. Boguslawski, L. Mahdjoubi, V. Zverovich, and F. Fadli, "Automated construction of variable density navigable networks in a 3D indoor environment for emergency response," *Autom. Construct.*, vol. 72, pp. 115–128, Dec. 2016.
[38] Y. Qiao, D. Han, J. Shen, and G. Wang, "A study on the route selection problem for ship evacuation," in *Proc. IEEE Int. Conf. Syst., Man, Cybern. (SMC)*, Oct. 2014, pp. 1958–1962.
[39] W.-J. Na, B.-H. Son, and W.-H. Hong, "Analysis of walking-speed of cruise ship passenger for effective evacuation in emergency," *Medico-Legal Update*, vol. 19, no. 2, p. 710, 2019.
[40] P. Guo, J. Xia, M. Zhou, R. A. Falconer, Q. Chen, and X. Zhang, "Selection of optimal escape routes in a flood-prone area based on 2D hydrodynamic modelling," *J. Hydroinformat.*, vol. 20, no. 6, pp. 1310–1322, Nov. 2018.
[41] H. Ortega-Arranz, D. R. Llanos, and A. Gonzalez-Escribano, "The shortest-path problem: Analysis and comparison of methods," *Synth. Lectures Theor. Comput. Sci.*, vol. 1, no. 1, pp. 1–87, Dec. 2014.

Kezhong Liu (Member, IEEE) received the B.S. and M.S. degrees in marine navigation from the Wuhan University of Technology (WUT), Wuhan, China, in 1998 and 2001, respectively, and the Ph.D. degree in communication and information engineering from the Huazhong University of Science and Technology, Wuhan, in 2006.

He is currently a Professor with the School of Navigation, WUT. His active research interests include indoor localization technology and data mining for ship navigation.

Yuting Ma is currently pursuing the Ph.D. degree in marine navigation with the Wuhan University of Technology (WUT), Wuhan, China.

Her research interests include emergency navigation and evacuation.

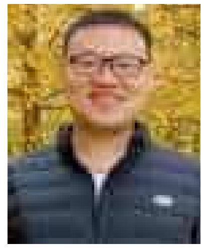

Mozi Chen (Member, IEEE) received the B.S. degree in electric engineering from the Hubei University of Technology, Wuhan, China, in 2013, and the M.S. degree in navigation engineering and the Ph.D. degree from the Wuhan University of Technology (WUT), Wuhan, in 2016 and 2020, respectively.

He is currently an Associate Researcher with WUT. His research interests include wireless sensing techniques and machine learning algorithms for human localization, emergency navigation, and activity recognition in mobile environment, i.e., cruise ships.

Kehao Wang received the B.S. degree in electrical engineering and the M.S. degree in communication and information system from the Wuhan University of Technology, Wuhan, China, in 2003 and 2006, respectively, and the Ph.D. degree from the Department of Computer Science, University of Paris-Sud XI, Orsay, France, in 2012.

In 2013, he joined the School of Information Engineering, Wuhan University of Technology, where he is currently an Associate Professor. His research interests include cognitive radio networks, wireless network resource management, and embedded operating systems.

Kai Zheng received the Ph.D. degree from the School of Geodesy and Geomatics, Wuhan University, Wuhan, China, in 2020.

He is currently an Associate Researcher with the Wuhan University of Technology, Wuhan. His research interests include GNSS precise positioning techniques.

Xuming Zeng received the Ph.D. degree in communication engineering from the China University of Geosciences, Wuhan, China, in 2018.

From 2016 to 2017, he was a joint training Ph.D. Student with the Department of Electrical and Computer Engineering, College of Engineering, Florida State University, Tallahassee, FL, USA. He currently holds the postdoctoral position with the Department of Traffic and Transportation Engineering, School of Navigation, Wuhan University of Technology, Wuhan, where he has been studying wireless ad hoc network for shipboard environment since 2018. His research interests include routing protocols, MAC, QoS, clustering, radio resource management, traffic engineering, and performance analysis, for both wired and wireless networks.

Appendix B: Paper II

Received June 27, 2020, accepted July 13, 2020, date of publication July 23, 2020, date of current version August 4, 2020.
Digital Object Identifier 10.1109/ACCESS.2020.3011545

ANT: Deadline-Aware Adaptive Emergency Navigation Strategy for Dynamic Hazardous Ship Evacuation With Wireless Sensor Networks

YUTING MA[1], KEZHONG LIU[1], (Member, IEEE), MOZI CHEN[1], (Graduate Student Member, IEEE), JIE MA[1], XUMING ZENG[1], KEHAO WANG[2], AND CONG LIU[3], (Member, IEEE)
[1]School of Navigation, Wuhan University of Technology, Wuhan 430000, China
[2]School of Electronics and Information Engineering, Wuhan University of Technology, Wuhan 430000, China
[3]Department of Computer Science, University of Texas at Dallas, Richardson, TX 75080, USA
Corresponding author: Mozi Chen (chenmz@whut.edu.cn)

This work was supported in part by the National Natural Science Foundation of China (NSFC) under Grant 51979216; and in part by the Major Project for the Technology Innovation of Hubei Province, China, under Grant 2017AAA120.

ABSTRACT Efficient and safe ship evacuation strategy plays a critical role in protecting passengers' lives when ships encounter accidents. Existing wireless sensor network (WSN)-based emergency navigation methods mainly consider the dynamics of hazards and accordingly plan evacuation paths to minimize human exposure to the environmental hazards, such as fire and smoke. However, without sufficient consideration of the ship capsizing time and the impact of dynamic ship inclination on the passengers' walking speed, these methods may fail to evacuate passengers before the deadline. In this paper, we propose ANT, a deadline-aware adaptive emergency navigation strategy for dynamic hazardous ship evacuation with WSNs, which informs each passenger about a hazard-avoided evacuation path to successfully reach lifeboats within the specified deadline under all circumstances. To achieve this aim, ANT analyzes the process of ship capsizing to predict the specific limited evacuation time and the worst-case traversal delay. Next, an online evacuation path planning strategy is proposed based on a real-time adaptive routing algorithm to maximize navigation efficiency while ensuring user safety. We evaluate ANT by conducting prototype experiments and extensive simulations. The results demonstrate that ANT improves the navigation success ratio by 40% and 5%, compared with state-of-the-art emergency navigation systems, namely, medial axis-based approach and ENO-based oscillation-free emergency navigation approach, respectively.

INDEX TERMS Emergency navigation, adaptive routing, ship evacuation, wireless sensor networks.

I. INTRODUCTION

Guarantee of the safety of passengers and crew of ships has received considerable attention since the International Convention for the Safety of Life at Sea was introduced by the International Maritime Organization [1]. As ship environmental hazards are dynamic and passengers are unfamiliar with the complex ship structure, accidents occurring in recent years (e.g., Costa Concordia disaster in 2012 [2]) have highlighted the chaos and catastrophic consequences of the actual ship evacuation without an intelligent location-based evacuation service [3]–[8]. Recent advances in wireless sensor networks (WSNs) have shown the potential of sensing hazards in the physical world and an in-situ interaction between people and the environment. The use of WSNs to explore dynamic environmental hazards and provide a real-time navigation service to users has garnered increasing attention.

To improve passenger safety during evacuation, significant efforts have been made to propose various WSN-assisted

The associate editor coordinating the review of this manuscript and approving it for publication was Mu Zhou.

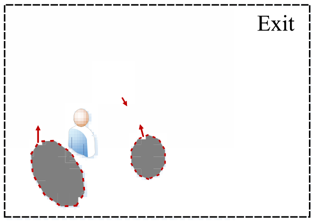
Exit

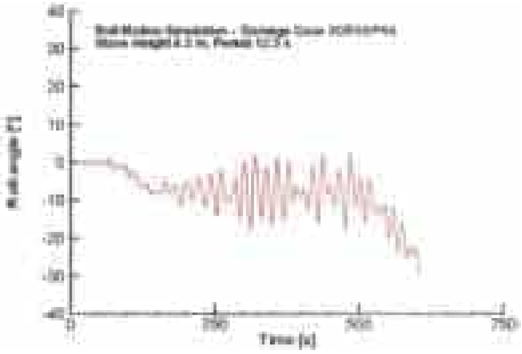

FIGURE 2. Time-history curve of the simulated ship roll motion for a specific case. Reprinted with permission from [22].

II. MOTIVATION AND PRELIMINARIES

In this section, we motivate our design by describing the unique characteristics of ship evacuation. Conventional oscillation-free navigation systems provide navigation paths by minimizing the probability of oscillation using the ENO as the path planning metric. Compared with the general environment, a damaged ship may cause two main challenges, namely, limited evacuation time and the impact on the passengers' movement speed, and make the existing methods unavailable. We now present the potential problems and insights observed from the analysis of ship accidents.

A. LIMITED EVACUATION TIME

Serious accidents at sea mainly include collisions with other ships and obstacles. According to [25], after a collision or grounding, there are risks of water ingress into the ship and sinking. In that case, the time available for ship evacuation is limited. Fig. 2 shows an example of a simulated ship roll motion behavior. We can observe that the average slope angle increases slowly at the beginning until at a certain point it starts accelerating. After a few large swings, the slope angle reaches 30° (which is regarded as the capsize criterion) and passengers' chances of survival dramatically decrease. Therefore, it is essential for the emergency navigation system to consider the limited evacuation time and navigate passengers to lifeboats before the ship capsizes. To predict the time available for ship evacuation, we consider relevant research as theoretical support. In [22], the capsizing time down to a significant wave height of 4.5 m is obtained directly using a ship motion simulation method. The method considers the loading condition of the vessel, extent and location of the damage, and sea condition in the area of operation. The probable survival time until capsizing T_c for the significant wave height lower than 4.5 m can be extrapolated with the following formula:

$$T_c = T_s \times e^{A+\frac{B}{h^2}}, \tag{1}$$

where T_s denotes the significant wave period and h indicates the significant wave height. The constants A and B can be calculated by capsizing simulations for higher wave heights using the same period T_s. In addition, considering that the presence of waves is not the only reason for ship's sinking after an accident occurs, many existing works also investigate the motion and flooding process of a damaged ship in calm water. In this paper, we refer to [26] to predict the survival time until capsizing for a ship in still water.

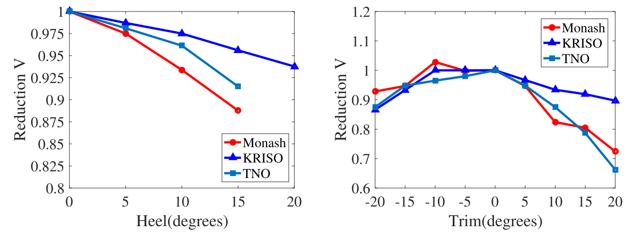

(a) (b)

FIGURE 3. Speed reduction factor with various trim or heel angles. Fig. 3 shows the experimental results obtained from Monash [22], KRISO [24], and TNO [28].

B. IMPACT OF SHIP INCLINATION ON THE WALKING SPEED

In addition to the limited evacuation time, another challenge of ship evacuation is ship inclination. It includes heel and trim, which may significantly slow down or block the movement speed of passengers [24], [27]. Various international research projects have been concerned with the reduction in the walking speed caused by ship inclination. Fig. 3 presents speed reduction data obtained from the evacuation analyses conducted by the following organizations:

- Korea Research Institute of Ship and Ocean Engineering (KRISO)
- The Netherlands Organization for Applied Scientific Research (TNO)
- The Monash University in Australia

As can be seen, the reduction in walking speed is represented as a function of the inclination angle. When the angle reaches the maximum, the speed becomes distinctly lower than that under level conditions. According to [22], the speed reduction r_{trans} in a laterally tilted corridor can also be calculated according to the heel angle ϕ:

$$r_{trans} = \begin{cases} -0.0067\phi + 1 & 0° \leq \phi < 15° \\ -0.0425\phi + 1.5375 & 15° \leq \phi < 35° \\ 0.05 & 35° \leq \phi \leq 45° \\ 0 & 45° < \phi \end{cases} \tag{2}$$

Similarly, we can compute the speed reduction in a longitudinally tilted corridor and stairs with a lateral or longitudinal slop. Based on the above-mentioned models, we can predict the worst-case passenger traversal delay bound by observing the ship inclination degree from ship inbuilt sensors.

III. NAVIGATION MODEL AND PROBLEM FORMULATION

In this section, we first present the navigation model and then formulate the problem and provide an example to show the intuitiveness of our approach. We consider the scenario that a user equipped with a portable device has to pass through

TABLE 1. Notations and definitions of the parameters of the model.

Notation	Meaning
$\mathscr{V}$	Set of sensors
$\mathscr{E}$	Set of edges between neighboring sensors
p	Navigation path
v_h	Hazardous sensor
v_a	User sensor
v_o	Exit sensor
v_i, v_j	Two neighboring landmarks
$\overrightarrow{v_iv_j}$	Connection between v_i and v_j
$\mathscr{V}'$	Set of landmarks
$\mathscr{E}'$	Set of segments between neighboring landmarks
$\mathscr{N}_i$	Set of front neighbor landmarks of v_i
$d_T(\overrightarrow{v_iv_j})$	Typical delay along the segment $\overrightarrow{v_iv_j}$
$d_W(\overrightarrow{v_iv_j})$	Maximum delay along the segment $\overrightarrow{v_iv_j}$
$d_T(p)$	Typical delay along the path p
$d_W(p)$	Maximum delay along the path p
$D(v_j, v_i)$	Duration of hazardous arrival at $\overrightarrow{v_iv_j}$ at the initial time t_0

a field containing dynamic hazards, and the user's speed changes depending on the inclination of the ship.

A. MODEL AND DEFINITIONS

Here, we provide an in-depth description of the model and definitions, with notations presented in Table 1.

The navigation scenario on a ship is mapped to a 2-D Euclidean plane, which is well covered by a WSN. The WSN is denoted by a directed graph $G = (\mathcal{V}, \mathcal{E})$, where $\mathcal{V}$ represents the set of sensors and $\mathcal{E}$ represents the set of edges between two neighboring sensors. Evacuees on the ship are required to arrive at the place where lifeboats are located. Therefore, the sensor closest to a lifeboat is defined as *exit sensor* v_o. Other sensors are divided into two types: *hazardous sensors* and *normal sensors*, which indicate sensors inside or outside of a hazardous region, respectively. The hazardous region is modeled as a convex hull of the subset of hazardous sensors. There may be multiple hazardous regions, and because of the dynamics of hazards, the sensor status may change with time (i.e., a normal sensor may be transformed into a hazardous sensor), as shown in Figs. 4 (a)–(c). In our study, we only consider one basic type of variation in hazards, i.e., expansion.

Considering the characteristics of the indoor environment of the ship, we exploit an exit sensor and sensors at staircases as the navigation landmarks to assist the user with movement. For example, v_a, v_1, v_2, and v_o in Fig. 4d represent four different landmarks. Let $\mathcal{V}'$ be the set of landmarks, $\mathcal{V}' \subset \mathcal{V}$. The connection between two adjacent landmarks (v_i and v_j) is defined as a segment $\overrightarrow{v_iv_j}$. Let $\mathcal{E}'$ represent the set of segments, $\mathcal{E}' \subset \mathcal{E}$. In this study, we base the design of our method on the navigation model $G' = (\mathcal{V}', \mathcal{E}')$. The user is continuously guided along the segment to the next landmark until he or she reaches the exit sensor. Each segment $\overrightarrow{v_iv_j}$ in

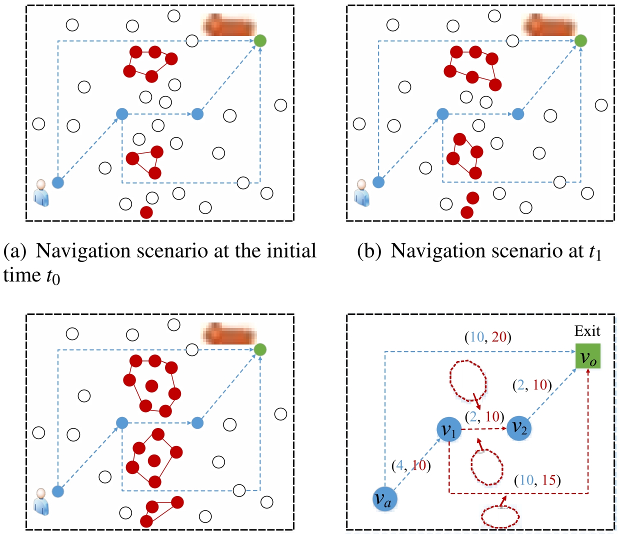

(a) Navigation scenario at the initial time t_0 (b) Navigation scenario at t_1 (c) Navigation scenario at t_2 (d) Navigation model

FIGURE 4. Navigation scenarios and the corresponding navigation model. The open circles represent normal sensors, red solid circles denote hazardous sensors, green solid circle represents an exit sensor, and blue solid circles indicate landmarks. The red dotted arrows in (d) represent the segments affected by hazards. Subgraphs (a)–(c) show the dynamics of the three hazards from t_0 to t_2.

the navigation model is labeled with two delay parameters: an estimate of the typical delay $d_T(\overrightarrow{v_iv_j})$ and a guaranteed maximum delay $d_W(\overrightarrow{v_iv_j})$ that may be encountered in traveling $\overrightarrow{v_iv_j}$ (here $0 < d_T(\overrightarrow{v_iv_j}) < d_W(\overrightarrow{v_iv_j})$). As shown in Fig. 4d, the blue number alongside each segment indicates $d_T(\overrightarrow{v_iv_j})$, and the red number denotes $d_W(\overrightarrow{v_iv_j})$.

Let $\mathcal{N}_j$ be all front neighbor landmarks of v_j in G'. $\mathcal{N}_j$ is defined as follows:

$$\mathcal{N}_j \triangleq \left\{v_i \mid \overrightarrow{v_iv_j} \in \mathcal{E}'\right\}$$

We define $D(v_j, v_i)$, $v_i \in \mathcal{N}_j$ to reflect the duration of hazardous arrival at $\overrightarrow{v_iv_j}$ (details of the calculation procedure of $D(v_j, v_i)$ are presented in Algorithm 1). All $D(v_j, v_i)$ constitute the set $\mathcal{D}_j$. $\mathcal{D}_j$ is defined as:

$$\mathcal{D}_j \triangleq \left\{D(v_j, v_i) \mid \overrightarrow{v_iv_j} \in \mathcal{E}'\right\}$$

Each landmark v_j in the navigation model is labeled with the set $\mathcal{D}_j$.

A navigation path p is a connected and cycle-free sequence of segments. The user sensor v_a and the exit sensor v_o are viewed as the origin and the terminal of the path, respectively:

$$p(v_a \to v_o) \triangleq \left\langle \overrightarrow{v_av_i}, \overrightarrow{v_iv_j}, \ldots, \overrightarrow{v_nv_o} \right\rangle$$

where $\overrightarrow{v_av_i} \in \mathcal{E}'$, $\overrightarrow{v_iv_j} \in \mathcal{E}'$, and $\overrightarrow{v_nv_o} \in \mathcal{E}'$. The costs $d_T(p)$ and $d_W(p)$ of path p are defined as:

$$d_T(p) \triangleq \sum_{\forall \overrightarrow{v_iv_j} \in p} d_T(\overrightarrow{v_iv_j})$$

and

$$d_W(p) \triangleq \sum_{\forall \overrightarrow{v_iv_j} \in p} d_W(\overrightarrow{v_iv_j})$$

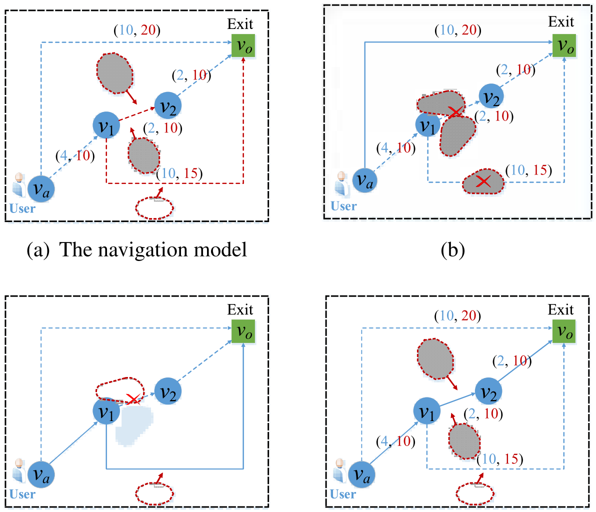

(a) The navigation model (b) (c) (d)

FIGURE 5. Intuitiveness of ANT. (a) Example graph of the navigation model, in which the three gray areas represent hazardous regions, red dotted arrows denote the segments affected by hazards, and blue arrows indicate all possible navigation paths. (b)–(d) Three different navigation routes that are selected based on the user's actual walking speed. The blue dotted arrows in (b)–(d) denote the paths chosen for the guided user with different velocities.

B. PROBLEM FORMULATION

Our objective is to find a *superior* path for a user who is trapped on the ship. We define a superior path to be the navigation path, p_{sup}, from the user sensor to the exit sensor with the minimum typical delay, while ensuring that the user escapes within a given deadline under all circumstances and avoids hazardous regions.

First, considering a set of segments, $\overrightarrow{v_iv_j}$, on path $p\,(v_a \rightarrow v_o)$, we present a precise definition of the superior path. Let $\mathcal{P}_i$ be all paths from v_i to v_o. We define $\mathcal{X}_i$ to represent all safe neighbors of v_i, i.e., there exists a certain path $p\,(v_i) \in \mathcal{P}_i$:

$$\mathcal{X}_i \triangleq \big\{v_j \mid d_W(\overrightarrow{v_iv_j}) + d_W(v_j \rightarrow v_y) \leq D(v_y, v_x) \\ -d_{v_a\rightarrow v_i},\, \overrightarrow{v_xv_y} \in p\,(v_i)\big\}$$

where $d_{v_a\rightarrow v_i}$ denotes the actual delay encountered from v_a to v_i, which is determined by the actual walking speed of the user.

Next, we define $\delta(v_i)$ as the minimum typical delay from v_i to exit v_o and $p_{sup}(v_i)$ as the path from v_i to v_o with $\delta(v_i)$. We have the following recurrence with respect to $\delta(v_i)$:

$$\delta(v_i) = \min_{v_j\in\mathcal{X}_i} \begin{cases} d_T(\overrightarrow{v_iv_j}) + \delta(v_j) \\ s.t.\;\; d_T(\overrightarrow{v_iv_j}) + d_W(v_j \rightarrow v_n) \leq D(v_n, v_m) \\ \quad -d_{v_a\rightarrow v_i}, \\ \overrightarrow{v_mv_n} \in p_{sup}(v_i) \end{cases}$$

Finally, a navigation path is considered to be superior if and only if for each v_i, v_j is determined by $\delta(v_i)$.

C. INTUITIVENESS OF ANT

Figs. 5 (b)–(d) provide an example to demonstrate the intuitiveness of our approach. In our scenarios, three gray areas indicate dynamic hazardous regions. The solid arrow represents the navigation path provided for the user. Subgraphs (b)–(d) show three different methods for navigating the user, depending on the user's actual walking speed. Considering the deadline C for emergency navigation on the ship, we assume $D(v_o, v_a) = D(v_o, v_2) = 27$ at the initial time; if $D(v_2, v_1) = 15$ and $D(v_o, v_1) = 20$ owing to the dynamic hazards, the selected path for the user is the solid arrow in (b). However, if $D(v_o, v_1) = 25$ and $D(v_2, v_1) = 15$, the user first traverses segment $\overrightarrow{v_av_1}$ and then selects $\overrightarrow{v_1v_2}$ or $\overrightarrow{v_1v_o}$ determined by the user's actual walking speed:

1) If the actual delay, $d_{\overrightarrow{v_av_1}}$, encountered across $\overrightarrow{v_av_1}$ does not exceed 5, the user subsequently takes route $v_1 \rightarrow v_2 \rightarrow v_o$ (as shown in (d)) yielding a typical delay $5 + 2 + 2 = 9$, while guaranteeing that the worst-case delay to v_o is $10 + 10 \leq 27$ - $d_{\overrightarrow{v_av_1}}$. Furthermore, the worst-case delay to v_2 is $10 \leq 15$ - $d_{\overrightarrow{v_av_1}}$, indicating that the user can avoid the dynamic hazards in traveling from v_1 to v_2 even if the worst-case delay is 10 along this segment.

2)However, if the actual delay, $d_{\overrightarrow{v_av_1}}$, encountered across $\overrightarrow{v_av_1}$ exceeds 5 (but $d_{\overrightarrow{v_av_1}} \leq 10$), the user can take route $v_1 \rightarrow v_o$ (Fig. 5c) and arrive at the exit sensor v_o within 15 (which is ≤ 27 - $d_{\overrightarrow{v_av_1}}$). Similarly, the user avoids the dynamic hazard in moving from v_1 to v_o even in the worst-case delay of 15 along this segment ($15 \leq 25$ - $d_{\overrightarrow{v_av_1}}$).

Thus, we can find that individual paths can be provided to users utilizing our method based on their actual walking speed. This ensures that evacuees reach the exit within the deadline while avoiding hazards.

IV. DESIGN

This section elaborates on the design of ANT. First, we present the framework of our method. Next, we provide details of ANT in the remainder of this section: quantifying the parameters of the navigation model, constructing two types of look-up tables, and guiding the movement of the user.

A. ANT FRAMEWORK

Our method is designed based on the principle of rapid routing with the guaranteed delay bound algorithm [29]. The basic process of our navigation method includes two main steps:

First, given the navigation model depicted in Fig. 4d, we establish look-up tables at each landmark during the preprocessing phase. These tables are used to determine the superior path. We construct two types of tables. One contains data in the form of a 3-tuple $(s,\, v_j,\, \delta)$, $0 < \delta < s$. The 3-tuple denotes that the path from v_i to the exit v_o, with the guaranteed worst-case delay bound s and the minimum typical delay δ, has $\overrightarrow{v_iv_j}$ as the outgoing segment from v_i. Let $\mathcal{V}''$ denote the set of landmarks affected by hazards ($v_u \in \mathcal{V}''$, if and only if there exist some segments connecting v_u with its front neighbors, which will be covered by dynamic hazards). Another table contains data in the form of a 2-tuple $(s(v_u), v_j)$, $s(v_u) > 0$, denoting that the navigation path $p\,(v_i \rightarrow v_u)$ with the guaranteed worst-case delay bound $s(v_u)$ has $\overrightarrow{v_iv_j}$ as the outgoing segment from v_i. The second type of entry is only constructed under the following condition: if we travel $\overrightarrow{v_iv_j}$, there will be no navigation path without segments that would be damaged by dynamic hazards.

Second, the user is navigated at each intermediate landmark v_i according to the tables in the following form: first, if $C - d_{\overrightarrow{v_av_i}} \geq s$, it is possible to take the corresponding segment $\overrightarrow{v_iv_j}$. Next, referring to another type of look-up table, if there is a remaining duration of hazardous arrival at $v_u \geq s(v_u)$, it is certain to select $\overrightarrow{v_iv_j}$.

Based on the actual walking speed of the user, our method can find a navigation path with the minimum typical delay, while enabling the user to reach the exit safely within C under all conditions. These circumstances raise two problems:

- Quantifying the parameters of the navigation model, including $d_T(\overrightarrow{v_iv_j})$ and $d_W(\overrightarrow{v_iv_j})$ on each segment $\overrightarrow{v_iv_j}$, and $\mathcal{D}_i$ attached to each landmark v_i.
- Constructing and using the two types of look-up tables to guide the user to the exit incrementally according to his actual speed.

The remainder of this section contains details of our design.

B. QUANTIFYING THE PARAMETERS OF THE NAVIGATION MODEL

This section presents the process of parameter assessment, which is the basis of constructing the look-up tables and guiding the movement of the user.

1) TYPICAL DELAY AND WORST-CASE DELAY

Ship inclination can significantly affect the movement of passengers, and consequently, the time required to traverse a certain segment also varies based on the changes in human speed. The onboard user walks at a constant speed of 0.8 m/s in rooms and corridors and 0.3 m/s on stairways [30]. Thus, we assume that the typical speed across segments is either 0.8 m/s or 0.3 m/s. In addition, we utilize the reduction factor of the walking speed when the inclination angles, including the trim and heel angles, reach 30° to assess the worst-case speed (here, this factor can be computed using Fig. 3). Let R_1 be the reduction factor for a 30° transverse to the walking direction and let R_2 be that in the walking direction. $d_W(\overrightarrow{v_iv_j})$ is computed as

$$d_W(\overrightarrow{v_iv_j}) = \frac{d_T(\overrightarrow{v_iv_j})}{R_1 \times R_2}. \tag{3}$$

2) $\mathcal{D}_j$ ON EACH LANDMARK v_j.

To evaluate $\mathcal{D}_j$ on each landmark v_j. We need to know the deadline C for emergency navigation in the dynamic hazardous ship indoor environment (here, C can be computed using (1)) and the duration of hazardous arrival at v_u.

It is necessary to traverse the segments affected by hazards before they become impassable. To predict these segments, the corresponding v_u, and the duration of hazardous arrival at v_u, we need to assess the dynamics (including the expansion direction and speed) of hazards. Fig. 6 shows the principle of determining v_u. In the figure, v_h is a hazardous

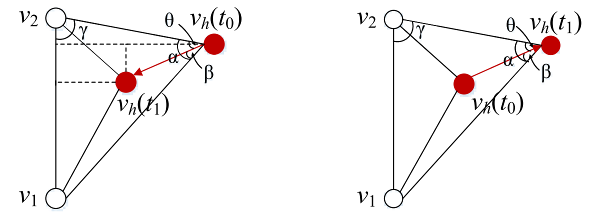

(a) v_h moves closer to a segment (b) v_h moves away from a segment

FIGURE 6. Moving tendency of the hazardous sensor v_h with a segment.

sensor, and $v_h(t_0)$ and $v_h(t_1)$ represent the locations of v_h at times t_0 and t_1, respectively. We insert v_2 into $\mathcal{V}''$ if the following conditions are satisfied. First, the hazardous node v_h is required to move closer to the segment $\overrightarrow{v_1v_2}$ instead of departing from it. Second, $\theta \leq \alpha$ and $\beta \leq \alpha$, where θ denotes the angle between $\overline{v_h(t_0)v_2}$ and $\overline{v_h(t_0)v_h(t_1)}$, α represents the angle between $\overline{v_h(t_0)v_2}$ and $\overline{v_h(t_0)v_1}$, and β indicates the angle between $\overline{v_h(t_0)v_h(t_1)}$ and $\overline{v_h(t_0)v_1}$. The corresponding duration of hazardous arrival at v_2 is computed as follows:

$$D(v_2, v_1) = \frac{dis_{\overline{v_2v_h(t_0)}} \times \sin\gamma}{vel_{v_h}^{\overrightarrow{v_1v_2}}}, \tag{4}$$

where γ denotes the angle between $\overrightarrow{v_2v_1}$ and $\overline{v_2v_h(t_0)}$ and $dis_{\overline{v_2v_h(t_0)}}$ indicates the distance between v_2 and $v_h(t_0)$. $vel_{v_h}^{\overrightarrow{v_1v_2}}$ represents the velocity of v_h toward $\overrightarrow{v_1v_2}$ (refer to [15] (Section 3.4.1) for a detailed description of the computation of $vel_{v_h}^{\overrightarrow{v_1v_2}}$).

Next, we can compute $\mathcal{D}_j$ on each landmark v_j. We initialize all $D(v_j, v_i)$ on each landmark v_j as follows:

$$D(v_j, v_i) = \begin{cases} +\infty & \text{j} \neq \text{o} \\ C & \text{j} = \text{o} \end{cases}. \tag{5}$$

The final $\mathcal{D}_j$ at each landmark v_j is determined according to Algorithm 1.

C. CONSTRUCTING THE TWO TYPES OF LOOK-UP TABLES

We construct the two types of look-up tables to guide the user's movement. Details of the algorithm for constructing these look-up tables are provided below.

- **Look-up table to the exit:** The look-up table TAB $[v_i]$ to the exit at landmark v_i consists of 3-tuples (s, v_j, δ), with the interpretation that the path with the minimum typical delay δ from v_i to the exit v_o and the guaranteed worst-case delay bound s, has $\overrightarrow{v_iv_j}$ as the outgoing segment from v_i. The reader is referred to [29] (Section IV) for a detailed description of the LOOK-UP TABLE SYNTHESIS Algorithm to construct TAB $[v_i]$ at each landmark v_i.
- **Look-up table to $\mathcal{V}''$:** This type of entry is only constructed under the following condition: if we traverse segment $\overrightarrow{v_iv_j}$, a navigation path $p(v_i)$ without any segments that will be damaged by dynamic hazards does not exist. The pseudocode for constructing the look-up table to $\mathcal{V}''$ is shown in Algorithm 2.

Algorithm 1 Computing $\mathcal{D}_j$

Input: Dynamics of hazards; $G' = (\mathcal{V}', \mathcal{E}')$;
Output: $\mathcal{D}_j$;
Initialize $\mathcal{D}_j$ for all $v_j \in \mathcal{V}'$, as in (3) above;
for *each landmark* $v_j \in \mathcal{V}'$ **do**
  for *each landmark* $v_i \in \mathcal{N}_j$ **do**
    for *each hazardous sensor* v_h **do**
      if *the angles in* $\triangle v_i v_j v_h$ *meet the conditions in Section* IV-B **then**
        Compute $\frac{dis_{v_h}^{\overrightarrow{v_i v_j}}}{vel_{v_h}^{\overrightarrow{v_i v_j}}}$;
        if $\frac{dis_{v_h}^{\overrightarrow{v_i v_j}}}{vel_{v_h}^{\overrightarrow{v_i v_j}}} < D(v_j, v_i)$ **then**
          $D(v_j, v_i) = \frac{dis_{v_h}^{\overrightarrow{v_i v_j}}}{vel_{v_h}^{\overrightarrow{v_i v_j}}}$;
        end
      end
    end
    Insert $D(v_j, v_i)$ into $\mathcal{D}_j$;
  end
end

Algorithm 2 Constructing Look-up Table to $\mathcal{V}''$

Input: TAB $[v_i]$ on each landmark v_i; $G' = (\mathcal{V}', \mathcal{E}')$;
Output: Look-up table to $\mathcal{V}''$;
$exist1$ = FALSE // Does $p(v_i)$, which contains $\overrightarrow{v_i v_j}$, include a segment affected by hazards?;
$exist2$ = FALSE // Should the look-up table to $\mathcal{V}''$ be constructed?;
$Count = 0$;
for *each landmark* $v_i \in \mathcal{V}'$ **do**
  for *each* v_j *existing in* TAB $[v_i]$ **do**
    for *each* $p(v_i)$*, which contains* $\overrightarrow{v_i v_j}$*,* **do**
      for *each segment* $\overrightarrow{v_x v_y} \in p(v_i)$*, which contains* $\overrightarrow{v_i v_j}$*,* **do**
        if $\overrightarrow{v_x v_y}$ *is affected by hazards* **then**
          $exist1$ = TRUE;
        end
      end
      if $exist1$ = TRUE **then**
        $Count$ ++;
      end
    end
    if $Count$ = *the number of* $p(v_i)$*, which contains* $\overrightarrow{v_i v_j}$*,* **then**
      $exist2$ = TRUE;
    end
    if $exist2$ = TRUE **then**
      Call LOOK-UP TABLE SYNTHESIS Algorithm to $\mathcal{V}''$;
    end
  end
end

- **An example:** Let us now consider the process of constructing both these types of look-up tables according to the navigation model shown in Fig. 4d. First, we construct the look-up table to the exit v_o, and then we construct the look-up table to $\mathcal{V}''$ (here $\mathcal{V}''$ includes v_2 and v_o).
  1) Look-up table to the exit v_o (see Fig. 7):

D. USER NAVIGATION

We now explain how to use the final look-up tables to guide the user to the exit. We assume $C = 25$, $D(v_o, v_1) = 25$, and $D(v_2, v_1) = 20$ at the initial time. Starting from v_a, the user first traverses $\overrightarrow{v_a v_1}$ (if $20 \le C < 25$, or $C \ge 25$ but $D(v_o, v_1) < 25$ and $D(v_2, v_1) < 20$, then the user takes $\overrightarrow{v_a v_o}$). Upon reaching v_1, the user checks to determine $C - d_{\overrightarrow{v_a v_1}}$, $D(v_o, v_1) - d_{\overrightarrow{v_a v_1}}$, and $D(v_2, v_1) - d_{\overrightarrow{v_a v_1}}$:

1) If $C - d_{\overrightarrow{v_a v_1}} \ge 20$ and $D(v_2, v_1) - d_{\overrightarrow{v_a v_1}} \ge 10$, then the user traverses $\overrightarrow{v_1 v_2}$;

2) If $C - d_{\overrightarrow{v_a v_1}} \ge 20$, $D(v_2, v_1) - d_{\overrightarrow{v_a v_1}} < 10$ but $D(v_o, v_1) - d_{\overrightarrow{v_a v_1}} \ge 15$, then the user traverses $\overrightarrow{v_1 v_o}$;

3) If $15 \le C - d_{\overrightarrow{v_a v_1}} < 20$ and $D(v_o, v_1) - d_{\overrightarrow{v_a v_1}} \ge 15$, then the user traverses $\overrightarrow{v_1 v_o}$.

V. EVALUATIONS

We evaluate the developed deadline-aware adaptive emergency navigation strategy, ANT. This section presents the performance results of both experiments on real hardware and extensive simulations.

A. EXPERIMENTS ON A REAL-WORLD PASSENGER SHIP

In this part, we introduce our experiments on a real-world passenger ship, "Yangtze Gold 7." Our testbed is implemented

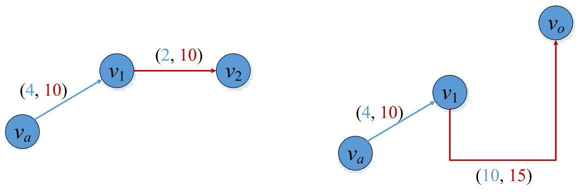

(a) Simplified model for v_2 (b) Simplified model for v_o

FIGURE 8. Simplified models for $\mathcal{V}''$.

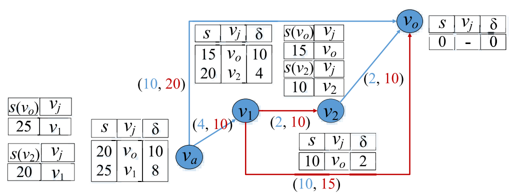

FIGURE 9. Final look-up tables.

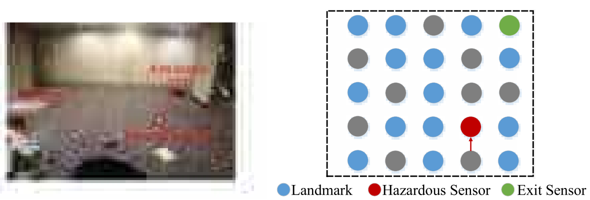

(a) (b)

FIGURE 10. Experimental setup. The hazardous region is assumed to expand as indicated by the red arrow.

of 1 m between two neighboring sensors. The sensor in the top-right corner (coordinate (5, 5)) is designated as the exit sensor, as shown in Fig. 10. We set one hazardous region consisting of one hazardous sensor because of the small-scale nature of the experiment, and the frequency and intensity of the update on hazards are utilized to represent the extent of the dynamics of hazards. Here, we select 14 sensors as the navigation landmarks based on the characteristics of the indoor environment of the ship to assist the user with movement. The typical walking speed and the worst-case speed are set to 1.2 m/s and 0.4 m/s, respectively. This allows us to compute both the typical delay and the worst-case delay for each segment based on the two speeds and the segment length. Next, we construct the two types of look-up tables at each landmark and base user navigation on these tables.

2) Look-up table to $\mathcal{V}''$ (v_2 and v_o): According to Algorithm 2, the look-up table to $\mathcal{V}''$ should be constructed on v_a and v_1, as shown in Fig. 9, based on the simplified model (illustrated in Fig. 8):

Fig. 11a depicts the escape time of our method when the human speed is set to 1.2 m/s. We see that the user always safely arrives at the exit within the deadline (the deadline is set to 23 s in our experiments). That is, the navigation success ratio of ANT reaches 100%. Fig. 11b shows the ANT efficiency in terms of path length. We can see that the path length varies with the movement speed of the user. This becomes even more significant in large-scale simulations for

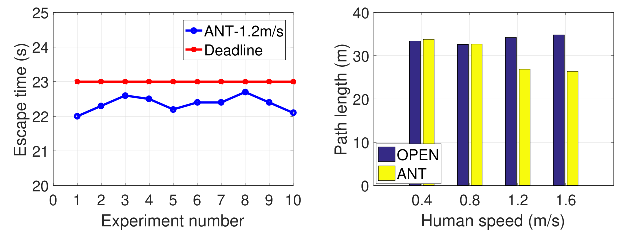

(a) (b)

FIGURE 11. (a) Escape time versus experiment number. (b) Path length versus human speed.

FIGURE 12. Experimental layout on a real-word passenger ship. Sensors are deployed at the locations colored red and green. We select the sensors at the green-colored locations as the landmarks.

assessing the navigation efficiency using ANT, as measured by the path length.

B. SIMULATION

In this part, we evaluate the effectiveness and scalability of ANT in a large-scale network through simulations. The performances of ANT and two state-of-the-art approaches are compared in terms of navigation efficiency and user safety perspective.

1) Simulation framework: Our simulation parameters are set using real-world passenger ship parameters. We recorded the scene parameters of the "Yangtze Gold " passenger ship, and the layout is shown in Fig. 12.

To evaluate the efficiency of ANT, we compare it with the OPEN approach [15] and MA approach [13] from four perspectives, namely, the average path length, user escape time, navigation success ratio, and minimum distance to hazardous regions. We use a network topology of a grid partitioned with 1024 to 16,384 nodes in a rectangular area. To examine the scalability, we vary the size of the network and the number of deployed nodes while retaining the same network density.

In the simulations, all users are required to arrive at the exit. We assume that hazards exhibit dynamics in only one pattern, i.e., expansion. During the simulations, we randomly insert three hazardous regions into the network and specify

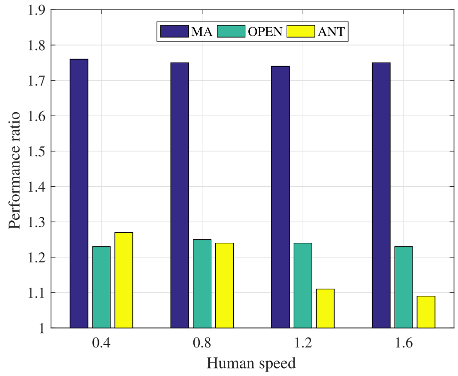

FIGURE 13. Performance ratio to the shortest path.

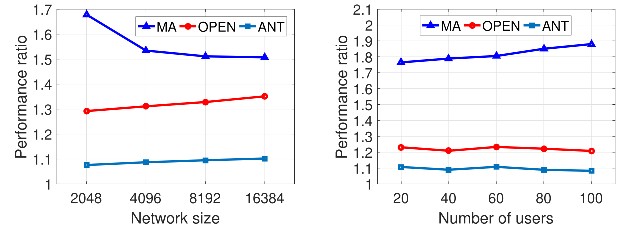

(a) Performance ratio versus network size (b) Performance ratio versus the number of users

FIGURE 14. Performance ratio to the shortest path when human speed = 1.2.

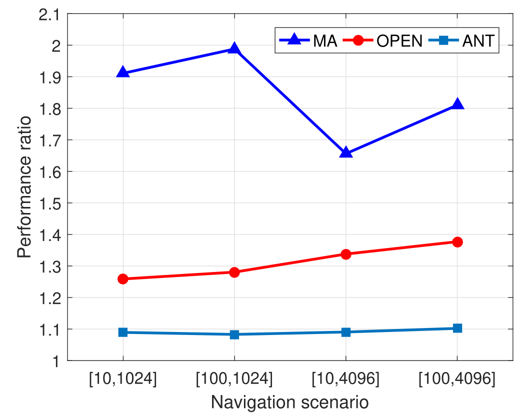

FIGURE 15. Performance ratio of the user escape time.

the dynamics of hazards as well as the walking speed of the users. The ratio of the size of each hazardous region to the total network size is maintained below 5%. Unless otherwise stated, we randomly generate 10 internal users in the field. The simulation results reported below are the average values after 20 runs.

We perform the simulation experiments written in Matlab in a personal computer (Operating System: Windows 10 Education) equipped with Intel Core i5-8400 CPU @ 2.8GHz and 8.0 GB memory. The total time needed for conducting our simulations is about 174 minutes.

2) Average length of navigation paths: We evaluate the efficiency of the path by comparing the length of the path provided by each approach L with the length of the shortest path that does not cross hazardous regions L_{OPT}. The performance ratio is defined as $\frac{L}{L_{OPT}}$. We uniformly deploy 1024 nodes in the sensor field. The worst-case speed (corresponding to the worst-case delay) and the typical speed (corresponding to the typical delay) are set to 0.4 and 1.2, respectively. Fig. 13 shows the performance ratio of the three approaches under different walking speeds. The results in the figure indicate the superior path efficiency of our method when the speed of human movement is equal to or greater than 1.2.

We further evaluate the scalability of our method in larger-scale networks. Specifically, we perform a group of simulations where the network size ranges from 2048 to 16,384, and the walking speed of the users is set to 1.2. Fig. 14a shows the performance ratio of the three approaches under different network sizes. As can be seen, MA maintains the ratio above 1.5, OPEN maintains the ratio at approximately 1.3, and our method achieves a ratio lower than 1.1. This result demonstrates that the performance ratio using our method presents distinct stability as the network size is increased. Starting from the current landmark, the user is navigated to the next superior landmark using the two types of look-up tables constructed by ANT, which means that the performance ratio does not depend on the size of the network.

We also evaluate the performance ratio by varying the number of users. We conduct a group of simulations in which the number of users is set to 20, 40, 60, 80, and 100 and the walking speed of the users is fixed at 1.2. The sensor field is uniformly partitioned with 1024 nodes. Fig. 14b shows the performance ratio to the shortest path under different numbers of users. We can see that MA has an increased ratio as the number of users is increased, whereas OPEN and our method maintain the ratio unchanged at approximately 1.2 and 1.1, respectively.

3) User escape time: The purpose of this group of simulations is to compare our method with MA and OPEN in terms of user escape time. A shorter escape time indicates a more efficient navigation path. In this simulation, 10 and 100 users are inserted into networks with sizes of 1024 and 4096, respectively. The walking speed of the users is set to 1.2. Fig. 15 shows the user escape time of the three approaches under different navigation scenarios. Our method yields a shorter escape time than the other two approaches. This is because our method can determine a safe path that avoids unnecessary detours according to the actual walking speed of the users.

4) Navigation success ratio: We evaluate the navigation success ratio of the three methods. The time available for passenger evacuation on a damaged ship is limited. Passengers must arrive at the exit before the deadline; otherwise, their navigation fails. Therefore, we can evaluate the navigation success ratio by calculating the possibility of reaching the exit within the deadline. In our simulation, this possibility is expressed as 1-$\frac{F(T)}{Q_u}$, where Q_u denotes the number of users and $F(T)$ is computed by (4).

$$F(T) = \begin{cases} 0 & T \le C \\ T-C & T > C \end{cases}, \tag{6}$$

where T denotes the user escape time.

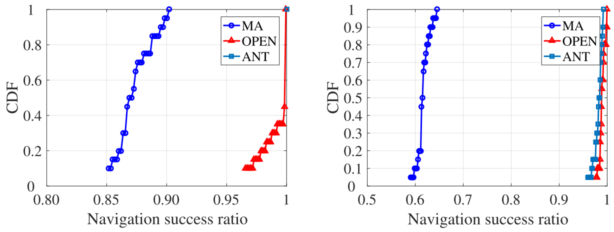

(a) Walking speed = 1.2 (b) Walking speed = 0.4

FIGURE 16. CDF of the navigation success ratio.

To compare the navigation success ratios, we consider the case in which 1024 nodes are uniformly deployed in the sensor field, and 100 users escape at the typical speed (1.2) or the worst-case speed (0.4). The deadline C is fixed at 25. Fig. 16a shows that our method outperforms OPEN and MA by always achieving a navigation success ratio of 100% when the walking speed is set to 1.2. MA and OPEN fail to ensure the navigation success in certain scenarios because they are likely to cause detours, which increases the user escape time and thus leads to the navigation failure.

Fig. 16b shows the cumulative distribution function (CDF) of the navigation success ratio of the three approaches when the speed of human movement is set to 0.4. We can see that the navigation success ratio of our method is similar to that of OPEN, where more than 96% of the users can be successfully navigated to the exit. This is because detours are inevitably included to ensure user safety when the speed of human movement is very low. Despite this, both OPEN and our method outperform MA in terms of the navigation success ratio.

Considering the influence of dynamic ship motion on the walking speed, we conduct a group of additional simulations to evaluate the navigation success ratio of the three approaches further. During the simulations, we assume that the change of the heel angle is an iterative process. Specifically, the angle increases from $-20°$ to $+20°$ and is incremented by $5°$ from segment to segment. Next, it decreases from $+20°$ to $-20°$ and is diminished by $5°$ from segment to segment. The process is repeated until users arrive at the exit node. According to the law of the change of the heel angle, we can calculate the speeds across segments (refer to the speed reduction data obtained by Monash in Fig. 3a). Here, the typical walking speed is set to 1.2, and 1024 nodes are uniformly deployed in the sensor field. The deadline C is fixed at 25. Fig. 17 shows the CDF of the navigation success ratio of the three approaches. We can see that our method outperforms OPEN and MA by achieving a nearly 100% navigation success ratio.

5) Minimum distance to hazardous regions: We evaluate the absolute safety of the path planned by the three approaches. Let B denote the minimum distance from the node on the path to hazardous regions and B_{OPT} denote the minimum distance to hazardous regions from the optimal path that maximizes B. The performance ratio is defined as $\frac{B}{B_{OPT}}$. A larger ratio indicates improved chances of the navigated user to avoid hazardous regions. Nevertheless, it is unnecessary to find a path for which the maximum performance ratio is achieved because that often means that the planned path is over-conservative, which can increase the time spent in the navigation environment, thereby reducing the overall safety of the guided users.

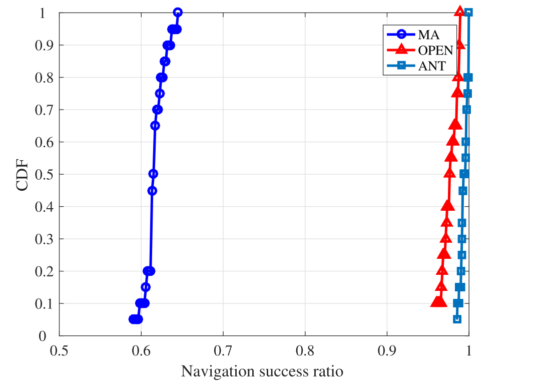

FIGURE 17. CDF of the navigation success ratio considering dynamic ship motion.

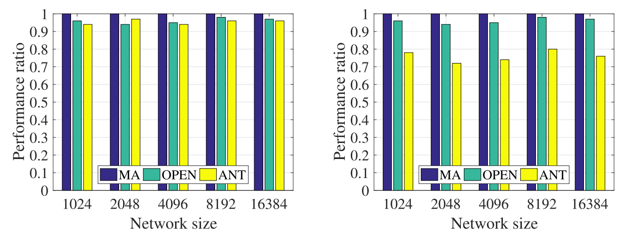

(a) Walking speed = 0.4 (b) Walking speed = 1.2

FIGURE 18. Performance ratio of the minimum distance to hazards.

Fig. 18a shows the performance ratio of the three approaches when the walking speed is set to 0.4. We can see that the performance ratio is not affected by the network size. The MA approach presents the optimal result with the ratio = 1. Both our method and OPEN have a performance ratio of approximately 0.95, which is slightly lower than that of MA. Fig. 18b shows the performance ratio when the speed is set to 1.2. In this case, the performance ratio of both MA and OPEN remains unchanged, whereas the ratio of our method is lower by approximately 20%, which does not indicate a considerable threat to user safety.

VI. CONCLUSION

Emergency navigation is essential for passengers (network users) on a damaged ship. Both user safety and navigation efficiency are critical requirements for successful navigation. Considering the deadline for ship evacuation and the influence of ship inclination on the walking speed, it is challenging to ensure passenger survival. In this study, based on graph theory, we design a deadline-aware adaptive emergency navigation strategy, ANT, for dynamic hazardous ship evacuation. Our method can identify a navigation path with the minimum typical delay while guaranteeing the avoidance of dynamic hazardous regions and respecting the specified deadline under all circumstances. Both small-scale experiments and extensive simulations are used to demonstrate the advantages of our method.

REFERENCES

[1] F. Stefanidis, E. Boulougouris, and D. Vassalos, "Ship evacuation and emergency response trends," in *Design and Operation of Passenger Ships*. 2019.

[2] D.-G. Yoon and C.-S. Kim, "Analysis report of the elapse for costa Concordia's disaster," *J. Korean Soc. Mar. Environ. Saf.*, vol. 18, no. 4, pp. 331–335, Aug. 2012.

[3] C. Nasso, S. Bertagna, F. Mauro, A. Marinò, and V. Bucci, "Simplified and advanced approaches for evacuation analysis of passenger ships in the early stage of design," *Brodogradnja*, vol. 70, no. 3, pp. 43–59, Sep. 2019.

[4] R. Bellas, J. Martínez, I. Rivera, R. Touza, M. Gómez, and R. Carreño, "Analysis of naval ship evacuation using stochastic simulation models and experimental data sets," *Mol. Cellular Biomechanics*, vol. 122, no. 3, pp. 971–995, 2019.

[5] M. Hu and W. Cai, "Evacuation simulation and layout optimization of cruise ship based on cellular automata," *Int. J. Comput. Appl.*, vol. 42, no. 1, pp. 36–44, Jan. 2020.

[6] J.-P. Wang, M.-R. Wang, J.-L. Zhou, Q.-J. Zuo, and X.-X. Shi, "Simulation based optimal evacuation plan in vertical ship lift: A case study," *Eng. Comput.*, vol. 37, no. 5, pp. 1757–1786, Jan. 2020.

[7] M. Chen, K. Liu, J. Ma, Y. Gu, Z. Dong, and C. Liu, "SWIM: Speed-aware WiFi-based passive indoor localization for mobile ship environment," *IEEE Trans. Mobile Comput.*, early access, Oct. 16, 2019, doi: 10.1109/TMC.2019.2947667.

[8] M. Chen, K. Liu, J. Ma, X. Zeng, Z. Dong, G. Tong, and C. Liu, "MoLoc: Unsupervised fingerprint roaming for device-free indoor localization in a mobile ship environment," *IEEE Internet Things J.*, early access, Jun. 22, 2020, doi: 10.1109/JIOT.2020.3004240.

[9] Q. Li, M. De Rosa, and D. Rus, "Distributed algorithms for guiding navigation across a sensor network," in *Proc. 9th Annu. Int. Conf. Mobile Comput. Netw. (MobiCom)*, 2003, pp. 313–325.

[10] M. Li, Y. Liu, J. Wang, and Z. Yang, "Sensor network navigation without locations," in *Proc. 28th Conf. Comput. Commun. (IEEE INFOCOM)*, Apr. 2009, pp. 2419–2427.

[11] D. Chen, C. K. Mohan, K. G. Mehrotra, and P. K. Varshney, "Distributed in-network path planning for sensor network navigation in dynamic hazardous environments," *IEEE. Trans. Wireless Commun. Mobile Comput.*, vol. 12, no. 8, pp. 739–754, Jun. 2012.

[12] G. Alankus, N. Atay, C. Lu, and O. B. Bayazit, "Adaptive embedded roadmaps for sensor networks," in *Proc. IEEE Int. Conf. Robot. Autom.*, Apr. 2007, pp. 3645–3652.

[13] J. Wang, Z. Li, M. Li, Y. Liu, and Z. Yang, "Sensor network navigation without locations," *IEEE Trans. Parallel Distrib. Syst.*, vol. 24, no. 7, pp. 1436–1446, Jul. 2013.

[14] C. Buragohain, D. Agrawal, and S. Suri, "Distributed navigation algorithms for sensor networks," in *Proc. 25th IEEE Int. Conf. Comput. Commun. (IEEE INFOCOM)*, Apr. 2006, pp. 1–10.

[15] L. Wang, Y. He, W. Liu, N. Jing, J. Wang, and Y. Liu, "On oscillation-free emergency navigation via wireless sensor networks," *IEEE Trans. Mobile Comput.*, vol. 14, no. 10, pp. 2086–2100, Oct. 2015.

[16] C. Wang, H. Lin, and H. Jiang, "CANS: Towards congestion-adaptive and small stretch emergency navigation with wireless sensor networks," *IEEE Trans. Mobile Comput.*, vol. 15, no. 5, pp. 1077–1089, May 2016.

[17] L. Wang, Y. He, Y. Liu, W. Liu, J. Wang, and N. Jing, "It is not just a matter of time: Oscillation-free emergency navigation with sensor networks," in *Proc. IEEE 33rd Real-Time Syst. Symp.*, Dec. 2012, pp. 339–348.

[18] A. A. Ahmed, M. Al-Shaboti, and A. Al-Zubairi, "An indoor emergency guidance algorithm based on wireless sensor networks," in *Proc. Int. Conf. Cloud Comput. (ICCC)*, Apr. 2015, pp. 1–5.

[19] A. Desmet and E. Gelenbe, "Reactive and proactive congestion management for emergency building evacuation," in *Proc. 38th Annu. IEEE Conf. Local Comput. Netw.*, Oct. 2013, pp. 727–730.

[20] H. Bi and E. Gelenbe, "Routing diverse evacuees with cognitive packets," in *Proc. IEEE Int. Conf. Pervas. Comput. Commun. Workshops (PERCOM WORKSHOPS)*, Mar. 2014, pp. 291–296.

[21] Z. Dong and C. Liu, "Analysis techniques for supporting hard real-time sporadic gang task systems," *Real-Time Syst.*, vol. 55, no. 3, pp. 641–666, Jul. 2019.

[22] P. Valanto, "Time-dependent survival probability of a damaged passenger ship ii-evacuation in seaway and capsizing," HSVA, Hamburg, Germany, Tech. Rep. 1661, 2006, pp. 42–62.

[23] E. Vanem and R. Skjong, "Collision and grounding of passenger ships–risk assessment and emergency evacuations," in *Proc. 3th Int. Conf. Collision Grounding Ships. (ICCGS)*, vol. 195, 2004, p. 202.

[24] D. Lee, J.-H. Park, and H. Kim, "A study on experiment of human behavior for evacuation simulation," *Ocean Eng.*, vol. 31, nos. 8–9, pp. 931–941, Jun. 2004.

[25] D. Pan, C. Lin, Z. Zhou, Y. Sun, Y. Sun, and Z. Liu, "Hydrostatic analyses of uprighting processes of a capsized and damaged ship," *Int. Shipbuilding Prog.*, vol. 65, no. 1, pp. 73–92, Jun. 2018.

[26] X. Zhang, Z. Lin, P. Li, D. Liu, Z. Li, Z. Pang, and M. Wang, "A numerical investigation on the effect of symmetric and asymmetric flooding on the damage stability of a ship," *J. Mar. Sci. Technol.*, vol. 2020, pp. 1–15, Feb. 2020.

[27] J. Sun, Y. Guo, C. Li, S. Lo, and S. Lu, "An experimental study on individual walking speed during ship evacuation with the combined effect of heeling and trim," *Ocean Eng.*, vol. 166, pp. 396–403, Oct. 2018.

[28] W. Bles, S. A. E. Nooy, and L. C. Boer, "Influence of ship listing and ship motion on walking speed," in *Proc. Int. Conf. Pedestrian Evacuation Dyn. (PED)*, 2002, pp. 437–452.

[29] S. Baruah, "Rapid routing with guaranteed delay bounds," in *Proc. IEEE Real-Time Syst. Symp. (RTSS)*, Dec. 2018, pp. 13–22.

[30] K. Yoshida, M. Murayama, and T. Itakaki, "Study on evaluation of escape route in passenger ships by evacuation simulation and full-scale trials," Res. Inst. Mar. Eng., Mitaka, Japan, Tech. Rep., 2001.

YUTING MA is currently pursuing the master's degree in marine navigation with the Wuhan University of Technology (WUT), Wuhan, China. Her research interests focus on emergency navigation and evacuation.

KEZHONG LIU (Member, IEEE) received the B.S. and M.S. degrees in marine navigation from the Wuhan University of Technology (WUT), Wuhan, China, in 1998 and 2001, respectively, and the Ph.D. degree in communication and information engineering from the Huazhong University of Science and Technology, Wuhan, in 2006. He is currently a Professor with School of Navigation, WUT. His active research interests include indoor localization technology and data mining for ship navigation.

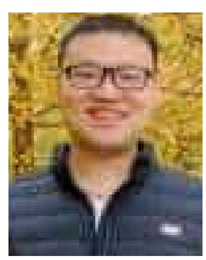

MOZI CHEN (Graduate Student Member, IEEE) received the B.S. degree in electric engineering from the Hubei University of Technology, China, in 2013, and the M.S. degree in navigation engineering from the Wuhan University of Technology (WUT), China, in 2016, where he is currently pursuing the Ph.D. degree. His research interests focus on wireless sensor networks and indoor localization.

JIE MA received the Ph.D. degree in computer science from the Huazhong University of Science and Technology, China, in 2010. He is currently an Associate Professor with the School of Navigation, Wuhan University of Technology. His researches include networked sensing systems, and data-driven intelligent transportation systems, supported by National Natural Science Foundation of China. He has over 20 published journal and conference papers in the related fields.

XUMING ZENG received the Ph.D. degree in communication engineering from the China University of Geosciences, Wuhan, China, in 2018. He is currently pursuing the Ph.D. degree in traffic and transportation engineering with the School of Navigation, Wuhan University of Technology, Wuhan, China. He has been studying wireless ad-hoc network for shipboard environment with the Wuhan University of Technology, since 2018. From 2016 to 2017, he was a joint training Ph.D. student with the Electrical and Computer Engineering, College of Engineering, Florida State University, Tallahassee, FL, USA. His research interests include routing protocols, MAC, QoS, clustering, radio resource management, traffic engineering, and performance analysis, for both wired and wireless networks.

KEHAO WANG received the B.S. degree in electrical engineering and the M.S. degree in communication and information system from the Wuhan University of Technology, Wuhan, China, in 2003 and 2006, respectively, and the Ph.D. degree from the Department of Computer Science, University of Paris-Sud XI, Orsay, France, in 2012. In 2013, he joined the School of Information Engineering, Wuhan University of Technology, where he is currently an Associate Professor. His research interests include cognitive radio networks, wireless network resource management, and embedded operating systems.

CONG LIU (Member, IEEE) received the Ph.D. degree in computer science from The University of North Carolina at Chapel Hill, in 2013. He is currently an Associate Professor with the Department of Computer Science, University of Texas at Dallas. His research interests include real-time systems and GPU. He has more than 30 published papers in premier conferences and journals. He received the Best Paper Award at the 30th IEEE RTSS and the 17th RTCSA.

Appendix C: Paper III

Ocean Engineering 263 (2022) 112403

Contents lists available at ScienceDirect

Ocean Engineering

journal homepage: www.elsevier.com/locate/oceaneng

Review

A survey of crowd evacuation on passenger ships: Recent advances and future challenges

Kezhong Liu [a], Yuting Ma [a], Mozi Chen [a,*], Kehao Wang [b], Kai Zheng [a]

[a] School of Navigation, Wuhan University of Technology, Wuhan, China
[b] School of Electronics and Information Engineering, Wuhan University of Technology, Wuhan, China

ARTICLE INFO

Keywords:
Building evacuation
Ship passenger evacuation
Passenger evacuation behavior
Passenger evacuation optimization
Passenger evacuation assessment

ABSTRACT

During ship emergencies, a reliable and efficient evacuation system is able to guide passengers to the appropriate muster stations as quickly as possible. The majority of the existing indoor evacuation systems provide emergency guidance for people trapped in general buildings. However, those systems fail to consider the unique challenges of ship passenger evacuation, such as the effect of ship motion on pedestrian motion and the feedback of pedestrian motion on ship inclination state. Consequently, evacuation guidance provided by these schemes may not always be optimal or may even make the evacuation worse due to the differences in the critical factors influencing emergency guiding between land-based buildings and passenger ships. This paper presents a systematic literature overview of recent advances in building evacuation, followed by a description of the challenges unique to evacuating passengers on vessels. Furthermore, the existing ship evacuation research is reviewed from three aspects, i.e., passenger behavior study, ship evacuation optimization, and evaluation of evacuation on passenger ships. A discussion of land-based evacuation schemes and prospects for ship evacuation is also presented.

1. Introduction

Over the past few years, passenger ships have become one of the most popular means of marine transportation and tourism (Fowler and Sorgaard, 2000; Yang et al., 2020). According to the data from Cruise Lines International Association (CLIA), the worldwide ocean cruise passenger capacity had a compound annual growth rate of 6.6% from 1990 to 2021 (Chiou et al., 2021). Fig. 1 shows the worldwide passengers carried from 1990 to 2021. Although modern cruise ships have made continuous progress in their structural designs, operating practices, marine technologies, and regulations in the past 20 years, passenger ship accidents still occurred with catastrophic consequences, e.g., the Costa Concordia disaster in 2012, which leads to 32 passengers/crew dead and more than 4000 injured (Mileski et al., 2014; Liu et al., 2022). According to Lloyds Register accident statistics, there were close to a hundred thousand deaths and injuries of vessels worldwide from 2000 to 2020, of which more than 5% were associated with inappropriate evacuation (Wang et al., 2022; Statistics, 2020). Therefore, an efficient evacuation scheme should be a favorable measure to reduce the losses of human lives in such catastrophes.

The existing evacuation works focus on designing land-based evacuation schemes (Li et al., 2019). As shown in Fig. 2, there are four kinds of guidance systems for evacuation in buildings on the land: (1) Signage-based evacuation scheme, (2) Leader-based evacuation scheme, (3) Mobile equipment (ME)-based evacuation scheme, and (4) Wireless Sensor Network (WSN)-based evacuation scheme. Earlier studies focused on the design of evacuation signage, including fixed and variable signage. The former is predetermined and does not respond to environmental dynamics, while the latter can adapt to changing hazard status or pedestrian flow to guide occupants (Chu et al., 2017). People may panic in emergency situation, especially when they are unfamiliar with the environment, leading to a poor understanding of evacuation signs, potentially resulting in a stampede and subsequent casualties. The deployment of evacuation leaders is an effective method to improve evacuation safety and efficiency. There are two types of leaders: human and robotic leaders. A mobile robot plays a role similar to that of a human leader in guided crowd evacuation. Moreover, mobile robots could be more advantageous in certain emergency cases where human leaders cannot be assigned to guide people out. Rapid development in intelligent wearable devices and mobile communication technologies has made ME-based evacuation possible. ME-based schemes typically assume the location information of people is available, which may not always be available in many

* Corresponding author.
E-mail addresses: kzliu@whut.edu.cn (K. Liu), 278827@whut.edu.cn (Y. Ma), chenmz@whut.edu.cn (M. Chen), kehao.wang@whut.edu.cn (K. Wang), kzheng@whut.edu.cn (K. Zheng).

https://doi.org/10.1016/j.oceaneng.2022.112403
Received 11 May 2022; Received in revised form 18 August 2022; Accepted 22 August 2022
Available online 5 September 2022

realistic situations (Fujihara and Yanagizawa, 2015; Mulloni et al., 2011; Gelenbe and Bi, 2014; Ikeda and Inoue, 2016; Iizuka and Iizuka, 2015; Wada and Takahashi, 2013; Fujihara and Miwa, 2012; Inoue et al., 2008; Chu and Wu, 2011; Chen et al., 2015; Chittaro and Nadalutti, 2008). The follow-up studies enable users to bootstrap their indoor evacuation services by themselves, avoiding the dependency on a pre-deployed localization system (Zheng et al., 2017; Shu et al., 2015; Yin et al., 2016; Dong et al., 2019; Teng et al., 2019; Li et al., 2020; Pan and Li, 2019). The ME-based systems neglect environmental dynamics, which may navigate users to hazardous areas. WSNs, capable of automatically monitoring environmental dynamics, should be incorporated into evacuation systems (Wang et al., 2014a). The WSN-assisted scheme can be divided into two categories: sensor-centric scheme, which is to find a direction for every single sensor, and user-centric scheme, which aims to provide customized guidance for each evacuee (Wu, 2017).

The above systems can effectively mitigate potential harm to building occupants in case of emergency. However, evacuating people on passenger vessels is still very challenging due to the unique characteristics of ship evacuation. For example, the impact of dynamic ship motion on pedestrian movement and the feedback of pedestrian movement on ship motion. Compared with the relatively mature land-based evacuation, the research on ship evacuation only started lately. There are mainly three kinds of research focusing on ship evacuation in terms of study intentions: (1) Investigating and analyzing the likely behavior of ship passengers in emergency situations; (2) Optimizing evacuation strategy for trapped passengers; (3) Evaluating ship evacuation performance. The first kind of research examines the characteristics of passengers (e.g., passengers' likely behavior when hearing an evacuation alarm) by conducting experiments, questionnaire surveys, or model-based simulations (Chen et al., 2016a; Wang et al., 2020; Valanto, 2006; Sun et al., 2018a). With respect to passenger evacuation optimization, most researchers focus on planning escaping routes (Ng et al., 2021), optimizing the staircase layout (Wang et al., 2022), and scheduling the time for issuing evacuation orders (Xie et al., 2020c). Ship passenger evacuation can be evaluated in two ways: advanced analyses and simplified analyses (Ni et al., 2017; Kang et al., 2019; Vilen et al., 2020; Galea et al., 2015; Wang et al., 2022; Cho et al., 2016; Sarshar et al., 2013; Xie et al., 2020b; Kana and Droste, 2019; Hifi, 2017; Vanem and Skjong, 2006). The simplified analysis considers a large passenger group as a whole. In contrast, every passenger is regarded as an individual with his/her characteristics in the advanced analysis.

This paper provides an analysis of ship passenger evacuation. The main contributions of our work are summarized as follows:

- A thorough analysis and comparison in recent advances in land-based indoor evacuation systems based on signage, leader, ME, and WSN, is presented.
- The specificities of passenger vessels, which result in the inapplicability of these land-based systems on ship passenger evacuation, are analyzed.
- The research about the evacuation on passenger vessels is reviewed from three perspectives, i.e., the likely behavior of passengers in emergency situations, the optimization of ship evacuation, and the evaluation of evacuation on passenger ships.
- Some comments on the land-based evacuation and the future research directions for the area of ship passenger evacuation are discussed.

This paper is organized as follows. Section 2 reviews the work pertaining to land-based evacuation with signage, leader, ME, and WSN. In Section 3, the unique characteristics and the recent research efforts about ship passenger evacuation are discussed, respectively. Finally, Section 4 presents our comments on the land-based evacuation schemes and the prospects for evacuating passengers on ships. The organization of our paper is illustrated in Fig. 3.

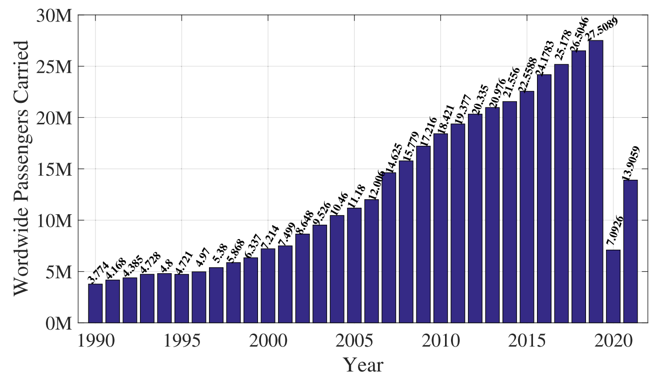

Fig. 1. Worldwide passengers carried from 1990 to 2021.

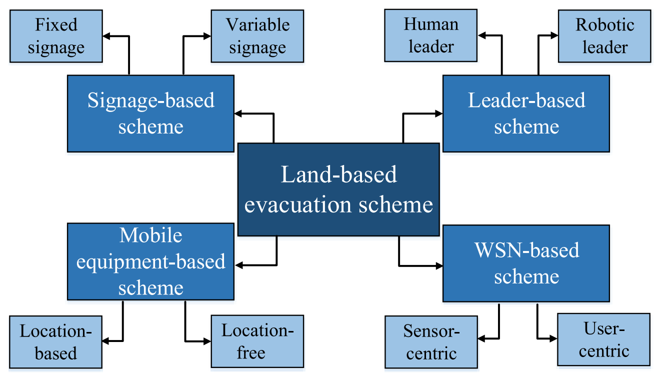

Fig. 2. Different types of crowd evacuation schemes.

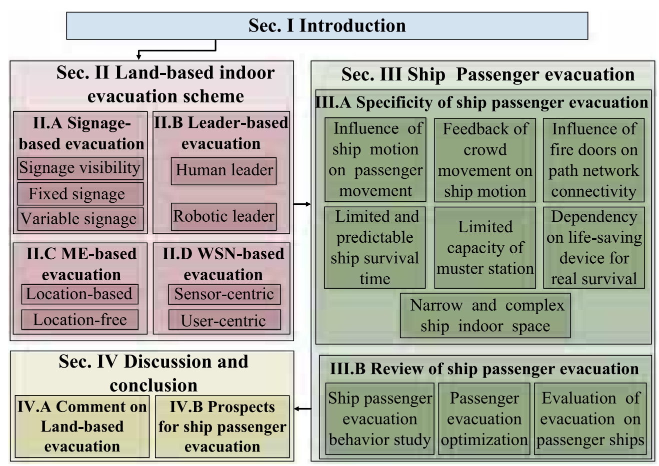

Fig. 3. Organization of this paper.

2. Land-based indoor evacuation scheme

A number of evacuation schemes for general buildings have been proposed, which can be classified into four groups, according to their guidance pattern: signage-based evacuation scheme, leader-based evacuation scheme, ME-based evacuation scheme, and WSN-based evacuation scheme (see Fig. 2). This section describes these different types of land-based indoor evacuation schemes.

2.1. Signage-based evacuation scheme

Signage systems are widely applied to large buildings such as urban rail transit stations, office buildings, and supermarkets. As a sort of

Table 1
Crowd evacuation with static signage.

Related work	Year	Optimization objective	Technique	Algorithm/Model	Scenario
Chen et al. (2009)	2009	Sign location	MCLP	Lagrangian relaxation algorithm	Single-floor supermarket
Chu and Yeh (2012)	2012	Sign location and number	MCLP with side constrains	Visibility graph	A transportation terminal
Motamedi et al. (2017)	2017	Sign location	Simulation	Grid-based model	SenriChuo station, A 440 m^2 rectangle area
Zhou et al. (2020)	2020	Sign location	Simulation	SF model	Beijing Subway Station
Yuan et al. (2018)	2018	Mixed layout of WS and GS	Simulation	SF model	A smoky hall

way-finding facility, the signage system does not only provide guidance to occupants who are unfamiliar with the layout of the building in normal situations, it also can offer safety information for evacuees in case of emergencies. Many studies have shown that the arrangement of signage is a feasible way to improve the efficiency of an emergency evacuation in most situations (Tang et al., 2009; Liu et al., 2011; Ronchi et al., 2012; Wang et al., 2014b; Cosma et al., 2016). Based on the response to contemporary evacuation situations, the existing signage-based evacuation system can be divided into fixed signage-based and variable signage-based guidance. The former is predetermined and cannot vary with the status of hazards and congestion, while the latter can respond to dynamic emergency conditions. This section presents a thorough review of the above-mentioned signage-based evacuation scheme.

2.1.1. Fixed signage-based evacuation scheme

The majority of existing signage-based evacuation schemes utilize static signs to provide stabilized guidance to evacuees unfamiliar with the building environment. Table 1 summarizes the previous work on crowd evacuation with static signs. Chen et al. formulated the location optimization for evacuation signs as a maximal-coverage location problem (MCLP) (Chen et al., 2009). Results showed that the proposed guidance arrangement scheme improved evacuation efficiency. However, it is not effective to simply optimize signage placement based on sign locations and visibility while ignoring the associated evacuation routes. Chu et al. found the position of signs that maximized coverage and constituted connected shortest paths by solving a maximum-coverage problem with side constraints (Chu and Yeh, 2012).

In addition, many researchers used simulations to reach efficient signage placement. Motamedi et al. utilized a Building Information Model (BIM) and a grid-based game engine to simulate the movement of pedestrians. Then the efficiency of the signage system design was investigated and optimized (Motamedi et al., 2017). Based on an improved social force model (SF), Yuan et al. proposed a mixed layout scheme of wall signs (WS) and ground signs (GS) with high evacuation efficiency in fire smoke (Yuan et al., 2018). Zhou et al. incorporated a perception probability model that quantified the probability pedestrians could notice and comprehend signs into a modified SF model to investigate crowd evacuation dynamics under the effects of different signage distribution schemes (Zhou et al., 2020).

2.1.2. Variable signage-based evacuation scheme

Since fixed signage cannot respond to the contemporary population density, it would more likely result in heavy congestion. Moreover, static guidance could also lead to pedestrians' frequent oscillations when hazards are on the evacuation routes predetermined by the fixed signs. Variable evacuation signage systems where signs change according to hazard status and pedestrian flow have attracted many researchers' attention in recent years (Tables 2 and 3). A series of studies have proved the effectiveness of the dynamic signage system. Hui et al. conducted experimental trials to test the comprehensibility and effectiveness of variable signs (Hui et al., 2014; Galea et al., 2017b,a). Considering the high cost of field experiments, Olyazadeh et al. exploited virtual environments (VEs) and questionnaires to investigate and evaluate dynamic signage for emergency evacuation (Olander et al., 2017; Galea et al., 2017a; Olyazadeh, 2013; Langner and Kray, 2014; Lin et al., 2017).

Some works take into account the effect of evolving emergencies and depend on the periodic recalculation of guidance information provided by signs to keep occupants safe (Veichtlbauer and Pfeiffenberger, 2011; Wang et al., 2008; Sharma et al., 2018; Luh et al., 2012; Cho et al., 2015a). Complying with the variable guidance, pedestrians can avoid hazardous areas and go out of the building with highest probability. However, frequent change in sign indications may cause possible confusion and reduce the credibility of guidance information disseminated by the signs. Wang et al. proposed that guidance should only be updated when emergency status varied significantly, as determined by emergency responders' subjective judgments (Wang et al., 2009). Desmet et al. scheduled the dynamic pointing directions of signage according to a capacity-reservation routing algorithm. Future capacity reservations can effectively forecast congestion and then assist subsequent path assignment (Desmet and Gelenbe, 2014). Chu et al. proposed a bi-level optimization approach to determine variable pedestrian evacuation guidance in buildings with convex polygonal interior spaces (Chu et al., 2017). The lower-level model utilized a modified floor field cellular automata model (FFCA) to predict congestion and passed the prediction to the upper-level model which used a decreased order of time (DOT) algorithm to calculate variable guidance.

2.2. Leader-based evacuation scheme

Many studies have proved that the staffing of trained evacuation leaders with complete knowledge of the layout of a building can guide evacuees to expected exits and significantly reduce the casualties (Spartalis et al., 2014; Yang et al., 2014; Wang et al., 2015b; Ma et al., 2017; Li et al., 2016; Yang et al., 2015; Vihas et al., 2012; Zhou et al., 2019b).

2.2.1. Human leader-based evacuation scheme

A trained human leader can issue guidance information and spread positive emotion. Over the past decades, several follow-the-leader evacuation models (e.g., SF model (Fig. 4a), vector field model (VF) (Fig. 4b), multi-grid model (Fig. 4c), and cellular automata model (CA) (Fig. 4d)) have been proposed, which can be used in leader effect understanding and leader distribution optimization (Tables 4 and 5).

Utilizing an extended dynamic communication field model (DCF), Wang *et al*. found the centripetal effect of evacuation assistants (Wang et al., 2015b). Yang et al. proposed a modified SF model to simulate guided crowd evacuation dynamics. Some phenomena, for example, pedestrians following the leader can escape with a faster velocity than those walking independently, were observed in the simulation results (Yang et al., 2014). Based on a CA-based model, Spartalis *et al*. discovered that a trained leader could not only trigger herding formations of crowds but activate alternative routes, which decreased congestion levels in specific passages and exits (Spartalis et al., 2014; Vihas et al., 2012). However, the effects of the staffing of guides are not always positive. Ma et al. found the dual effect of guides on pedestrian evacuation under limited visibility via an extended SF model (Ma et al., 2017). On the one hand, a few guides could already facilitate pedestrian evacuation when the neighbor density within the visual field was moderate. On the other hand, when the neighbors within the visual field were too many or too few, the effect of guides was usually negative.

Evacuation performance strongly correlates with the distribution and action of guiders. Yuan et al. proved the impact of the number

Table 2
Evaluating crowd evacuation with variable signage.

Related work	Year	Evaluation goal	Technique	Technique description	Scenario	Participant
Hui et al. (2014)	2014	Comprehensibility and Detectability	Survey, Experiment	An international web based survey, Field experiment	Queen Anne building	68
Olyazadeh (2013)	2013	Response time to dynamic signs, Effectiveness of exit signs, Realism of VR experiment	Experiment, Questionnaire	Immersive video environment	Three back projected wall (140 degree)	10
Lin et al. (2017)	2017	Effectiveness in evacuating through emergencies	Simulation	Agent-based model	Underground parking lot	110
Langner and Kray (2014)	2014	Impact on Mass Evacuation	Simulation	SF model	SC Preußen 06 e. V.	12,500
Olander et al. (2017)	2017	Impact on effectiveness of dissuasive exit signage	Questionnaire	Theory of affordances	An egress door within a virtually simulated office	46
Galea et al. (2017a)	2017	Effectiveness of ADSS, Most effective signage type	Experiment, Survey	An international web based survey, Field experiment	A rail station	200
Galea et al. (2017b)	2017	Effectiveness of improved ADSS	Experiment	Field experiment	Sant Cugat station	139

Table 3
Optimizing crowd evacuation with variable signage.

Related work	Optimization goal	Method	Method description	Validation
Cho et al. (2015b)	Shortening safe egress	Dijkstra algorithm	Reverse and simplify start and end nodes of Dijkstra algorithm by adding a virtual node	Simulation
Luh et al. (2012) and Wang et al. (2008, 2009)	Mitigating blocking	Divide-and-conquer	Dynamic programming method for each group subproblem, Lagrangian relaxation framework for Inter-group coordination	Numerical example, Simulation
Chu et al. (2017)	Reducing evacuation time	Bi-level optimization	FFCA for lower-level problem, DOT algorithm for upper-level problem	Numerical example
Sharma et al. (2018)	Supporting real-time reactive signage, Extensible, Energy-efficient, Scalable	DSS-SL	SDN forwarding devices, LED-based visible light communication scheme	–
Desmet and Gelenbe (2014)	Reducing evacuation time	Capacity-reservation algorithm	CPN, CCRP	Simulation

Table 4
The effect of human leader on crowd evacuation.

Related work	Year	Model	Scenario	Exit number	Exit size
Spartalis et al. (2014)	2014	CA model	20 m × 30 m retirement house	Three	0.8 m, 1.2 m
Yang et al. (2014)	2014	SF model	50 m × 50 m room	One	1 m
Li et al. (2016)	2016	Trace Model	Indoor classroom	Two	–
Vihas et al. (2012)	2012	CA model	A two-dimensional space with 17 sectors, a cubic space with 4 sectors	–	–
Wang et al. (2015b)	2015	Extended DCF model	26 m × 26 m room	One	0.8 m
Ma et al. (2017)	2017	SF model	15 m × 15 m room	One	4 m
Zhou et al. (2019b)	2019	SF model	Beijing's urban rail transit station	Three	3.4 m

of guiders on evacuation by using a CA-based model (Yuan and Tan, 2009). Hou et al. discovered that for evacuation under a single-exit scenario, only one or two leaders could exert a remarkable impact, while more leaders are expected for configurations with multi-exits (Hou et al., 2014). Wang et al. optimized the position of leaders while minimizing their number and observed that except for the distribution of leaders, other factors such as the number of evacuees guided by a leader, the visibility range of environments, and the leaders' speeds significantly affect evacuation efficiency (Wang et al., 2012; Zhang et al., 2021; Wang et al., 2015c, 2016). In addition, Cao et al. did not only derive the appropriate distribution of leaders but also optimized their guidance strategy (Cao et al., 2016; Zhou et al., 2019a; Yang et al., 2013).

2.2.2. Robotic leader-based evacuation scheme

Human leaders may arrive at the emergency site too late to assist crowd evacuation. In addition, they cannot be sent to guide evacuees out in some accidents like nuclear leakage because of security concerns. In such cases, the usage of robotic leaders could be attractive. Many simulators have been used to model robots and crowds to demonstrate the effectiveness of using robots for aiding emergency evacuations (Sakour and Hu, 2017).

Earlier works focused on indirectly evacuating evacuees utilizing autonomous robots, not involving human–robot interaction (Shell et al., 2005; Ferranti and Trigoni, 2008). Shell et al. described a multi-robot-based navigational aid deployment strategy with which a network of directional audio aids can be deployed automatically following an emergency with the assistance of a team of robots (Shell et al., 2005). Ferranti et al. devised two robot-assisted evacuation route discovery (ERD) mechanisms, namely Agent-to-Tag-ERD and Tag-to-Tag-ERD, with which robots can search for the shortest evacuation routes as soon as possible in parallel with their exploration of an unknown hazardous area (Ferranti and Trigoni, 2008).

Recently, the improvement in the trust in human–robot interaction makes it possible to guide occupants directly using emergency evacuation robots. Kim et al. designed a portable fire evacuation guide robot that can be thrown into fire scenes to explore the information about environmental conditions and trapped occupants, which would be transmitted to firefighters to determine a guide strategy that could be broadcast through the microphone and speaker system on the robot (Kim et al., 2009). Robinette et al. devised robots incorporating a model of human panic behavior to navigate evacuees safely to appropriate exits (Robinette and Howard, 2011). The above-mentioned robot-assisted evacuation systems require control and decision support from human operators. With the advance in integration techniques

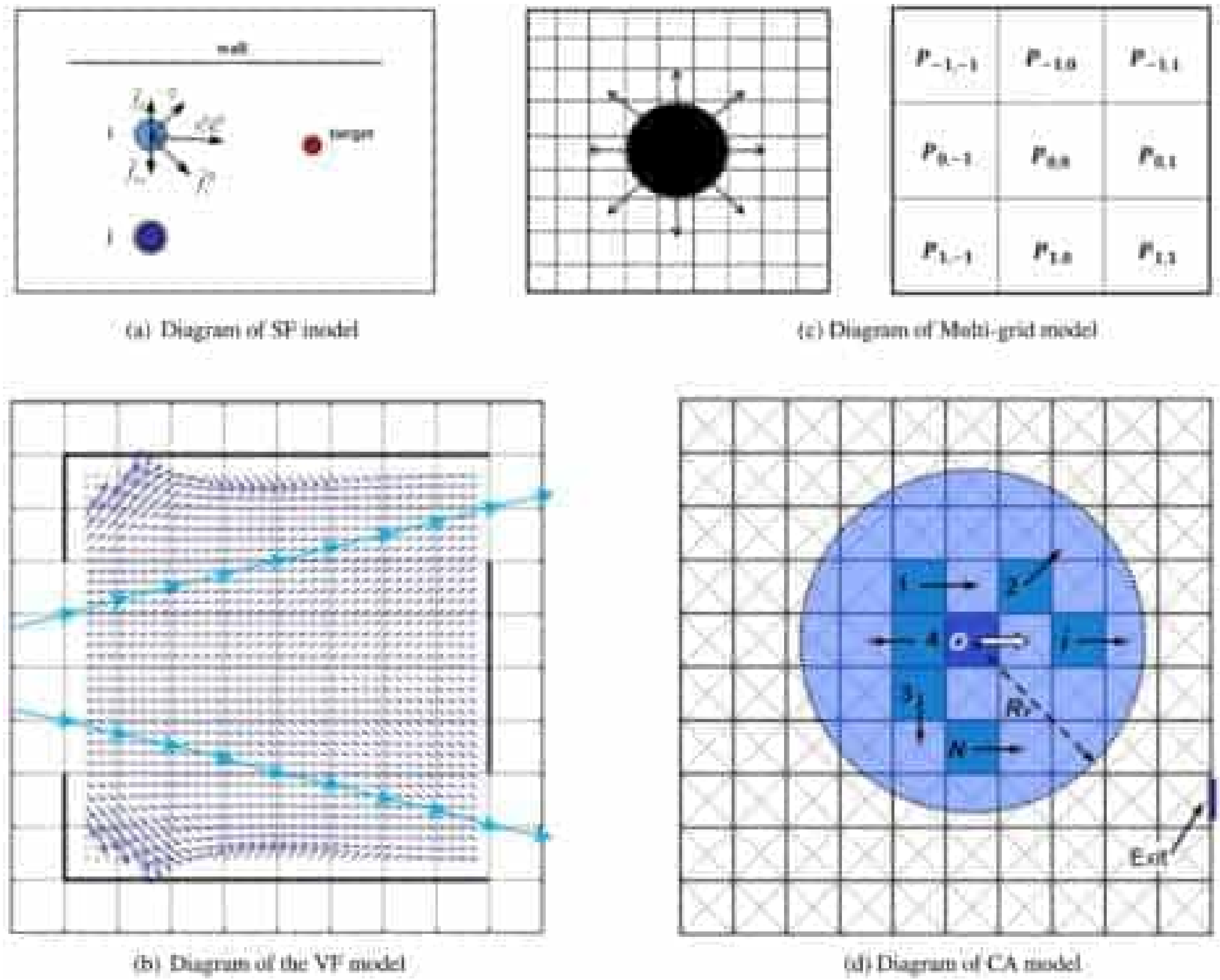

Fig. 4. Diagram of classical follow-the-leader evacuation model (Yuan and Tan, 2009; Okada and Ando, 2011; Cao et al., 2016; Yang et al., 2014).

Table 5
The influencing factors of human leader-based evacuation.

Related work	Year	Model	Influencing factor	Scenario	Exit number	Exit size
Okada and Ando (2011)	2011	VF model	Location, number	A room	Two	–
Ma et al. (2016)	2016	SF model	Location, number, visibility, distribution range of evacuees	20 m × 20 m room	One	1 m–20 m
Yuan and Tan (2009)	2009	CA model	Visibility, number	20 m × 20 m room	One	2 m
Wang et al. (2012)	2012	CA model, CF model	Location, number	26 m × 26 m room	One	0.4 m
Hou et al. (2014)	2014	SF model	Location, number, velocity, visibility	20 m × 20 m room	One, two, four	2 m
Cao et al. (2016)	2016	Multi-grid model	Guidance strategy, guider type, number and distribution	20 m × 10 m room	Two	1 m
Wang et al. (2015c)	2015	CA model, CF model	Walking speed, information transmission radius	26 m × 26 m room	One	0.8 m
Yang et al. (2015)	2015	SF model	Location, number	50 m × 50 m room	One	1 m
Wang et al. (2016)	2016	Multi-Information CF model	Sensing radius	0.4 m × 10 m T-shaped channel, 2 m × 24 m T-shaped channel	Two	2 m
Yang et al. (2013)	2013	Multi-agent model	Guiding route	80 × 80 area	Three	Radius 15, 10, 5
Zhou et al. (2019a)	2019	Hybrid bi-level model	Location, number, route	Beijing's urban rail transit station	Three	3.4 m
Zhang et al. (2021)	2021	E-AECM	Location	Spring city square of Jinan	–	–

and computing power, robots can evacuate occupants independently. Jiang *et al*. presented an adaptive dynamic programming approach (ADP) to control the motion of a robot for a desirable collective velocity (Jiang et al., 2017). Boukas et al. trained the intelligent emergency evacuation robots to attract evacuees heading towards saturated exits and redirect them to less blocked ones to ensure a faster and safer evacuation (Boukas et al., 2015; Tang et al., 2016; Wan et al., 2020; Zhang and Guo, 2015; Garrell et al., 2009).

2.3. ME-based evacuation scheme

Typical ME for assisting crowd evacuation includes smartphones and Augmented Reality (AR) headsets. This kind of equipment can present more useful and intuitive evacuation information than that provided by traditional techniques based on audio alarms and paper maps. In addition, with the fast development of AR and Virtual Reality (VR) technology, AR/VR-based wearable hardware such as the

Table 6
Crowd evacuation with ME.

Source	Location-based	Localization technique	Track-based	Tracking technique	Floor plan-based	Central server-based	Optimization objective	Capacity aware	Clustering aware
Iizuka and Iizuka (2015) and Wada and Takahashi (2013)	✓	GPS	×		✓	×	Evacuation time	×	×
Fujihara and Miwa (2012)	✓	GPS	×		✓	×	Evacuation time	✓	×
Ikeda and Inoue (2016)	✓	GPS	×		✓	✓	Evacuation time	×	×
Gelenbe and Bi (2014)	✓	Built-in camera	×		✓	✓	Survival rate	×	✓
Diao and Shih (2018) and Zhang et al. (2020c)	✓	Built-in camera	×		✓	✓	Evacuation time	×	×
Stigall and Sharma (2017)	✓	Built-in camera	×		✓	✓	Evacuation distance	×	×
Ahn and Han (2011)	✓	Built-in sensors	×		✓	✓	Evacuation time	×	×
Chen and Chung (2017) and Chen and Liu (2021)	✓	iBeacon	×		✓	✓	Evacuation time	✓	✓
Fujihara and Yanagizawa (2015)	✓	iBeacon	×		✓	×	True positive detection rate of guidance	×	×
Mulloni et al. (2011)	✓	Info points	×		✓	×	Evacuation distance	×	×
Fujihara and Miwa (2012)	✓	Wi-Fi	×		✓	×	Evacuation time	✓	×
Chen et al. (2015)	✓	RFID, iBeacon, RSSI-based	×		✓	✓	Evacuation time	✓	×
Chu (2010)	✓	NFC, RFID	×		✓	✓	Evacuation time	×	×
Nadalutti and Chittaro (2008) and Chittaro and Nadalutti (2008)	✓	RFID	×		✓	×	Navigation error, stops	×	×
Chu and Wu (2011)	✓	RFID	×		✓	✓	Distance, congestion, temperature	✓	×
Inoue et al. (2008)	✓	Radio beacon	×		✓	✓	Evacuation distance	×	×
Zheng et al. (2017)	×		✓	Image, IMU, WiFi	×	×	Spatial error, energy saving, path distance	×	×
Shu et al. (2015)	×		✓	IMU	×	×	Spatial error, energy saving	×	×
Zhang et al. (2020b) and Yin et al. (2016)	×		✓	WiFi, IMU	×	×	Spatial error, deviation detection time	×	×
Dong et al. (2019)	×		✓	Visual SLAM	×	×	Navigation success rate	×	×
Li et al. (2020)	×		✓	WiFi, IMU	×	×	Space error	×	×
Dong et al. (2020)	×		✓	Visual SLAM	×	✓	Navigation success rate, space error	×	×
Pan and Li (2019)	×		✓	IMU, iBeacon	×	✓	Navigation distance, navigation deviation, notification delay	×	×
Teng et al. (2019)	×		✓	Point clouds, IMU	×	✓	Tracking error, navigation success rate	×	×

wireless head-mounted display (HMD) has been introduced to study human evacuation behavior and train occupants. Using HMD-based VR experiments, Feng et al. investigated the response of evacuees to different types of information (e.g., crowd flow and exit signs) (Feng et al., 2021; Lin et al., 2020). Lin et al. examined the effect of repeated exposures to indoor environments on people's indoor wayfinding performance (Lin et al., 2019). In addition, Lovreglio et al. trained occupants to cope with emergencies in an earthquake or fire by using VR-based simulators (Lovreglio et al., 2018; Xu et al., 2014).

Based on the dependency on the pre-knowledge of user locations, the ME-based evacuation schemes are classified into two categories: location-based and location-free evacuation schemes using ME (Table 6). This section presents the review of the two schemes.

2.3.1. Location-based evacuation scheme using ME

Most of the existing ME-based evacuation schemes rely on the availability of location information on each user. Ikeda et al. exploited the built-in Global Positioning System (GPS) function to provide the position of smartphones (Ikeda and Inoue, 2016; Iizuka and Iizuka, 2015; Wada and Takahashi, 2013; Fujihara and Miwa, 2012). But it is challenging to receive satellite signals within a modern building. Therefore other location awareness systems become necessary for location-based indoor evacuation using ME. Chen et al. proposed that the location of each person can be periodically detected by his/her smartphone through signal strength-based localization or infrastructure-based positioning (e.g., radio-frequency ID (RFID) and iBeacon) (Chu, 2010; Nadalutti and Chittaro, 2008; Chittaro and Nadalutti, 2008; Chen et al., 2015; Chu and Wu, 2011; Shin et al., 2011). Gelenbe et al. identified evacuees' positions by the camera or sensors built in smartphones or AR headsets (Gelenbe and Bi, 2014; Zhang et al., 2020c; Ahn and Han, 2011; Stigall and Sharma, 2017). In addition, Mulloni *et al* exploited activity-based instructions to guide users from one info point to the next (Mulloni et al., 2011). In this system, only sparse 3D localization at selected info points in a building is necessary.

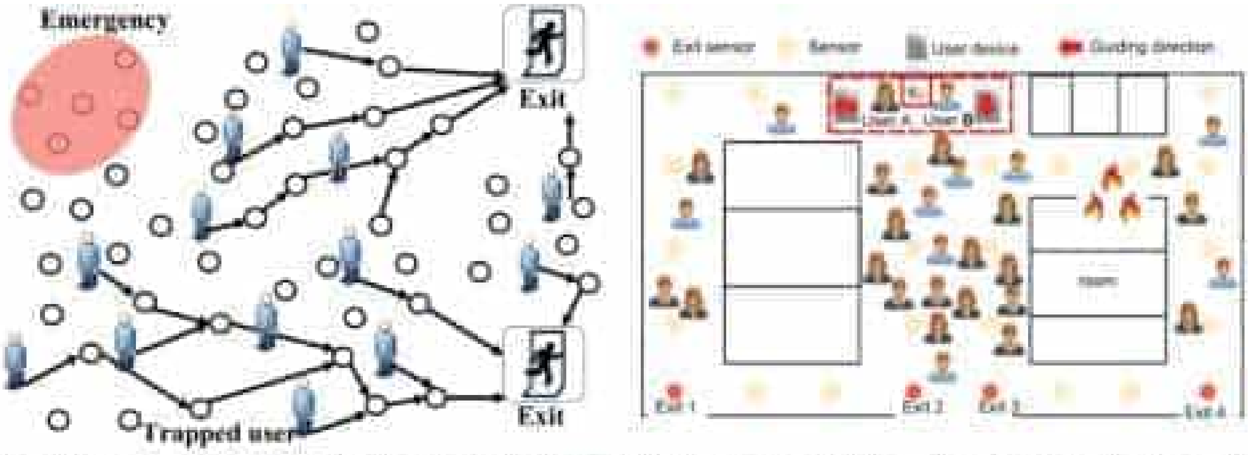

(a) A typical sensor-centric evacuation scheme using WSN (Wang et al., 2017). (b) A typical user-centric evacuation scheme using WSN (Wu, 2017).

Fig. 5. The typical sensor-centric and user-centric evacuation scheme using WSN (Wang et al., 2017). In (b), sensor s_1 can provide different guiding directions for the User A and User B even though both of them are located nearby s_1.

2.3.2. Location-free evacuation scheme using ME

The location information may not always be available in many realistic situations where emergency guidance is needed. Zheng et al. designed Peer-to-Peer (P2P) navigation systems on mobile phones, which enabled efficient navigation without resorting to pre-deployed location service and the availability of indoor maps (Zheng et al., 2017; Shu et al., 2015; Dong et al., 2019; Zhang et al., 2020b; Yin et al., 2016). In this kind of system, guiders recorded their traces in a variety of forms (e.g., pathway images, geomagnetic fields, or WiFi signals) and transmitted them to followers so that they could get prompt path instructions through their phones. However, P2P mode suffers from path deficiency in large complex indoor scenarios, which significantly hampers its application. Teng *et al*. merged the paths of different guiders into a global map by introducing a crowdsourcing scheme (Teng et al., 2019; Li et al., 2020; Pan and Li, 2019; Dong et al., 2020).

2.4. WSN-based evacuation scheme

WSN is a natural choice for supporting emergency evacuation, given the ubiquitous sensing and communication capability. Previous researches verified the effectiveness of WSN-assisted guiding mechanisms using simulations and real test-bed implementation approaches (Ahmed et al., 2015; Yin, 2015; Lung et al., 2016; Stigen, 2019). Fig. 5 shows the typical WSN-assisted emergency evacuation system. A number of sensor nodes are deployed in a building to monitor the time-varying environmental conditions, calculate guiding paths and send them to nearby evacuees equipped with radio modules. Existing WSN-assisted evacuation schemes can be divided into two classifications: the sensor-centric guiding scheme (Fig. 5(a)) and the user-centric guiding scheme (Fig. 5(b)). This section reviews the two types of evacuation schemes.

2.4.1. Sensor-centric evacuation scheme

In sensor-centric scheme, all people associated with the same sensor are provided with the same direction. Table 7 summarizes previous work on evacuation with WSNs. Some research assumed the availability of global knowledge about path topology and used global exhaustive search algorithms to determine optimal guiding routes. Buragohain et al. carried out a Breadth-First-Search (BFS) to calculate an optimal path. In addition, in order to reduce communication expenses, an adaptive skeleton graph was constructed in a distributed fashion (Buragohain et al., 2016). Filippoupolitis et al. used the Dijkstra algorithm to calculate the path with the minimum effective length (Filippoupolitis and Gelenbe, 2009). Wang et al. proposed a novel metric of path planning named Expected Number of Oscillations (ENO) to quantify the dynamics of emergency. Based on ENO information, the path minimizing the probability of oscillation was found using a global exhaustive search algorithm (Wang et al., 2014a). Chen et al. provided the fastest routes for people to reach exits based on the evacuation time estimated by an analytical model that took into account corridor capacity and length, exit capacity, and concurrent movement and distribution of people (Chen et al., 2012b). Shen et al. employed the Dinic Algorithm to provide evacuees with navigation service, which reduced congestion and increased the evacuated ratio in a short time (Shen et al., 2011).

Instead of global search, Tseng et al. executed path planning based on local search algorithms (Tseng et al., 2006; Zhou et al., 2012; Chen et al., 2012a; Wang et al., 2017, 2013, 2015a; Li et al., 2003; Chen et al., 2011, 2008; Pan et al., 2006; Chen et al., 2016b; Park and Corson, 1997; Pooja et al., 2019). Wang et al. computed an artificial potential field for the corresponding state to generate optimal guiding direction (Wang et al., 2017; Li et al., 2003; Chen et al., 2008, 2011; Pooja et al., 2019). Chen et al. assigned sensor nodes temporally ordered sequence numbers to construct a directed navigation graph in a localized manner (Tseng et al., 2006; Chen et al., 2012a; Zhou et al., 2012; Chen et al., 2016b; Park and Corson, 1997; Pan et al., 2006). Wang et al. sought for a global or local topological structure as a public infrastructure to provide navigation information for internal queries, through which unnecessary overhead of individually path planning is avoided (Wang et al., 2015a, 2013).

2.4.2. User-centric evacuation scheme

The user-centric guiding system provides navigation directions for each individual user rather than for each sensor. As shown in Fig. 5(b), the sensor s_1 can provide different guiding directions for User A and User B even though both of them are nearby s_1. The user-centric evacuation scheme relaxes the constraint on the number of guiding directions provided by a single sensor, which opens up more opportunities to optimize overall evacuation time. Wu et al. proposed a localized user-centric guiding protocol where the overall evacuation time is minimized with the consideration of the effect of hazards and the limited capacity of a certain sensor at a certain time slot (Wu, 2017).

3. Ship passenger evacuation

The consequences of an accident could be destructive for passenger ships, especially for luxury cruises. For example, thirty-two people were

Table 7
Crowd evacuation with WSNs.

Related work	Location-based/Location-free	Global/Local search	Method	Congestion-aware	Path metric
Buragohain et al. (2016)	Location-based	Global	BFS	×	Path length
Shen et al. (2011)	Location-based	Global	Dinic algorithm	✓	Evacuation time
Wang et al. (2014a)	Location-free	Global	OPEN	×	ENO
Chen et al. (2012b)	Location-based	Global	TORA	✓	Evacuation time
Pan et al. (2006), Tseng et al. (2006), Chen et al. (2012a) and Park and Corson (1997)	Location-based	Local	TORA	×	Path length
Zhou et al. (2012) and Chen et al. (2016b)	Location-based	Local	TORA	✓	Evacuation time
Filippoupolitis and Gelenbe (2009)	Location-based	Global	Dijkstra algorithm	×	Effective length
Li et al. (2003)	Location-free	Local	Artificial potential field	×	Distance to dangers
Chen et al. (2008)	Location-based	Local	Artificial potential field	✓	Evacuation time
Chen et al. (2011)	Location-free	Local	Artificial potential field	✓	Evacuation time
Wang et al. (2017) and Pooja et al. (2019)	Location-free	Local	Artificial potential field	✓	Distance to dangers
Wang et al. (2015a)	Location-free	Local	Level set method	✓	Congestion level, Path length
Wang et al. (2013)	Location-free	Local	Road map	×	Distance to dangers

killed when the Costa Concordia capsized in 2012. In case of such a catastrophe, an appropriate evacuation strategy should be applied to reduce casualties. The land-based indoor evacuation approaches mentioned in Section 2 cannot be used directly to guide evacuees on passenger ships due to the specificities of ships' internal structure and passengers' behavior during evacuation. Compared with the mature land-based indoor evacuation, the research on evacuation on passenger ships is relatively limited and mainly focuses on three aspects from the view of intentions: (1) Investigation of the likely evacuation behavior of passengers; (2) Optimization of passenger evacuation for decreasing casualties; (3) Evaluation of evacuation on passenger ships. This section first presents the latest guideline on evacuation analysis for passenger ships, issued by International Maritime Organization (IMO), and then analyze the unique characteristics of ship passenger evacuation. Finally, a survey of existing research efforts on the evacuation of passenger ships is given.

3.1. Evaluation of the IMO guideline on ship evacuation

The international regulation "Safe Return to Port" specifies the design criteria that guarantee the return of the ship to the port when a casualty occurs. In such a case, passengers should move to the so-called Safe Areas. If the given threshold of damage is exceeded, it is necessary to abandon the ship and evacuate passengers to survival crafts. In both cases, the evacuation analysis must be performed. The latest guidelines concerning evacuation analysis for passenger ships are dictated by IMO in MSC.1/Circ.1533 (IMO, 2007). The guidelines allow evacuation analysis by either the simplified or the advanced method. The simplified analysis is based on a macroscopic model, treating passengers as the fluid that runs through corridors and stairs as if they are tubes. In this sort of analysis, the geometry of doorways, stairs and corridors, and the initial density of passengers are considered to calculate the total evacuation duration and identify the possible bottlenecks (Nasso et al., 2019). The advanced method simulates individual passengers, taking into account the particular features of passengers, such as the walking speed and the reaction time to an emergency. In this method, IMO-certified software (e.g., EVI and AENEAS), based on VR, is used to calculate the travel duration, including the response duration.

The regulations on safe return to port and evacuation analysis are of primary importance in the early stage of design for passenger ships to upgrade the intrinsic ship safety in event of casualties. In addition, these regulations provide standard scenarios and indexes for the evaluation of ship evacuation systems. The performance of a proposed ship evacuation scheme should be evaluated in day and night scenarios, in which the initial distribution of passengers on board is different. The evacuation performance of a scheme should be measured in terms of the traversal time required for passengers to arrive at the Safe Areas when it is assumed that the accident does not exceed a fixed threshold. Otherwise, it should be measured by the duration until the launch of survival crafts.

3.2. Specificity of ship passenger evacuation

Based on the analysis of maritime accident investigation reports and case studies, as well as the data collection on a real passenger ship, this section describes the specificities of the evacuation environment and crowd behaviors during the emergency evacuation on passenger ships.

3.2.1. The influence of ship motion on passenger movement

The movement pattern of passengers on board is significantly different from that on the static ground because of the effect of ship inclination and motion. Many simulations and experiments have been performed to quantify the influence of ship inclination or motion on pedestrian speed. Fig. 6 presents the speed reduction data due to ship inclination from various international research projects (i.e., Fleet Technology Limited (FTL) and Fire Safety Engineering Group (FSEG) in the University of Greenwich, Research Institute of Marine Engineering of Japan (RIME) and National Maritime Research Institute of Japan (NIMR), Korea Research Institute of Ship and Ocean Engineering (KRISO), the Netherlands Organization for Applied Scientific Research (TNO), Australian Maritime Engineering Cooperative Research Centre (AME CRC), TraffGo HT GmbH using evacuation software AENEAS, and the Skate Key Laboratory of Fire Science in the University of Science and Technology of China (SKLFS)). In addition, Valanto et al., by means of evacuation software AENEAS, presented speed reduction factors in laterally and longitudinally tilted staircases as the function of ship inclination angle (see Eqs. (2)–(4)) (Valanto, 2006). ϕ denoted the slope angle; r_{trans} indicated the reduction factor in laterally tilted staircases; r_{longu} and r_{longd} were reduction factors when walking up and down longitudinally tilted staircases, respectively. Sun et al. exploited a ship corridor simulator to investigate the effect of heeling and trim on individual walking speed and group walking speed, respectively (Sun et al., 2018a,b). Chen et al. investigated the coupled-forced pedestrian movement features as a result of ship swaying using an agent-based pedestrian model (Chen et al., 2016a). Wang et al. carried out a series of walking experiments on a real ship to quantitatively evaluate the effect of different rolling angles on individual walking speed both on

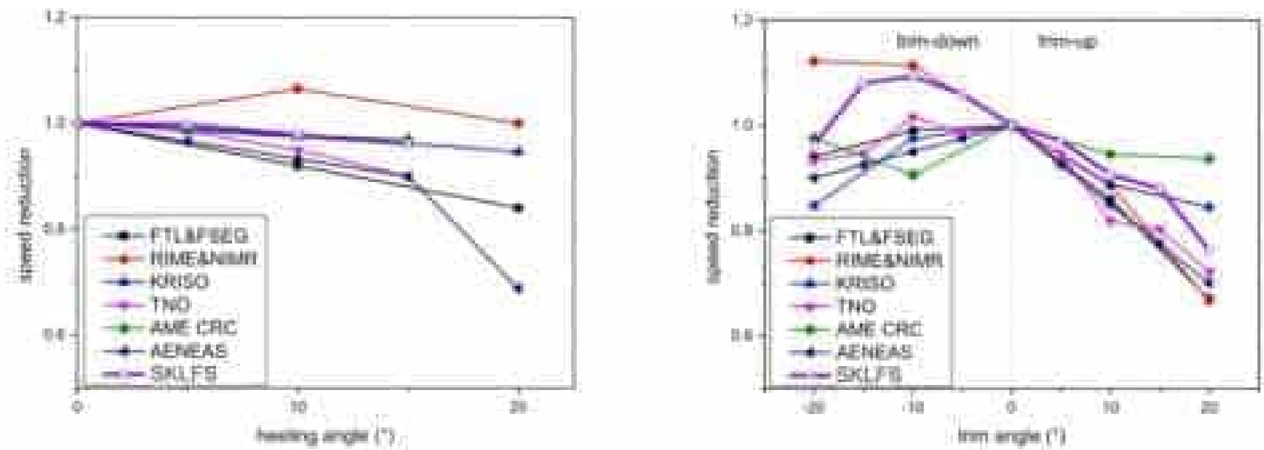

(a) Speed reduction as a function of transverse slope in a corridor (b) Speed reduction as a function of longitudinal slope in a corridor

Fig. 6. Speed reduction data under different situations from various international research projects.

flat terrains and staircases (Wang et al., 2021a).

$$r_{\text{trans}} = \begin{cases} -0.005\phi + 1 & 0^\circ \le \phi < 20^\circ \\ -0.085\phi + 2.6 & 20^\circ \le \phi < 30^\circ \\ 0.05 & 30^\circ \le \phi \le 40^\circ \\ 0 & 40^\circ < \phi \end{cases} \tag{1}$$

$$r_{\text{longu}} = \begin{cases} 0 & \phi < -45^\circ \\ 0.038\phi + 1.76 & -45^\circ \le \phi < -20^\circ \\ 1 & -20^\circ \le \phi < 0^\circ \\ -0.015\phi + 1 & 0^\circ \le \phi \le 20^\circ \\ -0.065\phi + 2 & 20^\circ \le \phi < 30^\circ \\ 0.05\phi + 2.1 & 30^\circ \le \phi \le 45^\circ \\ 0 & 45^\circ < \phi \end{cases} \tag{2}$$

$$r_{\text{longd}} = \begin{cases} 0 & \phi < -45^\circ \\ 0.05 & -45^\circ \le \phi < -30^\circ \\ 0.065\phi + 2 & -30^\circ \le \phi < -20^\circ \\ 0.015\phi + 1 & -20^\circ \le \phi < 0^\circ \\ 1 & 0^\circ \le \phi < 15^\circ \\ -0.032\phi + 1.48 & 15^\circ \le \phi \le 45^\circ \\ 0 & 45^\circ < \phi \end{cases} \tag{3}$$

3.2.2. The feedback of crowd movement on ship motion

Crowd movement, in turn, can affect the motion of a ship. On September 26, 2002, MV Le Joola capsized off the coast of The Gambia with 1863 deaths (Rothe et al., 2006). The ship was submerged in just five minutes. According to the analysis of the relative maritime accident investigation reports, it is found that lopsided crowd movement is one of the main reasons for such fast sinking, which dramatically decreased the allowable evacuation time. There were about five hundred passengers on the upper deck before the disaster occurred, which ascended the ship's center of gravity and thus reduced ship stability. It was, therefore, more vulnerable to severe weather and sea states. Moreover, passengers on the upper deck swarmed to the port side to avoid storms from the starboard side, which undeniably accelerated the capsizing of MV Le Joola. The sinking of Phoenix PC Diving also revealed that it was critical for an evacuation scheme to take into account the feedback of crowd movement on ship motion. When danger arose, passengers on Phoenix PC Diving stampeded to the starboard side, which sped up the ship's overturning. Within only three minutes, it sank in the ocean near Phuket, Thailand, causing 47 deaths (Chen, 2021).

3.2.3. The influence of fire doors on path network connectivity

Fire doors with different fire resistance ratings are installed to reduce the spread of fire and smoke between separate components of a passenger ship to enable safe egress from a vessel (Perez Villalonga, 2005). Certain fire doors on vessels are hidden in normal situations and can be closed in the event of a fire, which is different from the fire doors in general buildings. Once the fire door is closed, it can only be opened from one side of the door. That is to say, certain corridors on vessels are unidirectionally passable due to the existence of fire doors, which makes the evacuation scenario on a passenger ship distinguishing. In addition, it takes a certain amount of time to open the fire doors, so the calculation of the traversal time on the related passageways is different from common ones.

3.2.4. Limited and predictable ship survival time

A passenger ship is required to have sufficient hydrostatic stability to survive certain damage cases. However, the required stability cannot guarantee the survival of the ship in all cases, especially if the accident takes place in unfavorable weather conditions or sea states. In such cases, the survival time until capsizing for the ship is limited. In order to survive, passengers must flee from the damaged ship within the limited ship survival time. The value of ship survival time depends on the loading condition of a vessel, the type, location, and extent of damage, and the probable weather condition and sea state in an operation area. Valanto *et al*. determined a method to estimate the survival time (Valanto, 2006). Firstly, when the significant wave height is great than or equal to 4.5 m, the survival time can be obtained with the help of the numerical simulation of ship motion. Fig. 7 shows some typical examples of simulated ship roll motion until capsizing, where angle 30° is considered as the capsizing criterion. The estimation of the survival time for the significant wave height lower than 4.5 m using numerical simulation is very ineffective in terms of computation time. In such cases, the survival time can be extrapolated with the following formula:

$$T_c = T_s \times e^{A + \frac{B}{h^2}} \tag{4}$$

where T_c represents the survival time of a vessel. T_s and h indicate the significant wave period and height, respectively. The constants A and B can be calculated by numerical simulation for higher wave height with the same wave period.

3.2.5. Limited capacity of muster station

A passenger ship has multiple muster stations that are the equivalent of evacuees' destinations (Bucci et al., 2016). Different from the land building evacuation, the muster stations on passenger ships give a

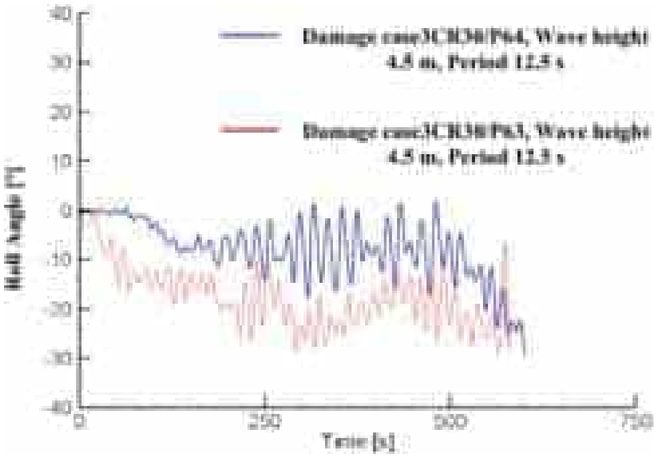

Fig. 7. Typical examples of simulated ship roll motion until capsizing.

limitation for routing selection due to the limited number of lifeboats and rafts in the stations (Qiao et al., 2014). When the embarkation and muster stations are not coincident, the capacity of each muster station is also limited due to the space limitation, which is determined in the ship design stage. Without considering the limited capacity of muster stations, passengers are likely to be guided to the stations that have no space to accommodate more evacuees, which would lead to a reassignment to another station, and thus inevitably prolongs the period required to navigate passengers to safety. Considering the resultant longer evacuation time, it is increasingly likely that passengers will eventually miss the limited ship survival time and consequently lose their lives when abandoning the ship becomes necessary.

3.2.6. Dependency on life-saving equipment for real survival

In case the damaged ship must be abandoned, passengers will be required to arrive at boarding stations and embark on lifeboats or rafts or jump into the water (Yoshida et al., 2001). In such cases, passengers need to equip themselves with life-saving equipment such as life vests and lifebuoys, which increases passengers' feelings of safety and their chance of survival. The minimum number of different life-saving equipment is defined in Safety of Life at Sea (SOLAS) regulations based on the size and passenger capacity of the ship (Ahola et al., 2014). Specifically, there are two life jackets in each passenger room, and at other specific locations (e.g., outside decks), a certain number of lifebuoys or jackets are distributed. If a passenger is not in the room when an emergency happens, it would be vital to consider the distribution of life-saving equipment in the path planning. For example, should they return to their cabins to collect life jackets, or should they head for other locations where pertinent appliances are placed?

3.2.7. Narrow and complex ship indoor space

The internal structure of a passenger ship is very complex, especially for state-of-the-art passenger ships with theaters, shops, swimming pools, and gyms (Stefanidis et al., 2019). Moreover, the width of corridors in cruises ranges from 1 m to 3 m, only allowing one or two passengers to pass simultaneously. However, with the increase in passenger capacity, there may be thousands of passengers on a cruise ship, which gives rise to congestion points. Without considering the heavy congestion and even blocking and trampling due to capacity constraints of pathways, it is likely to aggravate the extent of injuries and casualties.

3.3. Studies of ship passenger evacuation

There are three kinds of research focusing on ship passenger evacuation from the view of intentions, i.e., evacuation behavior study, passenger evacuation optimization, and evaluation of evacuation on passenger ships. Previous research on ship passenger evacuation is summarized in Table 8.

3.3.1. Passenger behaviors during evacuation

It is critical to study passengers' behaviors during a ship evacuation process. Valanto et al. investigated the moving characteristics of passengers considering the effect of ship inclination and motion (Valanto, 2006; Sun et al., 2018a; Chen et al., 2016a; Sun et al., 2018b; Wang et al., 2021a). Sun et al. investigated the effect of heeling and trim on individual walking speed using a ship corridor simulator (Sun et al., 2018a). Results showed that compared with trim angles, heeling angles had less impact on individual walking speed. Lu et al. explored the movement pattern of single file passengers under ship trim and heeling conditions (Sun et al., 2018b). Results indicated that as with individual walking speed, group speed was more vulnerable to heeling angles compared with trim angles. Moreover, the larger the inclination angle, the more the velocity between adjacent experimental subjects correlated. Chen *et al*. established an agent-based evacuation model taking into account the forced pedestrian movement pattern (Chen et al., 2016a). Simulations of single pedestrian movement indicated that pedestrian movement was significantly affected by the angle between pedestrian movement direction and ship swaying direction. Based on the primary data from a series of walking experiments on a real ship, Wang et al. analyzed the individual walking speed under different rolling conditions in two scenarios, i.e., flat terrains and staircases (Wang et al., 2021a). Other behaviors including cooperation with others, perception of wayfinding tools, proactive response to evacuation alarms, compliance with the crew, observation on others' actions, obedience to evacuation instructions, patient queuing, and return to the cabin when their families are left behind, were also investigated (Kwee-Meier et al., 2017; Wang et al., 2021b; Zhang et al., 2020a). In addition, Wang et al. addressed the demographic differences among these behaviors (Wang et al., 2020).

Some research focused on the factors affecting passengers' evacuation behaviors (Li et al., 2021). With the help of hypothesis testing, Zhang et al. analyzed the relationship between personnel characteristics (e.g., blood type and personality type) and evacuation behaviors (e.g., the first response to a fire alarm and the possibility of return for properties) (Zhang et al., 2020a). Ahola *et al*. conducted user studies in an authentic environment to assess the themes pertaining to passenger perception of safety (Ahola et al., 2014; Ahola and Mugge, 2017). Based on ship accident investigation reports, Nevalainen et al. found that both external stimuli, including alarm sound, abnormal noise, and the darkness caused by a blackout, and inner emotion could affect how passengers process and interpret environmental cues under emergencies (Nevalainen et al., 2015).

3.3.2. Passenger evacuation optimization

Regarding passenger evacuation optimization, the plan of escaping routes, the optimization of staircase layout, and the schedule of the time for issuing evacuation orders have attracted the attention of many researchers. Casareale et al. demonstrated the effectiveness of wayfinding systems in improving evacuation on cruise ships (Casareale et al., 2017). Ni *et al*. applied a goal-driven decision-making model to create a concrete escape plan (Ni et al., 2017). Ng et al. iteratively utilized a modification of the scheduling algorithm introduced by Leung and Ng to find a schedule for different groups at risk, which minimized the time of evacuating all people with the least total cost (Ng et al., 2021). Based on a SF model, Wang et al. optimized the staircase layout on a Ro-Ro vessel to reduce evacuation time (Wang et al., 2022). Xie proposed a surrogate-based optimization method to determine the time for issuing evacuation orders so that the assembly time could be minimized (Xie et al., 2020c).

Table 8
Ship passenger evacuation.

Research intentions	Research content	Technique	Implemented in
Passenger evacuation behavior	Moving characteristic	Simulation with agent-based models, Full-scale experiment on ships, Experiment with simulators	Valanto (2006), Sun et al. (2018a), Chen et al. (2016a), Sun et al. (2018b) and Wang et al. (2021a)
	Perception of wayfinding tools	Experiment in simulated conditions, Questionnaire survey	Wang et al. (2020), Kwee-Meier et al. (2017) and Wang et al. (2021b)
	External and internal factors affecting passengers' behaviors	Experiment in simulated conditions, Passenger ship accident investigation reports, Full-scale experiments on ships, Questionnaire survey	Ahola et al. (2014), Nevalainen et al. (2015), Ahola and Mugge (2017) and Zhang et al. (2020a)
Passenger evacuation optimization	Effectiveness of wayfinding solutions	Simulation with SF model	Casareale et al. (2017)
	Staircase layout optimization	Simulation with SF model	Wang et al. (2022)
	Optimization of issuance of passenger evacuation orders	Genetic algorithm	Xie et al. (2020c)
	Optimization of evacuation path	BFS, Leung–Ng fast approximation scheduling algorithm	Ni et al. (2017) and Ng et al. (2021)
Passenger evacuation evaluation	Reliability of evacuation	Bayesian network parameter learning method, Risk-based methodology, K2 structure learning algorithm	Wang et al. (2021c) and Vanem and Skjong (2006)
	Evacuation process estimation	Simulation with SF model, Modeling with Batch NHPP, Simulation with grid-based model, Dynamic Bayesian network, Markov decision process, Polynomial chaos expansion	Kang et al. (2019), Ni et al. (2017), Hifi (2017), Vilen et al. (2020), Galea et al. (2015), Sarshar et al. (2013), Kana and Droste (2019) and Xie et al. (2020a,b)

3.3.3. Evaluation of evacuation on passenger ships

The evacuation process can be analyzed in two ways: advanced analyses and simplified analyses. The advanced analysis treats each passenger as an individual with his/her characteristic and behavior. Ni *et al*. proposed an extended SF model that considered the resistance force from obstacles in cabins to govern the movement of passengers (Ni et al., 2017). Kang et al. incorporated the psychological tendency of pedestrians to slip downhill into the SF model to simulate evacuation behaviors on inclined shipwrecks (Kang et al., 2019). Vilen et al. evaluated two advanced evacuation analysis software packages, i.e., Evi and Pathfinder, in terms of numerical results and user experience (Vilen et al., 2020). Galea et al. did an experimental validation of the evacuation model maritimeEXODUS using two data sets generated from semi-unannounced assembly trials on a RO-PAX ferry and a cruise ship (Galea et al., 2015). Results showed that the model was capable of predicting the assembly process for the two vessels to a specified level of accuracy. In addition, Hifi et al. described a set of scenarios for performing advanced evacuation analysis and recommended a survey of population composition and ship familiarity before the evacuation analysis to improve analysis accuracy (Wang et al., 2022; Hifi, 2017). However, the advanced analysis is very time-consuming, and thus when a fast assessment of evacuation time is needed, it is not a suitable option. Cho *et al*. developed a simplified analysis solution that took a macroscopic view of the evacuation process, treating passengers as homogeneous particles in a fluid (Cho et al., 2016). Sarshar et al. developed a dynamic Bayesian network model that considered the most vital factors influencing congestion (e.g., panic, age, sex, and the presence of rescue personnel) to predict the probability of congestion during the entire process of an evacuation (Sarshar et al., 2013). Xie et al. established a surrogate model using a coupling technique of nested sampling and polynomial chaos expansion method to estimate passenger travel time uncertainty with acceptable accuracy (Xie et al., 2020b,a). Kana *et al*. presented a ship-centric Markov decision process model for evaluating the evacuation during the preliminary design phase of a passenger ship (Kana and Droste, 2019). The simplified analysis ignored the different elements of an evacuation process and thus could not mirror passengers' movement. Hifi et al. developed a parametric model that could produce a fast estimate of evacuation time while capturing the factors influencing the evacuation to satisfactory accuracy (Hifi, 2017).

The quantitative evaluation of evacuation on ships is also essential. Wang et al. investigated the main factors leading to evacuation failure and established a model using the K2 structure learning algorithm and the Bayesian network parameter learning method to quantify the probability of a successful evacuation (Wang et al., 2021c). Vanem et al. developed a risk-based approach to evaluate the evacuation performance associated with a specific passenger ship using the proposed set of evacuation scenarios (Vanem and Skjong, 2006).

4. Discussion and future directions

This section evaluates the above land-based evacuation schemes and delineates our insights into the future research perspectives for ship passenger evacuation.

4.1. Comment on land-based evacuation

Significant research works on building evacuation have been carried out. Based on different types of guidance patterns, a classification of land-based evacuation schemes is proposed, including signage-based evacuation, leader-based evacuation, ME-based evacuation, and WSN-based evacuation.

In Section 2.1, the review of land-based indoor evacuation with fixed and variable signage is provided. The latter can respond to contemporary environmental conditions and present up-to-date guiding information. However, pedestrians may not find signs in smoky conditions. Even under clear conditions, they are likely to neglect the signs at specific locations or cannot fully understand the content of signs during emergencies due to their anxiety and panic. In such emergencies, evacuation leaders with complete knowledge of the layout of a building can provide guiding instructions for occupants and significantly reduce casualties. Compared with human leaders, robotic leaders can be sent to guide evacuees out in several special accidents like nuclear leakage. An emergency evacuation system is requested to provide a time-critical guiding service. But for the leader-based evacuation system, it will take a significant amount of time to arrange leaders to appropriate locations. Therefore, evacuating through the equipped device (e.g., smartphone) regularly used in everyday life for all pedestrians is very attractive. However, the downsides to the three kinds of evacuation schemes are as follows: (1) Without real-time indoor environment monitoring, evacuation routes provided by these schemes are not necessarily passable due to the encroachment of hazards; (2) Passengers observing the same sign or leader or near the same beacon will escape along the same direction, which inevitably causes heavy congestions, trampling and possible injuries and casualties. The WSN-based evacuation scheme is capable of exploring dynamic environmental conditions by means of the collaborative detection of sensor nodes. But sensor-centric WSN-based evacuation scheme is only effective on the first downside mentioned above, while powerless to solve the second problem. Therefore, a user-centric WSN-based evacuation scheme will be a good choice for a modern building.

4.2. Prospects for ship passenger evacuation

Compared with the land-based evacuation, there are some specific features for passenger ship evacuation due to the uniqueness of ship structure, passenger behaviors onboard, and evacuation requirements at sea. Therefore, personalized evacuation approaches for ship passengers are indispensable. However, in contrast to the relatively mature land-based evacuation schemes, the research on ship evacuation is still in its infancy and focuses on investigating the likely behaviors of passengers. Design or optimization of evacuation routes targeting ship passengers is also critical but scarce. Drawing from the four types of land-based evacuation schemes mentioned in Section 2, the prospects for the evacuation system of modern cruise ships are discussed in this section.

A WSN with functionally-separated sensors like tilt sensors, hydraulic pressure sensors, temperature sensors, and smoke sensors is deployed on a modern cruise ship. When an emergency takes place, the sensors will initiate a danger alarm and transmit the current locations and levels of hazards to a path planning server. In addition, the current position of each passenger is detected using the received strength of wireless signals on his/her smartphone, and the sensor ID with the strongest signal strength is used to determine the passenger's position in the blueprint database of sensor deployment. That is to say, the proposed scheme does not require accurate location information on each passenger. The smartphone periodically sends the determined position to the path planning server. According to the obtained information, the server will compute a dedicated escape route for each individual and broadcast it to his/her smartphone. The reason for selecting smartphones as guides during emergencies is that nowadays almost everyone has a smartphone and familiarity with their own smartphones can increase passengers' feelings of safety. Fig. 8 shows the system architecture of our proposed emergency guiding scheme for ship passengers. Red rectangles represent sensor nodes deployed at muster stations, doors, and crossing points among corridors and/or doors on a passenger ship in advance. The Wi-Fi access point is used for maintaining the communication between the smartphones and the path planning server. The following is a list of properties of evacuation routes provided to passengers:

- The path is apart from hazardous regions and through which a passenger can arrive at a specific exit before the ship capsizes under all circumstances.
- The total evacuation time of passengers should be reduced as much as possible. To realize this goal, an evacuation system has to consider not just the relative distance from the passenger to the muster station, but the movement speed on the route, the capacity of the route, and the up-to-date distribution as well as the spatial–temporal mobility of all passengers.
- The evacuation routes should be provided to passengers in a real-time manner.
- Escaping along the provided route, each passenger would have obtained a piece of saving-life equipment when arriving at the muster station.
- Following the offered direction would not speed up the ship leaning to one side.
- Passengers would not be guided to a muster station that cannot accommodate more evacuees.
- Except for guaranteeing passengers' safety, the evacuation system should also maintain the integrity of a passenger ship as much as possible.

The proposed architecture is attractive but challenging, due to the restricted battery power of low-cost sensor nodes and the ad-hoc routing protocol of a WSN in a large and complicated ship indoor space. Specifically, as the information regarding the environment is forwarded over multiple hops towards a gateway, some sensors get more congested than others, depending on their location. Therefore, they deplete their batteries quickly, shortening the overall network lifetime. In addition, considering the dynamics of the hazardous environment, the routing protocol in WSN functions poorly in the evacuation application. Because in order to ensure passengers' safety, frequent flooding is required to update the escaping paths in the rapidly changing environment, which may trigger many simultaneous bursts of broadcast packets throughout the network and thus cause a large number of packet collisions. The calculation of all routes is performed in the path planning server. So in case it malfunctions during the emergency, our evacuation system will break down. Moreover, while the potential of our proposed architecture to improve access to real-time monitoring and even intuitive and reliable navigation instruction can be provided to evacuees, concerns about personal data privacy remain. User data may be inadequately disclosed or transmitted to commercial entities by smartphone applications (apps) for ship passenger evacuation.

With the emergence of Low Power Wide Area Network (LPWAN) technologies, one type of WSN, which is designed for long-range Internet of Things (IoT) services, the above challenges from WSNs will hopefully bear solved. LPWAN IoT devices consume low transmission power but have a communication distance of several kilometers, so they can directly transmit the information pertaining to the environment to the path planning server and thus avoid the network breakdown caused by packet collisions. In addition, benefiting from the development of edge computing, in the future the distributed approach can be used to provide paths for passengers so as to reduce and even release the dependency on the path planning server. Moreover, given the negative impacts of inadequate privacy disclosures, data protection becomes particularly important. On the one hand, the anonymization technology can be adopted for the utilization of the results of analysis of the exchanged data, which includes passengers' sensitive personalized contexts (e.g., information about passengers' physical and psychological status) (Shinzaki et al., 2016). On the other hand, government regulation and up-to-date technical scrutiny are also essential for avoiding privacy leakages (Huckvale et al., 2019).

In addition, with the development of Extended Reality (XR) technology, VR-based or AR-based experiments can be introduced as an alternative method of post-emergency investigation and hypothetical survey to study passenger behavior during ship emergencies. XR-based experiments can arouse passengers' behavioral responses to virtual emergencies and thus provide the opportunity to collect evacuation behavior data with relatively high ecological validity. Taking into account passengers' behaviors, the designed evacuation system will be more effective at ensuring the safety and reliability of evacuation in reality. Moreover, it is possible to develop VR-based Serious Games (SGs) to train passengers to utilize the proposed evacuation scheme to escape, which is an effective approach to acquiring and retaining evacuation knowledge. It is also possible to substitute smartphones in the proposed architecture with AR devices that can provide more intuitive guidance for passengers.

5. Conclusion

This paper provides a survey of research efforts on crowd evacuation both in general buildings and on passenger ships. A comprehensive

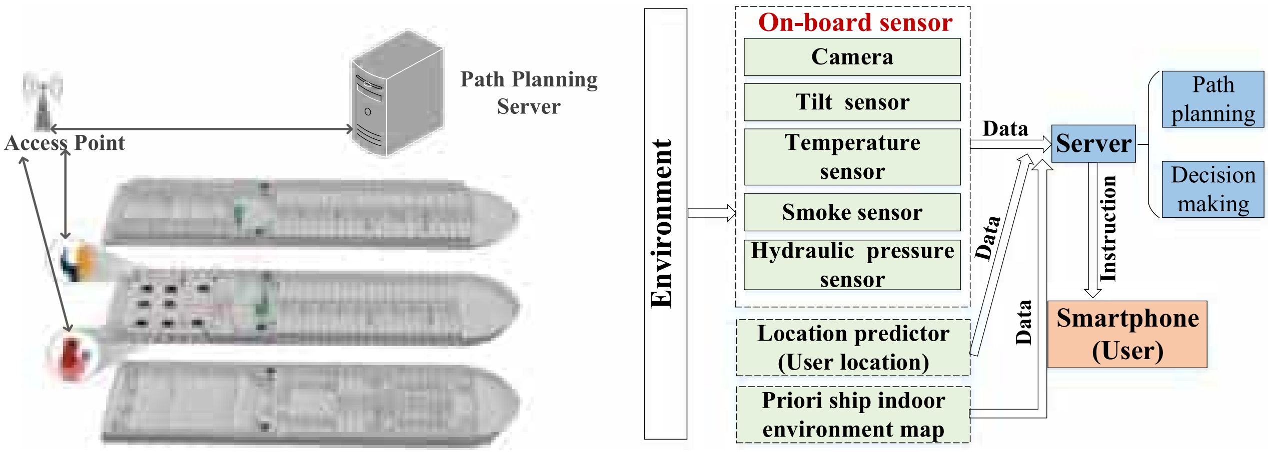

(a) Diagram of the emergency guiding system for ship passengers (b) System framework of emergency guiding for ship passengers

Fig. 8. System architecture of the emergency guiding scheme for ship passengers. (For interpretation of the references to color in this figure legend, the reader is referred to the web version of this article.)

analysis and synthesis of different kinds of guidance patterns for evacuation in land-based buildings, including signage-based, leader-based, ME-based, and WSN-based evacuation schemes, is presented. Those schemes are not used directly for ship passenger evacuation due to the unique challenges of guiding passengers on vessels. Section 3 analyzes the specificities of both evacuation environment and crowd behavior during the emergency evacuation on passenger ships. In addition, the existing work on evacuation for passenger ships are reviewed. Comments on land-based evacuation schemes and future research directions on ship passenger evacuation are also discussed. In the future, more intelligent and personalized guidance systems will be designed and implemented to improve the safety and efficiency of ship passenger evacuation.

Declaration of competing interest

The authors declare that they have no known competing financial interests or personal relationships that could have appeared to influence the work reported in this paper.

Data availability

Data will be made available on request.

Acknowledgments

The authors thank the anonymous reviewers for their insightful comments. This work was partially supported by the National Natural Science Foundation of China (NSFC) under Grant 51979216, and partially by the Natural Science Foundation of Hubei Province, China, under Grant 2021CFA001.

References

Ahmed, A.A., Al-Shaboti, M., Al-Zubairi, A., 2015. An indoor emergency guidance algorithm based on wireless sensor networks. In: 2015 International Conference on Cloud Computing. ICCC, IEEE, pp. 1–5.

Ahn, J., Han, R., 2011. Rescueme: An indoor mobile augmented-reality evacuation system by personalized pedometry. In: 2011 IEEE Asia-Pacific Services Computing Conference. IEEE, pp. 70–77.

Ahola, M., Mugge, R., 2017. Safety in passenger ships: The influence of environmental design characteristics on people's perception of safety. Applied Ergon. 59, 143–152.

Ahola, M., Murto, P., Kujala, P., Pitknen, J., 2014. Perceiving safety in passenger ships–User studies in an authentic environment. Saf. Sci. 70, 222–232.

Boukas, E., Kostavelis, I., Gasteratos, A., Sirakoulis, G.C., 2015. Robot guided crowd evacuation. IEEE Trans. Autom. Sci. Eng. 12 (2), 739–751.

Bucci, V., Marino, A., Mauro, F., Nabergoj, R., Nasso, C., 2016. On advanced ship evacuation analysis. In: Engineering Mechanics 2016-22nd International Conference. Institute of Thermomechanics Academy of Science of the Czech Repulic, pp. 105–112.

Buragohain, C., Agrawal, D., Suri, S., Distributed navigation algorithms for sensor networks. In: Proceedings of the 25th International Conference on Computer Communications. IEEE, pp. 1–10.

Cao, S., Song, W., Lv, W., 2016. Modeling pedestrian evacuation with guiders based on a multi-grid model. Phys. Lett. Sect. A: Gen. At. Solid State Phys. 380 (4), 540–547.

Casareale, C., Bernardini, G., Bartolucci, A., Marincioni, F., D'Orazio, M., 2017. Cruise ships like buildings: Wayfinding solutions to improve emergency evacuation. Build. Simul. 10 (6), 989–1003.

Chen, L., 2021. Research on the differences of disaster reports in Chinese and American media from the cross-cultural perspective. In: 2021 4th International Conference on Humanities Education and Social Sciences (ICHESS 2021). Atlantis Press, pp. 2716–2721.

Chen, W.-T., Chen, P.-Y., Wu, C.-H., Huang, C.-F., 2008. A load-balanced guiding navigation protocol in wireless sensor networks. In: IEEE GLOBECOM 2008-2008 IEEE Global Telecommunications Conference. IEEE, pp. 1–6.

Chen, L.-W., Cheng, J.-H., Tseng, Y.-C., 2012b. Evacuation time analysis and optimization for distributed emergency guiding based on wireless sensor networks. In: 2012 International Conference on Connected Vehicles and Expo. ICCVE, IEEE, pp. 130–135.

Chen, L.W., Cheng, J.H., Tseng, Y.C., 2015. Optimal path planning with spatial-temporal mobility modeling for individual-based emergency guiding. IEEE Trans. Syst. Man Cybern.: Syst. 45 (12), 1491–1501.

Chen, L.W., Cheng, J.H., Tseng, Y.C., 2016b. Distributed emergency guiding with evacuation time optimization based on wireless sensor networks. IEEE Trans. Parallel Distrib. Syst. 27 (2), 419–427.

Chen, L.-W., Chung, J.-J., 2017. Mobility-aware and congestion-relieved dedicated path planning for group-based emergency guiding based on internet of things technologies. IEEE Trans. Intell. Transp. Syst. 18 (9), 2453–2466.

Chen, P.Y., Kao, Z.F., Chen, W.T., Lin, C.H., 2011. A distributed flow-based guiding protocol in wireless sensor networks. In: Proceedings of the International Conference on Parallel Processing. IEEE, pp. 105–114.

Chen, C., Li, Q., Kaneko, S., Chen, J., Cui, X., 2009. Location optimization algorithm for emergency signs in public facilities and its application to a single-floor supermarket. Fire Saf. J. 44 (1), 113–120.

Chen, L.W., Liu, J.X., 2021. Time-efficient indoor navigation and evacuation with fastest path planning based on internet of things technologies. IEEE Trans. Syst. Man Cybern.: Syst. 51 (5), 3125–3135.

Chen, J., Ma, J., Lo, S., 2016a. Modelling pedestrian evacuation movement on a swaying ship. In: Traffic and Granular Flow'15. Springer, pp. 297–304.

Chen, D., Mohan, C.K., Mehrotra, K.G., Varshney, P.K., 2012a. Distributed in-network path planning for sensor network navigation in dynamic hazardous environments. Wirel. Commun. Mob. Comput. 12 (8), 739–754.

Chiou, M.-R., Chao, S.-L., Hsieh, H.-Y., 2021. The moderating role of service recovery on customer loyalty in the context of cruise passengers. Marit. Policy Manag. 48 (2), 150–166.

Chittaro, L., Nadalutti, D., 2008. A mobile RFID-based system for supporting evacuation of buildings. In: International Workshop on Mobile Information Technology for Emergency Response. Springer, pp. 22–31.

Cho, Y.-O., Ha, S., Park, K.-P., 2016. Velocity-based egress model for the analysis of evacuation process on passenger ships. J. Mar. Sci. Technol. 24 (3), 12.

Cho, J., Lee, G., Lee, S., 2015a. An automated direction setting algorithm for a smart exit sign. Autom. Constr. 59, 139–148.

Cho, J., Lee, G., Lee, S., 2015b. An automated direction setting algorithm for a smart exit sign. Autom. Constr. 59, 139–148.

Chu, L., 2010. A RFID-based hybrid building fire evacuation system on mobile phone. In: Proceedings of the 6th International Conference on Intelligent Information Hiding and Multimedia Signal Processing, IIHMSP 2010. IEEE, pp. 155–158.

Chu, J.C., Chen, A.Y., Lin, Y.-F., 2017. Variable guidance for pedestrian evacuation considering congestion, hazard, and compliance behavior. Transp. Res. C 85, 664–683.

Chu, L., Wu, S.J., 2011. A real-time decision support with cloud computing based fire evacuation system. In: Proceedings of the 16th North-East Asia Symposium on Nano, Information Technology and Reliability, NASNIT 2011. IEEE, pp. 45–48.

Chu, J.C., Yeh, C.-Y., 2012. Emergency evacuation guidance design for complex building geometries. J. Infrastruct. Syst. 18 (4), 288–296.

Cosma, G., Ronchi, E., Nilsson, D., 2016. Way-finding lighting systems for rail tunnel evacuation: A virtual reality experiment with Oculus Rift. J. Transp. Saf. Secur. 8 (sup1), 101–117.

Desmet, A., Gelenbe, E., 2014. Capacity based evacuation with dynamic exit signs. In: 2014 IEEE International Conference on Pervasive Computing and Communication Workshops (PERCOM WORKSHOPS). IEEE, pp. 332–337.

Diao, P.-H., Shih, N.-J., 2018. MARINS: A mobile smartphone AR system for pathfinding in a dark environment. Sensors 18 (10), 3442.

Dong, E., Liang, J., Wang, Z., Xu, J., Shangguan, L., Ma, Q., Yang, Z., 2020. Improving the applicability of visual peer-to-peer navigation with crowdsourcing. In: Proceedings of the 26th International Conference on Parallel and Distributed Systems (ICPADS). pp. 188–195.

Dong, E., Xu, J., Wu, C., Liu, Y., Yang, Z., 2019. Pair-navi: Peer-to-peer indoor navigation with mobile visual slam. In: IEEE Conference on Computer Communications. INFOCOM, IEEE, pp. 1189–1197.

Feng, Y., Duives, D.C., Hoogendoorn, S.P., 2021. Using virtual reality to study pedestrian exit choice behaviour during evacuations. Saf. Sci. 137, 105158.

Ferranti, E., Trigoni, N., 2008. Robot-assisted discovery of evacuation routes in emergency scenarios. In: Proceedings of the International Conference on Robotics and Automation. IEEE, pp. 2824–2830.

Filippoupolitis, A., Gelenbe, E., 2009. A distributed decision support system for building evacuation. In: Proceedings of the 2nd Conference on Human System Interactions. IEEE, pp. 323–330.

Fowler, T.G., Sorgaard, E., 2000. Modeling ship transportation risk. Risk Anal. 20 (2), 225–244.

Fujihara, A., Miwa, H., 2012. Effect of traffic volume in real-time disaster evacuation guidance using opportunistic communications. In: Proceedings of the 4th International Conference on Intelligent Networking and Collaborative Systems (INCoS). IEEE, pp. 457–462.

Fujihara, A., Yanagizawa, T., 2015. Proposing an extended ibeacon system for indoor route guidance. In: 2015 International Conference on Intelligent Networking and Collaborative Systems. IEEE, pp. 31–37.

Galea, E.R., Deere, S., Brown, R., Filippidis, L., 2015. An experimental validation of an evacuation model using data sets generated from two large passenger ships. Trans. - Soc. Naval Archit. Mar. Eng. 121 (3), 370–385.

Galea, E., Xie, H., Deere, S., Cooney, D., Filippidis, L., 2017a. An international survey and full-scale evacuation trial demonstrating the effectiveness of the active dynamic signage system concept. Fire Mater. 41 (5), 493–513.

Galea, E.R., Xie, H., Deere, S., Cooney, D., Filippidis, L., 2017b. Evaluating the effectiveness of an improved active dynamic signage system using full scale evacuation trials. Fire Saf. J. 91 (2001), 908–917.

Garrell, A., Sanfeliu, A., Moreno-Noguer, F., 2009. Discrete time motion model for guiding people in urban areas using multiple robots. In: 2009 IEEE/RSJ International Conference on Intelligent Robots and Systems (IROS). pp. 486–491.

Gelenbe, E., Bi, H., 2014. Emergency navigation without an infrastructure. Sensors 14 (8), 15142–15162.

Hifi, Y., 2017. Probabilistic Modelling of the Process of Evacuation for Ship Crises Management (Ph.D. thesis). University of Strathclyde.

Hou, L., Liu, J.-G., Pan, X., Wang, B.-H., 2014. A social force evacuation model with the leadership effect. Physica A 400, 93–99.

Huckvale, K., Torous, J., Larsen, M.E., 2019. Assessment of the data sharing and privacy practices of smartphone apps for depression and smoking cessation. JAMA Netw. Open 2 (4), e192542.

Hui, X., Galea, E.R., Lawrence, P.J., 2014. Experimental and survey studies on the effectiveness of dynamic signage systems. Fire Saf. Sci. 11, 1129–1143.

Iizuka, Y., Iizuka, K., 2015. Disaster evacuation assistance system based on multi-agent cooperation. In: 2015 48th Hawaii International Conference on System Sciences. IEEE, pp. 173–181.

Ikeda, Y., Inoue, M., 2016. An evacuation route planning for safety route guidance system after natural disaster using multi-objective genetic algorithm. Procedia Comput. Sci. 96, 1323–1331.

IMO, 2007. Guidelines for Evacuation Analysis for New and Existing Passenger Ships. MSC. 1/Circ. 1238, International Maritime Organization, London, UK.

Inoue, Y., Sashima, A., Ikeda, T., Kurumatani, K., 2008. Indoor emergency evacuation service on autonomous navigation system using mobile phone. In: 2008 Second International Symposium on Universal Communication. IEEE, pp. 79–85.

Jiang, C., Ni, Z., Guo, Y., He, H., 2017. Learning human–robot interaction for robot-assisted pedestrian flow optimization. IEEE Trans. Syst. Man Cybern.: Syst. 49 (4), 797–813.

Kana, A.A., Droste, K., 2019. An early-stage design model for estimating ship evacuation patterns using the ship-centric Markov decision process. Proc. Inst. Mech. Eng. M 233 (1), 138–149.

Kang, Z., Zhang, L., Li, K., 2019. An improved social force model for pedestrian dynamics in shipwrecks. Appl. Math. Comput. 348, 355–362.

Kim, Y.D., Kim, Y.G., Lee, S.H., Kang, J.H., An, J., 2009. Portable fire evacuation guide robot system. In: 2009 IEEE/RSJ International Conference on Intelligent Robots and Systems (IROS). IEEE, pp. 2789–2794.

Kwee-Meier, S.T., Mertens, A., Schlick, C.M., 2017. Age-related differences in decision-making for digital escape route signage under strenuous emergency conditions of tilted passenger ships. Applied Ergon. 59, 264–273.

Langner, N., Kray, C., 2014. Assessing the impact of dynamic public signage on mass evacuation. In: Proceedings of the 3rd ACM International Symposium on Pervasive Displays. pp. 136–141.

Li, Y., Cai, W., Kana, A.A., 2019. Design of level of service on facilities for crowd evacuation using genetic algorithm optimization. Saf. Sci. 120, 237–247.

Li, Y., Cai, W., Kana, A., Atasoy, B., 2021. Modelling route choice in crowd evacuation on passenger ships. Int. J. Marit. Eng. 163 (A2).

Li, Q., De Rosa, M., Rus, D., 2003. Distributed algorithms for guiding navigation across a sensor network. In: Proceedings of the 9th Annual International Conference on Mobile Computing and Networking. pp. 313–325.

Li, T., Han, D., Chen, Y., Zhang, R., Zhang, Y., Hedgpeth, T., 2020. IndoorWaze: A crowdsourcing-based context-aware indoor navigation system. IEEE Trans. Wireless Commun. 19 (8), 5461–5472.

Li, W., Li, Y., Yu, P., Gong, J., Shen, S., 2016. The Trace Model: A model for simulation of the tracing process during evacuations in complex route environments. Simul. Model. Pract. Theory 60, 108–121.

Lin, J., Cao, L., Li, N., 2019. Assessing the influence of repeated exposures and mental stress on human wayfinding performance in indoor environments using virtual reality technology. Adv. Eng. Inform. 39, 53–61.

Lin, H.-M., Chen, S.-H., Kao, J., Lee, Y.-M., Hsiao, G.L.-K., Lin, C.-Y., 2017. Applying active dynamic signage system in complex underground construction. Int. J. Sci. Eng. Res. 8 (2).

Lin, J., Zhu, R., Li, N., Becerik-Gerber, B., 2020. Do people follow the crowd in building emergency evacuation? A cross-cultural immersive virtual reality-based study. Adv. Eng. Inform. 43, 101040.

Liu, J., Zhang, J., Yan, X., Soares, C.G., 2022. Multi-ship collision avoidance decision-making and coordination mechanism in Mixed Navigation Scenarios. Ocean Eng. 257, 111666.

Liu, M., Zheng, X., Cheng, Y., 2011. Determining the effective distance of emergency evacuation signs. Fire Saf. J. 46 (6), 364–369.

Lovreglio, R., Gonzalez, V., Feng, Z., Amor, R., Spearpoint, M., Thomas, J., Trotter, M., Sacks, R., 2018. Prototyping virtual reality serious games for building earthquake preparedness: The Auckland City Hospital case study. Adv. Eng. Inform. 38, 670–682.

Luh, P.B., Wilkie, C.T., Chang, S.C., Marsh, K.L., Olderman, N., 2012. Modeling and optimization of building emergency evacuation considering blocking effects on crowd movement. IEEE Trans. Autom. Sci. Eng. 9 (4), 687–700.

Lung, C., Sabou, S., Buchman, A., 2016. Wireless sensor networks as part of emergency situations management system. In: 2016 IEEE 22nd International Symposium for Design and Technology in Electronic Packaging (SIITME). IEEE, pp. 240–243.

Ma, Y., Lee, E.W.M., Shi, M., 2017. Dual effects of guide-based guidance on pedestrian evacuation. Phys. Lett. Sect. A: Gen. At. Solid State Phys. 381 (22), 1837–1844.

Ma, Y., Yuen, R.K.K., Lee, E.W.M., 2016. Effective leadership for crowd evacuation. Physica A 450, 333–341.

Mileski, J.P., Wang, G., Beacham IV, L.L., 2014. Understanding the causes of recent cruise ship mishaps and disasters. Res. Transp. Bus. Manag. 13, 65–70.

Motamedi, A., Wang, Z., Yabuki, N., Fukuda, T., Michikawa, T., 2017. Signage visibility analysis and optimization system using BIM-enabled virtual reality (VR) environments. Adv. Eng. Inform. 32, 248–262.

Mulloni, A., Seichter, H., Schmalstieg, D., 2011. Handheld augmented reality indoor navigation with activity-based instructions. In: Mobile HCI 2011 - 13th International Conference on Human-Computer Interaction with Mobile Devices and Services. pp. 211–220.

Nadalutti, D., Chittaro, L., 2008. Presenting evacuation instructions on mobile devices by means of location-aware 3D virtual environments. In: Proceedings of the 10th International Conference on Human Computer Interaction with Mobile Devices and Services. pp. 395–398.

Nasso, C., Bertagna, S., Mauro, F., Marino, A., Bucci, V., 2019. Simplified and advanced approaches for evacuation analysis of passenger ships in the early stage of design. Brodogr.: Teor. Praksa Brodogr. Pomor. Teh. 70 (3), 43–59.

Nevalainen, J., Ahola, M.K., Kujala, P., 2015. Modeling passenger ship evacuation from passenger perspective. In: RINA, Royal Institution of Naval Architects - Marine Design 2015, Papers. pp. 121–129.

Ng, C.T., Cheng, T.C., Levner, E., Kriheli, B., 2021. Optimal bi-criterion planning of rescue and evacuation operations for marine accidents using an iterative scheduling algorithm. Ann. Oper. Res. 296 (1–2), 407–420.

Ni, B., Li, Z., Zhang, P., Li, X., 2017. An evacuation model for passenger ships that includes the influence of obstacles in cabins. Math. Probl. Eng. 2017, 1–21.

Okada, M., Ando, T., 2011. Optimization of personal distribution for evacuation guidance based on vector field. In: IEEE International Conference on Intelligent Robots and Systems. IEEE, pp. 3673–3678.

Olander, J., Ronchi, E., Lovreglio, R., Nilsson, D., 2017. Dissuasive exit signage for building fire evacuation. Applied Ergon. 59, 84–93.

Olyazadeh, R., 2013. Evaluating Dynamic Signage for Emergency Evacuation using an Immersive Video Environment (Ph.D. thesis). Citeseer.

Pan, M.-S., Li, K.-Y., 2019. EzNavi: an easy-to-operate indoor navigation system based on pedestrian dead reckoning and crowdsourced user trajectories. IEEE Trans. Mob. Comput. 20 (2), 488–501.

Pan, M.S., Tsai, C.H., Tseng, Y.C., 2006. Emergency guiding and monitoring applications in indoor 3D environments by wireless sensor networks. Int. J. Sensor Netw. 1 (1–2), 2–10.

Park, V.D., Corson, M.S., 1997. A highly adaptive distributed routing algorithm for mobile wireless networks. In: Proceedings of the 97th International Conference on Computer Communications, Vol. 3. INFOCOM, IEEE, pp. 1405–1413.

Perez Villalonga, F.J., 2005. Dynamic Escape Routes for Naval Ships (Ph.D. thesis). Monterey California. Naval Postgraduate School.

Pooja, S., Vandhana, P., Rakshana, A., Babiyola, A., 2019. MSEND: Modified situation-aware emergency navigation algorithm in wireless sensor networks. Internat. J. Engrg. Sci. 21129.

Qiao, Y., Han, D., Shen, J., Wang, G., 2014. A study on the route selection problem for ship evacuation. In: 2014 IEEE International Conference on Systems, Man, and Cybernetics. SMC, IEEE, pp. 1958–1962.

Robinette, P., Howard, A.M., 2011. Incorporating a model of human panic behavior for robotic-based emergency evacuation. In: Proceedings of the International Workshop on Robot and Human Interactive Communication. IEEE, pp. 47–52.

Ronchi, E., Nilsson, D., Gwynne, S.M., 2012. Modelling the impact of emergency exit signs in tunnels. Fire Technol. 48 (4), 961–988.

Rothe, D., Muzzatti, S., Mullins, C.W., 2006. Crime on the high seas: Crimes of globalization and the sinking of the Senegalese Ferry Le Joola. Crit. Criminol. 14 (2), 159–180.

Sakour, I., Hu, H., 2017. Robot-assisted crowd evacuation under emergency situations: A survey. Robotics 6 (2), 8.

Sarshar, P., Radianti, J., Granmo, O.C., Gonzalez, J.J., 2013. A dynamic Bayesian network model for predicting congestion during a ship fire evacuation. Lect. Notes Eng. Comput. Sci. 1, 29–34.

Sharma, P.K., Kwon, B.W., Park, J.H., 2018. DSS-SL: Dynamic signage system based on SDN with LiFi communication for smart buildings. Lect. Notes Electr. Eng. 474, 805–810.

Shell, D.A., Matari, C., Maja, J., 2005. Insights toward robot-assisted evacuation. Adv. Robot. 19 (8), 797–818.

Shen, L., Andong, Z., Xiaobing, W., Panlong, Y., Guihai, C., 2011. Efficient emergency rescue navigation with wireless sensor networks. J. Inf. Sci. Eng. 27 (1), 51–64.

Shin, H., Chon, Y., Cha, H., 2011. Unsupervised construction of an indoor floor plan using a smartphone. IEEE Trans. Syst. Man Cybern. C 42 (6), 889–898.

Shinzaki, T., Morikawa, I., Yamaoka, Y., Sakemi, Y., 2016. IoT security for utilization of big data: Mutual authentication technology and anonymization technology for positional data. Fujitsu Sci. Tech. J. 52 (4), 52–60.

Shu, Y., Shin, K.G., He, T., Chen, J., 2015. Last-mile navigation using smartphones. In: Proceedings of the Annual International Conference on Mobile Computing and Networking (MOBICOM), 2015-September. pp. 512–524.

Spartalis, E., Georgoudas, I.G., Sirakoulis, G.C., 2014. Ca crowd modeling for a retirement house evacuation with guidance. In: International Conference on Cellular Automata. Springer, pp. 481–491.

Statistics, R.B., 2020. Table 1. US Department of Homeland Security and US Coast Guard.

Stefanidis, F., Boulougouris, E., Vassalos, D., 2019. Ship evacuation and emergency response trends. Des. Oper. Passeng. Ships.

Stigall, J., Sharma, S., 2017. Mobile augmented reality application for building evacuation using intelligent signs. In: Proceedings of ISCA 26th International Conference on Software Engineering and Data Engineering (SEDE-2017). pp. 19–24.

Stigen, M., 2019. Applying Swarm to Unknown and Dynamic Environments in Evacuation Planning (Master's thesis). NTNU.

Sun, J., Guo, Y., Li, C., Lo, S., Lu, S., 2018a. An experimental study on individual walking speed during ship evacuation with the combined effect of heeling and trim. Ocean Eng. 166 (September 2017), 396–403.

Sun, J., Lu, S., Lo, S., Ma, J., Xie, Q., 2018b. Moving characteristics of single file passengers considering the effect of ship trim and heeling. Physica A 490, 476–487.

Tang, B., Jiang, C., He, H., Guo, Y., 2016. Human mobility modeling for robot-assisted evacuation in complex indoor environments. IEEE Trans. Hum.-Mach. Syst. 46 (5), 694–707.

Tang, C.H., Wu, W.T., Lin, C.Y., 2009. Using virtual reality to determine how emergency signs facilitate way-finding. Applied Ergon. 40 (4), 722–730.

Teng, X., Guo, D., Guo, Y., Zhou, X., Liu, Z., 2019. CloudNavi: Toward ubiquitous indoor navigation service with 3D point clouds. ACM Trans. Sensor Netw. 15 (1), 1–28.

Tseng, Y.-C., Pan, M.-S., Tsai, Y.-Y., 2006. Wireless sensor networks for emergency navigation. Computer 39 (7), 55–62.

Valanto, P., 2006. Time-dependent survival probability of a damaged passenger ship ii-evacuation in seaway and capsizing. In: HSVA Report. pp. 42–62.

Vanem, E., Skjong, R., 2006. Designing for safety in passenger ships utilizing advanced evacuation analyses - A risk based approach. Saf. Sci. 44 (2), 111–135.

Veichtlbauer, A., Pfeiffenberger, T., 2011. Dynamic evacuation guidance as safety critical application in building automation. In: International Workshop on Critical Information Infrastructures Security. Springer, pp. 58–69.

Vihas, C., Georgoudas, I.G., Sirakoulis, G.C., 2012. Follow-the-leader cellular automata based model directing crowd movement. In: International Conference on Cellular Automata. Springer, pp. 752–762.

Vilen, E., et al., 2020. Evaluation of Software Tools in Performing Advanced Evacuation Analyses for Passenger Ships (Master's thesis). Aalto University.

Wada, T., Takahashi, T., 2013. Evacuation guidance system using everyday use smartphones. In: 2013 International Conference on Signal-Image Technology & Internet-Based Systems. IEEE, pp. 860–864.

Wan, Z., Jiang, C., Fahad, M., Ni, Z., Guo, Y., He, H., 2020. Robot-assisted pedestrian regulation based on deep reinforcement learning. IEEE Trans. Cybern. 50 (4), 1669–1682.

Wang, X., Guo, W., Cheng, Y., Zheng, X., 2015b. Understanding the centripetal effect and evacuation efficiency of evacuation assistants: Using the extended dynamic communication field model. Saf. Sci. 74, 150–159.

Wang, X.-L., Guo, W., Zheng, X.-P., 2015c. Effects of evacuation assistant's leading behavior on the evacuation efficiency: Information transmission approach. Chin. Phys. B 24 (7), 070504.

Wang, X., Guo, W., Zheng, X., 2016. Information guiding effect of evacuation assistants in a two-channel segregation process using multi-information communication field model. Saf. Sci. 88, 16–25.

Wang, L., He, Y., Liu, W., Jing, N., Wang, J., Liu, Y., 2014a. On oscillation-free emergency navigation via wireless sensor networks. IEEE Trans. Mob. Comput. 14 (10), 2086–2100.

Wang, J., Li, Z., Li, M., Liu, Y., Yang, Z., 2013. Sensor network navigation without locations. IEEE Trans. Parallel Distrib. Syst. 24 (7), 1436–1446.

Wang, C., Lin, H., Jiang, H., 2015a. CANS: Towards congestion-adaptive and small stretch emergency navigation with wireless sensor networks. IEEE Trans. Mob. Comput. 15 (5), 1077–1089.

Wang, C., Lin, H., Zhang, R., Jiang, H., 2017. SEND: A situation-aware emergency navigation algorithm with sensor networks. IEEE Trans. Mob. Comput. 16 (4), 1149–1162.

Wang, X., Liu, Z., Loughney, S., Yang, Z., Wang, Y., Wang, J., 2021a. An experimental analysis of evacuees' walking speeds under different rolling conditions of a ship. Ocean Eng. 233, 108–997.

Wang, X., Liu, Z., Loughney, S., Yang, Z., Wang, Y., Wang, J., 2022. Numerical analysis and staircase layout optimisation for a Ro-Ro passenger ship during emergency evacuation. Reliab. Eng. Syst. Saf. 217, 108056.

Wang, X., Liu, Z., Wang, J., Loughney, S., Zhao, Z., Cao, L., 2021b. Passengers' safety awareness and perception of wayfinding tools in a Ro-Ro passenger ship during an emergency evacuation. Saf. Sci. 137, 105–189.

Wang, X., Liu, Z., Zhao, Z., Wang, J., Loughney, S., Wang, H., 2020. Passengers' likely behaviour based on demographic difference during an emergency evacuation in a Ro-Ro passenger ship. Saf. Sci. 129 (1), 104–803.

Wang, W.L., Lo, S.M., Liu, S.B., Kuang, H., 2014b. Microscopic modeling of pedestrian movement behavior: Interacting with visual attractors in the environment. Transp. Res. C 44, 21–33.

Wang, P., Luh, P.B., Chang, S.C., Marsh, K.L., 2009. Efficient optimization of building emergency evacuation considering social bond of evacuees. In: 2009 IEEE International Conference on Automation Science and Engineering, CASE 2009. IEEE, pp. 250–255.

Wang, P., Luh, P.B., Chang, S.-C., Sun, J., 2008. Modeling and optimization of crowd guidance for building emergency evacuation. In: 2008 IEEE International Conference on Automation Science and Engineering. IEEE, pp. 328–334.

Wang, Y., Wang, K., Wang, T., Li, X.Y., Khan, F., Yang, Z., Wang, J., 2021c. Reliabilities analysis of evacuation on offshore platforms: A dynamic Bayesian network model. Process Saf. Environ. Prot. 150, 179–193.

Wang, X., Zheng, X., Cheng, Y., 2012. Evacuation assistants: An extended model for determining effective locations and optimal numbers. Physica A 391 (6), 2245–2260.

Wu, F.-J., 2017. A sensor-assisted emergency guiding system: sensor-centric or user-centric? IEEE Trans. Veh. Technol. 67 (2), 1598–1611.

Xie, Q., Li, S., Ma, C., Wang, J., Liu, J., Wang, Y., 2020a. Uncertainty analysis of passenger evacuation time for ships' safe return to port in fires using polynomial chaos expansion with Gauss quadrature. Appl. Ocean Res. 101, 102190.

Xie, Q., Wang, P., Li, S., Wang, J., Lo, S., Wang, W., 2020b. An uncertainty analysis method for passenger travel time under ship fires: A coupling technique of nested sampling and polynomial chaos expansion method. Ocean Eng. 195, 106604.

Xie, Q., Zhang, S., Wang, J., Lo, S., Guo, S., Wang, T., 2020c. A surrogate-based optimization method for the issuance of passenger evacuation orders under ship fires. Ocean Eng. 209 (March), 107–456.

Xu, Z., Lu, X., Guan, H., Chen, C., Ren, A., 2014. A virtual reality based fire training simulator with smoke hazard assessment capacity. Adv. Eng. Softw. 68, 1–8.

Yang, Y., Dimarogonas, D.V., Hu, X., 2013. Optimal leader-follower control for crowd evacuation. In: Proceedings of the IEEE Conference on Decision and Control. IEEE, pp. 2769–2774.

Yang, X., Dong, H., Wang, Q., Chen, Y., Hu, X., 2014. Guided crowd dynamics via modified social force model. Physica A 411, 63–73.

Yang, X., Dong, H., Yao, X., Sun, X., Wang, Q., Zhou, M., 2015. Necessity of guides in pedestrian emergency evacuation. Physica A 442, 397–408.

Yang, D., Zhang, L., Luo, M., Li, F., 2020. Does shipping market affect international iron ore trade?–An equilibrium analysis. Transp. Res. E 144, 102107.

Yin, K., 2015. Fire evacuation simulation for the case of a non-symmetrical metro station using wireless sensor network. In: 2015 5th International Conference on Information Science and Technology, ICIST 2015. IEEE, pp. 141–146.

Yin, Z., Wu, C., Yang, Z., Lane, N., Liu, Y., 2016. PpNav: Peer-to-peer indoor navigation for smartphones. In: 2016 IEEE 22nd International Conference on Parallel and Distributed Systems. ICPADS, IEEE, pp. 104–111.

Yoshida, K., Murayama, M., Itakaki, T., 2001. Study on Evaluation of Escape Route in Passenger Ships by Evacuation Simulation and Full-Scale Trials. Research Institute of Marine Engineering, Japan.

Yuan, Z., Jia, H., Zhang, L., Bian, L., 2018. A social force evacuation model considering the effect of emergency signs. Simulation 94 (8), 723–737.

Yuan, W., Tan, K.H., 2009. Cellular automata model for simulation of effect of guiders and visibility range. Curr. Appl. Phys. 9 (5), 1014–1023.

Zhang, S., Guo, Y., 2015. Distributed multi-robot evacuation incorporating human behavior. Asian J. Control 17 (1), 34–44.

Zhang, Z., He, S., Shu, Y., Shi, Z., 2020b. A self-evolving WiFi-based indoor navigation system using smartphones. IEEE Trans. Mob. Comput. 19 (8), 1760–1774.

Zhang, Z., Liu, H., Jiao, Z., Zhu, Y., Zhu, S.-C., 2020c. Congestion-aware evacuation routing using augmented reality devices. In: 2020 IEEE International Conference on Robotics and Automation. ICRA, IEEE, pp. 2798–2804.

Zhang, G., Lu, D., Liu, H., 2021. IoT-based positive emotional contagion for crowd evacuation. IEEE Internet Things J. 8 (2), 1057–1070.

Zhang, J., Zhao, J., Song, Z., Gao, J., 2020a. Evacuation performance of participants in an offshore platform under smoke situations. Ocean Eng. 216, 107–739.

Zheng, Y., Shen, G., Li, L., Zhao, C., Li, M., Zhao, F., 2017. Travi-navi: Self-deployable indoor navigation system. IEEE/ACM Trans. Netw. 25 (5), 2655–2669.

Zhou, M., Dong, H., Wang, X., Hu, X., Ge, S., 2020. Modeling and simulation of crowd evacuation with signs at subway platform: A case study of Beijing subway stations. IEEE Trans. Intell. Transp. Syst. 1–13.

Zhou, M., Dong, H., Zhao, Y., Ioannou, P.A., Wang, F.Y., 2019a. Optimization of crowd evacuation with leaders in urban rail transit stations. IEEE Trans. Intell. Transp. Syst. 20 (12), 4476–4487.

Zhou, M., Liu, J., Ge, S., Dong, H., 2019b. Passenger cooperative guidance system for urban rail transit stations. In: 2019 Chinese Automation Congress. CAC, IEEE, pp. 2985–2990.

Zhou, J., Wu, C.-C., Yu, K.-M., Tsao, Y., Lei, M.-Y., Chen, C.-J., Cheng, S.-T., Huang, Y.-S., 2012. Crowd guidance for emergency fire evacuation based on wireless sensor networks. In: The 5th IET International Conference on Ubi-Media Computing (U-Media). pp. 303–308.

Appendix D: Paper IV

Rapid Crowd Evacuation for Passenger Ships Using LPWAN

Yuting Ma, Kezhong Liu, Mozi Chen, *Member, IEEE*, Yinhao Li, Rui Sun, and Rajiv Ranjan, *Senior Member, IEEE*

***Abstract*— An emerging evacuation path planning technique that uses Low Power Wide Area Networks (LPWAN) to enable real-time danger prediction and user-oriented path planning can ensure the safe and timely navigation of evacuees in complex scenarios such as cruise ships. However, most existing LPWAN-based evacuation models assume pedestrians' walking speed remains constant and ignore crowd congestion in corridors before exits, which is not appropriate for rocking ships. To overcome these issues, this paper proposes a congestion-relived guiding framework with dedicated path planning for emergency evacuation on passenger ships. The basic idea is to averagely minimize the total evacuation time while meeting the deadline for ship capsizing under all circumstances by selecting uncrowded paths for each passenger individually. First, we use probability distributions rather than constant numbers to represent walking time (also called delay) along passageways. A worst-case delay bound with a high level of trustworthiness is also estimated for each passageway under the boundary condition of ship capsizing. Next, we predict the congestion of corridors by modeling the spatiotemporal movement of passengers, and then distribute evacuation loads evenly among corridors to alleviate the congestion. The total expected evacuation time of all corridors is finally minimized based on the delay probability distribution and estimated congestion, and the deadline for ship evacuation under all circumstances is met with the worst-case delay bound. Simulation results show that our approach significantly reduces the total escaping time of crowd evacuation by 45% and 34% while improving the navigation success ratio by more than 20% and 80% compared with the state-of-the-art emergency evacuation systems, namely the look-up table guiding scheme and the group-based guiding evacuation scheme, respectively.**

***Index Terms*— Passenger ship evacuation, Internet of Things, user-centric guiding, rapid routing, load balancing.**

Manuscript received 21 November 2022; revised 25 June 2023 and 26 August 2023; accepted 7 September 2023. Date of publication 22 September 2023; date of current version 2 February 2024. This work was supported in part by the National Natural Science Foundation of China (NSFC) under Grant 51979216; and in part by the Natural Science Foundation of Hubei Province, China, under Grant 2021CFA001 and Grant 20221j0059. The Associate Editor for this article was N. Wang. *(Corresponding author: Kezhong Liu.)*

Yuting Ma and Mozi Chen are with the School of Navigation, Wuhan University of Technology, Wuhan 430063, China (e-mail: 278827@whut.edu.cn; chenmz@whut.edu.cn).

Kezhong Liu is with the School of Navigation, Wuhan University of Technology, Wuhan 430063, China, also with the National Engineering Research Center for Water Transport Safety, Wuhan 430063, China, and also with the Hubei Key Laboratory of Inland Shipping Technology, Wuhan 430063, China (e-mail: kzliu@whut.edu.cn).

Yinhao Li, Rui Sun, and Rajiv Ranjan are with the School of Computing, Newcastle University, NE1 7RU Newcastle upon Tyne, U.K. (e-mail: yinhao.li@newcastle.ac.uk; r.sun5@newcastle.ac.uk; raj.ranjan@newcastle.ac.uk).

Digital Object Identifier 10.1109/TITS.2023.3314081

I. INTRODUCTION

MODERN passenger liners have the capability of carrying thousands of passengers and therefore if an accident involving such ships occurs its consequences will be disastrous. The safety of large passenger ships thus has gained increasing attention in recent years. Evacuation, a protective action in ship emergency circumstances, is very important in improving passenger and crew safety.

Internet of Things (IoT), born with the ability to explore the dynamic environmental conditions and the movement of people, can be incorporated into an evacuation system to monitor and interact with the physical world [1], [2], [3], [4]. When an emergency occurs, nodes collect the information on current hazard situation as well as the up-to-date distribution of people and send it to the path planning server which can provide guiding information to users equipped with smartphones or personal digital assistants (PDAs), so that they can escape from the hazardous area [5].

A. Motivation

A diversity of specifically designed solutions for emergency evacuation with IoT has been proposed. On one hand, those works use wireless technologies such as IEEE 802.15.1 Bluetooth and IEEE 802.15.3 ZigBee low-rate wireless personal area networks (LR-WPANs) for sensor applications, which are not adapted to the ship evacuation scenario where it requires long-range transmission [6], [7], [8], [9], [10], [11], [12]. LPWAN can provide long-range communication, while simultaneously it is inexpensive and highly energy efficient with a battery life of more than ten years [13], [14]. Therefore it is particularly suitable for the IoT application in emergency evacuation on large cruise ships, which only needs to transmit tiny amounts of data on environmental conditions (e.g., hazard information) to a path planning server in long range. In this paper, we supersede the widely employed short-range radio technologies by LPWAN. Fig. 1 shows the schematic representation of our proposed emergency evacuation scheme. In our scheme, a number of LPWAN nodes are deployed at exits, doors, and crossing points among corridors and/or doors of a passenger ship to monitor the real ship indoor environment. In addition, all passengers are equipped with smartphones that can communicate with nodes. The current location of each passenger is detected using the received strength of wireless signals on his/her smartphone, and the node ID with

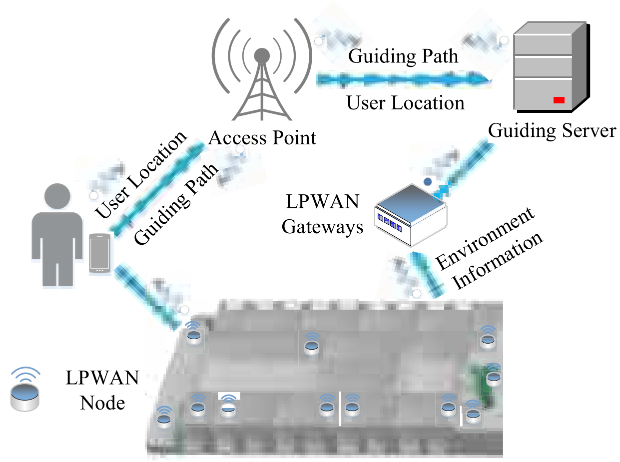

Fig. 1. Schematic representation of user-centric and congestion-relieved rapid emergency guiding scheme.

the strongest signal strength is used to determine the user's location in the blueprint database of node deployment. That is to say, we do not require accurate location information on each passenger in the proposed scheme. The smartphone periodically sends the determined position to the path planning server. When an emergency event is detected, the path planning server actively transmits a personalized evacuation path for each passenger to his/her smartphone and keeps updating it, according to the real-time collected information from users' smartphones and LPWAN nodes.

On the other hand, those works mostly address the emergency guiding in land-based buildings and do not sufficiently consider the unique characteristics of evacuation on passenger ships, such as the effect of changing inclination angles on passenger movement. Navigation solutions provided by those works deal with the situation where there is only a single constant numerical estimate of the delay/distance across individual passageways rather than a combination of probability distributions and upper bounds for delays of passageways. As a result, the planned escape paths are not necessarily optimal and even violate the deadline for ship evacuation, which is immensely perilous for passengers, due to the non-constant values of delay across individual passageways in an emergency on a passenger ship.

The prior work that is most related to ours assumed a model that characterizes each edge by a worst-case delay and a delay probability distribution. The performance objective considered in [15] is to identify safe paths that minimize the expected (i.e., average) delay. According to its provided solution, all passengers near a node, whose remaining deadlines are in the same interval, have to follow the same guiding direction of the next node. Considering the narrow corridors on passenger ships, escaping along the provided guiding direction is likely to cause a prolonged period required to evacuate passengers to the exit and even violate the specified deadline due to the possible waiting time resulting from congestion at certain passages or doors.

Before further introducing the motivation of this work, we present a formal definition as follows: the evacuation time of a path is defined as the sum of the moving time of corridors and the waiting delays of doors, exits, and crossing vertices.

Fig. 2 shows an illustrative example of the possible consequence of escaping along the guiding direction provided in [15] for 10 users, which helps to understand that it is indispensable to take into account the capacity of passageways/doors and the concurrent moving of different individuals in the design of passenger ship evacuation schemes. In the evacuation scenarios, the solid circles represent waypoints, and the green solid circle denotes the exit waypoint. The blue number alongside each edge between two waypoints indicates the expected delay that is computed using the delay probability distributions, and the red number denotes the worst-case delay which is the maximum delay that may be encountered in traveling the edge. In addition, the white number in each circle record the capacity of each waypoint. Based on the Hard-real-time routing algorithm in [15], the routing table at each waypoint is constructed, and all users, near the same waypoint and whose remaining deadlines are in the same interval, are guided to the same direction. According to temporal order, subgraphs (a)-(d) show the snapshots of evacuating 10 users in three intervals. We can see that there is no feasible route for the four users in red to take due to the needful waiting time caused by the congestion at v_1. We hope to utilize more idle and/or under-loaded paths such as the path $v_0 \rightarrow v_2 \rightarrow v_5$ as shown in Fig. 3 (the initial people distribution is the same as that at time t_0=0 in Fig. 2) evacuating the excessive users who will be delayed by the congestion and thus violate the specified deadline.

The above example reveals that it is unreliable to use the routing table provided by [15], and the congestion caused by the limited capacity of passageways/doors and the excessive number of people should be carefully taken into account in the design of evacuation for passenger ships. A safe and efficient evacuation approach should guide evacuees along the sub-optimal paths which are idle and/or underloaded so as to guarantee the eventual success of evacuation.

B. Contributions

Inspired by the above analysis, in this work, a user-centric congestion-relieved rapid path planning scheme is designed for evacuation guiding on passenger ships based on LPWAN (see Fig. 1). By considering the expected and worst-case delay across each passageway, corridor capacities, and the spatiotemporal mobility of all passengers together, our scheme can generate dedicated paths to minimize the total expected evacuation time while respecting a specified deadline. We first assign the passenger evacuation order according to the current evacuation time to make the difference of evacuation loading among passageways as balanced as possible and then plan dedicated escape routes accordingly based on the evacuation order.

The main contributions and novelty of this study are concluded as follows:

i) Currently, only LR-WPANs are of special concern in designing technology-assisted means to provide evacuees with navigation advice during emergencies. However, the ad-hoc deployment of LR-WPANs nodes in a large and complicated passenger ship will cause some nodes, especially near the

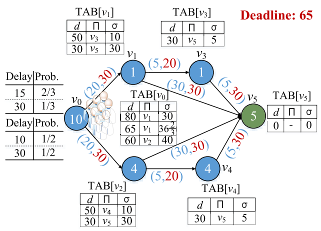
Deadline: 65
TAB[v_1]
TAB[v_3]
TAB[v_0]
TAB[v_5]
TAB[v_2]
TAB[v_4]
Delay Prob.
15 2/3
30 1/3
Delay Prob.
10 1/2
30 1/2
(20,30)
(5,20)
(30,30)
(5,30)

these path planning solutions, depending on the recalculation of navigation routes, may lead to users' oscillations. Frequent oscillations inevitably result in users remaining in danger for a longer period of time and eventually missing the chance of survival due to the blocking of all escape routes. Reference [9] proposed OPEN, a navigation approach that provides paths with the minimum probability of oscillations.

Without balancing the evacuation load in corridors and exits, the above-mentioned navigation schemes can guide evacuees to an over-congested route. Heavy congestion is likely to amplify users' panic and thus cause a higher threat to users' safety. Reference [22] proposed a distributed load-balanced guiding protocol that dispersed people to multiple exits according to the load of each path to achieve mild congestion and assist people in escaping quickly. Considering the vulnerability of users nearby dangers to congestion, [10] constructed a hazard level map tracking the evolution of boundaries of hazardous areas, so that users close to an emergency can be branched into different routes to avoid heavy congestion. Those approaches, however, neglect to consider path and exit capacities and therefore they are not enough to solve the congestion problem due to the different capacities of corridors/exits. Reference [23] took the evacuation capacities of exits into account. Each exit sensor is assigned a negative hazard potential value reversely proportional to its capability so that exits with higher evacuation capacities can attract more trapped users than exits with lower capacities. In [24], authors connected path capacity and moving speed. The artificial potential value of each sensor is determined by the moving speed of evacuees, distances to exits, as well as weighted exit capacities, and therefore the load of each road and exit can be balanced. Reference [11] designed an analytical model in which corridor length and capacity, exit capacity, and concurrent movement and distribution of people are considered together to further reduce the total evacuation time. Because these methods are to find a guiding direction for every single sensor for evacuating people nearby, a group of people near a sensor have to follow the same direction. Thus, the evacuation load of corridors cannot be fully balanced. Reference [25] relaxed the constraint on the number of direction assignments of every single sensor to design a user-centric guiding protocol, which provides a personalized guiding direction for each individual user and substantially reduces the total evacuation time. However, these methods neglected the high-level uncertainty of evacuation environments, they provided evacuation plans in a deterministic context which is not the case with researchers' considerations of uncertain real-world evacuation environments. Reference [26] considered the uncertainty of population distributions in endangered areas, and expressed them as Type-2 fuzzy variables of an uncertain path-based one-destination network flow model. Reference [27] took the uncertainty of travel time and risk into account and established a path-planning method based on multi-objective robust optimization to minimize the total cost function that combines the total evacuation time, the total risk, and the total congestion. Reference [28] presented a stochastic dynamic traffic assignment model, which represents the time-varying characteristics of the traffic flow, for emergency evacuations with the consideration of background traffic. However, these approaches are not suitable for the problem we seek to solve due to not incorporating the "hard" end-to-end deadline that is a fundamental part of ship emergency evacuation.

B. Evacuation on Passenger Ships

There is a significant research effort related to path optimization at sea aiming to aid ships in their navigation. Most of them focus on tackling the challenges associated with automatic collision avoidance concerning the maneuvering capabilities of ships as well as complying with maritime traffic rules [29], [30]. In addition, [31] constructed a space-air-sea-ground integrated monitoring network-based forecasting system for supporting the operational response of ships in distress. Compared with mature ship path planning, the work on passenger path planning on ships in case of emergencies is relatively limited.

The present studies on evacuation on passenger ships pay attention to simulating and modeling crowd behaviors under emergencies [32], [33], [34], [35]. Our paper does not focus on human behavior modeling or the belief-desire-intention (BDI) framework for emergency scenarios. These methods are beyond the scope of this paper and are not discussed here. The prior work pertaining to ours is [36]. Reference [36] took the limited ship survival time and the impact of ship motion on the movement speed of passengers into account. An adaptive emergency navigation strategy (ANT) based on rapid routing with guaranteed delay bounds algorithm was developed to determine hazard-free routes that typically experience the minimum delay while respecting the deadline by which passengers need to reach the embarkation points just beside the lifeboats or Marine Evacuation Systems (MES) under all circumstances. However, the related work finds optimal paths only using the typical-case and worst-case delay that characterize each passageway, while ignoring the waiting time due to congestion. In reality, if users evacuate along paths provided by ANT, it is likely to cause a prolonged typical period required to evacuate passengers to the exit and even violate the specified deadline considering the limited capacity of corridors/exits on ships. By far, a ship passenger evacuation solution is desired, which can provide safe and fast navigation service with IoT by taking multiple features (including the effect of ship motion on pedestrian motion, the limited ship survival time, the limited capacity of corridors/exits, and the up-to-date distribution and concurrent movement of passengers) into account.

III. System Model and Problem Statement

We address the scenario in which trapped passengers are navigated toward an exit. In practice, the exit could be the specified muster station on a passenger ship. The goal is to ensure the passengers' safe and timely evacuation.

In this section, we introduce the architecture overview of our proposed emergency guiding scheme, followed by the model and definitions. The third part describes the problem specification.

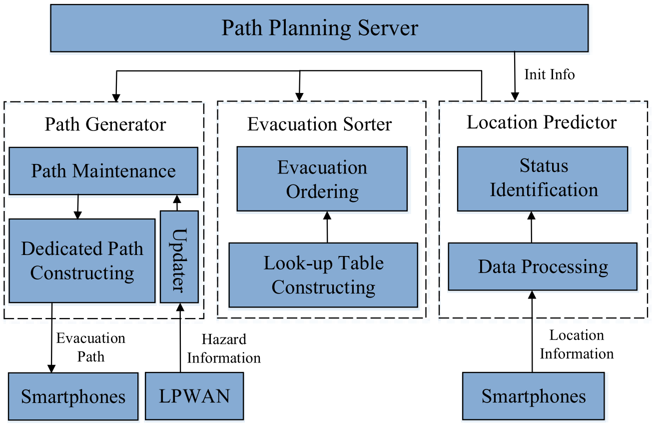

Fig. 4. Overview of our evacuation scheme.

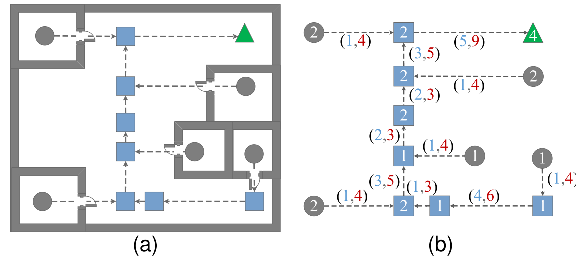

Fig. 5. Spatial modeling of indoor spaces. Squares, circles, and triangles represent crossing waypoints, door waypoints, and exit waypoints, respectively. (b) denotes $\mathcal{G}$ weighted by capacities and moving delay, where white numbers inside waypoints indicate their capacities, and blue numbers as well as red numbers alongside segments respectively represent the expected delays and worst-case delays across those segments.

A. System Architecture

Fig. 4 shows the architecture of our evacuation scheme, which consists of three main modules: location predictor, evacuation sorter, and path generator. These modules are integrated into the path planning server, providing a dedicated route for each user. First, the location predictor receives the location information on each user and then set the corresponding nodes as user nodes. Second, the evacuation sorter assigns evacuation orders to individuals for dedicated path planning by considering multiple features (i.e., the up-to-date distribution and concurrent movement of passengers, the moving time probability distribution across each corridor, and the capacities of corridors) together. Finally, the personalized paths are determined and sent to users' smartphones. Escaping along these provided paths can achieve the shortest expected total evacuation time, while guaranteeing to get passengers to the exit by the estimated deadline for ship evacuation.

To achieve improved performance, it is needed to re-plan evacuation paths for passengers until they reach the exit when the emergency environment changes due to the dynamic nature of hazards (e.g., expansion, contraction, clearance, and movement of hazardous areas). In addition, we assume that all passengers follow the offered indicators on their smartphones during evacuation.

B. Model and Definition

We model the LPWAN deployed in the indoor space of a passenger ship with one exit as a directed graph $\mathcal{G}$=($\mathcal{V}$, $\mathcal{E}$) as shown in Fig. 5, where $\mathcal{V}$ represents the set of waypoints (i.e., LPWAN nodes) and $\mathcal{E}$ is the set of segments (i.e., the walk paths between waypoints). The waypoints in $\mathcal{V}$ are classified into three types: exit waypoints, door waypoints, and crossing waypoints, which indicate the waypoints located at exits, doors, or crossing points among corridors and/or doors.

Each waypoint v_i is weighted by its capacity c_i (i.e., the number of passengers allowed to enter the waypoints per second). If the number of passengers remaining at a waypoint is greater than or equal to its capacity when an evacuee reaches, then the evacuation time of the evacuee equals his/her total moving time plus the waiting delay caused by the congestion. In addition, if two or more corridors with different capacities intersect each other, separate crossing waypoints are added to the directed graph for each corridor capacity. For each segment $\overrightarrow{v_i v_j}$, a probabilistic moving time function $P_{\overrightarrow{v_i v_j}}$ is specified. In our proposed model, $P_{\overrightarrow{v_i v_j}}$ is assumed to be the discrete probability distribution of the finite set of actual delays across the segment $v_i v_j$. That is, $P_{\overrightarrow{v_i v_j}}(d)$ is defined as the probability that the delay in traversing $\overrightarrow{v_i v_j}$ is d. In this paper, we suppose that $P_{\overrightarrow{v_i v_j}}$ is known a prior for all segments $\overrightarrow{v_i v_j} \in \mathcal{E}$. In addition, each segment $\overrightarrow{v_i v_j}$ is labeled with the expected delay $d_{\mathrm{T}}(\overrightarrow{v_i v_j})$ and the worst-case delay $d_{\mathrm{W}}(\overrightarrow{v_i v_j})$. $d_{\mathrm{T}}(\overrightarrow{v_i v_j})$ is an estimate of the expectation of all possible delays on the segment, which is computed as follows:

$$d_{\mathrm{T}}(\overrightarrow{v_i v_j}) = \sum_{\left\{d \mid P_{\overrightarrow{v_i v_j}}(d)>0\right\}} d \times P_{\overrightarrow{v_i v_j}}(d). \tag{1}$$

While $d_{\mathrm{W}}(\overrightarrow{v_i v_j})$ is the deterministic upper bound on the delay that will be encountered upon traversing the segment $\overrightarrow{v_i v_j}$.

C. Problem Formulation

In this work, we study the problem of escaping with a low expected delay from the current location to an exit in the constructed graph, while guaranteeing to arrive at the exit within the deadline for ship evacuation by considering 1) the expected and worst-case moving time across each segment, 2) the capacity of each waypoint, 3) the spatiotemporal mobility of individuals.

We first introduce some notations for formulating the objective of our emergency evacuation scheme. v_e denotes the exit waypoint and $\mathcal{V}_u$ is the set of the user waypoints. We assume that there are N users and path p_j is assigned user u_j, $1 \leq j \leq N$. Let v_i^j denote the i-th waypoint on path p_j. p_j is a waypoint sequence:

$$p_j \triangleq \left\langle v_u^j \equiv v_0^j, v_1^j, v_2^j, \ldots, v_k^j \equiv v_e \right\rangle.$$

where $v_u^j \in \mathcal{V}_u, \overrightarrow{v_{i-1}^j v_i^j} \in \mathcal{E}$ for $1 \leq i \leq k$, v_0^j and v_k^j respectively represent the waypoint location of user u_j and the exit.

Let $w_{\mathrm{W}}^j(i)$ and $w_{\mathrm{T}}^j(i)$ be the worst-case and expected waiting time at waypoint v_i^j respectively. The worst-case delay $d_{\mathrm{W}}(p_j)$ and expected delay $d_{\mathrm{T}}(p_j)$ of path p_j are defined in the following manner:

$$d_{\mathrm{W}}(p_j) = w_{\mathrm{W}}^j(0) + \sum_{i=1}^{k}(d_{\mathrm{W}}(\overrightarrow{v_{i-1}^j v_i^j}) + w_{\mathrm{W}}^j(i)). \tag{2}$$

$$d_{\mathrm{T}}(p_j) = w_{\mathrm{T}}^j(0) + \sum_{i=1}^{k}(d_{\mathrm{T}}(\overrightarrow{v_{i-1}^j v_i^j}) + w_{\mathrm{T}}^j(i)). \tag{3}$$

Let $T_{\mathrm{W}}^{(1,j)}(i)$ and $T_{\mathrm{T}}^{(1,j)}(i)$ respectively be the worst-case and expected time to evacuate from v_i^{j+1} for the last user of u_1, $u_2, \ldots, u_j$. The worst-case waiting time $w_{\mathrm{W}}^{j+1}(i)$ and expected waiting time $w_{\mathrm{T}}^{j+1}(i)$ of user u_{j+1} at waypoint v_i^{j+1} can be calculated by:

$$w_{\mathrm{W}}^{j+1}(i) = \begin{cases} 0, \text{if} T_{\mathrm{W}}^{(1,j)}(i) < \sum_{l=0}^{i-1}(d_{\mathrm{W}}(\overrightarrow{v_l^{j+1} v_{l+1}^{j+1}}) + w_{\mathrm{W}}^{j+1}(l)) \\ T_{\mathrm{W}}^{(1,j)}(i) - \sum_{l=0}^{i-1}(d_{\mathrm{W}}(\overrightarrow{v_l^{j+1} v_{l+1}^{j+1}}) + w_{\mathrm{W}}^{j+1}(l)), \\ \text{otherwise} \end{cases} \tag{4}$$

$$w_{\mathrm{T}}^{j+1}(i) = \begin{cases} 0, \text{if} T_{\mathrm{T}}^{(1,j)}(i) < \sum_{l=0}^{i-1}(d_{\mathrm{T}}(\overrightarrow{v_l^{j+1} v_{l+1}^{j+1}}) + w_{\mathrm{T}}^{j+1}(l)) \\ T_{\mathrm{T}}^{(1,j)}(i) - \sum_{l=0}^{i-1}(d_{\mathrm{T}}(\overrightarrow{v_l^{j+1} v_{l+1}^{j+1}}) + w_{\mathrm{T}}^{j+1}(l)), \\ \text{otherwise} \end{cases} \tag{5}$$

That is, if the worst-case (or expected) arrival time at v_i^{j+1} of user u_{j+1} is smaller than $T_{\mathrm{W}}^{(1,j)}(i)$ (or $T_{\mathrm{T}}^{(1,j)}(i)$), user u_{j+1} has to wait in the worst case (or the expected case) because some passengers are still jammed at v_i^{j+1}. Otherwise, there is no worst-case (or typical) waiting time at v_i^{j+1} for user u_{j+1} because there are no other passengers waiting at v_i^{j+1}. $T_{\mathrm{W}}^{(1,j)}(i)$ and $T_{\mathrm{T}}^{(1,j)}(i)$ can be calculated by:

$$T_{\mathrm{W}}^{(1,j)}(i) = \begin{cases} \sum_{l=0}^{i-1}(d_{\mathrm{W}}(\overrightarrow{v_l^j v_{l+1}^j}) + w_{\mathrm{W}}^j(l)), \text{if} v_i^j \notin p_{(1,j-1)} \\ \max(\sum_{l=0}^{i-1}(d_{\mathrm{W}}(\overrightarrow{v_l^j v_{l+1}^j}) + w_{\mathrm{W}}^j(l)), T_{\mathrm{W}}^{(1,j-1)}(i)), \\ \text{otherwise} \end{cases} \tag{6}$$

$$T_{\mathrm{T}}^{(1,j)}(i) = \begin{cases} \sum_{l=0}^{i-1}(d_{\mathrm{T}}(\overrightarrow{v_l^j v_{l+1}^j}) + w_{\mathrm{T}}^j(l)), \text{if} v_i^j \notin p_{(1,j-1)} \\ \max(\sum_{l=0}^{i-1}(d_{\mathrm{T}}(\overrightarrow{v_l^j v_{l+1}^j}) + w_{\mathrm{T}}^j(l)), T_{\mathrm{T}}^{(1,j-1)}(i)), \\ \text{otherwise} \end{cases} \tag{7}$$

We have the following base-case expressions $T_{\mathrm{W}}^1(i)$ and $T_{\mathrm{T}}^1(i)$:

$$T_{\mathrm{W}}^1(i) = \sum_{l=0}^{i-1} d_{\mathrm{W}}(\overrightarrow{v_l^1 v_{l+1}^1}). \tag{8}$$

$$T_{\mathrm{T}}^1(i) = \sum_{l=0}^{i-1} d_{\mathrm{T}}(\overrightarrow{v_l^1 v_{l+1}^1}). \tag{9}$$

Finally, the total worst-case and expected evacuation time of u_1, u_2, …, and u_j are respectively equal to:

$$d_{\mathrm{W}}(p_{(1,j)}) = \max(d_{\mathrm{W}}(p_1), d_{\mathrm{W}}(p_2), \ldots, d_{\mathrm{W}}(p_j)). \tag{10}$$

$$d_{\mathrm{T}}(p_{(1,j)}) = \max(d_{\mathrm{T}}(p_1), d_{\mathrm{T}}(p_2), \ldots, d_{\mathrm{T}}(p_j)). \tag{11}$$

The above estimation will be repeated until all evacuation time of u_1, u_2, …, and u_N are calculated. Our goal is to find a schedule minimizing the Total Evacuation Time (*TET*):

$$TET = \min((\max(d_{\mathrm{T}}(p_1), d_{\mathrm{T}}(p_2), \ldots, d_{\mathrm{T}}(p_N))), \tag{12}$$

subject to:

$$\max(d_{\mathrm{W}}(p_1), d_{\mathrm{W}}(p_2), \ldots, d_{\mathrm{W}}(p_N)) \leq DL. \tag{13}$$

where *DL* denotes the specified deadline for ship evacuation.

IV. User-Centric Congestion-Relieved Rapid Evacuation Method

In this section, we solve the congestion-relieved rapid path planning problem for user-centric emergency evacuation based on the work [15]. The procedure of our method is presented in pseudo-code form in Algorithm 1. The steps to determine the personalized route for each user, which can achieve the short total expected evacuation time while simultaneously guaranteeing that the total worst-case evacuation time is no more than the specified deadline for ship evacuation, are as follows:

- Modeling the indoor environment of a passenger ship
- Mapping individual locations
- Calculating congestion-relieved evacuation orders for each passenger
- Planning personalized evacuation paths

In Section III-A and Section III-B, we have the description of how to model ship indoor environment and map individual positions to the blueprint database of LPWAN node deployment. Regarding the modeling of the multi-floor ship indoor space, we add segments for stairs between floors. In the following, we elaborate on the planning of congestion-relieved evacuation orders and personalized evacuation routes.

In Algorithm 1, $\mathcal{P}$ denotes the set of the planned paths for all users, $ET_{\mathrm{T}}^{v_i}$ and $ET_{\mathrm{W}}^{v_i}$ are the evacuation tables added to each waypoint v_i respectively recording the expected and worst-case time required by all individuals to arrive at v_i. When an emergency event outside existing hazardous regions is detected, return to Line 1.

Algorithm 1 User-Centric Congestion-Relived Rapid Evacuation

Input: $\mathcal{G}$, $\mathcal{V}_u$
Output: $\mathcal{P}$
Construct evacuation graph;
for $i \leftarrow 1$ to N **do**
  Map users u_i to waypoints;
end
Call procedure Modified HRPG ($\mathcal{G}$=($\mathcal{V}$, $\mathcal{E}$), $\mathcal{V}_u$);
for $v_i \in \mathcal{V}$ **do**
  $ET_{\mathrm{T}}^{v_i}$={};
  $ET_{\mathrm{W}}^{v_i}$={};
end
while $N > 0$ **do**
  $d_{\mathrm{T}}(p_{min})$=min{$d_{\mathrm{T}}(p)|d_{\mathrm{W}}(p) \leq D$};
  for $v_j \in p_{min}$ **do**
    $ET_{\mathrm{T}}^{v_j^{p_{min}}}\left[d_{\mathrm{T}}(v_0^{p_{min}} \rightarrow v_j^{p_{min}})\right]$++;
    $ET_{\mathrm{W}}^{v_j^{p_{min}}}\left[d_{\mathrm{W}}(v_0^{p_{min}} \rightarrow v_j^{p_{min}})\right]$++;
    N--;
  end
end

A. Ordering of Evacuation for Each Individual

We design a congestion-relived scheme to determine the evacuation order based on the worst-case and typical evacuation time to the exit with the possible congestion caused by the escape of other users and the limited capacity of waypoints. The working flow of evacuation ordering for each individual is as follows.

1) Based on the algorithm in [15], the routes with specific expected delays while guaranteeing to respect the end-to-end deadline are determined for each user waypoint by only using the worst-case and expected delay across each segment. Note that we skip the comparison of the generated 3-tuples at user waypoints. That is, all tuples meeting the specified deadline are inserted for planning routes more efficiently. In addition, the 3-tuple in our scheme consists of d, p, and $d_{\mathrm{T}}(p)$ instead of d, π, and σ, with $d_{\mathrm{T}}(p)$ being the expected delay along the path p within the guaranteed worst-case delay bound d. The modified HRPG algorithm is shown in Algorithm 2 in the Appendix, where v_k represents the downlink neighbor of v_j. The set $\mathcal{N}_j^D$ of v_j's downlink neighbors is defined as follows:

$$\mathcal{N}_j^D \triangleq \left\{v_k \in \mathcal{V} | \overrightarrow{v_j v_k} \in \mathcal{E}\right\}$$

All users are sorted as u_1, u_2, $\ldots$, and u_N according to the planned escape routes p_1, p_2, $\ldots$, and p_N with the shortest expected evacuation time $d_{\mathrm{T}}(p_1)$, $d_{\mathrm{T}}(p_2)$, $\ldots$, and $d_{\mathrm{T}}(p_N)$ while guaranteeing users' arrival by the deadline under all circumstances, where $d_{\mathrm{T}}(p_1) \leq d_{\mathrm{T}}(p_2) \leq \ldots \leq d_{\mathrm{T}}(p_N)$. If two or more users have the same shortest expected evacuation time, the user with a longer second shortest evacuation time is selected first, and so on. If their all safe paths (i.e., paths that guarantee the user will meet the deadline even under worst-case circumstances) to exits have the same expected evacuation time, one of them can be simply randomly selected first. User u_1 is evacuated first along p_1.

2) The remaining users are sorted as u_2, u_3,..., and u_N by their paths p_2, p_3,..., and p_N with the shortest expected evacuation time $d_{\mathrm{T}}(p_2)$, $d_{\mathrm{T}}(p_3)$,..., and $d_{\mathrm{T}}(p_N)$, while guaranteeing users' arrival by the deadline under all circumstances. But we take the possible congestion caused by u_1 in this ordering. u_2 is selected to evacuate along the route p_2 after u_1. Note that now the order of evacuation may differ from the previous sorting due to the possible jam resulting from the escape of u_1 along the path p_1.

3) Likewise, the remaining users are sorted as u_3, u_4,..., and u_N by their paths p_3, p_4,..., and p_N with the shortest expected evacuation time $d_{\mathrm{T}}(p_3)$, $d_{\mathrm{T}}(p_4)$,..., and $d_{\mathrm{T}}(p_N)$, while guaranteeing users' arrival by the deadline under all circumstances. In this sorting, the possible congestion due to both u_1 and u_2 are considered. If the number n of users arriving at a waypoint v_i at the time t is less than or equal to the capacity c_i of v_i, then all of them can concurrently pass v_i at t without any delay. Otherwise, $n - c_i$ users will be delayed and evacuated at t+1. Similarly, if $n - c_i$ is still larger than c_i, then $n - 2c_i$ users only can pass v_i at t+2 and so on. The above process is repeated until all users are selected.

B. User-Centric Congestion-Relived Rapid Path Planning

The path with a minimum expected delay while meeting the deadline is planned based on the determined evacuation order, the expected and worst-case delay of each segment, the capacity of each waypoint, and the spatiotemporal mobility of users as follows. Before further introducing our proposed path planning method, we present some related definitions: v_{min}^j is the waypoint with the minimum capacity c_{min}^j in path p_j of user u_j.

1) Initially, the lookup tables constructed according to Algorithm 2 are added to each user waypoint. Based on the assigned evacuation order in Section IV-A, user u_1 is guided first. The expected and worst-case time required by u_1 to arrive at each waypoint v_i^1 along p_1 are recorded in $ET_{\mathrm{T}}^{v_i^1}$ and $ET_{\mathrm{W}}^{v_i^1}$ at all waypoints passed by u_1, respectively. In addition, the waypoint v_{min}^1 and its capacity c_{min}^1 in p_1 are also recorded.

2) Second, according to the determined evacuation order, the evacuation path p_2 with the minimum expected time $d_T(p_2)$ while meeting the deadline even under the worst case with the possible congestion caused by u_1 is provided to u_2. The expected and worst-case time it will take for u_2 to arrive at each waypoint along the path are respectively recorded in $ET_{\mathrm{T}}^{v_i^2}$ and $ET_{\mathrm{W}}^{v_i^2}$ at these waypoints. Note that if there are other users initially located at the same user waypoint as u_1, then $p_1 \equiv p_2 \equiv, \ldots, \equiv p_{c_m^1}$.

3) The aforementioned planning and recording process is repeated until the expected and worst-case time it will take for u_N to arrive at each waypoint along p_N are recorded in $ET_{\mathrm{T}}^{v_i^N}$ and $ET_{\mathrm{W}}^{v_i^N}$ at his/her passed waypoints respectively. By considering the spatiotemporal mobility of u_1, u_2,..., and u_{N-1} and the all possible safe routes for u_N, the expected evacuation time $d_{\mathrm{T}}(p_N)$ can be minimized, while at the same

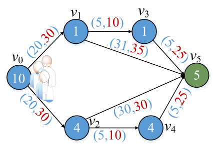
v_0
v_1
v_2
v_3
v_4
v_5
10
1
1
4
4
5
(20,30)
(20,30)
(5,10)
(31,35)
(5,25)
(30,30)
(5,25)
(5,10)

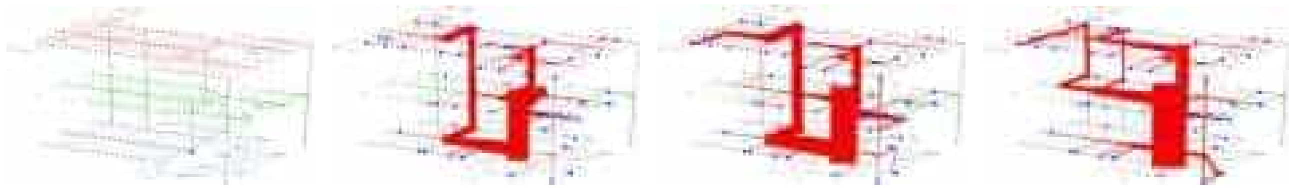

(a) The network of the second, third, and fourth floor of "Yangtze Gold 7" passenger ship with 346 nodes (b) Trace of users' egress paths using lookup table guiding scheme (c) Trace of users' egress paths using group-based guiding scheme (d) Trace of users' egress paths using our proposed guiding scheme

Fig. 7. Columns from left to right: (a) The original network with three floors and one exit (the green triangle). The segments on the first, second, and third floors are marked in blue, green, and red, respectively. Moreover, segments on the staircases are marked in black. (b) Trace of users' egress paths (highlighted in red) routed using the lookup guiding approach. (c) Trace of users' egress paths routed using the group-based guiding approach. (d) Trace of users' egress paths routed using our framework.

obtained by randomly selecting values from the interval $\left[d_{\mathrm{H}}(\overrightarrow{v_i v_j}), d_{\mathrm{W}}(\overrightarrow{v_i v_j})\right]$ as possible actual delays, which correspond to certain probabilities. $d_{\mathrm{H}}(\overrightarrow{v_i v_j})$ is estimated as follows:

$$d_{\mathrm{H}}(\overrightarrow{v_i v_j}) = \frac{l_{\overrightarrow{v_i v_j}}}{s_{\mathrm{H}}(\overrightarrow{v_i v_j})}. \tag{16}$$

where $s_{\mathrm{H}}(\overrightarrow{v_i v_j})$ is the walking speed when the ship inclination angle equals 0°. In our simulations, $s_{\mathrm{H}}(\overrightarrow{v_i v_j}) = 1.2$ m/s. The deadline for ship evacuation is estimated as follows:

$$DL = T_{\mathrm{S}} - T_{\mathrm{A}} - T_{\mathrm{EL}}. \tag{17}$$

where T_{S} denotes the total survival time until the ship will capsize, and T_{A} is the awareness time beginning upon initial notification of an emergency and ending when passengers accept the situation and start to move based on the provided navigation direction. T_{EL} denotes the sum of embarkation time and the launching time (i.e., the time required to provide for abandonment by the total number of persons on board). According to the guidelines approved by the Maritime Safety Committee (MSC), T_S equals 60 minutes, T_{A} equals 10 minutes, and T_{EL} equals 20 minutes in our simulations. That is, DL equals 30 minutes unless stated otherwise.

The number of inserted evacuees varies between 10 and 350. The number of hot-spot nodes is from 2 to 16. In each run of simulations, 50% evacuees are first randomly assigned to all waypoints and then the other 50% evacuees are randomly assigned to hot-spot nodes such that more passengers need to be guided at the hot-spot nodes than the other nodes. We perform the simulations written in Python on the Linux server equipped with Intel (R) Xeon (R) Silver 4210R CPU @ 2.40GHz and 125 GB memory. Each simulation is repeated 10 times and the average value is taken as the final result unless stated otherwise. We compare our scheme against the look-up table guiding method in [36] and the group-based guiding approach in [11]. The former guides evacuees to the neighbor that can achieve the minimum expected delay to the exit waypoint while ensuring the arrival within the specified deadline in the case of no congestion, while the latter provides groups of evacuees with the fastest paths based on the evacuation time estimated by their analytical model.

B. Simulation Results

Fig. 7 shows the possible evacuation paths by the three schemes mentioned in Section V-A for users in the simulated ship indoor environment. 100 user nodes and 20 hot spots are injected into the environment. We notice that it is different among the paths provided by the three approaches. We will further focus on four metrics for evacuation performance evaluation: total expected evacuation time, success ratio of evacuation, congestion distribution, and average escaping rate.

1) Total Evacuation Time: We evaluate the efficiency and safety of the evacuation service of our proposal in terms of the total expected and worst-case evacuation time of all injected users, respectively.

We inject 10, 40,…,310 users into the simulated indoor environment. The number of hot spots is set as 2. Fig. 8a shows the expected moving time of the three approaches under different numbers of users. This result demonstrates the superior evacuation efficiency using our method, especially in the scene with a high occupancy rate (more than 100 users). This is not much surprising as the look-up table method invariably requires that all users escape along optimal paths with minimum expected delays, which results in widespread congestion along the offered routes, while other less optimal (yet safe) will be idle throughout the evacuation. Therefore the performance of the look-up table method deteriorates when there are over 100 users. Moreover, we can see the performance of the group-based guiding approach is marginally better than that of the look-up table method. The main reason is group-based guiding scheme selects paths for users by jointly taking into account the capacity of nodes and parallel moving of users, which can efficiently alleviate possible congestion caused by other groups to minimize the total escaping time. Nevertheless, the performance of the group-based guiding approach remains unsatisfactory when many users exist near the same node, because a group of users near a node has to follow the same guiding direction to the same next landmark. That is, the evacuation load of passageways does not be fully balanced in this scheme, and thus the lowest total evacuation time for all users does not be achieved.

Fig. 8b shows the worst-case moving time. As the number of users continues to increase, the total worst-case time does not exceed the specified deadline for ship evacuation using our method. While it violates the deadline for the two other approaches in some cases. For example, when the number of users is more than 190 the deadline is violated using the look-up table method since it does not take the potential congestion into account. It is worth noticing that

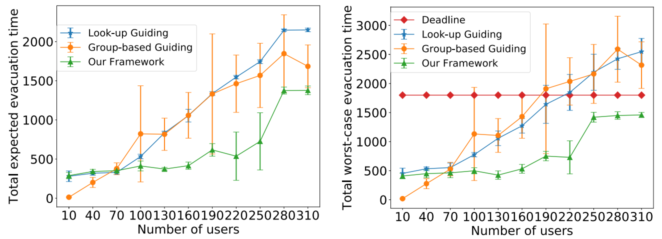

(a) Total expected evacuation time versus number of users
(b) Total worst-case evacuation time versus number of users

Fig. 8. Total evacuation time versus number of users.

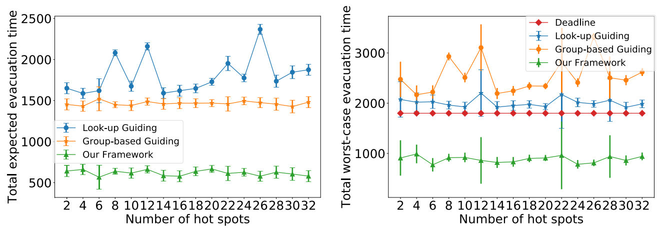

(a) Total expected evacuation time versus number of hot spots
(b) Total worst-case evacuation time versus number of hot spots

Fig. 9. Total evacuation time versus number of hot spots.

using the group-based method violates the deadline more than the look-up table approach because the group-based method does not consider the worst-case delay across each segment. In addition, the total expected and worst-case moving time of the three approaches seems to increase when there are growing users, which is caused by the inevitable waiting time considering the narrow corridors and the large number of users.

To test the robustness of our proposal against hot spots, we compare the total moving time with the different numbers of hot spots using the three evacuation schemes. We inject 250 users into the simulated ship indoor environment. The number of hot spots is from 2 to 32. From Fig. 9, we can observe that our method performs better than the other two approaches for all the numbers of hot spots.

2) Success Ratio of Evacuation: The purpose of this group of simulations is to compare our proposed method with two other schemes with respect to the evacuation success ratio. We consider four different cases: (i) 40 users being injected in the environment with 2 hot spots (named H2U40), (ii) 190 users being injected in the environment with 2 hot spots (named H2U190), (iii) 40 users being injected in the environment with 32 hot spots (named H32U40), (iv) 190 users being injected in the environment with 32 hot spots (named H32U190). In our simulations, missing the deadline is considered the only factor which leads to evacuation failure. Therefore, we evaluate the evacuation success ratio using the possibility of arriving at the exit along the provided path before the specified deadline for ship sinking, which is expressed as 1-$\frac{d_W(p)-DL}{d_W(p)}$ in the case where $d_W(p) \geq DL$. Otherwise, the possibility equals 1. Fig. 10 shows that our approach clearly outperforms the other two methods by always achieving a 100 percent evacuation success ratio in all scenarios. The look-up table guiding method and group-based guiding

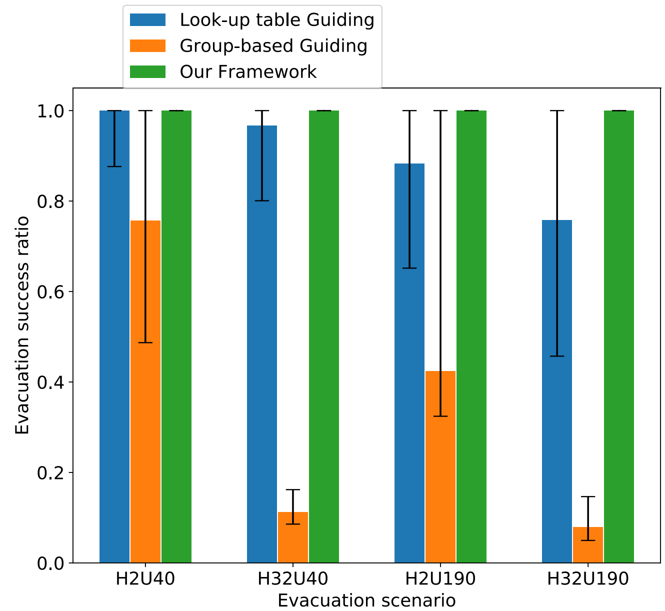

Fig. 10. Evacuation success ratio versus evacuation scenario.

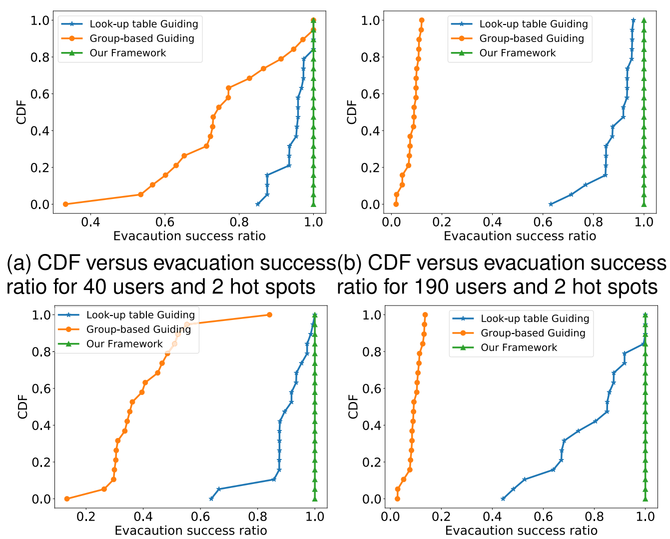

(a) CDF versus evacuation success ratio for 40 users and 2 hot spots
(b) CDF versus evacuation success ratio for 190 users and 2 hot spots
(c) CDF versus evacuation success ratio for 40 users and 32 hot spots
(d) CDF versus evacuation success ratio for 190 users and 32 hot spots

Fig. 11. CDF versus evacuation success ratio for different numbers of users and different numbers of hot spots.

approach fail to ensure evacuation success in some scenarios, because they do not take the congestion of corridors and worst-case delay on each segment into account, respectively. As a result, the worst-case evacuation times of all the users using the two methods are likely to exceed the specified deadline. We can also see the performance of the look-up table guiding method is better than that of the group-based guiding method. The reason is explicit: all the routes are scheduled without considering the worst-case delay across each segment using the group-based guiding scheme, and thus the total worst-case evacuation time most likely exceeds the specified deadline, which yields the evacuation failure.

We further simulate the cumulative distribution function (CDF) of the evacuation success ratio of the three approaches

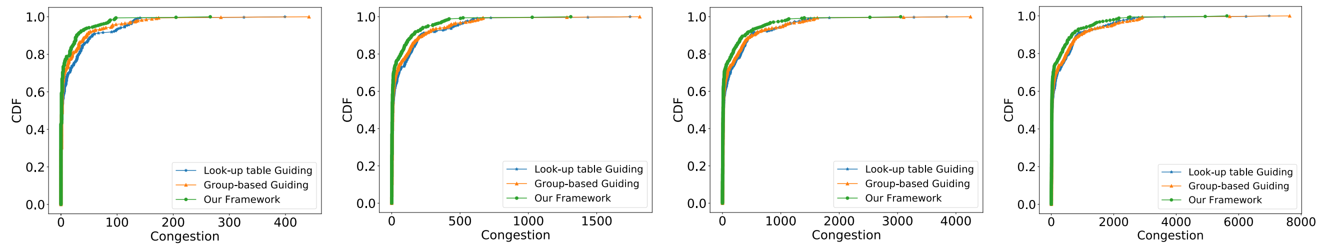

(a) CDF versus congestion for 300 paths (b) CDF versus congestion for 1000 paths (c) CDF versus congestion for 1700 paths (d) CDF versus congestion for 2400 paths

Fig. 12. CDF versus congestion for different numbers of users in the network with 20 hot spots.

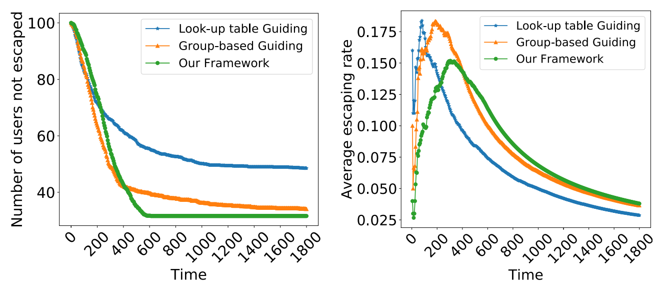

(a) Number of users not escaping every 5 seconds versus time for 32 hot spots and 100 users (b) Average escaping rate every 5 seconds versus time for 32 hot spots and 100 users

Fig. 13. Comparisons of the number of users not escaping and the average escaping rate every 5 seconds for 32 hot spots and 100 users.

Fig. 14. Collision location of the Costa Concordia disaster.

(a) The plan of the first floor

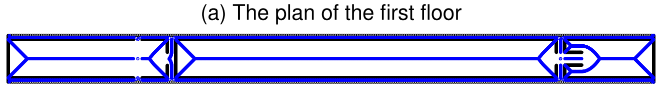

(b) The evacuation network of the first floor

Fig. 15. The evacuation network of the first floor of the Costa Concordia.

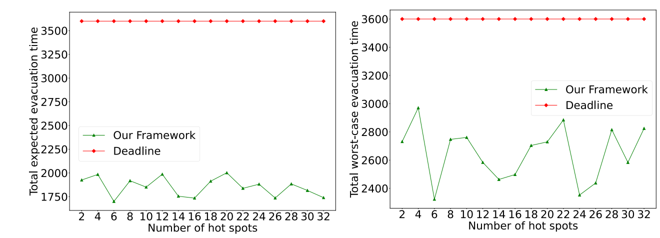

(a) Total expected evacuation time versus the number of hot spots (b) Total worst-case evacuation time versus the number of hot spots

Fig. 16. Total evacuation time for all people on the Costa Concordia using our approach under scenarios with different hot spots.

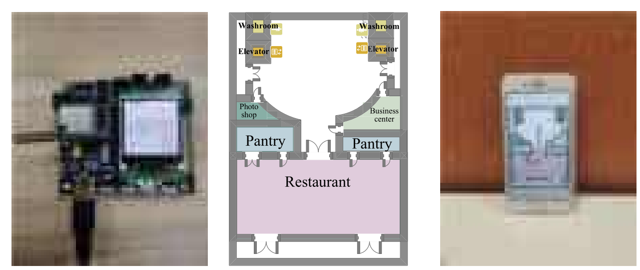

(a) (b) (c)

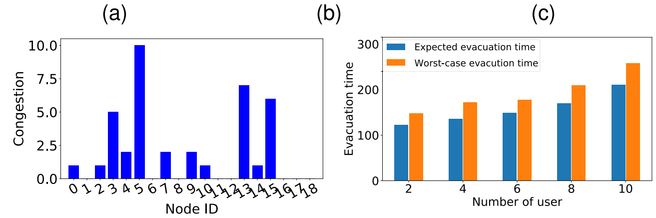

(d) The congestion of each node (e) Total expected and worst-case evacuation time

Fig. 17. System implementation of user-centric congestion-relieved emergency guiding.

under cases H2U40, H32U40, H2U190, and H32U190. Simulation results are the output of 20 runs of each approach under the different cases. It can be seen that 100 percent of users can be successfully directed to the exit using our method in the scenarios where 40 and 190 users have to be dispersed from the network with 2 and 32 hot spots, respectively. Our algorithm selects a path with the minimum expected evacuation time while guaranteeing to respect the specified deadline under all circumstances by jointly considering the capacity of the waypoints and the parallel moving of users. The cases in the four settings with our approach are better than those with the look-up table guiding method and group-based guiding method. It is increasingly likely that there is no feasible route for a user to take with more users in the simulated environment. Therefore, the performance under the setting with 40 users is better than that under the setting with 190 users for the other two approaches.

3) Congestion Distribution: We measured a segment's congestion by the number of scheduled paths the segment is involved in. The segments of routes are marked in red.

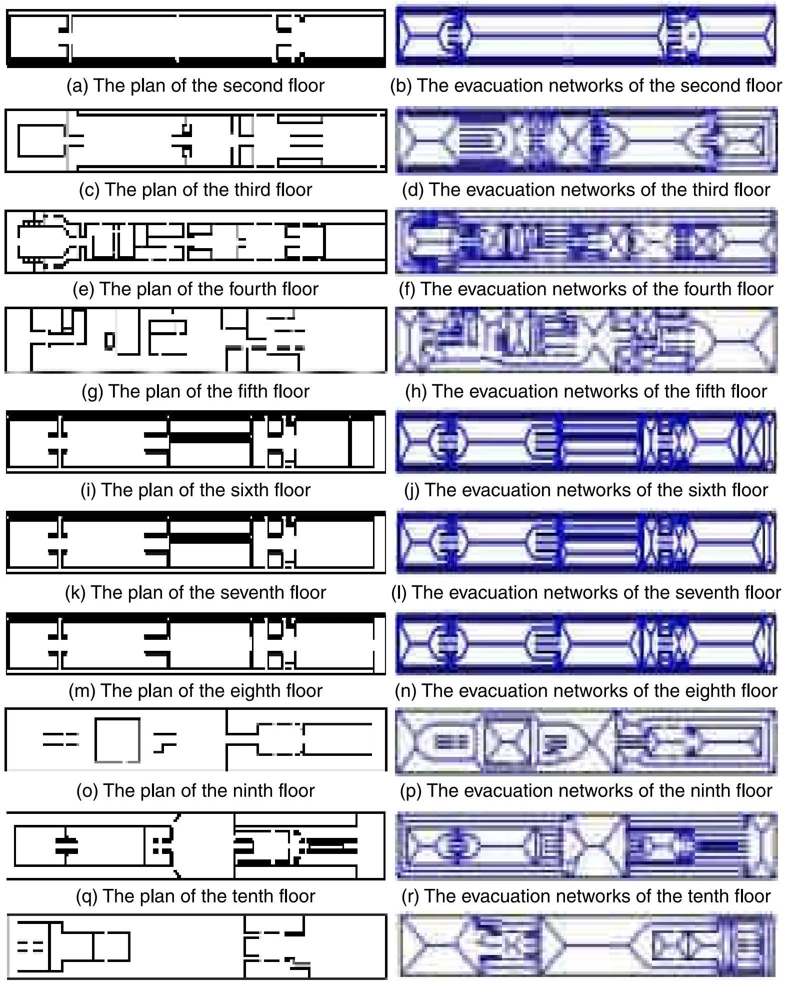

(a) The plan of the second floor (b) The evacuation networks of the second floor
(c) The plan of the third floor (d) The evacuation networks of the third floor
(e) The plan of the fourth floor (f) The evacuation networks of the fourth floor
(g) The plan of the fifth floor (h) The evacuation networks of the fifth floor
(i) The plan of the sixth floor (j) The evacuation networks of the sixth floor
(k) The plan of the seventh floor (l) The evacuation networks of the seventh floor
(m) The plan of the eighth floor (n) The evacuation networks of the eighth floor
(o) The plan of the ninth floor (p) The evacuation networks of the ninth floor
(q) The plan of the tenth floor (r) The evacuation networks of the tenth floor
(s) The plan of the eleventh floor (t) The evacuation networks of the eleventh floor

Fig. 18. The evacuation networks of the second to eleventh floors of the Costa Concordia.

The wider mark indicates heavier congestion of the segment, namely a more serious overuse by a specific evacuation approach mentioned in Section V-A. 100 users are generated in the simulated environment with 20 hot spots. As shown in Fig. 7, our proposed method has a better performance with respect to congestion distribution than the other two approaches, and it can discover a non-trivial path bypassing the over-congested parts. In comparison, the other two guiding approaches perform poorly.

To show the superiority of our framework in terms of nodes' congestion, we also simulate the CDF of congestion of the waypoints based on the 300, 1000, 1700, and 2400 paths (30, 100, 170, and 240 users for 10 times tests), respectively. It is observed that our proposed method has a better performance in all cases. Take the scenario where 300 paths are generated for example, most waypoints in our method are involved in less than 100 paths. In contrast, about 10 percent of the waypoints are extremely over-involved in more than 150 paths in the Look-up table method and Group-based guiding method. That is to say, those waypoints have to burden more than half of the users, which on one hand prolongs the total evacuation time, and on the other hand, increases the threat to user safety since it is more likely that heavy congestion will cause a stampede of the directed users.

4) Average Escaping Rate: Fig. 13a shows the comparisons of the number of users not escaping every five seconds for 32 hot spots for 100 users. Using our scheme, more users can be evacuated if the evacuation becomes unavailable (due to ship sinking, falling ceilings, damaged passageways, or blocked exits) before all users escape. On the other hand, Fig. 13b shows the comparisons of average escaping rates in Fig. 13a. It is clear that our scheme can guide users as many as possible during the most congested period.

C. Case Study

The proposed rapid crowd evacuation strategy was applied to the Costa Concordia (call sign: IBHD, IMO number: 9320544, MMSI number: 247158500) disaster that occurred at 21:45 on 13 January 2012, due to the collision with the reef at 42°21′55″N, 10°55′18″E in the Tyrrhenian Sea, as shown in Fig. 14 (all times used in this paper are local). Despite the relatively long survival time from 21:45 to 24:00, during which the ship listed and ultimately capsized at 24:00, the incident still resulted in 33 lives of passengers and crew on board. The factors that contributed to the death of 33 people are complicated, with the inadequate evacuation process playing a major part. Next, we will apply our proposed evacuation strategy to this accident to evaluate the effectiveness of our approach.

The simulated indoor environments are the first to eleventh floors, and we insert evacuees on the first, second, as well as sixth to eleventh floors of the ship. Fig. 15 shows the evacuation network of the first floor (the evacuation networks of the remaining floors are presented in Fig. 18). The exit waypoints are located beside the lifeboats on the fourth floor. 4229 trapped individuals are uniformly distributed in the evacuation network. The survival time of the ship is set to be 90 minutes, specifically from 21:45 to 23:15 when the list of the Costa Concordia to starboard reached 45°. Once the angle exceeds 45°, passengers on board will no longer be able to move. Due to the evacuation being conducted in the night scenario, the awareness time is set to 10 minutes. Considering the embarkation and launching time of 20 minutes, the estimated deadline for ship evacuation is 60 minutes (i.e., 90-10-20). Based on [37], the worst-case speed across each corridor segment is estimated to be 0.06 m/s (i.e., 1.2×0.05), while for staircase segments, it is 0 m/s. The probabilistic speed distribution across a corridor segment is obtained by selecting values from the interval $[0.06, 1.2]$ as possible actual speeds with associated probabilities, while for staircase segments, it is obtained by choosing values from $[0, 1.0]$. 1.2 and 1.0 respectively represent the average walking speed across corridor segments and staircase segments when the ship inclination angle equals 0°. Through the case study, we evaluate the effectiveness of our approach in terms of total evacuation time. Fig. 16 shows the total expected and worst-case evacuation time against hot spots using our method. It is worth noticing that both the total expected and worst-case evacuation times are shorter than the deadline for ship evacuation in all cases. This implies that all evacuees can successfully evacuate using our scheme. Here we consider the only factor causing the evacuation failure, is the excessing of the ship evacuation deadline. Therefore, by implementing our approach, it is possible to prevent the loss of lives that occurred in the Costa Concordia disaster, where 32 people died.

VI. Prototype Implementation

As shown in Fig. 17a, we implement a prototype testbed using SX1276 chips, which can transmit the information on sensor status to a path planning server, The server adopts an event-driven framework written in Python to generate guidance information and send it back to internal users. Our test bed consists of 19 nodes deployed on the second floor of The "Yangtze Gold 7" passenger ship (see Fig. 17b).

In our experiment, we mainly focus on the total expected and worst-case evacuation time as well as nodes' congestion (i.e., the number of routes that a node is involved in). During the experiments, two nodes are set as the hot spots, and we randomly choose two to ten initial positions of users.

Fig. 17d depicts the congestion of each node in the scenario with 10 user nodes. We can see that the majority of nodes are involved in less than 3 paths, and there are only 4 nodes overcrowded, which are involved in more than 5 paths. These overcrowded nodes are located near the exit. Fig. 17e shows the expected and worst-case total evacuation time under different numbers of users. It can be seen that both of them increase gracefully from about 100 to 200, and 150 to 250 as the number of users increases from 2 to 10, respectively.

VII. Conclusion and Discussion

Evacuation guiding is essential for passengers when an emergency event occurs on a vessel. Thus over the last decade, substantial research has been conducted to investigate passenger evacuation behavior, optimizing and evaluating passenger evacuation performance. Most if not all of these works apply the land-based indoor evacuation approaches to provide passengers onboard vessels with advice regarding the evacuation procedure during emergencies. However, these methods neglect the specific challenges of ship evacuation, which differ from other evacuation scenarios. For example, the deadline for ship evacuation, the dynamics of travel time across each passageway caused by the unstable surface, the limited corridor capacity, and the massive crowd mobility all play critical roles in designing evacuation schemes for passenger ships to ensure passenger safety and survival. Existing ship evacuation strategies mainly focus on the paths with the shortest evacuation distance or evacuation time on static walking conditions, while in reality, the walking speed of passengers may vary in time due to the changing inclination angle of a damaged ship, and thus navigation paths provided by these methods are not necessarily optimal and even impassable during emergencies. Furthermore, those methods do not incorporate the hard end-to-end deadline that is a fundamental part of the ship evacuation problem.

Thus, this study for the first time simultaneously takes into account the unique challenges of ship evacuation such as the effect of dynamic ship indoor walking environments and the deadline for ship evacuation, as well as other factors that are also vital to the safe and efficient evacuation of passengers on ships such as the limit of the capacity for passageways and the concurrent movement of massive crowds. We propose a user-centric congestion-relieved rapid path planning scheme for ship evacuation guiding based on LPWAN that can automatically explore the dynamics of danger and the movement of passengers. Firstly, a loading-based scheme is designed to assign passenger evacuation orders according to the expected delay across each segment, the corridor capacities, and the spatio-temporal movement of evacuees to make the difference of evacuation loading among passageways as balanced as possible. Then based on the determined evacuation order, together with other factors influencing the ship evacuation (e.g., the worst-case delay as well as the probabilistic delay function specified on each segment, the up-to-date distribution of passengers, and the capacities of passageways), dedicated escape routes are generated to minimize the total expected evacuation time while respecting an end-to-end deadline for ship evacuation despite the changing ship inclination status. The implementation and experimental results demonstrate the advantages of our scheme.

However, the ship evacuation system community still has a degree of skepticism regarding the applicability of our proposed scheme. Its difficulty mainly lies in modeling the delays across individual passageways on passenger ships. That is, how to design a probabilistic model capable of capturing dynamics of traversal times across segments caused by the changing ship inclination angle is the primary challenge for the implementation of our proposed scheme. In this paper, we mainly focus on the design of an evacuation protocol, given a specific model of delay. Therefore the design and refinement of a delay model is an interesting issue to be studied in order to further enhance and implement our emergency evacuation scheme for passenger ships in the future.

In addition, hazardous areas may vary (e.g., emergence, disappearance, expansion, or shrinkage) over time during an evacuation. Accordingly, navigation paths provided by our scheme for evacuees should be adapted due to the dynamics of hazards, which may cause evacuees' oscillation. Frequent oscillation inevitably results in a decrease of the chances of survival for evacuees. Thus, how to sufficiently address the dynamics of danger to minimize the passive reentrant as much as possible is left to our future work.

Last but not least, in our scheme, navigation decisions are computed and forwarded by a central path planning server, to all end users as they pass through pre-determined waypoints that guide them towards safe exit points. The server is potentially damaged or disconnected in the event of ship damage, which will result in the failure of the entire emergency evacuation system. In future research we plan to design novel decentralized emergency evacuation systems for guiding passengers to safety, that pre-locate advisory data to passengers in intermediate waypoints, and also combine passenger attributes (e.g., their age, gender, and resistance to hazards).

Appendix I

Fig. 2 shows the illustrative example of violating the specified source-to-destination deadline for multiple users using the approach in [15]. Fig. 2a indicates the example graph and the distribution of evacuees at the initial stage of the evacuation. All of the 10 people are located nearby the waypoint v_0. The deadline is assumed to be 65 units of time in this example. According to the advice provided by routing tables which are constructed based on the algorithm in reference [15], all the people are navigated to the waypoint v_1 along the segment $\overrightarrow{v_0v_1}$. Suppose that all of these people experience a delay of 30 time units across the segment $\overrightarrow{v_0v_1}$. Due to the waiting time caused by the limitation of the capacity of the vertex v_1 that only permits the passage of one person at a time, there are no feasible paths for the four people in red. That is, there is no segment to take from the waypoint v_1 for the four people, which will not violate the remaining deadline to the exit waypoint v_5, i.e., 29, and thus it will declare evacuation failure for them, as shown in Fig. 2b. Fig. 2c shows the distribution of the other six people at time 60. It is assumed that they encounter a delay of 30 across the segment $\overrightarrow{v_1v_5}$. we can see that the user in green is evacuated successfully from the exit waypoint v_5, and due to the capacity constraint of v_5, the other five people will escape from v_5 at the time 61, 62, 63, 64, and 65, respectively as shown in Fig. 2d. Therefore, the evacuation based on the algorithm in [15] is capable of guaranteeing the successful evacuation of six people as we illustrate above.

Fig. 3 shows the desired evacuation for the 10 users. Both The initial distribution of the 10 people and the specified source-to-destination deadline are the same as those of Fig. 2. The 10 people at the waypoint v_0 are divided into two groups: one, consisting of six people, escapes along the segment $\overrightarrow{v_0v_1}$, and the other, consisting of four people, escapes along the segment $\overrightarrow{v}_0v_2$. Suppose that both of the two groups of people experience a delay of 30 across the segments $\overrightarrow{v_0v_1}$ and $\overrightarrow{v_0v_2}$, respectively. Fig. 3a indicates the distribution at time 30. We can see that the four users can simultaneously pass through the waypoint v_2 at a time, while the other six users have to pass through the waypoint v_1 one by one considering the capacity limit of 1 person per time unit at v_1. At the time 35, the remaining deadline is 30, and thus there is still a feasible outgoing segment $\overrightarrow{v_1v_5}$ to take from the waypoint v_1 for the last user in the group of six. Fig. 3b and Fig. 3c show the distribution of people at the time 35 and 60, respectively. It is assumed that both of the two groups experience a delay of 30 while crossing the segments $\overrightarrow{v_1v_5}$ and $\overrightarrow{v_2v_5}$, respectively. From Fig. 3c, it is observed that all the people in the group of four and one person in the group of six are successfully evacuated from the exit waypoint v_5 at the time 60. Fig. 3d shows that all people are successfully navigated at the time 65. Comparing the evacuation in Fig. 2 and Fig. 3, it is explicit that the consideration of the capacity of corridors and exits, as well as the exploitation of the idle paths, will benefit the overall evacuation of all evacuees.

Algorithm 2 Modified HRPG Algorithm

Input: $\mathcal{G}$, $\mathcal{V}_u$
Output: TAB[v_u], $v_u \in \mathcal{V}_u$

Call procedure Initialize ($\mathcal{G} = (\mathcal{V}, \mathcal{E})$);
for $i = 1 \leftarrow (|\mathcal{V}| - 1)$ **do**
  for $\overrightarrow{v_iv_j} \in \mathcal{E}$ **do**
    if TAB$\left[v_j\right] \neq [\,]$ **then**
      for $(d_j, v_k, d_{\mathrm{T}}(j)) \in$ TAB $\left[v_j\right]$ **do**
        $d_i = d_{\mathrm{W}}(\overrightarrow{v_iv_j}) + d_j$;
        $d_{\mathrm{T}}(i) = d_{\mathrm{T}}(\overrightarrow{v_iv_j}) + d_{\mathrm{T}}(j)$;
        if $d_i \leq DL$ **then**
          Insert $(d_i, v_j, d_{\mathrm{T}}(i))$ into TAB[v_i];
        end
      end
    end
  end
end
for $v_i \in \mathcal{V}$ **do**
  if $v_i \in \mathcal{V}_u$ **then**
    for $(d, v_j, d_{\mathrm{T}}(i)) \in$ TAB [v_i] **do**
      Substitute $p(v_i \rightarrow v_e)$ for v_j ;
    end
  else
    Delete TAB[v_i]
  end
end

Algorithm 3 Initialize ($\mathcal{G} = (\mathcal{V}, \mathcal{E})$)

Input: $\mathcal{G}$
Output: TAB[v_i], $v_i \in \mathcal{V}$
for $v_i \in \mathcal{V}$ **do**
  if $v_i \neq v_e$ **then**
    TAB[v_i] = [ ];
  else
    TAB[v_e] = [0, NIL, 0];
  end
end

Fig. 6 presents an illustrative example of the implementation of our scheme in Fig. 6a. There are four users at v_0, and the source-to-destination deadline is specified as 65. TAB [v_0] denotes the lookup table at v_0 in the initialization phase. Fig. 6b, Fig. 6c, and Fig. 6d show the evacuation orders and the dedicated navigation paths for the four users using our scheme. The evacuation table is added to each waypoint along the planned path. The total expected evacuation time and worst-case evacuation time utilizing our scheme are respectively 50 and 65. Refer to Section IV-C for a detailed description of the procedure of our approach specifically for Fig. 6a.

Appendix II

This section presents the algorithms 2 and 3 introduced in Section IV.

Acknowledgment

The authors would like to thank the editors and anonymous reviewers for their valuable comments and suggestions on the earlier drafts of the article.

References

[1] K. Gai et al., "Blockchain-based privacy-preserving positioning data sharing for IoT-enabled maritime transportation systems," *IEEE Trans. Intell. Transp. Syst.*, vol. 24, no. 2, pp. 2344–2358, Feb. 2023.

[2] X. Xu, L. Zhang, S. Sotiriadis, E. Asimakopoulou, M. Li, and N. Bessis, "CLOTHO: A large-scale Internet of Things-based crowd evacuation planning system for disaster management," *IEEE Internet Things J.*, vol. 5, no. 5, pp. 3559–3568, Oct. 2018.

[3] A. C. Paredes, M. Malfaz, and M. A. Salichs, "Signage system for the navigation of autonomous robots in indoor environments," *IEEE Trans. Ind. Informat.*, vol. 10, no. 1, pp. 680–688, Feb. 2014.

[4] N. Al-Nabhan, N. Al-Aboody, and A. A. Al Islam, "A hybrid IoT-based approach for emergency evacuation," *Comput. Netw.*, vol. 155, pp. 87–97, May 2019.

[5] L.-W. Chen and J.-X. Liu, "Time-efficient indoor navigation and evacuation with fastest path planning based on Internet of Things technologies," *IEEE Trans. Syst., Man, Cybern., Syst.*, vol. 51, no. 5, pp. 3125–3135, May 2021.

[6] J. A. Gutierrez, L. Winkel, E. H. Callaway Jr., and R. L. Barrett Jr., *Low-Rate Wireless Personal Area Networks: Enabling Wireless Sensors With IEEE 802.15. 4*. Hoboken, NJ, USA: Wiley, 2011.

[7] L.-W. Chen, J.-H. Cheng, and Y.-C. Tseng, "Distributed emergency guiding with evacuation time optimization based on wireless sensor networks," *IEEE Trans. Parallel Distrib. Syst.*, vol. 27, no. 2, pp. 419–427, Feb. 2016.

[8] Q. Ren, L. Guo, J. Zhu, M. Ren, and J. Zhu, "Distributed aggregation algorithms for mobile sensor networks with group mobility model," *Tsinghua Sci. Technol.*, vol. 17, no. 5, pp. 512–520, Oct. 2012.

[9] L. Wang, Y. He, W. Liu, N. Jing, J. Wang, and Y. Liu, "On oscillation-free emergency navigation via wireless sensor networks," *IEEE Trans. Mobile Comput.*, vol. 14, no. 10, pp. 2086–2100, Oct. 2015.

[10] C. Wang, H. Lin, and H. Jiang, "CANS: Towards congestion-adaptive and small stretch emergency navigation with wireless sensor networks," *IEEE Trans. Mobile Comput.*, vol. 15, no. 5, pp. 1077–1089, May 2016.

[11] L.-W. Chen and J.-J. Chung, "Mobility-aware and congestion-relieved dedicated path planning for group-based emergency guiding based on Internet of Things technologies," *IEEE Trans. Intell. Transp. Syst.*, vol. 18, no. 9, pp. 2453–2466, Sep. 2017.

[12] A. Depari, A. Flammini, D. Fogli, and P. Magrino, "Indoor localization for evacuation management in emergency scenarios," in *Proc. Workshop Metrology Ind. 4.0 IoT*, Apr. 2018, pp. 146–150.

[13] K. Mekki, E. Bajic, F. Chaxel, and F. Meyer, "A comparative study of LPWAN technologies for large-scale IoT deployment," *ICT Exp.*, vol. 5, no. 1, pp. 1–7, Mar. 2019.

[14] L. Liu, Y. Yao, Z. Cao, and M. Zhang, "DeepLoRa: Learning accurate path loss model for long distance links in LPWAN," in *Proc. IEEE Conf. Comput. Commun.*, May 2021, pp. 1–10.

[15] K. Agrawal, S. Baruah, Z. Guo, J. Li, and S. Vaidhun, "Hard-real-time routing in probabilistic graphs to minimize expected delay," in *Proc. IEEE Real-Time Syst. Symp. (RTSS)*, Dec. 2020, pp. 63–75.

[16] M. Li, Y. Liu, J. Wang, and Z. Yang, "Sensor network navigation without locations," in *Proc. IEEE INFOCOM*, Apr. 2009, pp. 2419–2427.

[17] Q. Li, M. De Rosa, and D. Rus, "Distributed algorithms for guiding navigation across a sensor network," in *Proc. 9th Annu. Int. Conf. Mobile Comput. Netw.*, Sep. 2003, pp. 313–325.

[18] Y.-C. Tseng, M.-S. Pan, and Y.-Y. Tsai, "Wireless sensor networks for emergency navigation," *Computer*, vol. 39, no. 7, pp. 55–62, Jul. 2006.

[19] M. S. Pan, C. H. Tsai, and Y. C. Tseng, "Emergency guiding and monitoring applications in indoor 3D environments by wireless sensor networks," *Int. J. Sensor Netw.*, vol. 1, no. 1/2, p. 2, 2006.

[20] C. Buragohain, D. Agrawal, and S. Suri, "Distributed navigation algorithms for sensor networks," 2005, *arXiv:cs/0512060*.

[21] D. Chen, C. K. Mohan, K. G. Mehrotra, and P. K. Varshney, "Distributed in-network path planning for sensor network navigation in dynamic hazardous environments," *Wireless Commun. Mobile Comput.*, vol. 12, no. 8, pp. 739–754, Jun. 2012.

[22] W.-T. Chen, P.-Y. Chen, C.-H. Wu, and C.-F. Huang, "A load-balanced guiding navigation protocol in wireless sensor networks," in *Proc. IEEE GLOBECOM Global Telecommun. Conf.*, 2008, pp. 1–6.

[23] C. Wang, H. Lin, R. Zhang, and H. Jiang, "SEND: A situation-aware emergency navigation algorithm with sensor networks," *IEEE Trans. Mobile Comput.*, vol. 16, no. 4, pp. 1149–1162, Apr. 2017.

[24] P.-Y. Chen, Z.-F. Kao, W.-T. Chen, and C.-H. Lin, "A distributed flow-based guiding protocol in wireless sensor networks," in *Proc. Int. Conf. Parallel Process.*, Sep. 2011, pp. 105–114.

[25] F.-J. Wu, "A sensor-assisted emergency guiding system: Sensor-centric or user-centric?" *IEEE Trans. Veh. Technol.*, vol. 67, no. 2, pp. 1598–1611, Feb. 2018.

[26] J. Men, G. Chen, P. Chen, and L. Zhou, "A Gaussian type-2 fuzzy programming approach for multicrowd congestion-relieved evacuation planning," *IEEE Trans. Intell. Transp. Syst.*, vol. 23, no. 11, pp. 20978–20990, Nov. 2022.

[27] X. Yang, R. Zhang, Y. Li, and F. Pan, "Passenger evacuation path planning in subway station under multiple fires based on multiobjective robust optimization," *IEEE Trans. Intell. Transp. Syst.*, vol. 23, no. 11, pp. 21915–21931, Nov. 2022.

[28] T. Zhang, G. Ren, G. Cheng, Y. Yang, and M. Jin, "A stochastic dynamic traffic assignment model for emergency evacuations that considers background traffic," *IEEE Intell. Transp. Syst. Mag.*, vol. 14, no. 6, pp. 206–220, Nov. 2022.

[29] H. Yu et al., "Ship path optimization that accounts for geographical traffic characteristics to increase maritime port safety," *IEEE Trans. Intell. Transp. Syst.*, vol. 23, no. 6, pp. 5765–5776, Jun. 2022.

[30] W. Guan and K. Wang, "Autonomous collision avoidance of unmanned surface vehicles based on improved A-star and dynamic window approach algorithms," *IEEE Intell. Transp. Syst. Mag.*, vol. 15, no. 3, pp. 36–50, May 2023.

[31] Q. Pan et al., "Space-air-sea-ground integrated monitoring network-based maritime transportation emergency forecasting," *IEEE Trans. Intell. Transp. Syst.*, vol. 23, no. 3, pp. 2843–2852, Mar. 2022.

[32] K. Liu, Y. Ma, M. Chen, K. Wang, and K. Zheng, "A survey of crowd evacuation on passenger ships: Recent advances and future challenges," *Ocean Eng.*, vol. 263, Nov. 2022, Art. no. 112403.

[33] J. Chen, J. Ma, and S. Lo, "Modelling pedestrian evacuation movement on a swaying ship," in *Proc. 15th Int. Conf. Traf. Gra. Flow (TGF)*. Cham, Switzerland: Springer, 2016, pp. 297–304.

[34] J. Nevalainen, M. Ahola, and P. Kujala, "Modeling passenger ship evacuation from passenger perspective," in *Proc. Int. Mar. Des. Conf. (IMDC)*, 2015, pp. 121–129.

[35] Z. Kang, L. Zhang, and K. Li, "An improved social force model for pedestrian dynamics in shipwrecks," *Appl. Math. Comput.*, vol. 348, pp. 355–362, May 2019.

[36] Y. Ma et al., "ANT: Deadline-aware adaptive emergency navigation strategy for dynamic hazardous ship evacuation with wireless sensor networks," *IEEE Access*, vol. 8, pp. 135758–135769, 2020.

[37] P. Valanto, "Time-dependent survival probability of a damaged passenger ship II—evacuation in seaway and capsizing," Ham. Ship Model Basin Rep. (HSVAR), HSVA Rep. 1661, May 2005, vol. 625002, pp. 1–101.

Yuting Ma is currently pursuing the Ph.D. degree in marine navigation with the Wuhan University of Technology (WUT), Wuhan, China. Her research interests include emergency navigation and evacuation.

Kezhong Liu received the B.S. and M.S. degrees in marine navigation from the Wuhan University of Technology (WUT), Wuhan, China, in 1998 and 2001, respectively, and the Ph.D. degree in communication and information engineering from the Huazhong University of Science and Technology, Wuhan, in 2006. He is currently a Professor with the School of Navigation, WUT. His research interests include indoor localization technology and data mining for ship navigation.

Mozi Chen (Member, IEEE) received the B.S. degree in electric engineering from the Hubei University of Technology, China, in 2013, and the M.S. and Ph.D. degrees in navigation engineering from the Wuhan University of Technology (WUT), China, in 2016 and 2020, respectively. He is currently an Associate Researcher with WUT. His research work has been focusing on wireless sensing techniques and machine learning algorithms for human localization, emergency navigation, and activity recognition in mobile environment, i.e., cruise ships.

Yinhao Li received the M.Sc. degree in computer science from the China University of Geosciences and the Ph.D. degree from the School of Computing, Newcastle University, U.K., in 2022. His research interests include cloud computing, edge computing, and the Internet of Things.

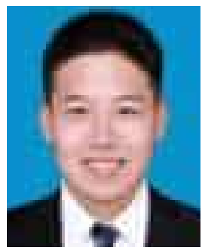

Rui Sun received the M.Sc. degree from the School of Computing, Newcastle University, under the supervision of Rajiv Ranjan. He is currently pursuing the Ph.D. degree in computer science with Newcastle University, under the supervision of Rajiv Ranjan. His research interests include federated learning, distributed machine learning, and the Internet of Things.

Rajiv Ranjan (Senior Member, IEEE) received the Ph.D. degree from the Department of Computer Science and Software Engineering, The University of Melbourne, in 2009. He is currently a Full Professor of computing science with Newcastle University, U.K. Before moving to Newcastle University, he was a Julius Fellow (2013–2015), a Senior Research Scientist, and a Project Leader of the Digital Productivity and Services Flagship of Commonwealth Scientific and Industrial Research Organization (CSIRO C Australian Government's Premier Research Agency). Prior to that, he was a Senior Research Associate (Lecturer Level B) with the School of Computer Science and Engineering, University of New South Wales (UNSW).

Appendix E: Paper V

D3QTP: Distributed Decentralized Deep Q-Learning with table-driven Pretraining for Ship Evacuation

Yuting Ma, Mozi Chen, Kezhong Liu, Erol Gelenbe, *Fellow, IEEE*

***Abstract*—Passenger Navigation control is essential to ship emergency evacuation systems. The conventional Collision-based search (CBS) is the mainstream approach for passenger navigation control problems (also called multi-agent path-finding problems (MAPF)). However, such approaches are computationally hopelessly infeasible, considering the large number of passengers and the large number of possible collisions in the crowded cruise ship environment. Due to the weak scalability, recent methods have applied reinforcement learning (RL) to learn decentralized policy in evacuation environments. MAPF for ship emergency evacuation using RL is attractive but challenging, on account of the dynamic nature of the emergency environment and the complex constraints on the path planning. In addition, there is no standard benchmark environment to train RL agents for navigation control during ship emergency evacuation. This paper designs the first time-varying ship evacuation environment to train RL agents for navigation control in an emergency situation. It consists of realistic features, e.g., floodwater spreading, bottlenecks, life-saving equipment, and dynamic ship motion. We also present an algorithm, Distributed Decentralized Deep Q-learning with Table-driven Pre-training (D3QTP) for unlabelled navigation control in ship emergency evacuation scenarios, that leverages the pretraining of the network weights of the Deep Q-Network (DQN)-based agent from the demonstration data to accelerate the learning process. Specifically, we first use the adaptive routing strategy to generate the demonstration data, which incorporates information on the routes that experience the smallest delay in expectation while guaranteeing respect for the limited time available for evacuation (LTAE) even under worst-case delays. The demonstration data is exploited to pre-train the agent. Then, the pre-trained DQN agent resumes to be trained in our proposed dynamic ship evacuation environment to learn the optimal navigation strategy. Simulation results show that the proposed approach outperforms its counterpart.**

***Index Terms*—Ship evacuation, Navigation control, Deep Q-networks, Pre-training, Demonstrations, Adaptive routing, Distributed learning.**

I. INTRODUCTION

Cruise ship transport is an important part of the passenger transportation network. In recent years, even with the presence of advanced accident prevention systems on board, passenger ship accidents still occur from time to time, and in many of which the casualty rates are disproportionally high [1], [2], [3], [4], [5]. For example, the South Korean ferry Sewol sank in 2014 where 304 people were either declared dead or missing [4]. As one of the most important modes of maritime emergency response, passenger evacuation plays a crucial role in increasing passengers' safety when a passenger ship is involved in a serious accident [6], [7], [8], [9], [10], [11].

Navigation control (also called multi-agent path-finding (MAPF)) is an essential component of the field of emergency evacuation and has important theoretical and practical significance. The current state-of-the-art (SOTA) approaches of MAPF can be mainly classified into two categories, i.e., the search-based methods and the reinforcement learning-based methods. The conventional search-based methods are able to plan paths for people if and only if the precise environment condition and its dynamic change (e.g., the estimates of the hazard spread model and the delay across pathways) are known [12], [13], [14]. However, in reality, modeling the dynamics of environmental conditions on a passenger ship is very challenging, especially considering the variety of the dynamics of danger and the time-varying delay across passageways.

Furthermore, the computational complexity of planning using search-based methods is a significant concern when the number of passengers and possible collisions with other passengers and hazards increase in crowded and perilous passenger ships. Besides, the performance of search-based methods is heavily dependent on the stable and fast communication between evacuees and the path planning server, which may not hold during an evacuation process on a passenger ship in practice.

Last but not least, the search-based methods assume homogeneity of all involved evacuees. That is to say, all evacuees perform actions based on the navigation guidance provided by search-based approaches perfectly so that they are homogeneous. However, such an assumption does not hold in many real-life scenarios due to the uncertain behavior of panic evacuees.

With the significant success of RL in various applications [15], [16], [17], [18], [19], researchers turn their attention to the MAPF using RL for emergency evacuation. However, compared with the RL-based MAPF for mobile robots in normal time, there is relatively limited research on pathfinding for people in emergency time utilizing RL is relatively limited, and even less research on RL-based ship evacuation. The previous works most related to ours are reported in [20] and [21]. [20] proposes a graph-based evacuation environment model consisting of fire spread, and bottlenecks to capture the building structure. However, the environmental setting in [20] still lacks key features (e.g., personal life-saving equipment (PLSE) and dynamic ship motion) of realistic ship evacuation

*This work was supported in part by the National Natural Science Foundation of China (NSFC) under Grant 51979216; and in part by the Natural Science Foundation of Hubei Province, China, under Grant No.2021CFA001 and Grant 20221j0059. *(Corresponding author: Kezhong Liu.)*

Yuting Ma and Mozi Chen are with the School of Navigation, Wuhan University of Technology, Wuhan 430063, China (e-mail: 278827@whut.edu.cn; chenmz@whut.edu.cn).

Kezhong Liu is with the School of Navigation, Wuhan University of Technology, Wuhan 430063, China; the National Engineering Research Center for Water Transport Safety, Wuhan 430063, China; and the Hubei Key Laboratory of Inland Shipping Technology, Wuhan 430063, China (e-mail: kzliu@whut.edu.cn).

Erol Gelenbe is with Université Côte d'Azur CNRS I3S, France; Department of Computer Engineering, Yaşar University, Bornova, Izmir, Turkey; and IITiS-PAN, Gliwice, Poland (e-mail: gelenbe.erol@orange.fr)

environments, and thus needs to be improved to allow for the efficient training of RL agents in the more authentic ship evacuation setting. In addition, [20] assumes people are moved by the agent one at a time so that the trained agent cannot handle collisions when people move simultaneously. Further, this article designs a Q-matrix transfer learning-assisted deep Q-learning method to train an agent in moving a person from one room to another. This method first requires a tabular style Q-learning, which becomes infeasible for our large multidimensional discrete state space in the pretraining environment. In [21], a single agent is trained for emergency navigation in ship indoor environments using a hierarchical reinforcement learning strategy. However, the proposed RL environment is too simplistic to model the realistic ship evacuation environment. Also, [21] treats other passengers as social force model-based agents instead of Rl-based agents, which loses sight of the coordination during online path planning.

To tackle the above issues, we plan passengers' paths for safe and efficient evacuation on a passenger ship via the RL-based algorithm which is model-free and thus can directly solve the task without explicitly estimating the environmental dynamics. Specifically, In this work, we propose a realistic learning environment for ship emergency evacuation to train RL agents to evacuate safely and efficiently. Realistic and key features like floodwater spread, bottlenecks of exits, PLSE (i.e., life jackets or lifebuoys), and dynamic ship motion, are incorporated into the designed environment. Considering the discrete control property of our problem and the high level of difficulty of our designed environment, we propose a distributed decentralized Deep Q-network (DQN) model with optimal table-driven pretraining to facilitate the navigation control of agents. We first use the knowledge of the actual delay distributions to establish routing tables for each grid center (i.e., waypoint), aimed at each muster station (i.e., goal waypoint), based on the optimal table-driven algorithm developed in [22]. According to the constructed routing tables at a waypoint, evacuees can determine the optimal outgoing action to take, minimizing the expected delay for the remaining traversal to destinations, given the remaining deadline. Next, we construct the Q-table to approximate the obtained routing tables so that it can properly reflect the expected delay to the destination, without a lengthy training process. Then, we pre-train a DQN model to imitate the built Q-table. The pre-trained DQN model will be trained on the complete ship evacuation environment to learn optimal navigation actions.

In addition, to make it easy to scale as the number of agents increases, we leverage decentralized Q-learning for the multi-agent partially observable system. That is to say, we treat each agent independently without learning a joint action value. To speed up learning, our model is trained in a distributed manner based on the Apex framework [23]. Simulation results show that our proposed method performs better than its counterpart.

Contributions. Our main contributions are summarized as follows.

- We propose the first learning environment close to the realistic ship evacuation setting, which contains key features like flooding, floodwater spread, uncertain crowd behavior, bottlenecks of muster stations, PLSE, and dynamic ship motion.
- We develop a novel deep Q-learning method with optimal table-driven pretraining for unlabeled navigation control of multi-agents in the proposed ship evacuation environment.
- We design a decentralized deep Q-learning method for scaling as the number of agents increases, and train the agent in a distributed manner to speed up the learning procedure.

Organization. The remainder of this paper is organized as follows. Section II introduces the RL concepts used in our work. The multi-agent navigation control (MANC) problem is formalized in Section III. Section IV and Section V respectively detail the proposed learning environment for ship emergency evacuation and the design of our model, i.e., the distributed decentralized deep Q-learning with table-driven pretraining (D3QTP). Simulation results are reported in Section VI. Section VII summarizes the SOTA path planning with conventional methods and RL-based methods. Finally, Section VIII concludes this paper.

II. Preliminaries

RL is a sub-field of machine learning, that can gradually learn the best actions for each system state, in regard to a specifically designed reward function, through interactions with environments. This section introduces the concepts and methods used in this paper, including the partially observable Markov game, Q-learning, and Deep Q-network.

A. Partially Observable Markov Game

We consider a partially observable discrete grid environment, where each agent can only observe the environment within its field of view (FOV). Therefore, the MANC problem can be modeled as a partially observable Markov game, represented as a tuple $\langle \mathcal{U}, \mathcal{S}, \{\mathcal{A}_i\}, \{\mathcal{O}_i\}, \mathcal{P}, \{\mathcal{R}_i\}, \gamma \rangle$. $\mathcal{U} \triangleq \{u_1, u_2, ..., u_n\}$ is the set of agents. $\mathcal{S}$ is the state space, describing all possible state configurations of the agents. $\mathcal{A}_i$ is the action space of agent u_i, which defines all possible actions of u_i. $\mathcal{O}_i(\mathcal{S} \longmapsto \mathcal{O}_i)$ is the observation space for agent u_i. $\mathcal{P}(s', o|s, a)$ is the state transition and observation probability function, where a and o are instances of $\mathcal{A}$ and $\mathcal{O}$. Agent u_i will receive the expected total rewards $\mathcal{R}_i(\mathcal{S} \times \mathcal{A} \longmapsto \mathbb{R})$, based on the states and its actions. $\mathcal{R}_i \triangleq \sum_{t=0}^{T} \gamma^t r_i^t$, where r_i^t is the reward received by agent u_i for the state and its action at time t, T is the time length, and γ represents the discount factor. The objective for each agent is to maximize $\mathcal{R}_i$. In Section IV, we will give a detailed introduction to the observation space, action space, and rewards.

B. Q-learning

Q-learning is an off-policy and value-based RL mechanism, that represents the policy as a Q-table. A Q-learning formulation includes (1) the state space $\mathcal{S}$; (2) the action space $\mathcal{A}$; (3) the Q-table consisting of Q-values, $Q(s_t, a_t)$, representing the expected value of discounted total reward of taking an action ($a_t \in \mathcal{A}$) at a state ($s_t \in \mathcal{S}$). Through iterative sampling from the environment, the Q-table is updated using the rewards obtained from these samples. The specific operation performed by a Q-learning-based agent at time t is as follows:

- The agent observes current state s_t ($s_t \in \mathcal{S}$).
- The agent selects and performs an action a_t ($a_t \in \mathcal{A}$).
- The agent observes next state s_{t+1}.
- The agent receives the reward r_t.
- Update $Q_t(s_t, a_t)$ according to the following equation:

$$\begin{aligned} Q_{t+1}(s_t, a_t) =& (1-\eta)\, Q_t(s_t, a_t) + \\ & \eta \left[r_t + \gamma \max_{a_{t+1}} Q_t(s_{t+1}, a_{t+1}) \right] \end{aligned} \tag{1}$$

Once the Q-table has converged, selecting the action with the maximum Q-value forms the best policy π^* which results in the maximum reward.

In our proposed approach, instead of the lengthy learning process of the agent, we directly construct the Q-table based on the routing tables obtained using a modification of the offline optimal table-driven algorithm introduced by [22].

C. Deep Q-Network

The tabular Q-learning approach becomes infeasible in environments with large multidimensional discrete or continuous state space. To tackle this problem, DQN learns a parameterized neural network $Q\ (s, a; \theta)$ (called Q-network) to approximate the optimal Q function $Q^*(s, a)$ [24], [25]. The Q-network is trained by minimizing the following loss function:

$$\mathcal{L}(\theta) = \mathbb{E}_{s,a,r,s'} \left[(Q(s, a; \theta) - y)^2 \right] \tag{2}$$

where y is the time difference target (TD target) to refine the Q-network, which can be defined as follows:

$$y = r + \gamma \max_{a_{t+1}} Q(s_{t+1}, a_{t+1}; \bar{\theta}) \tag{3}$$

where γ is the discount factor and $\bar{\theta}$ is the parameter of the target network, which can be updated periodically with the recent θ.

The gradient of the loss function is obtained by differentiating Equation (2):

$$\nabla_\theta L(\theta) = \mathbb{E}\left[(Q(s, a; \theta) - y) \nabla_\theta Q(s, a; \theta) \right] \tag{4}$$

Generally, agents need to condition on an observation-action history in partially observable environments. Therefore, we equip DQN with a Gate Recurrent Unit (GRU) [26] in our work.

III. Problem Definition

In the ship emergency evacuation scenario, the MANC problem is formalized as follows. Given an undirected graph G=($\mathcal{V}$, $\mathcal{E}$), $\mathcal{V}$ denotes the set of waypoints (i.e., the center of each grid), and $\mathcal{E}$ represents the set of edges (i.e., the connection between any two neighboring waypoints). Each edge $(u, v) \in \mathcal{E}$ is characterized by a probabilistic delay function $Pr_{(u,v)}$. For example, $Pr_{(u,v)}(x)$ denotes the probability that the delay experienced across the edge (u, v) is $x \in \mathcal{X}$, where $\mathcal{X}$ is assumed to be a finite set of positive integers in this paper. According to $Pr_{(u,v)}$, we can acquire the knowledge about the worst-case delay across each edge (u, v), which is defined as $d_W(u, v)$. In addition, the expected delay across each edge (u, v) is defined as $d_E(u, v) = \sum_x (Pr_{(u,v)}(x) \cdot x)$. We consider an agent set $\mathcal{U}$ where each agent $u_i, 1 \le i \le n$ is located at a unique start waypoint $s_i \in \mathcal{V}$. Besides, m goal (destination) waypoints, denoted $g_j \in \mathcal{V} (1 \le j \le m)$, are inserted into our graph model. A capacity parameter is specified on each goal waypoint, denoted c_j. A path p_i^j from the start waypoint s_i to the goal waypoint g_j for each agent u_i is a sequence of adjacent waypoints, p_i^j is designated as follows:

$$p_i^j \triangleq \langle s_i \equiv v_0^i, v_1^i, v_2^i, ..., v_k^i \equiv g_j \rangle.$$

where either $(v_{l-1}^i, v_l^i) \in \mathcal{E}$ $(1 \le l \le k)$, indicating the movement of agent u_i across an edge, or v_{l-1}^i and v_l^i are identical waypoints $(1 \le l \le k)$, indicating the wait of agent u_i at a waypoint. The worst-case delay and expected delay across the path p_i^j are respectively denoted as:

$$d_W(p_i^j) \triangleq \textstyle\sum_{l=1}^k d_W(v_{l-1}, v_l).$$

$$d_E(p_i^j) \triangleq \textstyle\sum_{l=1}^k d_E(v_{l-1}, v_l).$$

We classify collisions between two agents into two types: waypoint collision, occurring when both agents reach the same waypoint simultaneously, and edge collision, happening when both agents traverse the same edge from opposite directions. The collision involving agents and hazards exhibits similarities to those between two agents.

In addition, a quantity of PLSE is assigned in certain waypoints, called supply waypoints. The supply waypoints are not infinite reservoirs of PLSE. That is to say, the quantity of PLSE at a supply waypoint will decrease when an agent takes a piece of equipment from it. It is also worth noticing that in our work we consider the unlabeled navigation problem where the agent-to-goal assignment is not one-to-one and matches arbitrarily. In practice, the number of goal waypoints (i.e., muster stations in ship evacuation scenarios) is much less than that of agents (i.e., passengers).

Problem statement. For a given deadline D from start waypoints to goal waypoints, a solution to MANC is a set of paths free of collision with other agents and hazards while guaranteeing that $d_W(p) \le D$ and that each agent can get a piece of PLSE along his path. The quality of the solution is measured by the total arrival time for all agents at the goal waypoints.

IV. Learning Environment

We propose the first benchmark learning environment that is specifically designed to train RL agents for MANC for ship emergency evacuation. The learning environment includes realistic dynamics that frequently arise in real-world ship emergency scenarios. We elaborate on the observation space, action space, reward design, and key features of the proposed environment in the rest of this section.

A. Obsevation space

The environment has a gird-based structure to represent the model of the indoor space of a passenger ship with more than one goal waypoint. Fig. 1 shows a small case example. Because of the local observation ability of agents in practice, we consider a partially observable environment where each agent can only observe the setting in its limited FOV (3×3 FOV in our work). All agents are at the center of their FOV. Similar to the recent approaches which learned to find paths in a discrete grid world environment, the observation information is separated into different channels to simplify the learning task for agents. Specifically, the observation space consists of 4 binary matrices:

- A binary matrix $\mathbf{M}_{\mathrm{o}}$ showing the static obstacles inside the FOV.
- A binary matrix $\mathbf{M}_{\mathrm{a}}$ expressing the positions currently occupied by other agents if they are within the FOV.
- A binary matrix $\mathbf{M}_{\mathrm{g}}$ representing the goal waypoints (if within the FOV).
- A binary matrix $\mathbf{M}_{\mathrm{s}}$ expressing the positions of supply waypoints (if within the FOV).

Regarding the information about goal waypoints (if within the FOV), except for goal locations, agents also have access to the one-hot goal type representation $\mathbb{G}$ to avoid exceeding the bottleneck value of the goal waypoints. $\mathbb{G}$ can take two different values: $\mathbb{G} = +a_1$ if the number of agents in the goal does not exceed its bottleneck value and $-a_1$ otherwise. In regard to the supply waypoints (if within the FOV), agents also need to know the information about the remaining quantity of PLSE at the supply waypoints, which is stored in a matrix represented as $\mathbf{M}_{\mathrm{q}}$.

In addition, we include three reference channels in the input of the Q-network. The first is a binary matrix showing the single-agent fastest waypoint inside the FOV, denoted as $\mathbf{M}_{\mathrm{r}}$. By choosing the single-agent fastest waypoint, the agent can reach a goal waypoint with the minimum expected delay while guaranteeing never not to exceed a hard deadline in a single-agent setting. We apply an off-route penalty for deviating from the single-agent fastest waypoint in our reward structure (see IV-C). The second is a binary matrix $\mathbf{M}_{\mathrm{f}}$ showing the feasible waypoints (see V-A) inside the FOV. Since agents need to keep safe from hazards, they have access to a matrix $\mathbf{M}_{\mathrm{h}}$ representing the degree of hazard for each position inside the FOV. The degree of hazard is denoted by a positive number, and its maximum value belongs to the positions where hazards are located. If a hazard is spreading more rapidly towards a position, the position is associated with a higher value of the hazard degree.

Three additional inputs to each agent are the information about its current status, i.e., the remaining deadline rd_i to some goal waypoint for agent u_i, the waypoint v_{u_i} occupied by u_i, and one-hot agent type representation $\mathbb{F}$. $\mathbb{F}$ can take six different values. For an agent who is equipped with a piece of PLSE, $\mathbb{F} = a_2$ if the agent has reached some goal waypoint, a_3 if the agent reaches some supply waypoint with PLSE, and a_4 otherwise; For an agent who is not equipped with a piece of PLSE, $\mathbb{F} = -a_2$ if the agent has arrived at some goal waypoint, $-a_3$ if the agent arrives at some supply waypoint with PLSE, and $-a_4$ otherwise.

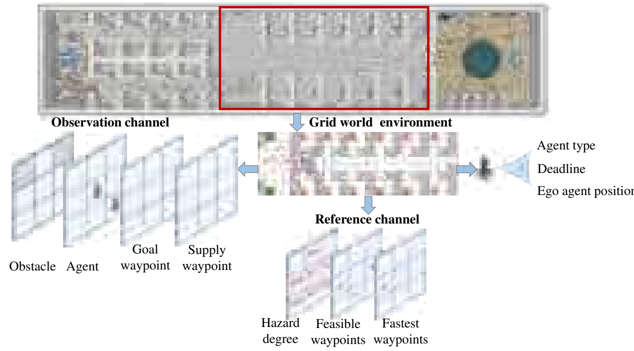

Fig. 1. Grid world environment example. The purple square shows the 3×3 FOV centered around an agent. The two green grids with lifeboats are goal waypoints, and the gray grids denote obstacles. Each grid is associated with a red number representing its degree of hazard. The maximum initial hazard degree set as 1.5 in our experiment is assigned to the precarious location indicated by a red exclamation mark. A certain number of life jackets are located at twelve supply waypoints. The black solid points at the centers of grids denote waypoints, and the black solid lines connecting two neighbor waypoints are the edges.

B. Action space

As commonly done in a grid world, each agent has a discrete action set in our setting. Specifically, at each time step, agents can select from 6 possible actions: moving up/down/left/right, picking up a piece of PLSE, or staying still. During training or execution, agents may take some invalid actions, such as moving to an infeasible waypoint, an obstacle, or another agent. However, we do not filter out these invalid actions to enhance the learning robustness. If an invalid action is selected, the related agent is recovered to its previous state until it selects a valid action. That is to say, an agent can stay still for multiple successive timesteps. Actually, once fully trained, agents rarely choose invalid actions.

C. Reward design

As described in Section III, there are some constraints on the path computed for each agent for MANC in ship emergency evacuation scenarios:

- Through the path, each agent can reach a goal without violating the deadline under all circumstances.
- Through the path, each agent can avoid collision with obstacles, other agents, or dynamic hazards.
- Through the path, each agent can get a piece of PLSE.

Subject to these constraints, the optimization objective of MANC in ship emergency evacuation scenarios is to minimize the expected traversal delay for each agent. Table I summarizes our designed reward structure.

$\delta(a)$ is the actual delay associated with the action a taken by an agent, which depends on the delay distribution $Pr_{(u,v)}$ where *(u, v)* is the traversal edge caused by action a. In consideration of the average movement speed under normal "at sea" conditions ($1\ m/s$) and the worst-case inclination states ($0.1\ m/s$) [27], we have $1\ s \leq \delta(a) \leq 10\ s$ in our

TABLE I
REWARD STRUCTURE

Action	Reward
Move penalty $[Up/Down/Left/Right]$	-0.2$\times\lvert\delta(a)\rvert\times l(v,t)$
Stay off goal penalty	-2.75
Off-route penalty	-2.25λ_1
Stay on goal reward ($\mathbb{G}=+a_1,\mathbb{F}=+a_2$)	0
Stay on goal penalty ($\mathbb{G}=+a_1,\mathbb{F}=-a_2$)	-0.6
Stay on goal penalty ($\mathbb{G}=-a_1,\mathbb{F}=+a_2$)	-0.6
Stay on goal penalty ($\mathbb{G}=-a_1,\mathbb{F}=-a_2$)	-2.1
Pick up a piece of PLSE penalty ($\mathbb{F}=+a_3$)	-4.5
Pick up a piece of PLSE reward ($\mathbb{F}=-a_3$)	0
Pick up a piece of PLSE penalty ($\mathbb{F}=+a_4$)	-4.5
Pick up a piece of PLSE penalty ($\mathbb{F}=-a_4$)	-4.5
Collision with agents/obstacles penalty	-5
Infeasible move penalty	-4.5
Finishing reward	+60

experiment. $l(v,t)$ is the degree of hazard for waypoint v at time *t*. The value of $l(v,t)$ ranges from $+0.5$ to $+2.5$ in our experiment. Therefore, the move reward ranges from -5 to -0.1. Following such a move reward function ensures that the reward of a move action depends on the actual move delay and the degree of hazard of the waypoint that the agent moves to. The move action is penalized more heavily if the agent takes a longer delay to get to the next waypoint with a higher degree of hazard, which forces the agent to avoid the collision with hazards and seek a path with the minimum expected delay.

Agents are penalized slightly more for staying still than moving (if not on a goal waypoint) to incentivize exploration when $l(v,t)\leq 1$. Since we estimate the single-agent fastest waypoint, we introduce an off-route penalty for the agent that does not move to the estimated single-agent fastest waypoint. In our experiment, the value of the off-route penalty is set as $-2.25\lambda_1$ where λ_1 controls the weight of the off-route reward. We also set a penalty to the agent that reaches a goal waypoint. The specific value of this penalty is determined by the agent type representation $\mathbb{F}$ and the goal type representation $\mathbb{G}$. Agents additionally get a reward for picking up a piece of PLSE, which is decided on the agent type representation $\mathbb{F}$. Deviating from the feasible waypoints (called infeasible action) leads to a -4 reward. Agents receive a $+60$ reward if they all arrive at goal waypoints.

D. Key features

The key features of our proposed learning environment to mimic the real-world ship emergency evacuation scenario are defined as follows.

1) Dynamic ship motion. It is important to take into account the influence of ship motions on traversal delay across individual edges. However, most if not all of the environment settings of current SOTA RL-based methods for MAPF assume that the rewards for different move actions are the same and constant [20], [28], [29], [30], [31]. Such a hypothesis neglects the discrepancy and uncertainty of the estimations of the delay on the edges, which are caused by ship motions in the seaway. Therefore, the resulting policies are trained to find paths with the minimum number of steps rather than traversal time in realistic ship evacuation scenarios (defined as path detour problem). To address the detour problem, we specify a probabilistic delay function on each edge, which is assumed to be precise (known and static) in our work. Therefore, agents receive different rewards for the four move actions Up, Down, Left, and Right, depending upon the probability distributions of the actual delays experienced across individual edges. Besides, a worst-case delay bound that may be encountered across each edge is inferred from the specified delay probability distributions, and such worst-case delay bounds can be used for seeking feasible waypoints (see V-A).

2) PLSE. Different from the evacuees in buildings, evacuees on board are required to wear PLSE to increase the likelihood of survival in case the ship must be abandoned [32]. The minimum standard for PLSE is defined in the Safety of Life at Sea (SOLAS) regulations, based on the size and passenger capacity of a cruise ship [33]. Generally, two life jackets are available in each passenger cabin, and a designated quantity of lifebuoys or life jackets is additionally placed in other specific locations such as aft decks. In this work, we set supply waypoints, where PLSE is located. The information about the supply waypoints (if within the FOV), including their locations and the remaining quantity of PLSE, is treated as part of the agents' observation. Besides, unlike most of the existing RL-based methods for MAPF which only consider 5 possible actions (move Up/Down/Left/Right and stay still) for each agent, we add a pick-up action to our action space. The reward for pick-up action is automatically controlled by the agent type representation $\mathbb{F}$. Agents are given a zero reward if $\mathbb{F}=-a_3$, and a negative reward otherwise for picking up a piece of PLSE, which forces agents to obtain only one piece of PLSE. The quantity of remaining PLSE will decrease by 1 at a supply waypoint after an agent takes a picking-up action at that waypoint. In our experiment, no PLSE is placed at goal waypoints.

3) Bottleneck. We put an upper limit on the number of evacuees that a goal waypoint can accommodate to alleviate the congestion problem arising at goal waypoints. The bottleneck information of a goal waypoint is provided to agents if they can observe the goal waypoint inside their FOV. We classify a goal waypoint into two types, represented by $\mathbb{G}$, depending on whether or not it reaches its bottleneck. $\mathbb{G}=+a_1$ denotes an underloaded goal waypoint where the number of evacuees does not exceed its bottleneck. Conversely, $\mathbb{G}=-a_1$ represents an overloaded goal waypoint where the number of evacuees reaches or even exceeds its bottleneck. The value of $\mathbb{G}$ affects the rewards received by agents who stay at goal waypoints. Specifically, an agent will get a negative reward for staying at a goal waypoint if $\mathbb{G}=-a_1$, which compels the agent to seek an underloaded goal. It is worth noticing that the reward for staying at a goal waypoint is also influenced by the value of $\mathbb{F}$. To incentivize picking up a piece of PLSE, we penalize slightly more for $\mathbb{F}=-a_2$ than $\mathbb{F}=+a_2$, under both $\mathbb{G}=+a_1$ and $\mathbb{G}=-a_1$.

4) Floodwater spreading. In ship emergency evacuation scenarios, hazards may dynamically spread. Based on the hazard spread direction, each waypoint is initially assigned a hazard degree denoted as $l(v,t_0)$, ranging from 0.5 to 1.5. A higher initial hazard degree is associated with the waypoint towards which a hazard is spreading, and the maximum value of $l(v, t_0)$ belongs to the precarious waypoints inside a dangerous region. $l(v, t)$ is updated gradually as follows:

$$l(v, t+1) = l(v, t) + \sigma(v), \forall v \in \mathcal{V} \tag{5}$$

where $\sigma(v)$ is a small positive value specifically designated for each waypoint and determined by the hazard spreading direction. A higher value of $\sigma(v)$ for a waypoint indicates a more rapid hazard spread towards that waypoint. In our experiment, the value of $l(v, t)$ ranges from $+0.5$ to $+2.5$. The information about the hazard degree inside the FOV works as a channel to be input to the Q-network. Agents get different rewards for moving (Up/Down/Left/Right) to different waypoints with different degrees of hazard. Specifically, an agent is penalized more for moving into a waypoint with a higher hazard degree, driving the agent to select a safer direction.

5) LTAE. In this work, we consider the emergency scenario where the ship must be abandoned. In such a case, the time available for evacuation of passengers and crew is limited [34]. That is, evacuees need to reach goal waypoints within a hard deadline under all circumstances. To respect the hard deadline, we use the information about the worst-case delay across each edge to identify feasible waypoints to ensure safety. A binary matrix showing the feasible waypoints inside the FOV serves as a channel input into the Q-network. In addition, we add a penalty if an agent selects an infeasible waypoint, forcing the agent to take feasible actions. The definition and calculation of feasible waypoints are detailed in Section V-A.

6) Terminal Condition. The terminal state is achieved when there are no agents at the waypoints except for the goal waypoints.

The pseudo-code for our proposed learning environment for MANC for ship evacuation is given in Algorithm 1. v is the waypoint that agent u_i reaches after taking action a_i, and u is the waypoint ocuupied by agent u_i before taking action a_i. $N_{PLSE}(v)$ denotes the quantity of PLSE at waypoint v.

Algorithm 1: Learning environment for MANC for ship evacuation

```
Input: Observation channels, Reference channels,
       Agent status
while not Terminal do
    a_i = u_i.action(O_i);
    if not Terminal then
        if F ≡ +a_2 then
            if G ≡ +a_1 then
                r_i = 0;
            else
                r_i = −0.6;
            end
        else if F ≡ −a_2 then
            if G ≡ +a_1 then
                r_i = −0.6
            else
                r_i = −2.1;
            end
        else
            if u ≠ v then
                rd_i = D − t;
                if off-route action then
                    r_i = −2.25λ_1;
                else if infeasible action then
                    r_i = −4.5;
                else if collision then
                    r_i = −5;
                else
                    r_i = −0.2 × |δ(a_i)| × l(v, t);
                end
            else if u ≡ v and a_i is stay still then
                rd_i = D − t;
                if collision then
                    r_i = −5;
                else
                    r_i = −2.75;
                end
            else if u ≡ v and a_i is pick up then
                rd_i = D − t;
                if F = +a_3 then
                    r_i = −4.5, N_PLSE(v) −= 1;
                else if F = −a_3 then
                    r_i = 0, N_PLSE(v) −= 1;
                else
                    r_i = −4.5;
                end
            end
        end
    end
end
```

V. DISTRIBUTED DECENTRALIZED DEEP Q-LEARNING WITH TABLE-DRIVEN PRETRAINING

In this section, we present a novel approach referred to as D3QTP, that combines DQN, Q-learning, and the table-driven algorithm, for our proposed learning environment for MANC in ship evacuation scenarios. Fig. 2 shows an architectural overview of the proposed D3QTP method. The main idea of D3QTP is to pre-train the RL agent by fitting it to a Q-matrix which is produced using the table-driven algorithm. In addition, we utilize Ape-X architecture to speed up deep Q-learning.

This section introduces the method for directly obtaining the Q-matrix based on a modification of the optimal table-driven algorithm, followed by the pretraining of the DQN to have the information about the single-agent fastest waypoint incorporated in it. The third part presents the Q-network design of the agent trained on the complete learning environment for MANC in ship evacuation scenarios.

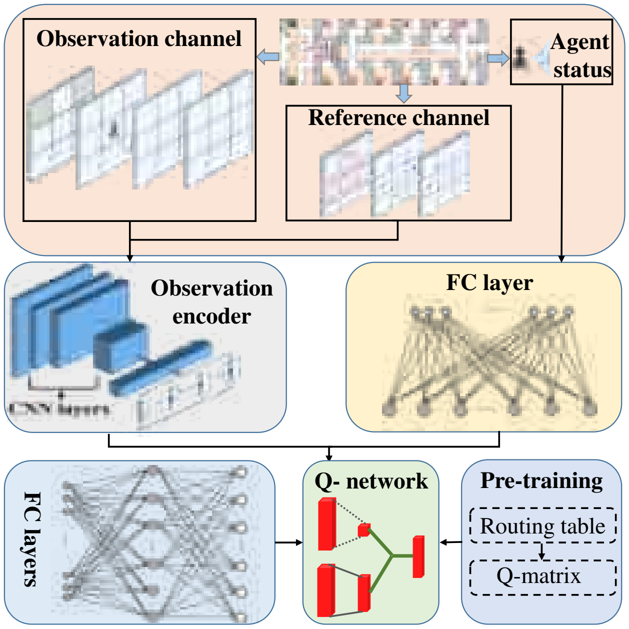

Fig. 2. Overview of the proposed D3QTP method.

A. Table-driven Q-matrix construction

Before further introducing the method for constructing the table-driven Q-matrix, we present a formal definition of feasible waypoints as follows: a waypoint v is considered to be a feasible waypoint, if and only if there is some path from v to some goal waypoint such that the worst-case delay of getting from the current waypoint u to v plus the worst-case delay across the path does not exceed the current remaining deadline to the goal waypoint, and vice verse.

1) Table-driven algorithm. In our work, we extend the table-driven algorithm (refer to [22]) to construct a routing table of 4-tuples for each waypoint, targeting different goal waypoints and different neighbor waypoints. All 4-tuples in a routing table consist of g, π, wd, and ed where wd are distinct for the same goal waypoint and neighbor waypoint. Let us take a particular 4-tuple $(g_0, \pi_0^v, wd_0^v, ed_0^v)$ in a routing table TAB$[v]$ for instance. $(g_0, \pi_0^v, wd_0^v, ed_0^v)$ denotes that if an agent takes a move action to the waypoint π_0^v, it will experience an expected delay of ed_0^v from current waypoint v to goal waypoint g_0, for a worst-case delay bound of wd_0^v to g_0. Algorithm 2 provides the pseudo-code for generating routing tables. QL is a list of waypoints whose current routing table TAB$[v]$ values have not been used to update the values of routing table TAB$[u]$. $\xi_v^g(wd^u - x)$ denotes the expected delay from v to goal waypoint g for a deadline of $wd^u - x$. Note that if there is no 4-tuple in the routing table at v whose third component (i.e., wd^v) is smaller than $wd^u - x$, we will set $\xi_v^g(wd^u - x) = +\infty$.

2) Q-matrix construction: Upon obtaining the routing table, we calculate the feasible waypoints and Q-matrix using the obtained routing table. All feasible waypoints for agent u_i with a remaining deadline rd_i at waypoint u comprise the set of feasible waypoints, defined as $\mathcal{V}_f(u, rd_i)$:

$$\mathcal{V}_f(u, rd_i) = \{v | (u, v) \in \mathcal{E}, wd_{min}^u(v) \le rd_i\}, \qquad (6)$$

Algorithm 2: Routing table construction

for *each goal waypoint* g **do**
  for *each waypoint* $v \in \mathcal{V}$ **do**
    TAB$[v] = empty$;
    TAB$[g] = (g, -, 0, 0)$;
  end
  $QL = \{g\}$;
  while QL *is not empty* **do**
    Remove the waypoint v in the front of QL;
    for *each edge (u,v) that leads to v* **do**
      for *each 4-tuple* $(g, \pi_0^v, wd_0^v, ed_0^v)$ *in* v **do**
        for x_0 *such that* $Pr_{(u,v)}(x_0) > 0$ **do**
          $wd^u = wd_0^v + x_0$;
          $ed^u = \sum_{\{x | Pr_{(u,v)}(x) > 0\}} Pr_{(u,v)}(x)(x + \xi_v^g(wd^u - x))$;
          Add (g, v, wd^u, ed^u) to TAB$[u]$;
          Remove $(g, v, \grave{wd}^u, \grave{ed}^u)$ with $ed^u < \grave{ed}^u$ and $wd^u \le \grave{wd}^u$
        end
      end
    end
  end
end

where $wd_{min}^u(v)$ is defined as:

$$wd_{min}^u(v) = \min\{wd^u | (g, \pi^u, wd^u, ed^u) \in \text{TAB}[u], \pi^u \equiv v\}. \qquad (7)$$

Next, we describe how to build the Q-matrix using the routing table without the need for a lengthy learning process. Algorithm 3 shows the complete pseudo-code to get the Q-matrix.

Algorithm 3: Q-matrix construction

for *each waypoint* $u \in \mathcal{V}$ **do**
  for *each deadline* $rd_i \in [wd_{min}^u, wd_{max}^u]$ **do**
    for *each action moving from u to v* **do**
      if $v \in \mathcal{V}_f(u, rd_i)$ **then**
        $Q_{(u, rd_i, v)} = -\lambda_2 \times \min\{\frac{ed^u}{wd^u} | (g, \pi^u, wd^u, ed^u) \in TAB[u], \pi^u \equiv v \cap rd_i \ge wd^u\}$;
      else
        $Q_{(u, rd_i, v)} = -1 \times \lambda_2$
      end
    end
  end
end

From Algorithm 3, we can see that a small Q-value is assigned to an action moving to an infeasible waypoint compared to the actions moving to feasible waypoints. Additionally, different Q-values are determined for actions moving to different feasible waypoints, depending on the resulting expected delay to some goal waypoint by taking these actions. The range of the Q-values can be automatically controlled by a multiplicative factor λ_2.

B. Q-matrix based pretraining

Once the Q-matrix is obtained, we pre-train the weights of the Q-network to incorporate the information included in the Q-matrix (i.e., information on feasible waypoints and fastest waypoints) by overfitting the Q-network on the Q-matrix. More specifically, we flatten the Q-matrix to a long vector to serve as the labels for the Q-network. We also add a small amount of noise to each element of the Q-matrix to offset the imbalance among them:

$$Q_{(u,rd_i,v)} = \begin{cases} Q_{(u,rd_i,v)} + \alpha, if Q_{(u,rd_i,v)} < \overline{Q}_{u,rd_i} \\ Q_{(u,rd_i,v)} - \alpha, if Q_{(u,rd_i,v)} \geq \overline{Q}_{u,rd_i} \end{cases} \tag{8}$$

where α is a hyperparameter, and $\overline{Q}_{u,rd_i}$ is the average value of the Q-values for the state (u, rd_i). If $Q_{(u,rd_i,v)}$ is smaller than $\overline{Q}_{u,rd_i}$, α is added to $Q_{(u,rd_i,v)}$. Otherwise α is subtracted from $Q_{(u,rd_i,v)}$. Through conditional addition or subtraction, the agent can avoid bias on a particular set of actions. After pretraining, the agent knows the information on the feasible waypoints as well as the fastest waypoints, and therefore dealing with other aspects of the learning environment like PLSE, bottlenecks, and floodwater spreading becomes easier. Algorithm 4 shows the pseudo-code for Q-matrix based pretraining.

Algorithm 4: Q-matrix based pretraining

```
Input: Q-matrix
for i ← 0 to T_pretrain do
    for each (u, rd_i) do
        O_i = Q-network.predic((u, rd_i));
    end
    L(θ_i) = 1/2 (O_i − Q-matrix)^2;
    θ_{i+1} = θ_i + η∇L(θ_i)
end
return θ*
```

C. D3QTP

After pertaining, the agent is trained in our proposed learning environment for MANC in ship evacuation scenarios to learn the optimal evacuation schedule. In this section, we detail the design of the agent Q-network, followed by an introduction of a distributed training strategy.

1) Agent Q-network design. We use a dueling DQN with recurrent units to approximate the agent's policy in the partially observable environment, which maps the current observation of its surroundings to the Q-value of each action. As pictured in Fig. 3, we use an 8-layer convolutional network and a Gate Recurrent Network (GRU) to encode the observation, taking inspiration from [29]. Specifically, the eight-channel matrices ($3 \times 3 \times 8$ tensor) representing the local observation are passed through two independent convolutions and three residual blocks, each containing two convolutional layers. In parallel, the information on the remaining deadline rd_i, the occupied waypoint by the agent v_{u_i}, and the agent type representation $\mathbb{F}$ are passed through a fully connected (FC) layer, and then concatenated with the encoded observation. The concatenation of the two pre-processed inputs is fed into two FC layers and finally adopted by the pre-trained Q-network. A residual shortcut connects the output of the concatenation layer to the input layer of the Q-network. The output layer consists of the Q-values for each action. In this work, we calculate the Q-values in a dueling manner and the optimal action is selected by the maximum Q-value. The final loss function is a 2-step TD error: $L(\theta) = Huber(R_t - Q(s_t, a_t, \theta))$ where R_t is the time difference target of the agent, s_t and a_t are its state and action.

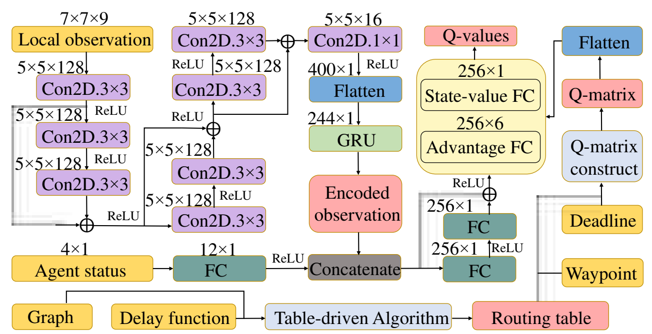

Fig. 3. D3QTP architecture. The local observation is first encoded by eight convolutional layers and then fed into a GRU to generate the intermediate message. The agent status is passed through a fully connected layer. Both of these pre-processed inputs are concatenated and fed into a residual block consisting of two FC layers. The output of the residual block is introduced into the pre-trained Q-network to calculate the state value and action advantages, which are merged for the final Q-values.

2) Distributed prioritized experience replay. To speed up the training process, we utilize the Ape-X architecture [23], which distributes RL by parallelizing experience data generation and selection with a shared replay memory, such that more high-priority data can be gathered to facilitate the parameter optimization. Fig. 4 illustrates the overview of our distributed deep Q-learning (DQL) framework, where multiple independent actors (sixteen actors in our experiment) running on CPUs generate experience in their own environment instances, and a single learner on GPU updates the network.

VI. Experiments

We conduct experiments on the proposed learning environment for MANC in ship evacuation scenarios and compare the D3QTP method with SOTA RL algorithms to verify the performance of our method in finding an optimal evacuation schedule for all the agents in the environment.

A. Experimental setup

The final task in our experiment is to train 38 agents in a $135m \times 19m$ environment that simulates a real-world ship deck, i.e., the second deck of the Yangtze Gold 7 cruise. Fig. 5 depicts the general arrangement of the cruise's second floor and the initial distribution of agents. In each episode, the agents' starting positions are randomized under the premise

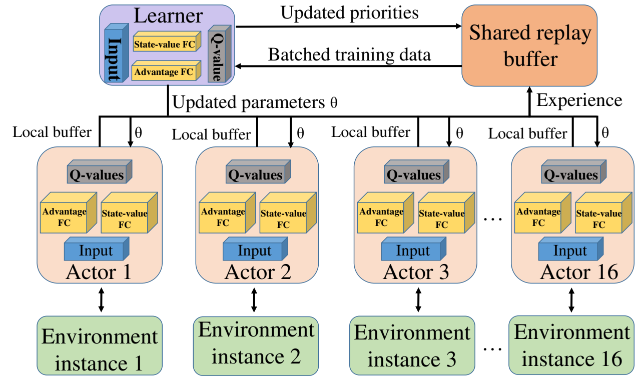

Fig. 4. The overview of the distributed DQL framework. Sixteen actors generate data in their own instances of environment, adding to a shared prioritized replay buffer. A single learner samples the most useful experiences from the buffer and updates the network and priorities of the experiences.

that the agents are not at goal waypoints. Note that no agents occupy a position already taken by another agent during the initialization phase. The green grids represent the goal waypoints, each associated with a bottleneck set to 223. The hazard starts in the red grid and spreads toward the north as shown in Fig. 5 (b) with the red arrow.

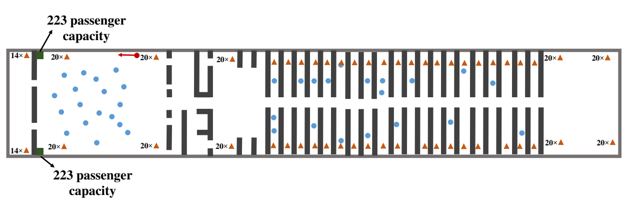

Fig. 5. Experiment setup. Gray blocks are static obstacles and blue circles are agents' initial positions. Orange triangles represent the locations of supply waypoints, and the black numbers beside them indicate the quantity of PLSE present. Green squares denote goal waypoints, each with a capacity of 223. The red circle represents the hazard location, and the red arrow indicates the hazard spread direction.

For other parameter settings during training, the upper limit on the episode length is 512. Once this limit is reached, the training loop breaks and a new episode starts. We set the training episodes to 9000 in the experiments. Unless otherwise stated, the FOV size is 3×3, λ_1 is 0.5, and λ_2 is 4.5. We train the network with a batch size of 192, a discount factor (γ) of 0.99, and an Adam optimizer with default parameters and a dynamic learning rate beginning at 10^{-4}. In order to allow more precise convergence, the learning rate decays by fifty percent at 100k step and 300k step. We use the ϵ-greedy action-selection strategy to encourage exploration throughout training. The value of ϵ taken by the actor begins at 0.6 and decreases by 50% at the 5k episode. All the training parameters are the same for D3QTP and the other three methods.

We develop our learning environment and model in Python with the help of Torch. All experiments were performed on a desktop computer, equipped with 18 cores of an Intel(R) Core(TM) i9-7980XE, 125GB RAM, and an NVIDIA Cooperation TU102 GPU.

B. Results

1) Average Reward. We measure the average reward acquired by all agents for each episode using D3QTP, original DQN, and original Double DQN (DDQN) approaches, as shown in Fig. 6. All approaches are implemented under the same environment settings. It is evident that our proposed method reaches the optimal average reward more rapidly than the other three methods and consistently maintains the optimal performance. This indicates the crucial role of the table-driven pre-training module in facilitating convergence and ensuring stability. Pre-trained agents possess some important information about the environment, and therefore their learning process becomes easier. Table II displays the numerical results for the average reward, maximum and minimum reward, and standard deviation of reward using the above-mentioned three methods. Clearly, using our D3QTP approach, we observe a substantial increase in the average reward alongside a notable improvement in the maximum reward.

TABLE II
COMPARISON OF AVERAGE REWARD VALUE OVER DIFFERENT APPROACHES

Approach	Average reward	SD	Maximum reward	Minimum reward
DQN	-2477.93	28.53	-1812.7	-2542.6
DDQN	-2525.29	32.627	-2276.46	-2545.55
D3QTP	-1503.51	277.94	-1334.22	-2529.12

2) Average evacuation time. We measure the average evacuation time taken by all agents for each episode as shown in Fig. 7. It is evident that our D3QTP algorithm converges to a shorter evacuation time more quickly, compared to the other two approaches which behave in a highly unstable manner and fail to reach the optimal solution. Table III presents the numerical results regarding the average evacuation time across 9100 episodes, the minimum evacuation time reached during training, and the standard deviation of evacuation time.

TABLE III
COMPARISON OF EVACUATION TIME OVER DIFFERENT APPROACHES

Approach	Average evacuation time	SD	Minimum evacuation time
DQN	581.071	81.38	532.684
DDQN	581.071	50.08	524.526
D3QTP	554.888	86.75	512

3) With and without reference channel. To investigate the contributions of the reference channels in solving MANC problems in ship evacuation scenarios, we develop a baseline model and two D3QTP variants. Specifically, the baseline model does not contain the feasible waypoints channel and fastest waypoints channel. The two D3QTP variants, denoted as Baseline (+Feasible) and Baseline (+Fastest) are formed by respectively adding the feasible waypoints channel and fastest waypoints channel to the input of the baseline model. All training parameters used in the three developed models are identical to those used in D3QTP.

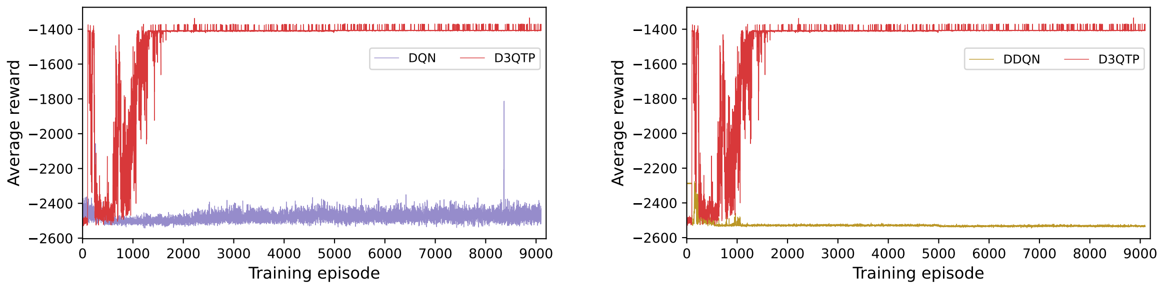

(a) The comparison result of the average reward of D3QTP with original DQN

(b) The comparison result of the average reward of D3QTP with original DDQN

Fig. 6. Comparison of the average reward of D3QTP, with original DQN and DDQN.

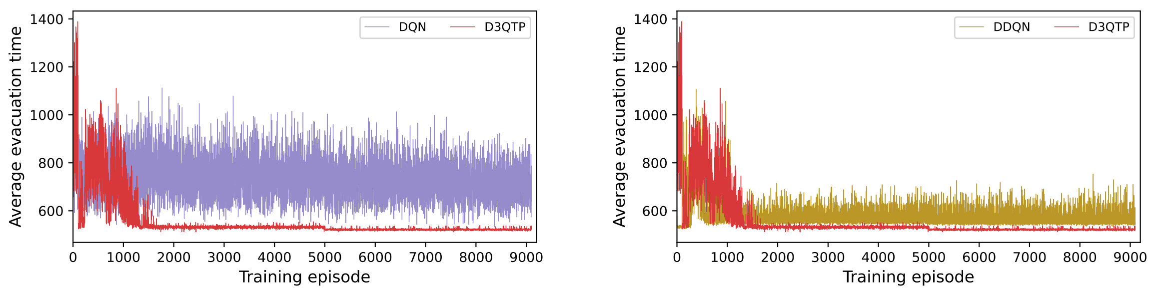

(a) The comparison result of the average evacuation time of D3QTP with DQN

(b) The comparison result of the average evacuation time of D3QTP with DDQN

Fig. 7. Comparison of the average evacuation time of D3QTP, with DQN and DDQN.

We compare the average evacuation time and reward of the Baseline model with the Baseline (+Feasible) model as shown in Fig. 8 (a) and (c) to demonstrate the functionality of the feasible waypoints channel. Fig. 8 (b) and (d) display the comparison of the average evacuation time and reward of the Baseline model and Baseline (+Fastest) model. It is obvious that the incorporation of both the feasible waypoints channel and the fastest waypoints channel makes the Baseline model behave better. The evacuation time drastically fluctuates and is highly unstable when using the Baseline model. In contrast, both the Baseline (+Feasible) and Baseline (+Fastest) models demonstrate convergence and stability in terms of average evaluation time. The Baseline model struggles to adapt to the complex learning environment due to the lack of guidance from reference channels, making its learning process more challenging. The numerical results for the average evacuation time, maximum and minimum evacuation time reached during training, and standard deviation of evacuation time are displayed in Table IV.

Regarding the average reward, we can see that the Baseline model fails to improve the average reward obtained by agents, ultimately converging to a suboptimal reward level. While both the Baseline (+Feasible) and Baseline (+Fastest) models show an increase in average reward during training, and it is able to stabilize at a superior reward level compared to the Baseline model.

In addition, We also evaluate the success rate, which is defined as the ratio of agents successfully reaching the goal waypoints within a given amount of time (i.e., 1800 seconds in our experiment) to the total number of agents. Fig. 9 illustrates the resultant success rate for the three models. We can observe that the Baseline (+Feasible) model and Baseline (+Fastest) model can respectively attain a success rate above ** after ** episodes, whereas the Baseline model is not capable of improving the success rate.

VII. Related work

This section first reviews previous research on crowd evacuation in both land-based built environments and ships. Notably, some interesting studies on evacuation planning [35], [36], [37], [38], [39], [40], which utilize a simulation-optimization framework integrating microscopic simulation, are beyond the scope of this paper and thus not elaborated on here. Subsequently, we discuss the study of reinforcement learning-based MAPF.

A. Global path planning for emergency evacuation

Global path-planning algorithms (e.g., Dijkstra, A*, RRT, Ant Colony Optimization, Genetic algorithm, etc.) can be utilized for evacuation routing by minimizing the route length or the exposure value, or maximizing the safe distance from the source node to the exit node, based on the existing 2D/3D map of a built environment. [41] solved the optimization of evacuation time by employing both a space potential formulation and a proportional swapping process. However, these approaches mostly consider the emergency as a static phenomenon and dynamically update navigation paths in case the emergencies change. Therefore, the navigation paths provided by those methods are not necessarily passable in

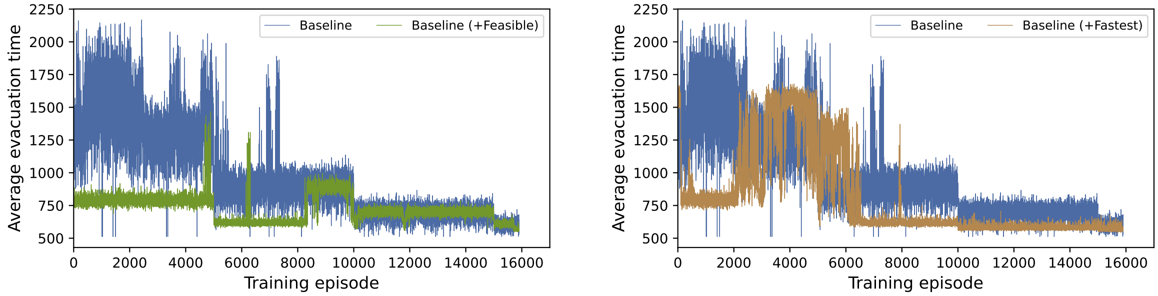

(a) The comparison result of average evacuation time of Baseline model with Baseline (+Feasible) model

(b) The comparison result of average evacuation time of Baseline model with Baseline (+Fastest) model

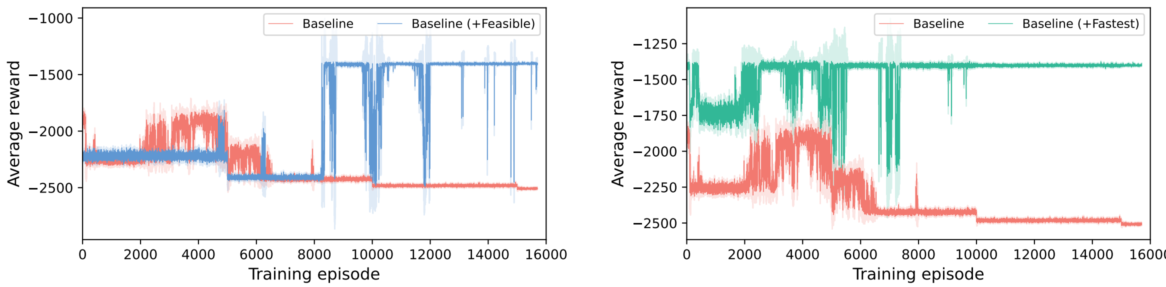

(c) The comparison result of average reward of Baseline model with Baseline (+Feasible) model

(d) The comparison result of average reward of Baseline model with Baseline (+Fastest) model

Fig. 8. Comparison of the average evacuation time and reward of Baseline model with Baseline (+Feasible) model and Baseline (+Fastest) model.

TABLE IV
COMPARISON OF EVACUATION TIME OVER DIFFERENT TRAINING MODELS

Approach	Average evacuation time	Maximum evacuation time	Minimum evacuation time	SD
Baseline model	983.013	1715.71	561.342	314.529
Baseline (+Feasible) model	702.802	1467.29	541.737	308.95
Baseline (+Fastest) model	767.401	1689.39	542.974	104.710

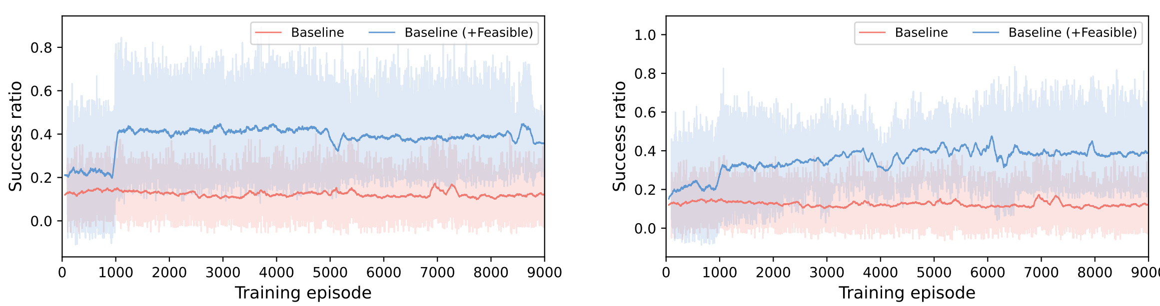

(a) The comparison result of success ratio of Baseline model with Baseline (+Feasible) model

(b) The comparison result of success ratio of Baseline model with Baseline (+Fastest) model

Fig. 9. Comparison of the success ratio of Baseline model with Baseline (+Feasible) model and Baseline (+Fastest) model.

the end because evacuees are likely to be led to emerging dangers due to the dynamics of dangers. The follow-up work addresses the jeopardization of the dynamics of danger. [42] proposed the Expected Number of Oscillations (ENO) concept to quantify the dynamics of emergency and then find navigation paths with the minimum probability of oscillations for the evacuated. In addition, [43] proposed a tailored Dijkstra shortest-path algorithm with the introduction of the concept of impedance conduction for considering the crowd dynamics along paths. [44] developed a multi-input-single-output model to predict crowd dynamics for regulating pedestrian flows more effectively during an evacuation process. In [45], system identification is proposed to model crowd dynamics and build prediction models for developing a behavioral controller that obtains the optimal distance-keeping instructions.

B. Local path planning for emergency evacuation

Undesirably, the global path planning methods require the completeness and determinacy of the information regarding the parameters that are needed to decide the optimal paths, which contradicts many realistic situations where emergency guidance is needed. Therefore, the follow-up studies release the requirement that all the information about the hazards and exits is precisely known prior to path computation, which greatly enhances their applicability to more practical scenarios. Using these **local path-planning** methods (e.g., Artificial potential field method and Reinforcement learning method), the guidance direction is decided for the trapped users based on the environmental conditions of their local neighborhood. For example, [46] applied the partial-reversal concept to the temporally ordered routing algorithm to assist users in avoiding passing through a hazardous region. [47] adopted mobile devices to act as sensors, communicate in a peer-to-peer manner via short-range radio, and guide their users through the evacuation process by conducting shortest route planning based on what is known about the environment.

However, these methods neglect the fact that the evacuation system for passenger ships is a safety-critical system without compromising safety guarantees. That is to say, the emergency navigation system should be capable of offering guidance directions that guarantee the time to the exit does not exceed the specified upper bound (i.e., the survival or capsizing time) even under the worst-case circumstances (e.g., the case where the roll angle reaches the 30°). [48] considered the impact of both dynamic hazards and upper bound on worst-case traversal time as well as the end-to-end time available for evacuation to determine hazard-free routes typically experiencing the smallest escaping time, while guaranteeing to respect the specified end-to-end upper bound for the survival time until capsizing under all circumstances. However, [48] based the emergency navigation system on the precise a priori estimates of the typical delay are available in [48]. That is to say, the estimates are known and static, which is not applicable to the practical evacuation scenario on passenger ships.

C. Reinforcement learning-based MAPF

Some researchers offload the online computational burden to an offline RL procedure due to its capability of handling high-dimensional state-space representations. RL-based MAPF methods can take advantage of historical data and flexibly encapsulate environmental uncertainty. These methods can be categorized into two main types: RL-based centralized planning approaches and RL-based decentralized planning approaches. Centralized planning approaches learn a joint action for all agents based on access to the observations and rewards of all agents during learning. [49] proposed a hierarchical RL method that incorporates an upper-level agent for learning the timing of releasing placed online customers and arrived crowd drivers, along with lower-level agents for route planning for crowd drivers and company vehicles to minimize the total costs. [50] applies deep reinforcement learning (DRL) technology to determine the directional instructions for evacuation signs with the help of metaverse to enable evacuees to choose the most efficient route for leaving the building in the least amount of time. In this study, the evacuation signage system is treated as an agent. [51] developed a multi-agent attention model to solve the vehicle routing problem instantly through lengthy offline training facilitated by multi-agent reinforcement learning. [31] introduced attention and BicNet-based multi-agent path planning algorithm which is under the actor-critic reinforcement learning framework to learn the optimal combination of individual actions in dynamic environments. The limitation of these centralized learning approaches is that they scale poorly to a large number of agents.

Some research has applied RL to learn decentralized policies, where each agent follows a policy individually and makes decisions based on its local observations. [52] proposed an RL algorithm inspired by Q-learning and Deep Deterministic Policy Gradient algorithms to train an agent to suggest high-quality conflict resolution maneuvers to the ownship based on observations within a circular area of interest. [53] proposed a decentralized RL framework for joint dynamic emergency vehicle (EMV) routing and traffic signal control so as to reduce both EMV travel time and non-EMV travel time. In [54], decentralized deep RL agents bargain with each other to solve both the vehicle route allocation problem and gain sharing problem simultaneously. Considering the inherent nature of individual drivers' compliance, [55] introduced a regional route guidance framework with the utilization of deep RL to send customized route plans to compliant individuals, aiming to reduce their trip costs while compromising partial system utility. [56] evaluates the last-mile relief distribution solutions generated by two decentralized deep RL approaches – specifically value function approximation (VFA) and policy function approximation (PFA). [28] presents a framework that combines reinforcement and imitation learning from an expert centralized multi-agent path-finding planner to teach fully decentralized policies in a partially observable world. To increase the training performance and efficiency, [30] proposed a decentralized multi-agent RL approach for path planning, which integrates evolutionary training that gradually eliminates the low-performance policies during training. [29] combines communication with decentralized deep Q-learning to enable agents to learn cooperation to handle the MAPF problem in congested situations.

VIII. CONCLUSION

This paper addresses the problem of MANC in ship evacuation scenarios using a model-free off-policy RL method. Compared to model-based and on-policy methods, our approach requires less time and information to adjust agents' optimal paths for our designed MANC environment, which simulates realistic ship evacuation scenarios. The features such as floodwater spreading, bottlenecks of goal waypoints, PLSE, and dynamic ship motion are taken into account in the proposed learning environment. We develop a novel RL-based method, i.e., the distributed decentralized deep Q-learning with table-driven pretraining (D3QTP), for better training in the environment. A table-driven algorithm is used to construct routing tables, based on which a Q-matrix can be calculated directly without undergoing a lengthy learning process. Then, the produced Q-matrix is employed to pre-train the agent to possess the information on the fastest waypoints. Finally, the pertained agent is distributed and trained in our learning environment to learn the optimal ship evacuation schedule. Through extensive experiments on a simulated ship deck environment, we demonstrate the superior performance of our proposed method compared with state-of-the-art RL approaches, such as DQN and DDQN. Also, the comparisons of a baseline model with three D3QTP variants prove the significance of the reference channels.

However, our work relies on the availability of precise (known and static) delay distributions on edges, which are challenging to obtain in reality. Therefore an important direction for future work is to handle cases where the delay distributions are unknown or dynamic.

Declaration of Competing Interest

The authors declare that they have no known competing financial interests or personal relationships that could have appeared to influence the work reported in this paper.

Acknowledgments

The authors would like to thank the editors and anonymous reviewers for their valuable comments and suggestions on the earlier drafts of the article. This research is supported in part by the National Natural Science Foundation of China (NSFC) under Grant 51979216; and in part by the Natural Science Foundation of Hubei Province, China, under Grant No.2021CFA001 and Grant 20221j0059.

References

[1] X. Wang, G. Xia, J. Zhao, J. Wang, Z. Yang, S. Loughney, S. Fang, S. Zhang, Y. Xing, and Z. Liu, "A novel method for the risk assessment of human evacuation from cruise ships in maritime transportation," *Reliability Engineering & System Safety*, vol. 230, p. 108887, 2023.

[2] E. Eliopoulou, A. Alissafaki, and A. Papanikolaou, "Statistical analysis of accidents and review of safety level of passenger ships," *Journal of Marine Science and Engineering*, vol. 11, no. 2, p. 410, 2023.

[3] J. Montewka, T. Manderbacka, P. Ruponen, M. Tompuri, M. Gil, and S. Hirdaris, "Accident susceptibility index for a passenger ship-a framework and case study," *Reliability Engineering & System Safety*, vol. 218, p. 108145, 2022.

[4] D. Kee, G. T. Jun, P. Waterson, and R. Haslam, "A systemic analysis of south korea sewol ferry accident–striking a balance between learning and accountability," *Applied ergonomics*, vol. 59, pp. 504–516, 2017.

[5] C.-J. Chae, K. H. Kim, and S. Y. Kang, "Limiting ship accidents by identifying their causes and determining barriers to application of preventive measures," *Journal of Marine Science and Engineering*, vol. 9, no. 3, p. 302, 2021.

[6] S. Fang, Z. Liu, X. Wang, J. Wang, and Z. Yang, "Simulation of evacuation in an inclined passenger vessel based on an improved social force model," *Safety science*, vol. 148, p. 105675, 2022.

[7] Y. Yue, W.-m. Gai, and Y.-f. Deng, "Influence factors on the passenger evacuation capacity of cruise ships: Modeling and simulation of full-scale evacuation incorporating information dissemination," *Process Safety and Environmental Protection*, vol. 157, pp. 466–483, 2022.

[8] H. Arshad, J. Emblemsvåg, G. Li, and R. Ostnes, "Determinants, methods, and solutions of evacuation models for passenger ships: A systematic literature review," *Ocean Engineering*, vol. 263, p. 112371, 2022.

[9] H. Arshad, J. Emblemsvåg, and X. Zhao, "A data-driven, scenario-based human evacuation model for passenger ships addressing hybrid uncertainty," *International Journal of Disaster Risk Reduction*, p. 104213, 2023.

[10] S. Fang, Z. Liu, X. Yang, X. Wang, J. Wang, and Z. Yang, "A quantitative study of the factors influencing human evacuation from ships," *Ocean Engineering*, vol. 285, p. 115156, 2023.

[11] X. Wang, Z. Liu, S. Loughney, Z. Yang, Y. Wang, and J. Wang, "Numerical analysis and staircase layout optimisation for a ro-ro passenger ship during emergency evacuation," *Reliability Engineering & System Safety*, vol. 217, p. 108056, 2022.

[12] J. Li, D. Harabor, P. J. Stuckey, H. Ma, and S. Koenig, "Symmetry-breaking constraints for grid-based multi-agent path finding," in *Proceedings of the AAAI Conference on Artificial Intelligence*, vol. 33, no. 01, 2019, pp. 6087–6095.

[13] A. Felner, R. Stern, S. Shimony, E. Boyarski, M. Goldenberg, G. Sharon, N. Sturtevant, G. Wagner, and P. Surynek, "Search-based optimal solvers for the multi-agent pathfinding problem: Summary and challenges," in *Proceedings of the International Symposium on Combinatorial Search*, vol. 8, no. 1, 2017, pp. 29–37.

[14] G. Sharon, R. Stern, A. Felner, and N. R. Sturtevant, "Conflict-based search for optimal multi-agent pathfinding," *Artificial Intelligence*, vol. 219, pp. 40–66, 2015.

[15] A. Juliani, V.-P. Berges, E. Teng, A. Cohen, J. Harper, C. Elion, C. Goy, Y. Gao, H. Henry, M. Mattar *et al.*, "Unity: A general platform for intelligent agents," *arXiv preprint arXiv:1809.02627*, 2018.

[16] O. Vinyals, T. Ewalds, S. Bartunov, P. Georgiev, A. Vezhnevets, M. Yeo, A. Makhzani, H. Küttler, J. Agapiou, J. Schrittwieser *et al.*, "Starcraft ii: A new challenge for reinforcement learning. arxiv 2017," *arXiv preprint arXiv:1708.04782*.

[17] Ł. Kidziński, S. P. Mohanty, C. F. Ong, J. L. Hicks, S. F. Carroll, S. Levine, M. Salathé, and S. L. Delp, "Learning to run challenge: Synthesizing physiologically accurate motion using deep reinforcement learning," in *The NIPS'17 Competition: Building Intelligent Systems*. Springer, 2018, pp. 101–120.

[18] G. Brockman, V. Cheung, L. Pettersson, J. Schneider, J. Schulman, J. Tang, and W. Zaremba, "Openai gym," *arXiv preprint arXiv:1606.01540*, 2016.

[19] A. Sweigart, *Making Games with Python & Pygame*, 2012.

[20] J. Sharma, P.-A. Andersen, O.-C. Granmo, and M. Goodwin, "Deep q-learning with q-matrix transfer learning for novel fire evacuation environment," *IEEE Transactions on Systems, Man, and Cybernetics: Systems*, vol. 51, no. 12, pp. 7363–7381, 2020.

[21] X. Zeng, K. Liu, Y. Ma, and M. Chen, "Dc-hen: A deadline-aware and congestion-relieved hierarchical emergency navigation algorithm for ship indoor environments," in *2023 IEEE International Conference on Mobility, Operations, Services and Technologies (MOST)*. IEEE, 2023, pp. 44–54.

[22] K. Agrawal, S. Baruah, Z. Guo, J. Li, and S. Vaidhun, "Hard-real-time routing in probabilistic graphs to minimize expected delay," in *2020 IEEE Real-Time Systems Symposium (RTSS)*. IEEE, 2020, pp. 63–75.

[23] D. Horgan, J. Quan, D. Budden, G. Barth-Maron, M. Hessel, H. Van Hasselt, and D. Silver, "Distributed prioritized experience replay," *arXiv preprint arXiv:1803.00933*, 2018.

[24] V. Mnih, K. Kavukcuoglu, D. Silver, A. Graves, I. Antonoglou, D. Wierstra, and M. Riedmiller, "Playing atari with deep reinforcement learning," *arXiv preprint arXiv:1312.5602*, 2013.

[25] V. Mnih, K. Kavukcuoglu, D. Silver, A. A. Rusu, J. Veness, M. G. Bellemare, A. Graves, M. Riedmiller, A. K. Fidjeland, G. Ostrovski *et al.*, "Human-level control through deep reinforcement learning," *nature*, vol. 518, no. 7540, pp. 529–533, 2015.

[26] J. Chung, C. Gulcehre, K. Cho, and Y. Bengio, "Empirical evaluation of gated recurrent neural networks on sequence modeling," *arXiv preprint arXiv:1412.3555*, 2014.

[27] D. Zhang, M. Zhao, T. Ying, and Y. Gong, "Passenger ship evacuation model and simulation under the effects of storms," *Xitong Gongcheng Lilun yu Shijian/System Engineering Theory and Practice*, vol. 36, no. 6, pp. 1609–1615, 2016.

[28] G. Sartoretti, J. Kerr, Y. Shi, G. Wagner, T. S. Kumar, S. Koenig, and H. Choset, "Primal: Pathfinding via reinforcement and imitation multi-agent learning," *IEEE Robotics and Automation Letters*, vol. 4, no. 3, pp. 2378–2385, 2019.

[29] Z. Ma, Y. Luo, and H. Ma, "Distributed heuristic multi-agent path finding with communication," in *2021 IEEE International Conference on Robotics and Automation (ICRA)*. IEEE, 2021, pp. 8699–8705.

[30] Z. Liu, B. Chen, H. Zhou, G. Koushik, M. Hebert, and D. Zhao, "Mapper: Multi-agent path planning with evolutionary reinforcement learning in mixed dynamic environments," in *2020 IEEE/RSJ International Conference on Intelligent Robots and Systems (IROS)*. IEEE, 2020, pp. 11 748–11 754.

[31] H. Guan, Y. Gao, M. Zhao, Y. Yang, F. Deng, and T. L. Lam, "Ab-mapper: Attention and bicnet based multi-agent path planning for dynamic environment," in *2022 IEEE/RSJ International Conference on Intelligent Robots and Systems (IROS)*. IEEE, 2022, pp. 13 799–13 806.

[32] K. Yoshida, M. Murayama, and T. Itakaki, "Study on evaluation of escape route in passenger ships by evacuation simulation and full-scale trials," *Research Institute of Marine Engineering, Japan*, 2001.

[33] M. Ahola, P. Murto, P. Kujala, and J. Pitknen, “Perceiving safety in passenger ships–user studies in an authentic environment,” *Safety science*, vol. 70, pp. 222–232, 2014.

[34] P. Valanto, “Time-dependent survival probability of a damaged passenger ship ii-evacuation in seaway and capsizing,” *HSVA Report*, no. 1661, pp. 42–62, 2006.

[35] M. A. Lopez-Carmona and A. P. Garcia, “Adaptive cell-based evacuation systems for leader-follower crowd evacuation,” *Transportation research part C: emerging technologies*, vol. 140, p. 103699, 2022.

[36] W. Wu, W. Yi, X. Wang, and X. Zheng, “A force-based model for adaptively controlling the spatial configuration of pedestrian subgroups at non-extreme densities,” *Transportation Research Part C: Emerging Technologies*, vol. 152, p. 104154, 2023.

[37] S. Li, J. Zhuang, and S. Shen, “A three-stage evacuation decision-making and behavior model for the onset of an attack,” *Transportation Research Part C: Emerging Technologies*, vol. 79, pp. 119–135, 2017.

[38] N. Shiwakoti and M. Sarvi, “Enhancing the panic escape of crowd through architectural design,” *Transportation research part C: emerging technologies*, vol. 37, pp. 260–267, 2013.

[39] M. Haghani and M. Sarvi, “Simulating dynamics of adaptive exit-choice changing in crowd evacuations: Model implementation and behavioural interpretations,” *Transportation research part C: emerging technologies*, vol. 103, pp. 56–82, 2019.

[40] A. Poulos, F. Tocornal, J. C. de la Llera, and J. Mitrani-Reiser, “Validation of an agent-based building evacuation model with a school drill,” *Transportation research part C: emerging technologies*, vol. 97, pp. 82–95, 2018.

[41] R.-Y. Guo, “Potential-based dynamic pedestrian flow assignment,” *Transportation Research Part C: Emerging Technologies*, vol. 91, pp. 263–275, 2018.

[42] L. Wang, Y. He, W. Liu, N. Jing, J. Wang, and Y. Liu, “On oscillation-free emergency navigation via wireless sensor networks,” *IEEE Transactions on Mobile Computing*, vol. 14, no. 10, pp. 2086–2100, 2014.

[43] B. Yu, “Consideration of tactical decisions in microscopic pedestrian simulation: Algorithm and experiments,” *Transportation research part C: emerging technologies*, vol. 119, p. 102742, 2020.

[44] M. A. Lopez-Carmona and A. P. Garcia, “Multiple-input-single-output prediction models of crowd dynamics for model predictive control (mpc) of crowd evacuations,” *Transportation research part C: emerging technologies*, vol. 154, p. 104268, 2023.

[45] M. A. Lopez-Carmona, “System identification for the design of behavioral controllers in crowd evacuations,” *Transportation research part C: emerging technologies*, vol. 144, p. 103913, 2022.

[46] Y.-C. Tseng, M.-S. Pan, and Y.-Y. Tsai, “Wireless sensor networks for emergency navigation,” *Computer*, vol. 39, no. 7, pp. 55–62, 2006.

[47] K.-F. Richter, M. Shi, H.-S. Gan, and S. Winter, “Decentralized evacuation management,” *Transportation Research Part C: Emerging Technologies*, vol. 31, pp. 1–17, 2013.

[48] Y. Ma, K. Liu, M. Chen, J. Ma, X. Zeng, K. Wang, and C. Liu, “Ant: Deadline-aware adaptive emergency navigation strategy for dynamic hazardous ship evacuation with wireless sensor networks,” *IEEE Access*, vol. 8, pp. 135 758–135 769, 2020.

[49] C. Xiang, Z. Wu, Y. Zhou, and J. Tu, “Dual-decoder attention model in hierarchical reinforcement framework for dynamic crowd logistics problem with batch-matching,” *Transportation Research Part C: Emerging Technologies*, vol. 157, p. 104417, 2023.

[50] J. Gu, J. Wang, X. Guo, G. Liu, S. Qin, and Z. Bi, “A metaverse-based teaching building evacuation training system with deep reinforcement learning,” *IEEE Transactions on Systems, Man, and Cybernetics: Systems*, vol. 53, no. 4, pp. 2209–2219, 2023.

[51] K. Zhang, F. He, Z. Zhang, X. Lin, and M. Li, “Multi-vehicle routing problems with soft time windows: A multi-agent reinforcement learning approach,” *Transportation Research Part C: Emerging Technologies*, vol. 121, p. 102861, 2020.

[52] D.-T. Pham, P. N. Tran, S. Alam, V. Duong, and D. Delahaye, “Deep reinforcement learning based path stretch vector resolution in dense traffic with uncertainties,” *Transportation research part C: emerging technologies*, vol. 135, p. 103463, 2022.

[53] H. Su, Y. D. Zhong, J. Y. Chow, B. Dey, and L. Jin, “Emvlight: A multi-agent reinforcement learning framework for an emergency vehicle decentralized routing and traffic signal control system,” *Transportation Research Part C: Emerging Technologies*, vol. 146, p. 103955, 2023.

[54] S. Mak, L. Xu, T. Pearce, M. Ostroumov, and A. Brintrup, “Fair collaborative vehicle routing: A deep multi-agent reinforcement learning approach,” *Transportation Research Part C: Emerging Technologies*, vol. 157, p. 104376, 2023.

[55] S. Jiang, C. Q. Tran, and M. Keyvan-Ekbatani, “Regional route guidance with realistic compliance patterns: Application of deep reinforcement learning and mpc,” *Transportation Research Part C: Emerging Technologies*, vol. 158, p. 104440, 2024.

[56] R. van Steenbergen, M. Mes, and W. van Heeswijk, “Reinforcement learning for humanitarian relief distribution with trucks and uavs under travel time uncertainty,” *Transportation Research Part C: Emerging Technologies*, vol. 157, p. 104401, 2023.

[57] L. Baird, “Residual algorithms: Reinforcement learning with function approximation,” in *Machine Learning Proceedings 1995*. Elsevier, 1995, pp. 30–37.

[58] D. P. Kingma and J. Ba, “Adam: A method for stochastic optimization,” *arXiv preprint arXiv:1412.6980*, 2014.

[59] A. Graves and A. Graves, “Long short-term memory,” *Supervised sequence labelling with recurrent neural networks*, pp. 37–45, 2012.

[60] M. Tan, “Multi-agent reinforcement learning: Independent vs. cooperative agents,” in *Proceedings of the tenth international conference on machine learning*, 1993, pp. 330–337.

[61] A. Tampuu, T. Matiisen, D. Kodelja, I. Kuzovkin, K. Korjus, J. Aru, J. Aru, and R. Vicente, “Multiagent cooperation and competition with deep reinforcement learning,” *PloS one*, vol. 12, no. 4, p. e0172395, 2017.

[62] I. M. Organization, “Guidelines for evacuation analysis for new and existing passenger ships,” *MSC. 1/Circ. 1238*, 2016.

[63] C. Nasso, S. Bertagna, F. Mauro, A. Marinò, and V. Bucci, “Simplified and advanced approaches for evacuation analysis of passenger ships in the early stage of design,” *Brodogradnja: Teorija i praksa brodogradnje i pomorske tehnike*, vol. 70, no. 3, pp. 43–59, 2019.

[64] C. Wang, H. Lin, R. Zhang, and H. Jiang, “Send: A situation-aware emergency navigation algorithm with sensor networks,” *IEEE Transactions on Mobile Computing*, vol. 16, no. 4, pp. 1149–1162, 2016.

[65] M. Everett, Y. F. Chen, and J. P. How, “Motion planning among dynamic, decision-making agents with deep reinforcement learning,” in *2018 IEEE/RSJ International Conference on Intelligent Robots and Systems (IROS)*. IEEE, 2018, pp. 3052–3059.

[66] M. Zhou, H. Dong, Y. Zhao, P. A. Ioannou, and F.-Y. Wang, “Optimization of crowd evacuation with leaders in urban rail transit stations,” *IEEE transactions on intelligent transportation systems*, vol. 20, no. 12, pp. 4476–4487, 2019.

Yuting Ma is currently pursuing a Ph.D. degree in marine navigation from the Wuhan University of Technology (WUT), Wuhan, China. Her research interests focus on emergency navigation and evacuation.

Kezhong Liu received the B.S. and M.S. degrees in marine navigation from the Wuhan University of Technology (WUT), Wuhan, China, in 1998 and 2001, respectively. He received the Ph.D. degree in communication and information engineering from the Huazhong University of Science and Technology, Wuhan, China, in 2006. He is currently a professor at the School of Navigation, WUT. His active research interests include indoor localization technology and data mining for ship navigation.

Mozi Chen received the B.S. degree in electric engineering from the Hubei University of Technology, China, in 2013, the M.S. degree in navigation engineering from the Wuhan University of Technology (WUT), China, in 2016, and the Ph.D. degree from the WUT, China, in 2020. He is currently an associate researcher at WUT. His research work has been focused on wireless sensing techniques and machine learning algorithms for human localization, emergency navigation, and activity recognition in mobile environments, i.e., cruise ships.

Erol Gelenb received the Ph.D. degree from the Polytechnic Institute of New York University in 1970. His previous full professorships include the University of Liege, Belgium (1974-79), University of Paris-Saclay (1979-1986), University of Paris V (1986-1994), Duke University, USA (1993-1998), University of Central Florida (1998-2003), and Imperial College (2004-2020). Known for pioneering the field of modeling and performance evaluation of computer systems and networks throughout Europe. He invented the random neural network and the eponymous G-networks. His many awards include the ACM SIGMETRICS Life-Time Achievement Award and the in Memoriam Dennis Gabor Award of the Hungarian Academy of Sciences.

Appendix F: Paper VI

sensors

Article

Impact of IoT System Imperfections and Passenger Errors on Cruise Ship Evacuation Delay

Yuting Ma [1,2,*], Erol Gelenbe [1,3,4,*] and Kezhong Liu [2]

[1] Instytut Informatyki Teoretycznej i Stosowanej Polskiej Akademii Nauk, 44-100 Gliwice, Poland
[2] School of Navigation, Wuhan University of Technology, Wuhan 430063, China; kzliu@whut.edu.cn
[3] Université Côte d'Azur, CNRS, I3S, 06100 Nice, France
[4] Department of Computer Engineering, Yaşar University, Bornova, 35500 Izmir, Turkey
* Correspondence: yma@iitis.pl (Y.M.); gelenbe.erol@orange.fr (E.G.)

Abstract: Cruise ships and other naval vessels include automated Internet of Things (IoT)-based evacuation systems for the passengers and crew to assist them in case of emergencies and accidents. The technical challenges of assisting passengers and crew to safety during emergencies include various aspects such as sensor failures, imperfections in the sound or display systems that are used to direct evacuees, the timely selection of optimum evacuation routes for the evacuees, as well as computation and communication delays that may occur in the IoT infrastructure due to intense activities during an emergency. In addition, during an emergency, the evacuees may be confused or in a panic, and may make mistakes in following the directions offered by the evacuation system. Therefore, the purpose of this work is to analyze the effect of two important aspects that can have an adverse effect on the passengers' evacuation time, namely (a) the computer processing and communication delays, and (b) the errors that may be made by the evacuees in following instructions. The approach we take uses simulation with a representative existing cruise ship model, which dynamically computes the best exit paths for each passenger, with a deadline-driven Adaptive Navigation Strategy (ANS). Our simulation results reveal that delays in the evacuees' reception of instructions can significantly increase the total time needed for passenger evacuation. In contrast, we observe that passenger behavior errors also affect the evacuation duration, but with less effect on the total time needed to evacuate passengers. These findings demonstrate the importance of the design of passenger evacuation systems in a way that takes into account all realistic features of the ship's indoor evacuation environment, including the importance of having high-performance data processing and communication systems that will not result in congestion and communication delays.

Keywords: passenger evacuation; naval vessels; cruise ships; emergency systems; information technology support; processing delays; congestion in communication systems

check for updates

Citation: Ma, Y.; Gelenbe, E.; Liu, K. Impact of IoT System Imperfections and Passenger Errors on Cruise Ship Evacuation Delay. *Sensors* **2024**, *24*, 1850. https://doi.org/10.3390/s24061850

Academic Editor: Nick Harris

Received: 20 January 2024
Revised: 19 February 2024
Accepted: 8 March 2024
Published: 13 March 2024

1. Introduction

In case of emergencies, evacuation methods are critical to managing people and vehicles in a manner that guarantees their safety [1,2]. These methods rely on the sensing, communication, and signaling technologies that are required to (a) know where people and vehicles are located and (b) how one can communicate with them or inform them about ongoing conditions so as to (c) direct them along effective pathways towards safety.

Research in this area includes the use of sensing and communication technologies [3], crowd monitoring [4], hazard modeling and prediction [5], evacuation simulation and evacuation path planning [6]. In particular, offline simulation of evacuation schemes aids the design and comparison of the sensing and communication technologies, and of the algorithms [7] that improve or optimize the performance and robustness of evacuation strategies.

Thus, emergency management simulation research addresses simulations that represent the movement of people who congregate in sports arenas, touristic sites, and other leisure venues [8,9], as well as in large ships [10], in the presence of unusual and extreme conditions such as the breakdown of some facilities or adversarial situations such as fire or panic.

With the increased popularity of the cruise ship industry worldwide, more attention has been paid to passenger safety in maritime transportation [11]. Although advanced accident prevention systems are deployed in modern passenger ships, maritime transport accidents unfortunately occur, such as the Sewol Ferry accident in South Korea that caused 304 casualties on 16 April 2014 [12], the Chinese Eastern Star accident that caused 42 casualties on 1 June 2015 [13], and the collision of two passenger ships in the Padma River in Bangladesh, resulting in 26 deaths on 3 May 2021 [14]. Therefore, effective evacuation methods for passengers on cruise or passenger ships are of great importance [15], and significant research is recently being conducted in this area [16].

Since such accidents or emergencies cannot be artificially created or reproduced or easily observed for data analysis when they occur, the simulation of human evacuation on ships has become a key tool in the design of both civilian and military naval vessels [17–19].

In particular, the IMO (International Maritime Organization) has published circulars regarding the simulation of naval vessel evacuation both for passenger and roll-on-roll-off ships. In 2016, it also issued approvals for guidelines regarding the simulation of evacuation both for new and existing passenger ships [20]. However, the actual technology that is used in supporting passenger evacuation, such as the computers, communication systems, visible panels, loudspeaker announcements, and other sensors and actuators, can themselves have some imperfections that are exacerbated during an emergency. Furthermore, passengers can also be panicked and confused during such events. Thus, this paper focuses on the effect—*on the time taken by passengers to exit the ship* —of:

1. Computation and communication delays in the sensing, communication and computer processing technologies in the vessel, including the processing delays in the computers that provide instructions to the evacuees [21,22];
2. Errors that the passengers may make in following instructions. Such errors can be caused by panic, human error or the lack of visibility of direction panels, and the difficulty of understanding loudspeaker announcements due to noise.

Our study uses a simulation framework to evaluate the outcome of these factors on the time needed by passengers to reach a safe exit, based on multiple simulation runs using the AnyLogic simulator [23] described in Section 2. The present research does not consider some other features that can impact the speed and safety of human beings during emergencies [7,24], including the time needed to traverse passages and staircases as a function of the health and age of different passengers. However, our simulations include the effect of the changes in the tilt of the ship which will affect the traversal times.

While AnyLogic is used as part of our simulation tool, we do not claim or suggest that this tool should be used for real-time decision making during an emergency. We expect that the software used to manage evacuations during the emergency would include a fast discrete-event purpose-built simulator which updates—in real-time—the dynamic spread of hazards that are reported via sensors installed in the cruise ship, or in any other built structures such as buildings, campuses or cities, which require emergency evacuation.

The remaining sections of this paper are structured as follows: The related research about evacuation in passenger ships and built structures is reviewed in Section 1. A detailed description of the ship emergency evacuation simulator is provided in Section 2, while the simulation results regarding the impact of delay and lost messages, which result from communication system congestion, are given in Section 3. Then, Section 4 presents the possible impact of uncertainties in human behavior. In Section 5, we discuss potential extensions and open aspects of our work and present our conclusions.

Related Work

There has been extensive work on using the IoT to support emergency management [25], and advanced systems such as Unmanned Aerial Vehicles (UAVs) have also been suggested as a means for observation and sensing [26] during emergencies. While the current study does not assume that evacuees were identified and tracked during the evacuation, there has been work on the issue of localization of specific groups, such as elderly people who may have greater difficulty in reaching exits safely [27].

While the use of path optimization algorithms in emergency evacuation is quite common [28] to minimize evacuation delay or minimize the risk to evacuees using prior 2D/3D knowledge [29,30], the decisions regarding the choice of paths do not always include the effects of unexpected or new hazards that may be encountered. The Expected Number of Oscillations (ENO) [31] has been used to quantify the dynamic changes due to spreading hazards, so that a small ENO indicates the paths do not change often under the effect of possible dangers and are therefore to be preferred. Indeed, methods that try to predict the optimum paths may not result in the safest paths, and the information available prior to an emergency may not match the realistic developments that may occur as an emergency unfolds. Therefore, recent studies do not require that all possible hazards be known for optimization purposes and tend to lead to results that have more value in practice [7,32].

Methods such as Social Potential Fields (SPF) [33] and local neighborhood techniques [34,35] with possible partial reversal can also help evacuees avoid entering hazardous areas. However, most studies do not consider the need to provide directions that assure that the "time needed to reach the exit" for each evacuee remains under a required specified bound determined by the characteristics of the worst-case dynamic characteristics of the ship.

Thus, this paper uses the Adaptive Navigation Strategy (ANS) evacuation algorithm, an extension of Rapid Routing with Guaranteed Delay Bounds [36], which was previously named ANT in [37], creating potential confusion with other well-known "ant colony" optimization techniques. ANS incorporates a guaranteed exit deadline bound, for each evacuee in each location. When dealing with ships, this deadline bound can be obtained, as already indicated above, from the recommendations of the IMO. We note that various organizations in various countries and regions have made corresponding safety recommendations for office buildings, apartment buildings, factories, university campuses, etc. Note that **all the work cited in this paper** is summarized in Table 1.

Table 1. Summary of the related work in this paper.

	Focus	Related work
Evacuation Review	Crowd monitoring	[4,6,25]
	Disaster detection & prediction	[3,6,25]
	Evacuation modelling	[6,11,15,19]
	Evacuation path planning	[6,11,15,28,30]
	Accident type	**Related work**
Ship Accident	Ship sinking	[12,13]
	Ship collision	[14]
	Simulation model	**Related work**
Evacuation Simulation	Agent-based model	[1,8,9,17,20,32]
	Social force model	[10,21,23,24]
	Social potential field model	[33]
	Flow model	[17,20]

Table 1. *Cont.*

	Planning method	Related work
Path Planning	A*	[5]
	Swarm optimization algorithm	[26]
	Proactiv & reactive method	[29]
	Cognitive packet network-based method	[7,38,39]
	OPEN	[31]
	Social potential field	[7]
	Temporally ordered routing algorithm	[34]
	Directional pathfinding method	[35]
	Table-driven method	[36]
	ANS	[37]
	Dinic algorithm	[40]
	Minimum spanning tree	[41]
	Hazard potential field	[42]
	Analysis method	**Related work**
Risk Analysis	Bayesian network	[16]
	Failure modes and effects analysis & analytic hierarchy process & fuzzy rule-based Bayesian reasoning & ER	[22]
	Method	**Related work**
Person Localization	Hybrid optimized fuzzy threshold extreme learning machine	[27]
	Method	**Related work**
Decision Rule Learning	Coevolutionary fuzzy rule miner	[2]
	Method	**Related work**
Evacuation Analysis & Layout Optimization	FDS+EVAC	[18]
	Method	**Related work**
Wireless Energy Transmission	Four-stage transmission	[43]
	Method	**Related work**
Activity & Data Detection	Multi-armed bandit	[44]

2. The Simulation Framework

We now describe the simulation framework that we use to evaluate the effects of both the computer and communication technology delay in providing routing instructions to evacuees, and the uncertainties related to the evacuees' behavior, within an event-driven simulation framework. This framework contains two parts:

- The first part is the simulation software AnyLogic 8.8-8.8.2: Please state the version number of the software. I have added the version number. in which the layout of the physical where the evacuation occurs is incorporated. The "pedestrian" software library of AnyLogic adopts the Social Potential Field model to determine the direction of the movement of each evacuee.
- Secondly, we add a path-planning module written in Python that computes the evacuation direction for evacuees based on ANS, which is described below. This module

transfers the computed instructions to the AnyLogic simulation software at each simulation step when the movement instructions need to be updated.

- ANS is implemented in our simulator to move evacuees along the path with minimum delay, avoiding the harmful effects caused by dynamic hazards. ANS assumes knowledge about the propagation of hazards (velocity and direction), and the average and maximum delay across each edge in the paths.
- As hazards progress in the simulation, ANS calculates the direction each evacuee should take to avoid hazards. In a real evacuation, this direction should be computed and then communicated to each evacuee via a wired or wireless network. In previous work, the possible delays of this communication were not taken into account.
- However, wireless or wired networks and computational servers that are used for decision making are likely to experience congestion, especially in emergency situations when decisions and communications are frequently updated and many messages are sent to evacuees and to the staff in the ship. This congestion can cause delays in updates regarding the navigation direction, and transmitting network packets and hence messages can be lost, and decisions may lead to errors due to the arrival of delayed instructions or facts, used by decision algorithms, that have been modified by events [43,44]. While most prior work neglects these effects, the present paper specifically evaluates their effect on the time required for the evacuation.
- Also, the passengers being evacuated may themselves be unable to follow the instructions they receive due to noise, panic, or misunderstanding.
- Thus, these delays and possible errors due to Information and Communication Technology (ICT), including network packet losses, as well as the possible effects of panic or misunderstandings by the evacuees, will be simulated and evaluated in this paper.

2.1. The Supporting IoT System

The IoT could, in principle, use the personal identification of each passenger via "smart badges", "RFID" (radio-frequency identity), or communicating "wristwatches". However, such devices requiring radio-frequency communications can be unreliable within naval vessels. Indeed, large ships typically have high steel content with possible local Faraday cage effects, as well as the refraction and reflection of high-frequency radio waves. In addition, the numerous electric motors (e.g., for ventilation and lifts) and ongoing automatic switching of equipment (e.g., on–off of air-conditioning equipment, multiple refrigerators, fans), as well as multi-path reflections, can lead to substantial radio-frequency interference. Other means of sophisticated local communication, such as high-frequency ultrasound or modulated light signals, may potentially be used, but in this paper, we assume that individual identification of the location of each passenger is not available.

The ship that we are simulating will have an ICT infrastructure that includes a **high-speed local area network (LAN)** equipped with switches and routers that conveys packet-based data communications between all the sensors and actuators together with WiFi hubs as needed. The LAN is connected to a **Data Center (DC)**, that is used to compute the emergency instructions for the evacuees, as well as for storing and processing other information related to the passenger ship. The LAN topology, as well as the DC itself, will be designed in advance for appropriate redundancy and reliability to adequately face emergency situations.

Infrared sensors connected to the ICT infrastructure may be placed throughout the vessel (in cabins, corridors, etc.) to detect human presence without identifying the individual. Of course, such sensors can also detect hazards such as high temperatures caused by fire, and electrical short circuits. There will also be a variety of temperature and smoke sensors. Passage locations and common areas (e.g., restaurants, decks, bars, and lounges) are typically equipped with video cameras to estimate the number of people present, and also for the purpose of security.

In addition, throughout the ship and connected to the ICT infrastructure via the LAN, there will be various **Emergency Direction Providers (EDPs)**. These will activate in an emergency and will have red/white signs throughout the locations of the ship, which flash and provide directions to the passengers, with instructions such as "Exit Here", "Turn Right", "Turn Left", "Go Straight", "Wait Here", etc., to provide directions to help evacuate the passengers. These instructions will be computed by the DC and sent over the LAN to the EDPs.

In case of an emergency, the DC runs the ANS evacuation algorithm to determine for the passengers, the **Evacuation Movement Recommendations (EMRs)**. Thus, the simulations in the present paper evaluate the effectiveness of the EMRs in the presence of the following:

- Delays in the reception of the EMRs at the locations of the EDPs throughout the vessel. These delays can be caused by LAN delays and congestion, and DC delay and congestion during an emergency.
- Errors made by evacuees in following instructions from the EDPs during an emergency evacuation due to confusion and panic.

2.2. System Parameters for the Simulation

The indoor environment we simulate is the second, third, and fourth floors of the Yangtze Gold 7 Cruise Ship, as shown in Figures 1 and 2, with 346 nodes from which evacuees originate or pass through, including connection points between corridors or rooms through which evacuees may pass, and a single exit node for the evacuation. There are also 600 passageway segments and 5 staircase segments at the edges of the graph that connect these nodes.

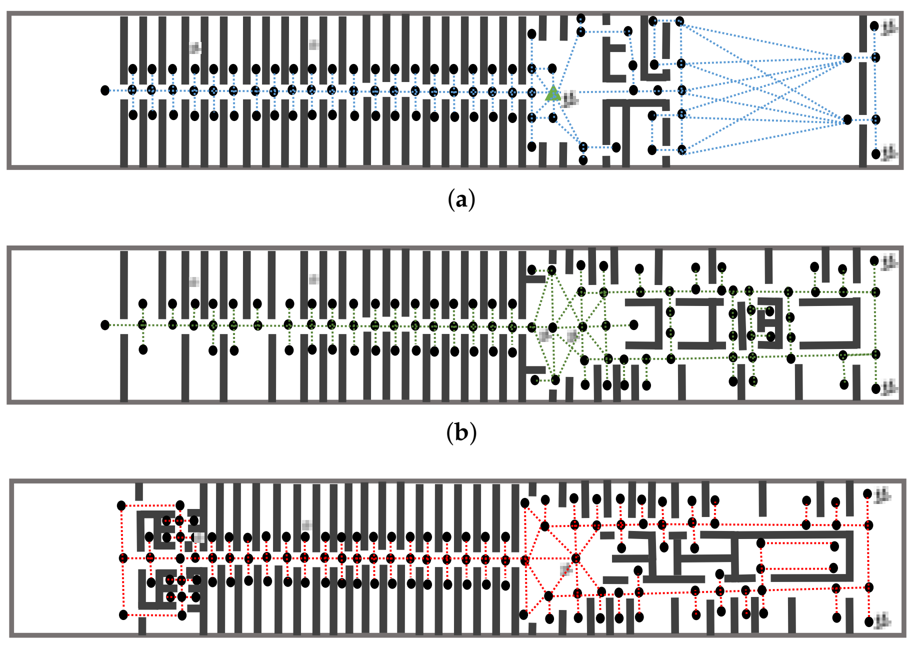

(**a**)

(**b**)

(**c**)

Figure 1. Schematic description of the layout for the Yangtze Gold 7 Cruise ship over three passenger floors (second, third, and fourth). This layout is used for simulating all the effects studied in this paper, including the delays in communicating the guidance information to the evacuees, and the possible uncertainty in the behavior of the evacuees. Here, (**a**–**c**) show the layout of the physical space of the second, third, and fourth floors.

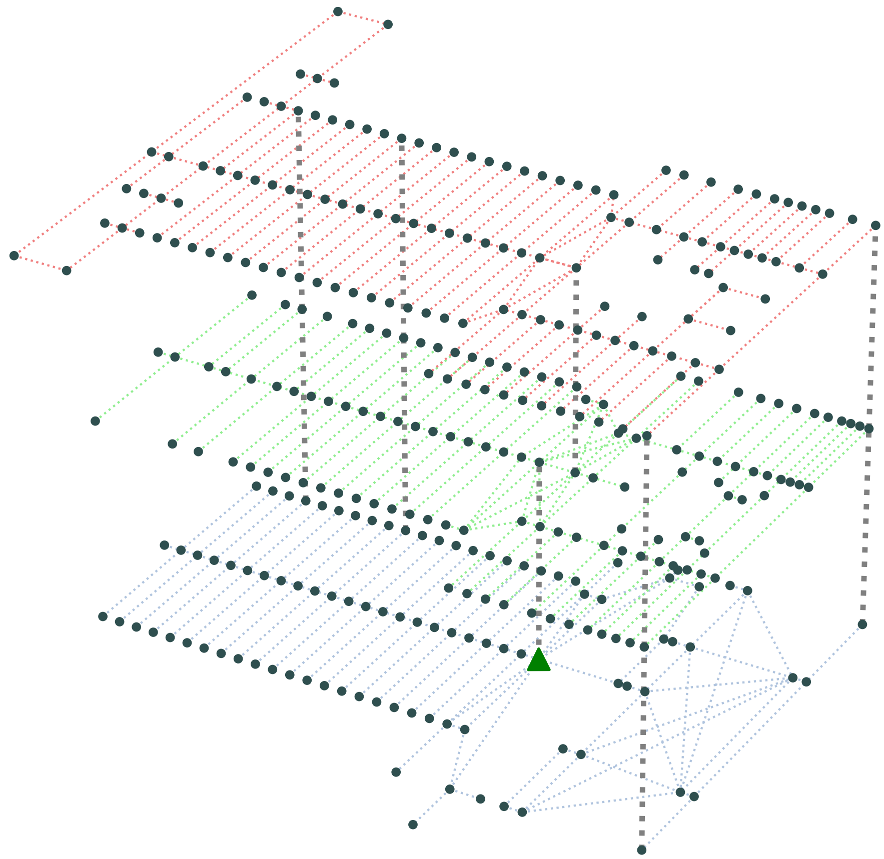

Figure 2. The evacuation graph representation of the physical space, showing the nodes where routing decisions are communicated to the evacuees via the EMRs.

The simulation uses the worst-case evacuee movement speed to estimate the time required for evacuees to cross each segment, which is 0.067 m/s. The average traversal time for each segment is estimated from the passengers' average speed of movement calculated based on the average speed at which an evacuee walks when the ship is horizontal is taken to be 0.67 m/s. In addition, the total time available to a passenger to evacuate the ship when they receive the "evacuate" message can be estimated as follows:

$$T_D = T_S - T_A - T_{EL}, \quad (1)$$

where T_S is the ship's survival duration (e.g., until it capsizes), T_A is the delay between the start of the emergency until the "evacuate" message is received by the evacuees, and T_{EL} is the time needed to embark on a lifeboat and for the lifeboat. The MSC (Maritime Safety Committee) [20] has estimated that T_S = 60 min, T_A = 5 min, T_{EL} = 25 min; thus, T_D = 30 min.

2.3. Layout of the Simulation Framework

The simulation layout for the Yangtze Gold 7 cruise ship's three passenger floors in Figure 2, shows the "dots" (i.e., nodes) which are locations where passengers may be staying or meeting (e.g., cabins, lobby, and restaurant), while the edges show the passageways, stairs, or corridors. The simulation also allows the inclusion of the effect of the inclination angle when the ship is damaged, which can change at regular intervals. This can affect the average traversal time encountered across each individual corridor or staircase which changes (shorter or longer time) with the inclination.

Each simulation is initialized by locating the evacuees (passengers) at random over the nodes, and each simulation is repeated over 100 rounds where the initial locations each time are randomized in the same way.

3. Impact of Delays in Computing and Communications on Passenger Evacuation

The ANS provides each evacuee, at each of the nodes of all the evacuation paths in the ship, an estimate of the next-step hazard-free node that the evacuee should enter to head toward the exit, based on the estimated total minimum delay to the exit from its current location. Since conditions may rapidly change with time during an evacuation, the computer and communication system that computes these directions and forwards the decisions to the nodes on each path may be congested during an evacuation. Thus, the resulting messages to evacuees may be delayed or lost.

Therefore, in this section, we analyze the impact of these possible delays, which are caused by performance imperfections and congestion of the underlying Information Technology System (ITS). To this effect, we **define the "information lag" (*IL*)** which refers to any generic node in the ship evacuation topology. $IL = 0$ means that each node in the evacuation topology of nodes and paths has received, from the ITS system, the exact direction recommendation which is based on the current true location of the evacuees at each node.

On the other hand, $IL = 1$ means that each node provides information to the evacuees regarding the next move they should make based on the location of the evacuees just prior to the current arrival of evacuees to their current node. Thus, $IL = 1$ means that the computation and transmission of the information are delayed by one step.

We also define the **"probability of delay" (*PoD*)**, which indicates whether the information lag is $IL = 1$ with probability PoD or $IL = 1$ with probability $1 - PoD$. PoD is a value that is probabilistically attributed to each node, since the delay may differ from node to node due to the communication system delays.

In the rest of this section, we evaluate the effect of PoD on the evacuation system's performance. All simulation results that are shown are obtained by drawing the probability PoD separately for each of the nodes and for 100 independent simulations under the same initial conditions. The figures that are shown for each simulation also show the 95% confidence intervals.

Evaluation of the Average Evacuation Time

The first evaluation is conducted to determine the **average evacuation time in seconds, from all of the 346 nodes**, relative to the ideal case with $IL = 0$.

Figure 3a plots the average evacuation time from all 346 starting nodes until the exit as a function of PoD. Figure 3b shows the performance ratio of average evacuation time for different values of PoD to the average for the ideal case of $PoD = 0$. Averages are taken over all nodes and based on 100 distinct independent simulations. We also show the standard deviation (black bars) for the evacuation time from all 346 nodes. These curves show clearly that as PoD increases to 0.5, the increase in average evacuation delay is quasi-linear, but for higher values, the increase continues but more slowly. When $PoD = 1$ for all nodes, the average evacuation time over all nodes is 50% higher than $PoD = 0$ (where the ITS provides up-to-date information to all nodes).

In addition, we also implement a group of simulations to evaluate the **average evacuation time, in seconds, for passengers located in cabins**. Figure 4a shows the effect of the probabilities PoD on the evacuation time of passengers that start from cabins. The performance ratio of the average evacuation time from cabins relative to the case $PoD = 0$ is given in Figure 4b, showing that it increases with PoD.

We also evaluate the **average evacuation time for passengers that are initially located in the restaurant**. Figure 5a presents the results for passengers who started the evacuation from the restaurant. It appears that the information processing delay has a smaller influence in this case, as compared to the evacuation time of passengers from the cabins when the delay probability PoD is low, such as $PoD = 0.1$ and $PoD = 0.2$.

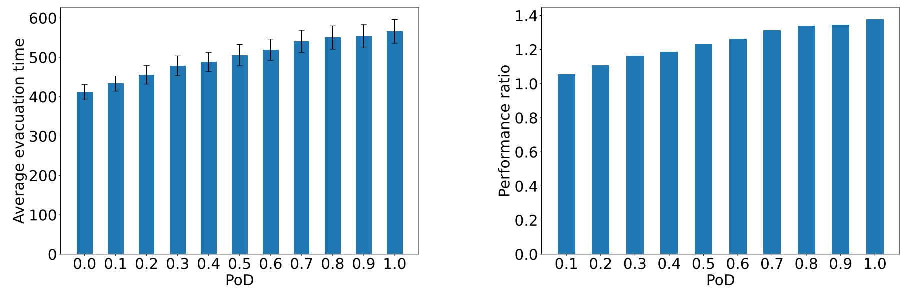

(**a**) (**b**)

Figure 3. The average evacuation time in seconds from all 346 nodes to the exit (**a**) as a function of PoD (x-axis), and (**b**) the performance ratio of the average evacuation times as compared to the ideal case of $PoD = 0$. Averages are over all nodes for 100 distinct independent simulations, with the standard deviation (the black bars) for the evacuation time.

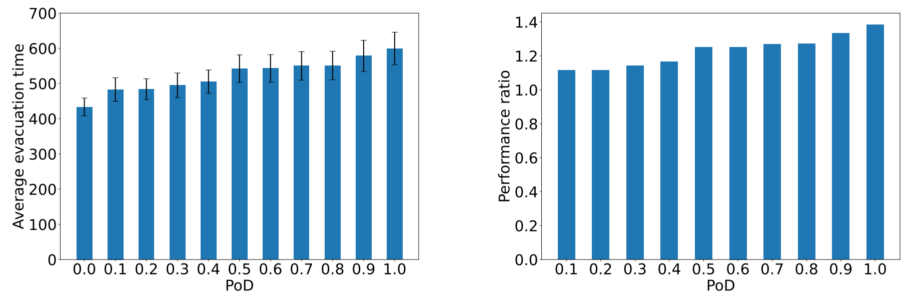

(**a**) (**b**)

Figure 4. The average evacuation time from the cabins to the exit given in seconds (**a**) as a function of PoD (x-axis), and (**b**) the performance ratio of the average evacuation time as compared to the ideal case of $PoD = 0$. Averages are taken over all passengers starting from cabins for 100 distinct independent simulations. The standard deviation (the black bars) of the evacuation time is also shown.

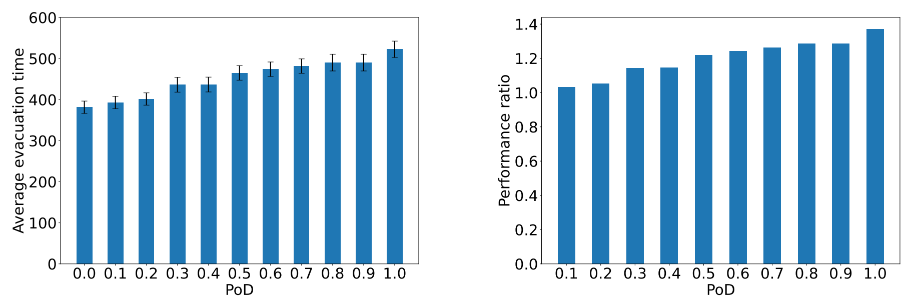

(**a**) (**b**)

Figure 5. The average evacuation time in seconds for passengers that are initially located in the restaurant (**a**) as a function of PoD (x-axis), and (**b**) the resulting performance ratio as compared to the ideal case of $PoD = 0$. Averages are taken over all passengers who were initially in the restaurant for 100 distinct independent simulations. The standard deviation of their evacuation time is shown with the black bars.

Finally, we perform a group of simulations in which half of the passengers are initially placed at random in cabins while the other half start from the restaurant, and we vary the total number of passengers. Note we assume that there are at most two passengers per cabin.

As shown in Figure 6a, the evacuation time grows with the number of passengers. This is mainly attributed to the increased waiting time resulting from the more serious congestion due to a large scale of passengers being evacuated. The evacuation time also increases with PoD, regardless of the number of passengers.

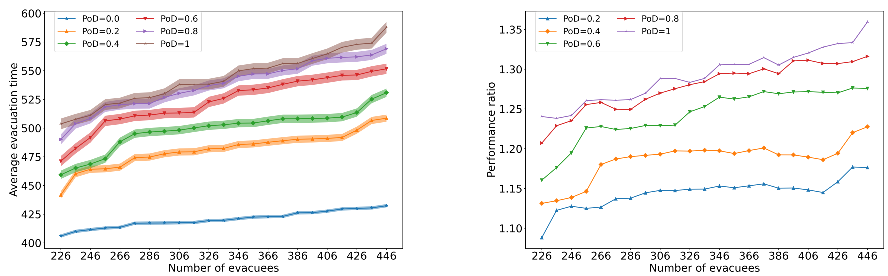

(**a**) (**b**)

Figure 6. The average evacuation time in seconds, with a 95% confidence interval, taken by different numbers of passengers where half of them originate in the cabins while the other half start from the restaurant (**a**), and (**b**) the performance ratio of the average evacuation time as compared to the ideal case with $PoD = 0$.

Figure 6b shows the change in the ratio of average evacuation time as a function of the number of passengers and of PoD. The performance ratio is always larger than 1, which indicates that as PoD grows, then the evacuation also duration grows, and the growth rate is higher for larger PoD.

4. The Effect of Uncertain Passenger Behaviour

During emergencies, the evacuees may panic or find it hard to read or hear instructions for evacuation. We model this by the choice of evacuees to miss the correct direction and take another one at random.

Therefore, in this section, we investigate the impact of the non-compliance with the evacuation suggestion. To this effect, we define the **"probability of error"** denoted as PoE, which indicates whether a passenger does not obey the provided evacuation direction with probability PoE or moves along the provided direction with probability $1 - PoE$. PoE is a value that is a probability that is chosen itself at random and attributed to each passenger, since the behavior may differ from passenger to passenger.

The Average Evacuation Time

First, we conduct simulations to measure the evacuation time, from all of the 346 nodes to the exit under various values of PoE. Figure 7 presents the ratio of average evacuation times relative to the case $PoE = 0$, where passengers fully comply with the ITS recommendation. Clearly, all the values of the performance ratio exceed 1, which shows that the behavior uncertainty of passengers prolongs the average evacuation time in seconds. We can observe that with the increase in the probability with which passengers ignore the evacuation guidance, the performance ratio in average evacuation time in seconds also increases. However, compared to PoD, the uncertain behavior of passengers has a less pronounced effect on the average evacuation time in seconds.

We also carry out a set of simulations to evaluate the impact of behavior uncertainty on the evacuation time of passengers who are initially located at random at nodes representing passenger cabins. Figure 8 plots the average evacuation time and the performance ratio compared to the case $PoE = 0$. The standard deviation is also shown. It can be observed that the average evacuation time increases with the probability of behavior uncertainty. When $PoE = 0.5$, the average evacuation time increases by almost 40% relative to $PoE = 0$.

Furthermore, it is worth noticing that the passengers in cabins are more significantly affected by their uncertain behavior compared to the results in Figure 7.

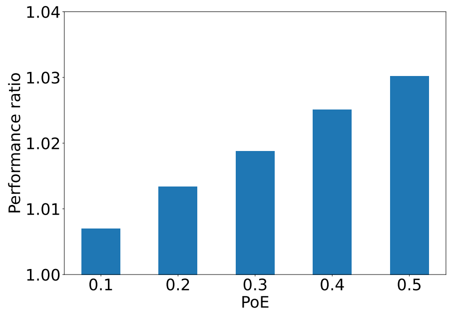

Figure 7. The performance ratio in average evacuation time in seconds from the 346 nodes to the exit compared to the ideal case $PoE = 0$.

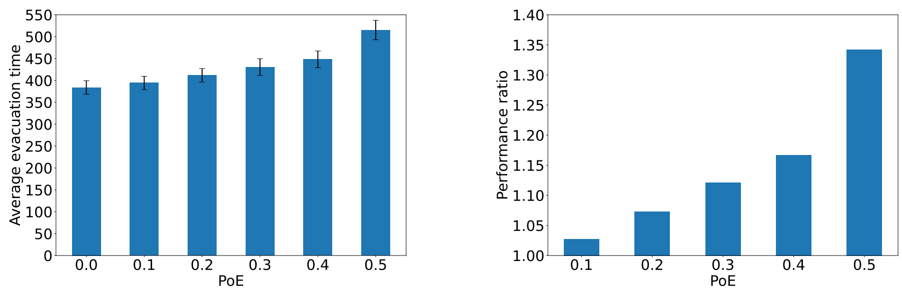

(**a**) Growth of the average evacuation time in seconds for passengers leaving from the cabins, as a function of PoE.

(**b**) Performance ratio of the average evacuation time as compared to the ideal case $PoE = 0$, shown as a function of PoE.

Figure 8. The average evacuation time in seconds taken by passengers in cabins and the performance ratio of the average evacuation time compared to the ideal case $PoE = 0$.

The average evacuation time in seconds for passengers in the restaurant is also measured as shown in Figure 9. We can see that failing to exit according to the instructions impairs the evacuation scheme and lengthens the evacuation of passengers from the restaurant. Again, it appears that this uncertain behavior has a milder effect on the average evacuation time for passengers in the restaurant compared to passengers leaving from the cabins.

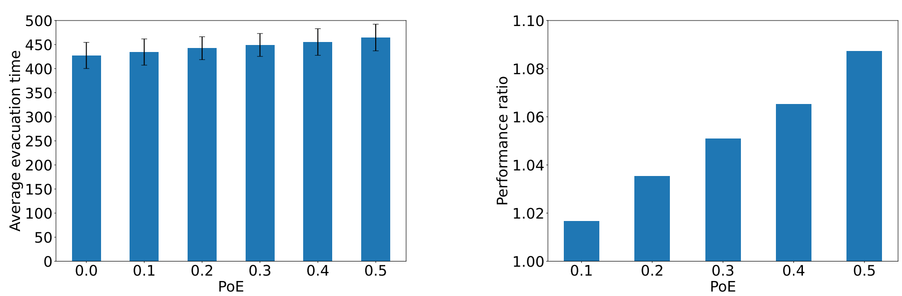

(**a**) The average evacuation time in seconds for passengers in the restaurant as a function of PoE.

(**b**) The ratio of the average evacuation time for increasing values of PoE, compared to the ideal case $PoE = 0$ for passengers exiting from the restaurant.

Figure 9. The average evacuation time in seconds for passengers in the restaurant and the performance ratio in average evacuation time compared to the ideal case $PoE = 0$.

We also measure the average evacuation time for different numbers of passengers with different probabilities of not following the evacuation directions. Here, half of the passengers start from the restaurant while the other half start from their cabins. Figure 10 plots the average evacuation time with the 95% confidence interval for different numbers of passengers with different probabilities of uncertain behavior. We can see that the average evacuation time increases with the probability of uncertain behavior. Nevertheless, we observe that behavior uncertainty has a much smaller effect on the average evacuation time, particularly if the passenger does not exceed 300. Again, behavior uncertainty has a much lower impact than PoD, showing that the ANS method is more resilient to uncertainties in evacuee behavior than to delays in the information technology system used for directing evacuees.

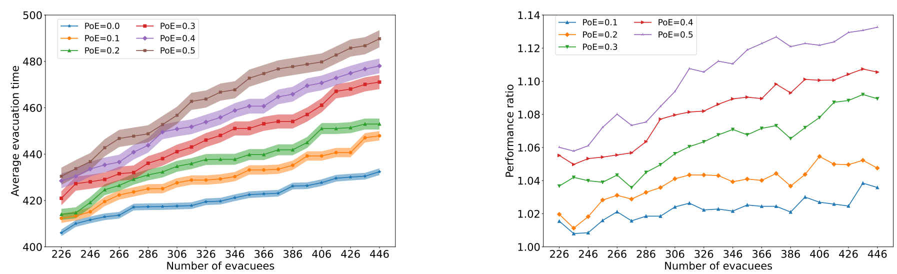

(**a**) We evaluate the effect of the evacuees' errors or panic, represented by the probability PoE of not following an evacuation instruction, and observe the increase in the average evacuation time in seconds, with a 95% confidence interval, as a function of the total number of passengers, assuming that half of the passengers originate in the cabins, while the other half start from the restaurant, for different values of PoE.

(**b**) We observe the relative increase of the evacuation time with respect to the case ideal case where $PoE = 0$, as a function of the total number of evacuees, due the evacuees' errors or panic, for different values of PoE of not following an evacuation instruction. Here, half of the passengers originate in the cabins, while the other half start from the restaurant.

Figure 10. This figure evaluates the impact of the effect of errors or panic by the evacuees, as represented by the probability PoE. On the left, we show the increase in the average evacuation time in seconds, with a 95% confidence interval, as a function of the total number of passengers, assuming that half of the passengers originate in the cabins, while the other half start from the restaurant, for different values of PoE. Under the same conditions on the number of passengers starting from the cabins and the restaurant, the right-hand side figure shows the increase in the relative performance ratio in average evacuation time as compared to the ideal case with $PoE = 0$ for different values of PoE and as a function of the total number of evacuees (passengers).

5. Conclusions and Future Work

Large transportation systems such as trains, passenger ships and aircraft require reliable and effective emergency evacuation to ensure the safety and passengers. Thus, much research has addressed the design of technology-assisted means to direct passengers effectively during emergencies, with algorithms and methods that maximize fast and optimized means for evacuation [39]. Thus, the present work addresses some of the key side effects of technology-assisted emergency evacuation that includes extensive simulations of a realistic and existing ship scenario.

Assuming that ongoing situational information is gathered by sensor networks [40–42] and then processed to provide optimum decisions and communicated to the evacuees as they progress towards the designated exits, our work has included the effects of imperfections in the technology support such as communication and processing delays for instructions to arrive at the evacuees, as well as the effects of mistakes that evacuees themselves may make during an evacuation.

We see that delayed decisions which are forwarded to all end evacuees as they pass through pre-determined "nodes" that guide them towards safety will create substantial evacuation delays for the evacuees. Similarly, we have observed that mistakes that are made by passengers due to panic or misunderstanding of the instructions also will increase the evacuation delays, but to a lesser extent as compared to delays due to the technology.

Thus, further research is needed to support evacuee safety in such complex and dynamic environments with many rapidly changing effects that may overwhelm both the ICT-based emergency management system [38] and the ability of evacuees to follow instructions. We suggest that future research could include these delaying factors in advance and design novel decentralized emergency navigation systems that pre-locate advisory data and related computational means in key system intermediate locations, combining centralized decisions with local decision making individual evacuee decision aids and hand-held mobile devices [35].

Author Contributions: Conceptualization, E.G.; relevant literature, E.G.; problem definition, E.G.; methodology, Y.M.; software, Y.M.; validation, Y.M.; formal analysis, Y.M.; identifying technical errors, E.G.; investigation, K.L.; resources, K.L.; data curation, Y.M.; writing—first draft preparation, Y.M.; writing—rewriting and editing, E.G.; visualization, Y.M.; supervision, E.G.; funding acquisition, E.G.; funding acquisition, K.L. All authors have read and agreed to the published version of the manuscript.

Funding: This research was funded by the Institute of Theoretical & Applied Informatics (IITIS-PAN), Polish Academy of Sciences, via a Research Assistantship for Yuting Ma, the European Union's Horizon Europe research and innovation programme, DOSS Project, under grant agreement No 101120270 for Erol Gelenbe, and the National Natural Science Foundation of China (NSFC) OF FUNDER Grant no. 51979216.

Institutional Review Board Statement: Not applicable.

Informed Consent Statement: Not applicable.

Data Availability Statement: The data presented in this study are available on request from the first author.

Acknowledgments: The authors would like to thank the editors and anonymous reviewers for their valuable comments and suggestions on earlier drafts of the article.

Conflicts of Interest: The authors declare no conflicts of interest.

References

1. Chu, H.; Yu, J.; Wen, J.; Yi, M.; Chen, Y. Emergency evacuation simulation and management optimization in urban residential communities. *Sustainability* **2019**, *11*, 795. [CrossRef]
2. Luo, L.; Zhang, B.; Guo, B.; Zhong, J.; Cai, W. Why they escape: Mining prioritized fuzzy decision rule in crowd evacuation. *IEEE Trans. Intell. Transp. Syst.* **2022**, *23*, 19456–19470. [CrossRef]
3. Birajdar, G.S.; Singh, R.; Gehlot, A.; Thakur, A.K. Development in building fire detection and evacuation system—A comprehensive review. *Int. J. Electr. Comput. Eng. (IJECE)* **2020**, *10*, 6644–6654. [CrossRef]
4. Singh, U.; Determe, J.F.; Horlin, F.; De Doncker, P. Crowd monitoring: State-of-the-art and future directions. *IETE Tech. Rev.* **2021**, *38*, 578–594. [CrossRef]
5. Choi, M.; Chi, S. Optimal route selection model for fire evacuations based on hazard prediction data. *Simul. Model. Pract. Theory* **2019**, *94*, 321–333. [CrossRef]
6. Ibrahim, A.M.; Venkat, I.; Subramanian, K.; Khader, A.T.; Wilde, P.D. Intelligent evacuation management systems: A review. *ACM Trans. Intell. Syst. Technol. (TIST)* **2016**, *7*, 1–27. [CrossRef]
7. Gelenbe, E.; Bi, H. Emergency Navigation without an Infrastructure. *Sensors* **2014**, *14*, 15142–15162. [CrossRef] [PubMed]
8. Meschini, S.; Accardo, D.; Locatelli, M.; Pellegrini, L.; Tagliabue, L.C.; Di Giuda, G.M. BIM-GIS integration and crowd simulation for fire emergency management in a large diffused university. In Proceedings of the 40th International Symposium on Automation and Robotics in Construction, Chennai, India, 4–7 July 2023; pp. 357–364.
9. Chu, H.; Yu, J.; Wen, J.; Huang, Y. Evacuation simulation and emergency management optimization in urban residential communities. In *IOP Conference Series: Earth and Environmental Science*; IOP Publishing: Bristol, UK, 2019; Volume 234, p. 012040.
10. Fang, S.; Liu, Z.; Zhang, S.; Wang, X.; Wang, Y.; Ni, S. Evacuation simulation of an Ro-Ro passenger ship considering the effects of inclination and crew's guidance. *Proc. Inst. Mech. Eng. Part M J. Eng. Marit. Environ.* **2023**, *237*, 192–205. [CrossRef]
11. Liu, K.; Ma, Y.; Chen, M.; Wang, K.; Zheng, K. A survey of crowd evacuation on passenger ships: Recent advances and future challenges. *Ocean. Eng.* **2022**, *263*, 112403. [CrossRef]
12. Kim, S.K. The Sewol ferry disaster in Korea and maritime safety management. In *Maritime Disputes in Northeast Asia*; Brill Nijhoff: Leiden, The Netherlands, 2017; pp. 183–199.
13. Suo, X.; Fu, G.; Wang, C.; Jia, Q. An application of 24 Model to analyse capsizing of the Eastern Star ferry. *Pol. Marit. Res.* **2017**, *24*, 116–122. [CrossRef]

14. Abdullah, A.; Mia, M.J. Inland waterway transport accident analysis of Bangladesh: Based on location, time, and regression approach. *arXiv* **2023**, arXiv:2305.10279.
15. Sarvari, P.A.; Cevikcan, E.; Ustundag, A.; Celik, M. Studies on emergency evacuation management for maritime transportation. *Marit. Policy Manag.* **2018**, *45*, 622–648. [CrossRef]
16. Li, H.; Ren, X.; Yang, Z. Data-driven Bayesian network for risk analysis of global maritime accidents. *Reliab. Eng. Syst. Saf.* **2023**, *230*, 108938. [CrossRef]
17. Nasso, C.; Bertagna, S.; Mauro, F.; Marinò, A.; Bucci, V. Simplified and advanced approaches for evacuation analysis of passenger ships in the early stage of design. *Brodogr. Teor. Praksa Brodogr. Pomor. Teh.* **2019**, *70*, 43–59. [CrossRef]
18. Wang, X.; Liu, Z.; Loughney, S.; Yang, Z.; Wang, Y.; Wang, J. Numerical analysis and staircase layout optimisation for a Ro-Ro passenger ship during emergency evacuation. *Reliab. Eng. Syst. Saf.* **2022**, *217*, 108056. [CrossRef]
19. Arshad, H.; Emblemsvåg, J.; Li, G.; Ostnes, R. Determinants, methods, and solutions of evacuation models for passenger ships: A systematic literature review. *Ocean. Eng.* **2022**, *263*, 112371. [CrossRef]
20. International Maritime Organization. Revised Guidelines for Evacuation Analysis for New and Existing Passenger Ships; MSC. 1/Circ. 1533. 2016. Available online: https://www.imorules.com/MSCCIRC_1533.html (accessed on 6 June 2016).
21. Fang, S.; Liu, Z.; Wang, X.; Wang, J.; Yang, Z. Simulation of evacuation in an inclined passenger vessel based on an improved social force model. *Saf. Sci.* **2022**, *148*, 105675. [CrossRef]
22. Wang, X.; Xia, G.; Zhao, J.; Wang, J.; Yang, Z.; Loughney, S.; Fang, S.; Zhang, S.; Xing, Y.; Liu, Z. A novel method for the risk assessment of human evacuation from cruise ships in maritime transportation. *Reliab. Eng. Syst. Saf.* **2023**, *230*, 108887. [CrossRef]
23. Niu, C.; Wang, W.; Guo, H.; Li, K. Emergency Evacuation Simulation Study Based on Improved YOLOv5s and Anylogic. *Appl. Sci.* **2023**, *13*, 5812. [CrossRef]
24. Xie, Q.; Guo, S.; Zhang, Y.; Wang, C.; Ma, C.; Li, Q. An integrated method for assessing passenger evacuation performance in ship fires. *Ocean. Eng.* **2022**, *262*, 112256. [CrossRef]
25. Ray, P.P.; Mukherjee, M.; Shu, L. Internet of things for disaster management: State-of-the-art and prospects. *IEEE Access* **2017**, *5*, 18818–18835. [CrossRef]
26. Alawad, W.; Halima, N.B.; Aziz, L. An Unmanned Aerial Vehicle (UAV) System for Disaster and Crisis Management in Smart Cities. *Electronics* **2023**, *12*, 1051. [CrossRef]
27. Ghorpade, S.N.; Zennaro, M.; Chaudhari, B.S. IoT-based hybrid optimized fuzzy threshold ELM model for localization of elderly persons. *Expert Syst. Appl.* **2021**, *184*, 115500. [CrossRef]
28. Bi, H.; Gelenbe, E. A Survey of Algorithms and Systems for Evacuating People in Confined Spaces. *Electronics* **2019**, *8*, 711. [CrossRef]
29. Desmet, A. A Modelling Approach to Human Navigation in Constrained Spaces. Ph.D. Thesis, Department of Electrical & Electronic Engineering, Imperial College London, London, UK, 2014.
30. Wiandt, B.; Kokuti, A.; Simon, V. Application of Collective Movement in Real Life Scenarios: Overview of Current Flocking Solutions. *Scalable Comput. Pract. Exp.* **2015**, *16*, 233–248. [CrossRef]
31. Wang, L.; He, Y.; Liu, W.; Jing, N.; Wang, J.; Liu, Y. On oscillation-free emergency navigation via wireless sensor networks. *IEEE Trans. Mob. Comput.* **2014**, *14*, 2086–2100. [CrossRef]
32. Filippoupolitis, A.; Hey, L.; Loukas, G.; Gelenbe, E.; Timotheou, S. Emergency response simulation using wireless sensor networks. In Proceedings of the Ambi-Sys '08: 1st International Conference on Ambient Media and Systems, Brussels, Belgium, 11–14 February 2008; Ambi-Sys '08; pp. 1–7.
33. Reif, J.; Wang, H.; Fields, S.P. *A Distributed Behavior Control for Autonomous Robots*; Duke University: Durham, NC, USA, 1995.
34. Tseng, Y.C.; Pan, M.S.; Tsai, Y.Y. Wireless sensor networks for emergency navigation. *Computer* **2006**, *39*, 55–62. [CrossRef]
35. Kokuti, A.; Gelenbe, E. Directional Navigation Improves Opportunistic Communication for Emergencies. *Sensors* **2014**, *14*, 15387–15399. [CrossRef]
36. Baruah, S. Rapid routing with guaranteed delay bounds. In Proceedings of the 2018 IEEE Real-Time Systems Symposium (RTSS), Nashville, TN, USA, 11–14 December 2018; IEEE: Piscataway, NJ, USA, 2018; pp. 13–22.
37. Ma, Y.; Liu, K.; Chen, M.; Ma, J.; Zeng, X.; Wang, K.; Liu, C. ANT: Deadline-aware adaptive emergency navigation strategy for dynamic hazardous ship evacuation with wireless sensor networks. *IEEE Access* **2020**, *8*, 135758–135769. [CrossRef]
38. Filippoupolitis, A. An adaptive system for movement decision support in building evacuation. In *Computer and Information Sciences, Proceedings of the 25th International Symposium on Computer and Information Sciences, London, UK, 22–24 September 2010*; Springer: Berlin/Heidelberg, Germany, 2010; pp. 389–392.
39. Akinwande, O.J.; Bi, H.; Gelenbe, E. Managing crowds in hazards with dynamic grouping. *IEEE Access* **2015**, *3*, 1060–1070. [CrossRef]
40. Li, S.; Zhan, A.; Wu, X.; Chen, G. ERN: Emergence rescue navigation with wireless sensor networks. In Proceedings of the 2009 15th International Conference on Parallel and Distributed Systems, Shenzhen, China, 8–11 December 2009; IEEE: Piscataway Township, NJ, USA, 2009; pp. 361–368.
41. Pan, M.S.; Tsai, C.H.; Tseng, Y.C. Emergency guiding and monitoring applications in indoor 3D environments by wireless sensor networks. *Int. J. Sens. Netw.* **2006**, *1*, 2–10. [CrossRef]
42. Wang, C.; Lin, H.; Zhang, R.; Jiang, H. SEND: A situation-aware emergency navigation algorithm with sensor networks. *IEEE Trans. Mob. Comput.* **2016**, *16*, 1149–1162. [CrossRef]

43. Shi, E.; Zhang, J.; Chen, S.; Zheng, J.; Zhang, Y.; Ng, D.W.K.; Ai, B. Wireless energy transfer in RIS-aided cell-free massive MIMO systems: Opportunities and challenges. *IEEE Commun. Mag.* **2022**, *60*, 26–32. [CrossRef]
44. Dong, J.; Zhang, J.; Shi, Y.; Wang, J.H. Faster activity and data detection in massive random access: A multiarmed bandit approach. *IEEE Internet Things J.* **2022**, *9*, 13664–13678. [CrossRef]

Appendix G: Paper VII

IoT Performance for Maritime Passenger Evacuation

Yuting Ma
IITiS-PAN, Gliwice, PL,
Wuhan University of Technology, China
yma@iitis.pl

Erol Gelenbe
IITiS-PAN, Gliwice, PL,
Université Côte d'Azur, Nice, FR,
King's College London, UK
seg@iitis.pl

Kezhong Liu
Wuhan University of Technology
Wuhan, China
kzliu@whut.edu.cn

***Abstract*—The safe and swift evacuation of passengers from Maritime Vessels, requires an effective Internet of Things (IoT) as well as an information and communication technology (ICT) infrastructure. However, during emergencies, delays in IoT and ICT systems that guide evacuees, can impair the evacuation process. This paper presents explores the impact of the key IoT and ICT elements. The methodology builds upon the deadline-aware adaptive navigation strategy (ANT), which offers the path segment that minimizes the evacuation time for each evacuee at each decision instant. The simulations on a real cruise ship configuration, show that delays in the delivery of correct instructions to evacuees can significantly hinder the effectiveness of the evacuation. Our findings stress the need to design robust and computationally fast IoT and ICT systems to support the evacuation of passengers in ships, and underscores the key role played by the IoT in the success of passenger evacuation and safety.**

***Index Terms*—ship evacuation, IoT, emergencies, passenger safety, IoT and ICT performance**

I. Introduction

During emergencies, the effectiveness of evacuation methods is crucial for ensuring the safety of people and vehicles [1], [2]. Such methods rely on technologies encompassing sensing, communication, and signaling, and play pivotal roles in (a) locating individuals and vehicles, (b) communicating with them to relay information about ongoing conditions, and (c) guiding them to safety along efficient pathways, as detailed in an extended version of this paper [3]. Research in this field uses sensing and communication technologies [4], crowd monitoring [5], hazard modeling and prediction [6], evacuation simulation [7], and evacuation path planning [8], [9]. Offline simulation of evacuation strategies facilitates the design and comparison of sensing and communication technologies, and of algorithms [10] that enhance or optimize the performance and robustness of evacuation strategies.

This research was supported by the Institute of Theoretical and Applied Informatics, Polish Academy of Sciences (IITIS-PAN) and the European Union's Horizon Europe research and innovation programme under Grant Agreement No 101120270 – DOSS. It was partially by the National Natural Science Foundation of China (NSFC), Grant No. 51979216 and the Natural Science Foundation of Hubei Province, China, Grants No. 2021CFA001 and 20221j0059.

Emergency management simulation research addresses the movement of people in scenarios, including sports arenas, tourist sites, leisure venues [11], [12], and large ships [13], under unusual conditions or adversarial situations like facility breakdowns, fires, or panic. With the global growth of the cruise ship industry, passenger safety in maritime trANTportation has gained increased attention [14]. Despite advanced accident prevention systems, maritime accidents still occur, underscoring the importance of effective evacuation methods for passenger ships [15]. Recent research in this area has seen considerable developments [16]. Due to the difficulty of artificially creating or reproducing maritime emergencies, simulation of human evacuation on ships has become essential for designing both civilian and military naval vessels [17]–[19]. Notably, the International Maritime Organization (IMO) has issued Circulars and guidelines for evacuation simulation in passenger ships [20]. However, existing research and guidelines often overlook realisttic features impacting human behavior during emergencies [10], [21], such as variations in traversal times and the impact of technology-induced delays and message loss [22], [23]. This paper investigates the influence of these unpredictable factors on the performance of contemporary simulation methods for vessel evacuation.

The paper employs a simulation framework to assess the impact of imperfections resulting from communication technologies, such as lost or delayed messages, and from passenger misunderstandings or panic during emergency management simulations. The tool utilized for this investigation is built on the AnLogic simulator [24], as detailed in Section II. The subsequent sections are organized as follows: Section I-A reviews related work on evacuation in passenger ships and built structures, Section II provides a detailed description of the ship emergency evacuation simulation, and Section III presents simulation results regarding the impact of communication system congestion. Finally, Section IV offers conclusions and suggestions for future research.

A. Related work

Emergency management systems guide evacuees with **path-planning** algorithms, such as Dijkstra, A*, RRT, ANT Colony Optimization, Genetic algorithms, and others, to minimize evacuation delay or maximize the distance from hazard nodes to the exit node, utilizing 2D/3D maps of built environments [25], [26]. However, the resulting paths may become impractical as they include unexpected hazards such as fire, flooding, or failures in emergency management systems. Efforts have been made to address dynamIic dangers using the Expected Number of Oscillations (ENO) concept [27], quantifying emergency dynamics and exploring paths with the smallest probability of frequent changes. Global path planning methods often require complete system specifications, contradicting realistic scenarios. Subsequent studies relax this requirement, allowing for path computation without precise prior knowledge of all hazard and exit information [10], [28]. Methods such as Artificial Potential Fields and local neighborhood techniques [29], [30], possibly with partial reversal, help evacuees avoid hazardous areas. However, most studies overlook the necessity of providing directions ensuring that the ”time needed to reach the exit” for each evacuee remains under a specified upper bound (e.g., ship survival or capsizing time) in worst-case scenarios. Thus, this paper adopts the ANT (Adaptive Navigation Strategy) evacuation algorithm [31], explicitly incorporating a guaranteed exit deadline for each evacuee in each location. This deadline bound is derived from the International Maritime Organization (IMO) recommendations for ships.

II. The Simulation framework

The simulation framework we employ assesses the impact of computer and communication technology delays in providing routing instructions to evacuees within an event-driven framework that comprises two integral parts: (1) AnyLogic Simulation Software [24]: This software incorporates the layout of the physical environment where the evacuation takes place, and utilizes a ”pedestrian” software library employing a force model, akin to social potential fields for evacuee movement, and (2) Path-Planning Module in Python that computes evacuation directions based on ANT, an extension of the Rapid Routing with Guaranteed Delay Bounds algorithm [31], [32]. This module conveys computed instructions to the AnyLogic software at each simulation step when movement instructions are updated. We implement the ANT algorithm with the following features:

- ANT moves evacuees along paths with minimal delay, mitigating harmful effects from dynamic hazards. The algorithm assumes knowledge of hazard propagation (velocity and direction), as well as typical and worst-case delay across each edge of each path.
- As hazards progress, ANT calculates the direction for each evacuee to avoid hazards. In a real evacuation, this direction should be computed and communicated to evacuees via a wired or wireless network. Notably, prior work has often overlooked the possible delays in this communication.

Networks and servers used for decision-making may experience congestion, especially in emergencies when decisions and communications are frequent. This congestion can lead to delays in navigation direction updates, packet losses, and errors in decisions due to the use of delayed or obsolete data in decision algorithms [33], [34]. While previous studies often neglect these effects, this paper specifically evaluates their impact on evacuation time. Furthermore, potential delays and errors stemming from technology, including network packet losses and server failures. This simulation framework is a comprehensive tool for assessing the intricate dynamics of evacuation scenarios, including the technology-induced delays.

A. System Parameters for the Simulation

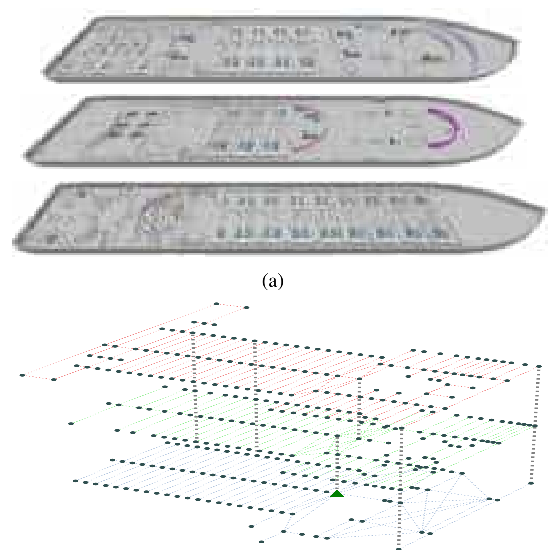

(a)

(b)

Fig. 1. Schematic description of the layout for the Yangtze Gold 7 Cruise ship over its three passenger floors (second, third, and fourth). This layout is used for simulating the effects that are studied in this paper, i.e., the delays in communicating the guidance information to the evacuees. Here (a) is the layout of the physical space of the second, third, and fourth floors, and (b) is the evacuation graph model of the physical space.

We simulate the indoor environment of the second, third, and fourth floors of the Yangtze Gold 7 Cruise Ship, illustrated in Figure 1. The simulation includes 346 nodes representing origin points, passageways, connection points between corridors or rooms, and a single exit node for evacuation. The graph also encompasses 600 passageway segments and 5 staircase segments connecting these nodes.

In our simulation setup, the worst-case traversal time across each segment is computed based on the worst-case traversal speed of evacuees, set at 0.067 meters/second.

Conversely, the typical traversal time for each segment reflects the average walking speed on a passenger ship under normal safe conditions, set at 0.67 meters/second. The total time available for evacuation, denoted as T_D, is estimated for evacuees who receive the "evacuate" message:

$$T_D = T_S - T_A - T_{EL}, \quad (1)$$

where: T_S is the ship's survival duration until capsizing (e.g., 60 minutes), T_A is the delay between the start of the emergency until the "evacuate" message is received (e.g., 5 minutes), T_{EL} is the sum of embarkation time and lifeboat launching time for evacuees reaching the exit point. Guidelines from the Maritime Safety Committee (MSC) [20] specify $T_S = 60$ minutes, $T_A = 5$ minutes, and $T_{EL} = 25$ minutes, resulting in $T_D = 30$ minutes, unless otherwise stated. This simulation framework captures essential parameters for evaluating evacuation strategies in maritime emergency scenarios.

B. The IoT and Information and Communication (IC) Environment

The IoT and ICT environment that is being considered, is composed of:

1) A centralized Data Center (DC) that stores the list of passengers and staff who are present on the passenger ship. This list is updated when the passengers or staff board the ship, as well as when anyone leaves the ship for various normal reasons, as well as when a passenger is evacuated through a designated exit.
2) The DC also computes the **Evacuation Recommendations (ERs)** and movement directions for all the passengers during an evacuation using the ANT algorithm.
3) A wired communication high-speed Local Area Network (LAN) that runs throughout the ship, with appropriate switching equipment. The LAN is connected to WiFi Hubs and sensors that are placed throughout the ship, including in the cabins, lounges, restaurants, and the passageways and corridors used for normal movement of passengers and staff, and also used for evacuation.
4) The cabins and passageways contain Infrared Sensors that can detect human presence in different locations. These infrared sensors do not detect the identity of human beings, but simply their presence. Infrared sensors can also be used to detect high temperatures caused by fire and electrical short circuits.
5) Passageways and Common Rooms (Restaurants and Lounges) can also contain Video Camera Sensors, that help to count the number of people in a given area, and also help find people who may have lost their way, and are also used for security.
6) Finally, also connected to the LAN, are *Direction Providers which turn ON during an emergency*. These may be red/white flashing signs that say "Go Straight", "Turn Right", "Turn Left", "Wait Here", etc. to provide directions to evacuees during an emergency. They are activated by the ANT algorithm's ERs that are computed by the DC described in Item 1 above.

While the individual personal identification of passengers is not considered explicitly for the IoT system in this paper, systems using wireless "RFID" (radio-frequency identity), and "wristwatches" that broadcast the identity of the wearers, can also be used. However, IoT devices with wireless communications may be less reliable inside ships, due to the high metal and steel content of the naval structures, and the resulting absorption, reflection, and refraction of high-frequency radio signals, resulting in high interference and signal attenuation, which may require sophisticated bandwidth management, radio-frequency repeaters, and signal processing.

C. Layout of the Simulation Framework

The schematic diagram of the simulation layout for the three passenger floors of the Yangtze Gold 7 Cruise ship is shown in Figure 2. On the right-hand side, the dotted diagram illustrates "dots" representing nodes, which signify locations where passengers may congregate or gather (e.g., cabins, the lobby, and the restaurant). The edges in the diagram depict passageways, stairs, or corridors. The simulation incorporates the effect of the inclination angle of the damaged ship, which can change at regular intervals. This inclination can impact the average traversal time across each corridor or staircase, varying with changes in inclination (resulting in shorter or longer traversal times). Thus the ANT provides the best advice that includes the estimate of traversal time, which may change due to the ship's inclination. Each simulation is initiated by placing evacuees (passengers) over the nodes. The simulation is then repeated for 100 rounds, and the initial locations of the evacuees are randomized in each round. This approach ensures robustness and comprehensiveness in evaluating evacuation strategies.

III. Impact of Computing and Communication Delays on Evacueees

The ANT algorithm provides evacuees a recommendation regarding the next-step hazard-free node that the evacuee should navigate towards the exit, at each node along all evacuation paths on the ship. The recommendation is not based on the evacuee's individual identity, and is generic for all evacuees, and is based on the total minimum delay estimation from the current location to the exit. However, emergency conditions are dynamic and subject to rapid changes, and the computer and communication system responsible for computing and forwarding these directions may face congestion during an evacuation. As a result, messages to evacuees may be delayed or lost.

In this section, we analyze the impact of these potential delays caused by performance imperfections and congestion in the Information Technology System (ITS). We introduce the concept of "information lag" (IL) for any generic node in the ship evacuation topology. $IL = 0$ signifies that each node has received the exact direction recommendation from the ITS system based on the current true location of evacuees. Conversely, $IL = 1$ implies that each node provides information to evacuees based on the status of all nodes, derived from the location of evacuees just before their current arrival at the node. Thus, $IL = 1$ denotes a delay of one step in the computation and transmission of information. We also define the "probability of delay" (PoD), indicating whether the information lag is $IL = 1$ with a probability of PoD, or $IL = 0$ with a probability of $1 - PoD$. PoD is a probabilistic attribute assigned to each node, considering that the delay may vary from node to node due to communication system delays.

In the following analysis, we evaluate the effect of PoD on the evacuation system's performance. Simulation results are obtained by assigning the probability PoD separately for each node in 100 independent simulations under the same initial conditions. The figures presented for each simulation also include the 95% confidence intervals.

A. Evaluation of the Evacuation Times

We first determine the average evacuation time from all 346 nodes concerning the ideal case with $IL = 0$. Figure 2 (a) illustrates the average evacuation time from all 346 starting nodes to the exit as a function of PoD. Figure 2 (b) presents the performance ratio of average evacuation time for various PoD values relative to the average for the ideal case of $PoD = 0$. The averages are taken over all nodes and based on 100 distinct independent simulations. The standard deviation is also shown as black bars for the evacuation time from all 346 nodes. These curves demonstrate a quasi-linear increase in average evacuation delay as PoD increases to 0.5, and a more gradual increase for higher values. When $PoD = 1$ for all nodes, the average evacuation time over all nodes is 50% higher than $PoD = 0$, where the ITS provides up-to-date information to all nodes.

Additionally, we perform a set of simulations to evaluate the average evacuation time for passengers located in cabins. Figure 3 (above) illustrates the average evacuation time in seconds, taken by passengers originating from cabins, affected by different probabilities PoD. The performance ratio in average evacuation time for passengers in cabins, relative to the case $PoD = 0$, is shown in Figure 3 (b). It is evident that the evacuation of passengers from cabins worsens with the increase in PoD.

Moreover, we investigate the average evacuation time for passengers located in the restaurant. Figure 4 (a) illustrates the average evacuation time of passengers within the restaurant. Notably, we observe that IL has a milder impact on the evacuation time of restaurant patrons compared to passengers in cabins, particularly when PoD is low, such as $PoD = 0.1$ and $PoD = 0.2$

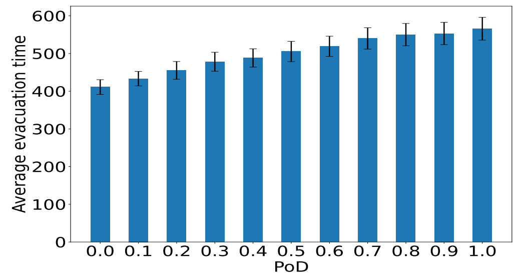

(a)

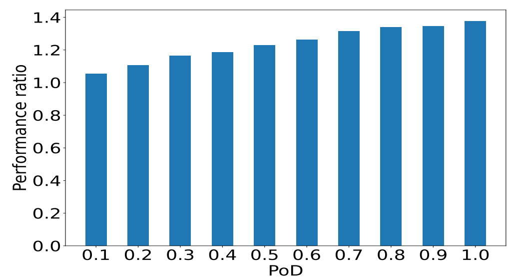

(b)

Fig. 2. The average evacuation time, in seconds, from all 346 nodes to the exit (above), as a function of PoD (x-axis), and (below) the performance ratio in average evacuation time as compared to the ideal case of $PoD = 0$. Averages are over all nodes for 100 distinct independent simulations, with the standard deviation (the black bars) for the evacuation time.

Additionally, other simulations assess the average evacuation time for varying numbers of passengers, influenced by different PoD values. In this simulation set, half of the passengers are randomly distributed in cabins, while the remaining half occupy the restaurant. Notably, the cabin capacity is limited to two passengers at most. As depicted in Figure 5 (a), the average evacuation time demonstrates an increase with a growing number of passengers. This escalation is primarily attributed to heightened waiting times resulting from more pronounced congestion caused by the evacuation of a larger number of passengers. Moreover, we observe that the average evacuation time rises with PoD, irrespective of the number of passengers. Figure 5 (b) presents the performance ratio in average evacuation time for varying passenger numbers under different probabilities of PoD. The performance ratio consistently exceeds 1, indicating that a larger PoD leads to an extended evacuation duration, with a more pronounced impact observed for higher PoD values.

IV. Conclusions and Further Research

Ensuring reliable emergency evacuation is vital, and IoT systems to support evacuation and guide evacuees have been the object of much research [35], [36]. However, challenges arise during emergencies due to congestion and damage to the IoT system supporting an evacuation, as

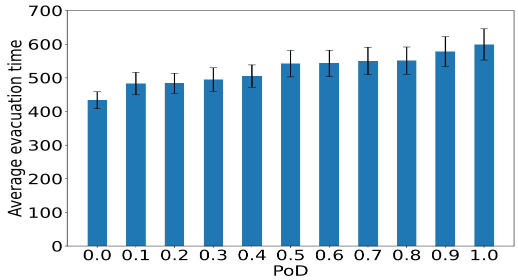

(a)

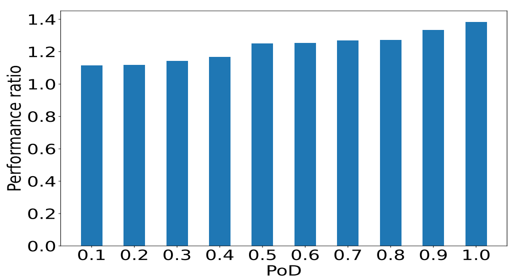

(b)

Fig. 3. The average evacuation time in seconds, taken by passengers in cabins to the exit (left), as a function of PoD (x-axis), and (right) the performance ratio in average evacuation time as compared to the ideal case of $PoD = 0$. Averages are taken over all passengers starting from cabins for 100 distinct independent simulations, with the standard deviation (the black bars) for the evacuation time.

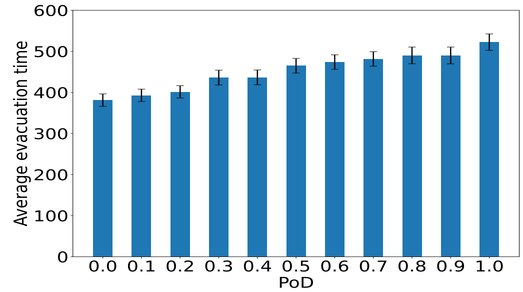

(a)

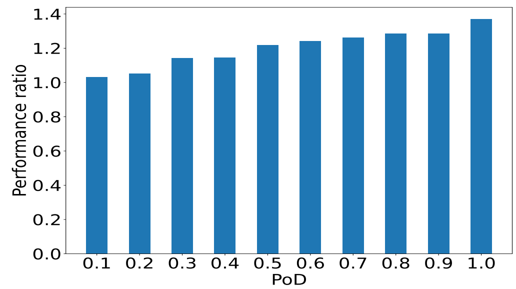

(b)

Fig. 4. The average evacuation time in seconds, taken by passengers in the restaurant to the exit (left), as a function of PoD (x-axis), and (right) the performance ratio in average evacuation time as compared to the ideal case of $PoD = 0$. Averages are taken over all passengers in the restaurant for 100 distinct independent simulations, with the standard deviation (the black bars) for the evacuation time.

well as to damages in the built environment. We have focused on the evacuation of passengers from a cruise ship during an emergency, and has considered the ICT and IoT system that is needed to enable the timely evacuation of the passengers crew and staff. In particular, the impact of the IoT through sensor networks [37], [38], and the computing and communication system, on the effectiveness of the navigation advice provided to passengers, was studied.

This study represents the first examination of the significant side effects of ICT and IoT performance influencing emergency evacuation in practical ship scenarios. With extensive simulations, the paper investigates the impact of the delay in receiving correct movement instructions by the passengers, on the evacuation performance during a ship emergency. The simulations incorporate parameters from the real passenger cruise ship "Yangtze Gold 7" and its evacuation system, and assess the repercussions of information delays that affect human evacuees. In future research, it will be useful to proactively incorporate the delaying factors, to design innovative decentralized emergency navigation systems that locally pre-compute and store in a distributed manner the needed advisory data at key system intermediate nodes, and combine centralized decisions with individual evacuee decision aids.

REFERENCES

[1] E. Gelenbe and F.-J. Wu, "Future research on cyber-physical emergency management systems," *Future Internet*, vol. 5, no. 3, pp. 336–354, 2013.

[2] L. Luo, B. Zhang, B. Guo, J. Zhong, and W. Cai, "Why they escape: Mining prioritized fuzzy decision rule in crowd evacuation," *IEEE Transactions on Intelligent Transportation Systems*, vol. 23, no. 10, pp. 19 456–19 470, 2022.

[3] Y. Ma, E. Gelenbe, and K. Liu, "Impact of iot system imperfections and passenger errors on cruise ship evacuation delay," *Sensors*, vol. 24, no. 6, 2024. [Online]. Available: https://www.mdpi.com/1424-8220/24/6/1850

[4] G. S. Birajdar, R. Singh, A. Gehlot, and A. K. Thakur, "Development in building fire detection and evacuation system-a comprehensive review," *Int. J. Electr. Comput. Eng.(IJECE)*, vol. 10, pp. 6644–6654, 2020.

[5] U. Singh, J.-F. Determe, F. Horlin, and P. De Doncker, "Crowd monitoring: State-of-the-art and future directions," *IETE Technical Review*, vol. 38, no. 6, pp. 578–594, 2021.

[6] M. Choi and S. Chi, "Optimal route selection model for fire evacuations based on hazard prediction data," *Simulation Modelling Practice and Theory*, vol. 94, pp. 321–333, 2019.

[7] H. Bi and E. Gelenbe, "A survey of algorithms and systems for evacuating people in confined spaces," *Electronics*, vol. 8, no. 6, 2019. [Online]. Available: https://www.mdpi.com/2079-9292/8/6/711

[8] A. M. Ibrahim, I. Venkat, K. Subramanian, A. T. Khader, and P. D. Wilde, "Intelligent evacuation management systems: A review," *ACM Transactions on Intelligent Systems and Technology (TIST)*, vol. 7, no. 3, pp. 1–27, 2016.

[9] J. Li, F. Zhang, M. Li, and J. Li, "An evacuation time correction method for passenger ships fire considering passenger panic."

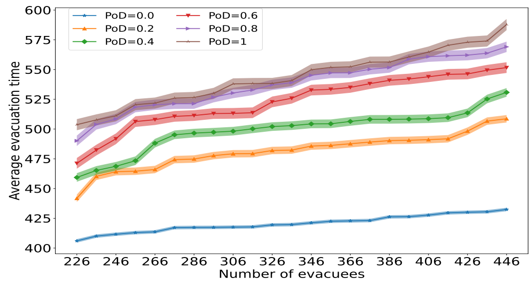

(a)

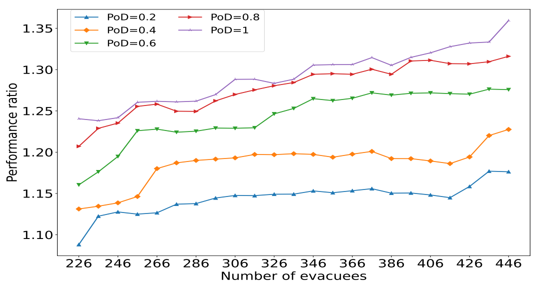

(b)

Fig. 5. The average evacuation time in seconds, with a 95% confidence interval, taken by different numbers of passengers where half of them originate in the cabins, while the other half start from the restaurant (above), and (below) the performance ratio in average evacuation time as compared to the ideal case w$PoD = 0$.

[10] E. Gelenbe and H. Bi, "Emergency navigation without an infrastructure," *Sensors*, vol. 14, no. 8, pp. 15 142–15 162, 2014. [Online]. Available: https://www.mdpi.com/1424-8220/14/8/15142

[11] S. Meschini, D. Accardo, M. Locatelli, L. Pellegrini, L. C. Tagliabue, G. M. Di Giuda *et al.*, "Bim-gis integration and crowd simulation for fire emergency management in a large diffused university," *PROCEEDINGS OF THE... ISARC*, pp. 357–364, 2023.

[12] H. Chu, J. Yu, J. Wen, and Y. Huang, "Evacuation simulation and emergency management optimization in urban residential communities," in *IOP Conference Series: Earth and Environmental Science*, vol. 234, no. 1. IOP Publishing, 2019, p. 012040.

[13] S. Fang, Z. Liu, S. Zhang, X. Wang, Y. Wang, and S. Ni, "Evacuation simulation of an ro-ro passenger ship considering the effects of inclination and crew's guidance," *Proceedings of the institution of mechanical engineers, part M: journal of engineering for the maritime environment*, vol. 237, no. 1, pp. 192–205, 2023.

[14] K. Liu, Y. Ma, M. Chen, K. Wang, and K. Zheng, "A survey of crowd evacuation on passenger ships: Recent advances and future challenges," *Ocean Engineering*, vol. 263, p. 112403, 2022.

[15] P. A. Sarvari, E. Cevikcan, A. Ustundag, and M. Celik, "Studies on emergency evacuation management for maritime transportation," *Maritime Policy & Management*, vol. 45, no. 5, pp. 622–648, 2018.

[16] H. Li, X. Ren, and Z. Yang, "Data-driven bayesian network for risk analysis of global maritime accidents," *Reliability Engineering & System Safety*, vol. 230, p. 108938, 2023.

[17] C. Nasso, S. Bertagna, F. Mauro, A. Marinò, and V. Bucci, "Simplified and advanced approaches for evacuation analysis of passenger ships in the early stage of design," *Brodogradnja: Teorija i praksa brodogradnje i pomorske tehnike*, vol. 70, no. 3, pp. 43–59, 2019.

[18] X. Wang, Z. Liu, S. Loughney, Z. Yang, Y. Wang, and J. Wang, "Numerical analysis and staircase layout optimisation for a ro-ro passenger ship during emergency evacuation," *Reliability Engineering & System Safety*, vol. 217, p. 108056, 2022.

[19] H. Arshad, J. Emblemsvåg, G. Li, and R. Ostnes, "Determinants, methods, and solutions of evacuation models for passenger ships: A systematic literature review," *Ocean Engineering*, vol. 263, p. 112371, 2022.

[20] I. M. Organization, "Guidelines for evacuation analysis for new and existing passenger ships," *MSC. 1/Circ. 1238*, 2016.

[21] Q. Xie, S. Guo, Y. Zhang, C. Wang, C. Ma, and Q. Li, "An integrated method for assessing passenger evacuation performance in ship fires," *Ocean Engineering*, vol. 262, p. 112256, 2022.

[22] S. Fang, Z. Liu, X. Wang, J. Wang, and Z. Yang, "Simulation of evacuation in an inclined passenger vessel based on an improved social force model," *Safety science*, vol. 148, p. 105675, 2022.

[23] X. Wang, G. Xia, J. Zhao, J. Wang, Z. Yang, S. Loughney, S. Fang, S. Zhang, Y. Xing, and Z. Liu, "A novel method for the risk assessment of human evacuation from cruise ships in maritime transportation," *Reliability Engineering & System Safety*, vol. 230, p. 108887, 2023.

[24] C. Niu, W. Wang, H. Guo, and K. Li, "Emergency evacuation simulation study based on improved yolov5s and anylogic," *Applied Sciences*, vol. 13, no. 9, p. 5812, 2023.

[25] A. Desmet, "A modelling approach to human navigation in constrained spaces," *PhD Dissertation, Dept. of Electrical & Electronic Engineering, Imperial College London*, 2014.

[26] B. Wiandt, A. Kokuti, and V. Simon, "Application of collective movement in real life scenarios: Overview of current flocking solutions," *Scalable Comput. Pract. Exp.*, vol. 16, no. 3, pp. 233–248, 2015.

[27] L. Wang, Y. He, W. Liu, N. Jing, J. Wang, and Y. Liu, "On oscillation-free emergency navigation via wireless sensor networks," *IEEE Transactions on Mobile Computing*, vol. 14, no. 10, pp. 2086–2100, 2014.

[28] A. Filippoupolitis et al., "Emergency response simulation using wireless sensor networks," in *Proceedings of the 1st International Conference on Ambient Media and Systems*, ser. Ambi-Sys '08. Brussels, BEL: ICST (Institute for Computer Sciences, Social-Informatics and Telecommunications Engineering), 2008.

[29] Y.-C. Tseng, M.-S. Pan, and Y.-Y. Tsai, "Wireless sensor networks for emergency navigation," *Computer*, vol. 39, no. 7, pp. 55–62, 2006.

[30] A. Kokuti and E. Gelenbe, "Directional navigation improves opportunistic communication for emergencies," *Sensors*, vol. 14, no. 8, pp. 15 387–15 399, 2014. [Online]. Available: https://www.mdpi.com/1424-8220/14/8/15387

[31] Y. Ma, K. Liu, M. Chen, J. Ma, X. Zeng, K. Wang, and C. Liu, "Ant: Deadline-aware adaptive emergency navigation strategy for dynamic hazardous ship evacuation with wireless sensor networks," *IEEE Access*, vol. 8, pp. 135 758–135 769, 2020.

[32] S. Baruah, "Rapid routing with guaranteed delay bounds," in *2018 IEEE Real-Time Systems Symposium (RTSS)*. IEEE, 2018, pp. 13–22.

[33] E. Shi, J. Zhang, S. Chen, J. Zheng, Y. Zhang, D. W. K. Ng, and B. Ai, "Wireless energy transfer in ris-aided cell-free massive mimo systems: Opportunities and challenges," *IEEE Communications Magazine*, vol. 60, no. 3, pp. 26–32, 2022.

[34] J. Dong, J. Zhang, Y. Shi, and J. H. Wang, "Faster activity and data detection in massive random access: A multiarmed bandit approach," *IEEE Internet of Things Journal*, vol. 9, no. 15, pp. 13 664–13 678, 2022.

[35] C. Wang, H. Lin, R. Zhang, and H. Jiang, "Send: A situation-aware emergency navigation algorithm with sensor networks," *IEEE Transactions on Mobile Computing*, vol. 16, no. 4, pp. 1149–1162, 2016.

[36] H. Chu, J. Yu, J. Wen, M. Yi, and Y. Chen, "Emergency evacuation simulation and management optimization in urban residential communities," *Sustainability*, vol. 11, no. 3, 2019. [Online]. Available: https://www.mdpi.com/2071-1050/11/3/795

[37] M.-S. Pan, C.-H. Tsai, and Y.-C. Tseng, "Emergency guiding and monitoring applications in indoor 3d environments by wireless sensor networks," *International Journal of Sensor Networks*, vol. 1, no. 1-2, pp. 2–10, 2006.

[38] S. Li, A. Zhan, X. Wu, and G. Chen, "Ern: Emergence rescue navigation with wireless sensor networks," in *2009 15th International Conference on Parallel and Distributed Systems*. IEEE, 2009, pp. 361–368.

Appendix H: Paper VIII

Article

IoT Driven Scheduling for Congestion Avoidance in Human Emergency Evacuation

Erol Gelenbe[1,2,3]* 0000-0001-9688-2201 and Yuting Ma[1,*]

[1] IITiS-PAN, Gliwice, Poland; seg@iitis.pl; yma@iitis.pl
[2] Université Côte d'Azur CNRS I3S, France
[3] Dept. of Engineering, King's College London
* Correspondence: seg@iitis.pl; yma@iitis.pl

Abstract: The efficient and timely management of human evacuation during emergency events is an important area of research where the Internet of Things (IoT) can be of great value. Significant areas of application for optimum evacuation strategies include buildings, sports arenas, cultural venues such as museums and concert halls, and naval vessels such as crowded cruise ships. In many cases, the evacuation process is complicated by the constraints on space and movement, such as corridors, staircases, and passageways, that can cause congestion and slowdown in evacuations. In such circumstances, the IoT can be used to sense the presence of evacuees in different locations, hazards, and also sense congestion, and decide based on sensing to guide the evacuees dynamically in the most effective direction to limit or eliminate congestion and maximize safety. This paper uses an analytical queueing network approach to analyze an emergency evacuation system and suggests the use of the IoT to direct evacuees in a manner that reduces the congestion downstream by moving them forward when other evacuees exit the system. The IoT-based approach is analyzed using a realistic representation of evacuation from an existing commercial cruise ship, with a queueing network model and several routing rules. Numerical examples are used to demonstrate the value of communications and the IoT in evacuating evacuees in a timely manner, within the constrained space of a Cruise Ship.

Keywords: Emergency Evacuation; Internet of Things; Naval Vessels; Cruise Ships; Evacuation Delay; G-Networks

1. Introduction

The management of major emergencies, to minimize loss of life and maximize human well-being, minimize loss of property and economic damage, is an active and well-established area of research. Such emergencies frequently occur in peacetime, and tragically also occur during warfare as we see today [1,2]. Commonly occurring recent examples of emergencies that require rescue and evacuation include:

- The frequent fires that occur around the Mediterranean coast, in particular during the summer period [3].
- The annual hurricane season in the southeastern United States, including Florida, that can require the evacuation of millions of people along congested roads [4].
- Seasonal floodings that occur regularly in various parts of the world, including in Europe, such as the floods in northeastern Spain in 2024 [5].
- Accidents or malevolent events that have occurred over recent years in theaters, sports arenas, large hotels, and during cultural or sports events [6,7].
- Accidents with cruise ships, as discussed in Section 1.3.
- Industrial accidents in factories, building sites, and underground or overground mines [8,9].

Though each event is distinct and different, all these events are characterized by a few common characteristics:

- Physical space is constrained, either because it is a built environment with buildings and roadways, some of which become blocked during the emergency.
- Civilians have to be evacuated rapidly, while emergency personnel such as ambulances, police, firemen, expert volunteers, have to enter the area rapidly.
- The civilian evacuees include both able-bodied people, and others who have to be helped or carried out, due to young or old age, or injuries.
- Part of the area contains health hazards, such as fires, smoke, or high levels of pollution or noxious materials or gases.

Thus, addressing these challenges has often required the use of specialized and complex cyber-physical systems [10], and substantial work has been conducted on algorithmic methods to address them [11,12]. A key issue in this area is to understand the performance of the methods that are used to address such emergencies, such as exit times for civilians, expected survival rates, speed with which emergency staff and equipment arrive at the scene, and other metrics, which can require sophisticated modelling techniques [13].

The need to address these challenges in a comprehensive modelling approach that attempts to encompass all the significant aspects of an emergency has resulted in a long line of simulation studies [14], and several special-purpose simulation tools have been developed [15]. The highly distributed structure of such events, with a large number of autonomous human and possibly robotic agents interacting with each other and affecting the outcome, has given rise to both agent-based simulators [16] and analytical modelling studies [17].

1.1. Technical Challenges

In addition to the need for realistic simulations, emergency evacuations have several common technical challenges that are worth mentioning. They all require emergency personnel to be able to search the relevant areas so as to find hazards and victims. Thus, some work has sought inspiration from the efficiency with which some animal species can search for food, for other animals of the same species, or for safe areas for their activities, and from other techniques, such as foraging and the behavior of physical systems when they identify and locate targets for physical or chemical interactions [18].

Another common aspect is the need to make "good" decisions, but not necessarily optimal decisions, in a very short time. This requires software-based decision aids [19] and fast and accurate decision algorithms. Since these decisions are embodied in physical space and time, computational models that explicitly represent and exploit space would be particularly useful [20].

Since evacuees should be able to move (or be moved) rapidly and efficiently to exit areas, or other areas where they can be safe and receive adequate care, emergency management needs efficient routing algorithms, while we know that many such algorithms are computationally intensive [21], and may not be adequate for providing decisions in real time with partial and incomplete information [22]. Thus, fast machine learning based algorithms have been suggested using Reinforcement Learning (RL) [23], inspired by smart network packet routing. Because of the possible lack of information and coordination between different parts of the system, emergency evacuation can also lead to excessive congestion caused by evacuees or their vehicles using common paths, so that approaches that use shared Cloud Computing for common decision making have also been suggested [24].

Many of the above considerations underline the need of communications for emergency evacuation systems, where public mobile networks may be "down" due to physical events or lack of sources of electricity [25]. In such cases, one must seek communication technologies that are self-aware and self-organize [26], and which also adapt to possible congestion in the network. Thus, disruption-tolerant communication systems [27] and opportunistic delay-tolerant communication systems have been suggested [28].

As soon as communications are discussed in the context of emergency management, one must also consider the issues of cybersecurity [29], as well as how smart cyberattack detection can be carried out without prior knowledge of the cyberattacks that an emergency may encounter. In addition, such cyberattacks can aim at the security of the end users, but also aim directly at the signalling schemes that allow the network to establish and maintain the communications [30].

While all these aspects are important to emergency management systems, in the next Section we will turn more specifically to the evacuation of Cruise Ships, which is the subject of this dissertation.

1.2. The Cruise Industry

The cruise industry is a vital component of the global tourism sector, having experienced the fastest growth prior to the COVID-19 pandemic, and contributing significantly to the global economy, job creation, and cultural exchange. According to the State of the Cruise Industry Report 2025 published by Cruise Lines International Association (CLIA), the ocean cruise industry experienced a compound annual growth rate of 6.3% in passenger amounts from 1990 to 2025. As shown in Fig. 1, while the ocean cruise industry was brought to a standstill for nearly two years by the COVID-19 pandemic, it has demonstrated a rapid rebound. By 2023, cruise travel had already reached 106% of the pre-COVID levels of 2019, with 29.1 million passengers sailing, indicating the strong resilience of cruise tourism in the face of global downturns.

Simultaneously, fifteen new cruise ships, with a combined passenger capacity of 38, 629, are expected to be completed by 2025 (see Table 1). This influx will increase the global ocean cruise passenger capacity to 704, 200 across 370 vessels. We can also see from Table 1 that large cruise ships, offering a wide array of onboard activities and amenities, have indeed become a dominant force in the cruise industry. Such vessels typically feature highly complex internal layouts, comprising multiple decks with restaurants, theaters, shopping areas, pools, and other entertainment venues, as well as hundreds of passenger cabins (see Fig. 2), and are considered one of the safest ways to travel. Although the frequency of large cruise ship accidents has decreased significantly over the last decade owing to the introduction of new safety regulations and guidelines, improved crew training schemes, and technological innovations, the consequences of such accidents remain catastrophic.

The next section collates and analyzes ship accidents that have occurred during this century, with particular focus on the role of evacuation in these accidents, in order to highlight the importance of effective evacuation and to identify key factors to consider when designing emergency evacuation approaches for passengers on vessels.

Table 1. New ocean cruise ships scheduled for completion in 2025.

Cruise company	Cruise ship	Estimated completion data	Passenger capacity
TUI Cruises	Mein Schiff Relax	Q1	4,000
MSC Cruises	World America	Q1	5,400
Norwegian	Aqua	Q1	3,571
Asuka/NYK	Asuka III	Spring	744
Royal Caribbean	Star of the Seas	Q2	5,610
Oceania	Allura	Q2	1,200
Viking Ocean	Viking Vesta	Q2	998
Ritz-Carlton	Luminara	Q3	456
Princess	Star Princess	Q3	4,300
SunStone (Aurora Expeditions)	Douglas Mawson	Q3	186
Four Seasons	Four Seasons I	Q4	180
Celebrity	Xcel	Q4	3,260
Windstar	Star Seeker	Q4	224
Disney	Adventure	Q4	6,000
Disney	Destiny	Q4	2,500

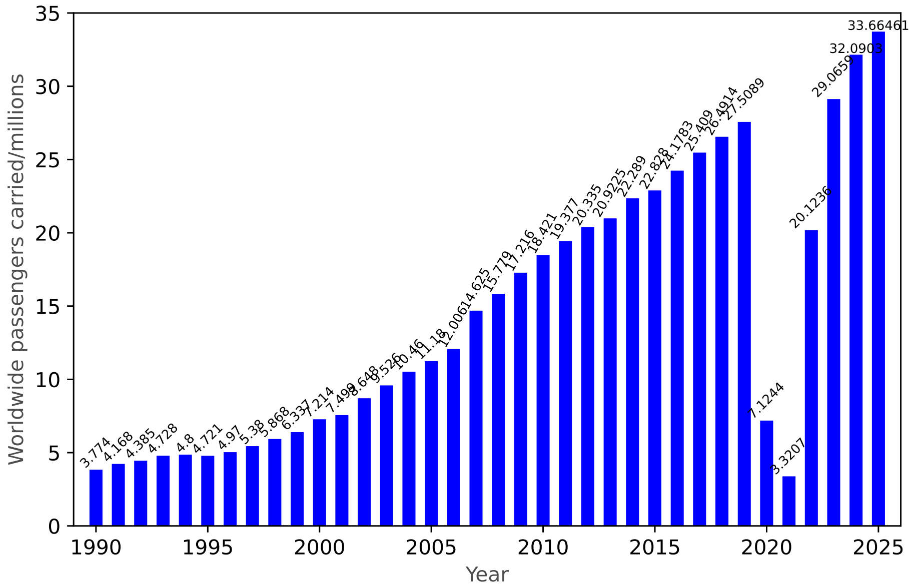

Figure 1. Number of global cruise ship passengers from 1990 to 2025.

Figure 2. Schematic view of the Cruise Ship Monster of the Deep.

1.3. Marine Casualties and Incidents

Grounding (or stranding), contact, collision, and fire constitute the predominant categories of accidents for passenger ships of all subtypes, including cruise ships, pure passenger ships, and passenger Ro-Ro cargo vessels. Such events generally pose a serious threat to the viability of the ship, crew, passengers, and cargo. According to the Annual Overview of marine casualties and incidents 2024 published by the European Maritime Safety Agency (EMSA), there are a total of 6370 passenger ships involved in marine casualties and incidents in the territorial seas of European Union (EU) member states during the period from 2014 to 2023, resulting in 2149 injuries and 54 fatalities. Among these marine casualties and incidents, 53.4% are classified as less serious, 28.4% as serious, 2.7% as very serious, and 15.5% as marine incidents (see Fig. 3). In addition to passenger ship accidents in the territorial seas of EU member states, accidents also occur from time to time in other seas. In 2002, the MV Le Joola RO-RO ferry capsized off the coast of The Gambia, resulting in $1,863$ fatalities and 64 survivors, ranking as the third-worst peacetime disaster in maritime history. There are several immediate factors playing a role in this disaster, including poor cargo stowage, severe passenger overloading, engine failure, adverse weather, and improper evacuation. With regard to the evacuation process, the excess passengers concentrated on the upper decks, making the ship highly unstable. Moreover, to take cover from the storm, they rushed en masse to one side, which further aggravated the hull tilt and significantly accelerated the capsizing. In 2006, the MS al-Salam Boccaccio 98, a RO-RO passenger ferry, sank in the Red Sea, resulting in over 1,000 deaths. The immediate cause of the sinking was identified as the buildup of seawater in the hull during firefighting operations in the engine room, which induced a severe listing and ultimately led to the ship capsizing. According to the Panama Maritime Authority Preliminary Investigation Report, at $19:09$, the fire alarm on MS al-Salam Boccaccio 98 was activated, providing visual and audible alerts on the control panel at the bridge, but orders to evacuate the vessel were never given or carried out as per established procedures. The majority of passengers remained waiting for evacuation instructions from the master until the vessel sank. In 2014, the ferry MV Sewol foundered while en route from Incheon to Jeju in South Korea under calm sea conditions. Out of 476 passengers and crew, only 172 people survived this disaster. The primary cause of the sinking was an unreasonably sudden turn to starboard, which triggered a shift of cargo to port and, in turn, induced a heavy listing and the eventual capsizing. The captain ordered passengers to stay in their cabins rather than mobilizing an evacuation of passengers while the Sewol ferry was listing. Therefore, this accident is considered to be a man-made disaster, since all passengers could have survived if adequate evacuation procedures had been implemented. In 2021, the passenger ferry MV Avijan-10 caught fire on the Sugandha River. This accident resulted in more than 40 deaths and more than 100 injuries. Most of the victims either died from the fire or drowned during their escape. Analysis of the aforementioned ship accidents indicates that the complete elimination of maritime accidents is practically unrealistic, and that inappropriate post-accident evacuation is one of the major factors contributing to the associated catastrophic consequences.

Conversely, the implementation of effective evacuation procedures can substantially mitigate maritime accidents in terms of a reduction in resultant fatalities and injuries. In 2013, the MV Grandeur of the Seas, carrying 2,224 passengers and a crew complement of 796, was on fire. Once the emergency situation was declared, the crew was first sent to their emergency stations, and passengers were directed to their muster stations. Therefore, despite the serious and large conflagration causing significant structural damage, no personal injuries were reported among passengers or crew members, thanks to the timely and effective emergency evacuation. Similarly, all individuals aboard the Yangtze Grand View No. 7 cruise ship were safely evacuated to shore within 29 minutes, with no reported injuries.

In summary, the evacuation decision plays a crucial role in protecting the lives of those on board when a passenger ship is involved in a serious accident. Evacuation planning for passengers on a damaged ship is a highly complex transshipment problem, affected by factors such as the propagation of hazards, the spatial and temporal distribution of evacuees and life-saving appliances, the dynamic inclinations of the ship, the capacity of muster stations, and the survival time of the vessel. In addition, the design of evacuation strategies is influenced by the underlying support infrastructure available on board a ship. All cruise ships are required by the International Convention for the Safety of Life at Sea (SOLAS) to have pre-deployed static evacuation plans to direct evacuees to muster stations in the event of an emergency. These plans must indicate the current area or cabin of passengers, the designated assembly area, the locations of lifeboats and liferafts, and the escape routes. Static evacuation plans are designed to provide paths with the shortest distance to muster stations, but they neglect other essential factors influencing evacuation efficiency and passenger safety. In recent years, intelligent ships equipped with advanced technologies such as the Internet of Things (IoT) have gradually become the norm in the cruise industry. Various sensor-based evacuation approaches have been proposed to provide dynamic evacuation plans that can react to changing conditions on board and are able to adapt guidance using real-time data collected by sensors.

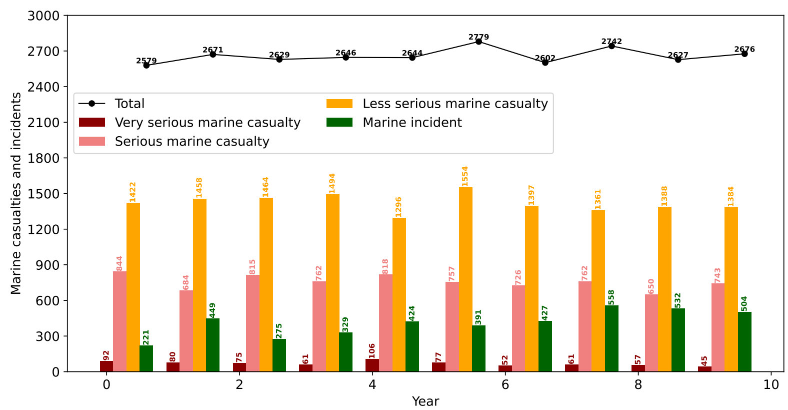

Figure 3. Evolution of the number of marine casualties and incidents over time, presented by order of severity.

Thus, in Section 2, we first review related work. Then in Section 3, the mathematical modelling approach that we use is detailed. Section 4 discusses the "pacing or regulating" scheme, which we call the "Pull Policy", to guarantee that congestion does not form in the various parts of the emergency evacuation system. In Section 5, we present numerical results concerning the Pull Policy, and a heuristic extension that sends messages simultaneously to all source nodes, and different routing rules that we have examined. Finally, Section 6 presents our conclusions for this work and suggests future research directions.

2. Related Work

Emergency evacuation methods are studied to improve the safety of people, property, and vehicles [31,32], and they increasingly rely on modern Internet of Things (IoT) technologies such as sensing, decision making, and communications. These methods are studied to assist human evacuees and vehicles, by locating and guiding them towards safety by relaying information about ongoing conditions, and guiding them along the fastest and safest pathways [33–35]. Such methods can be enhanced with crowd monitoring [36], hazard modeling and prediction [37], and the automatic selection of evacuation paths [38]. The study of emergency evacuation faces the obvious difficulty of artificially reproducing emergencies. Thus, modelling and simulation have become essential in this context [39,40], and such techniques are routinely used for the design and comparison of appropriate methods and algorithms [41] that are designed to improve or optimize the effectiveness and robustness of evacuation procedures.

Both modeling and simulation rely on two distinct methodologies: (i) mathematical modeling (MM) [42], which we are very familiar with from engineering and physics, and which has long been used for the study of communication, computer, networks and transportation systems [43,44], where systems of equations are used to represent reality, and (ii) discrete event simulation (DES) [45] where the events in a system are captured in a computer program which represents in great detail the sequence of events which are supposed to unfold over time within the real world that we wish to represent, with probabilistic (or not perfectly known) transitions being represented by random variables. While DES can require substantial programming efforts and lengthy computation time, but offers the possibility of representing the system very accurately, MM may offer faster computational algorithms, but requires the solution of a mathematical model, which may not be readily available or may be intractable.

One of the challenges in simulation scenarios is that evacuees may rush towards the designated exits, causing congestion and even injuries among the evacuees. Thus this paper studies the use of signalling via IoT devices, from the exit points towards the sources of evacuees, so that congestion does **not** occur on the exit paths. The approach is based on sending messages from the exit points to the source nodes where evacuees initially congregate, to "pace" or "regulate traffic" at the source locations of the evacuees, so that they may move forward at steady intervals which match the exit times of evacuees from the exit points, guaranteeing that large queues of evacuees and hence congestion will not occur in the intermediate corridors, staircases, and passageways of the system being considered.

We also investigate the use of routing policies where evacuees are directed in a static manner, for instance via sign-posting, to take the exit paths that can minimize overall delay. To this effect, we use an analytical model that allows us to numerically compute the outcome of such strategies when applied to a realistic cruise ship evacuation problem.

Emergency management simulation research addresses the movement of people in scenarios, including sports arenas, tourist sites, leisure venues [46,47], and large ships [48,49], in adversarial situations where some of the infrastructure may have broken down, and where hazards such as fire and the effect of human panic may further impair the evacuation process, such as large scale naval transport [50,51] and other areas of emergency management [52,53]. To this effect, some general-purpose software tools have also been developed to facilitate the simulation of complex evacuation scenarios [54].

On the other hand, emergency management systems are designed to guide evacuees using path-planning or dynamical algorithms to minimize evacuation delay and maximize the distance between the safe paths being used and the hazards and congestion that may occur. Such methods use 2D/3D maps of the built or natural environment in which the evacuation is occurring [55], and compute changes in the paths when unexpected congestion and hazards such as fire, flooding, or failures in communication systems occur. Situations where dynamic dangers can exist require techniques for establishing relatively stable evacuation paths even when unexpected hazards emerge, as has been done using the "Expected Number of Oscillations (ENO)" concept [56] that identifies paths that have the smallest probability of frequent changes. While global path planning methods can require complete system specifications that are unavailable in realistic scenarios, several recent studies avoid this requirement by allowing the path computation to proceed without precise prior knowledge of all hazards, and without detailed information about all possible exits [57].

In the naval transport industry, the International Maritime Organization (IMO) regularly issues circulars and recommendations for the simulation of evacuation procedures in evacuee ships [58], where the interaction between the human evacuees and the physically constrained environment has been studied extensively in recent research [59–61].

Methods from Artificial Potential Fields and adaptive routing [62,63], possibly with partial reversal, have also been designed to assist evacuees in avoiding hazards. While many studies overlook the need to provide directions that guarantee that the "time to reach the exit" for each evacuee is below a specified upper bound that guarantees survivability, other work [64] that was built on the AnLogic simulator [65], has explicitly incorporated the guarantee of an exit deadline for each evacuee in the system, as recommended for ship evacuation by the International Maritime Organization. The research in [66,67] has investigated both the imperfections in IoT systems, such as communication delays or message loss, and the effect of the possible panic of evacuees, on the effectiveness of emergency evacuation procedures in cruise ships.

3. The Evacuation System as a Network of Queues

The evacuation system is composed of:

- The n locations that evacuees enter or exit that we call *nodes*,
- Corridors and staircases which connect the locations, and
- Exit points which allow the evacuees to leave the vessel.

This structure is represented by a *directed acyclic graph* G, where the locations are the set of nodes $V = \{1, \ldots, n\}$, and directed arcs $A(i,j)$ that represent the corridors, passageways, or staircases, and the direction of each arc represents the direction the evacuees take during an emergency evacuation. Any pair of nodes (i,j) can only be connected by a single directed arc $A(i,j)$ from i to j, or $A(j,i)$, but not both. If $A = [A(i,j)]_{[n\times n]}$ is the binary matrix where $A(i,j) = 1$ if and only if there is an arc from i to j, we have $A(i,i) = 0$ and $A(i,j).A(j,i) = 0,\ \forall\, i,\ j \in V$.

V is composed of three disjoint subsets: the set of source nodes S, the set of exit (sink) nodes F, and the set of intermediate nodes I, so that $V = S \cup F \cup I$, where:

$$\begin{aligned} S &= \{i:\ \textit{such that}\ A(j,i) = 0,\ \forall\, j \neq i\}, \\ F &= \{i:\ \textit{such that}\ A(i,j) = 0,\ \forall j \neq i\}, \\ I &= \{i:\ \textit{such that}\ i \notin S \cup F\}\ . \end{aligned}$$

This means that source nodes do not have predecessors, sink nodes do not have successors, while intermediate nodes have both successors and predecessors in the graph G. We also assume that G has an important property which is necessary for a graph that represents an evacuation system: each node is connected to at least one of the sinks by at most $n-1$ arcs. In other words, an evacuee can go from any node of G to a sink node by traversing at most $n-1$ directional arcs (which are staircases or passageways).

The mathematical model we use to evaluate the total average delay for an evacuee, from any source to any exit point in the evacuation system, is a network of queues. We assume that each queue's capacity is unbounded, which means that the corridors, passageways, and staircases have been designed to be large enough so that they are never completely filled by people.

3.1. The Maximum Arrival Rates of Evacuees into Corridors

We assume that each source node $s \in S$ is a corridor K_s which receives the evacuees exiting from individual cabins (or also possibly common rooms such as restaurants, lounges, etc.), according to independent, identically, and exponentially distributed inter-arrival times (a Poisson process) of rate λ_s. The evacuees traverse the corridor in a time of average value τ_s, and enter at rate λ_s into a waiting area H_s, where they queue in First-In-First-Out (FIFO) order. For a corridor s of length L_s which contains C_s cabins aligned along the sides of the corridor, where evacuees walk on average at v m/sec (meters per second), the average time it takes an evacuee to go from her cabin to the waiting point H_s is $\tau_s =\ 0.5\ L_s v^{-1}$.

Since there are C_s cabins in the corridor K_s, and assuming that there are evacuees in each cabin and that evacuees exit cabins singly, we can assume that the maximum total exit rate of evacuees, in people per second, into the corridor K_s is:

$$\lambda_s = \frac{C_s}{\tau_s} = \frac{2vC_s}{L_s} \ . \tag{1}$$

In the queueing model used in this paper, when $A(i,j) = 1$, the staircase, passageway, or corridor $K(i,j)$ that connects node i to node j, for $i \in S \cup I$ and $j \in I \cup F$, is represented by a FIFO queue with independent and exponentially distributed service times of average value $\mu_{i,j}^{-1}$. If $j \in I$, an evacuee leaving queue $K(i,j)$ will enter another queue $K(j,l)$ such that $A(j,l) = 1$ with probability $P(j,l)$ and $\sum_{v_l \in I \cup F} A(j,l)P(j,l) = 1$. Finally, evacuees in K_f, $f \in F$, exit the system in FIFO order with an exit rate β_f, which is the parameter of an independent and identically distributed exponential service time at the final node.

4. Routing of Evacuees

In this section, we first describe the rules that will be compared for the routing of evacuees through the system. We will then introduce the "Pull Policy", which uses messages from the exit point to tell evacuees to leave their waiting areas and access the evacuee system towards the exit. The basic idea is that if evacuees are allowed to enter a passageway or staircase as soon as they arrive to its entrance, then this will add to the congestion at that staircase or passageway, so that admission and routing rules are needed that can help address this issue.

We will compare four routing methods to select the subsequent link that an evacuee joins from any of the nodes in the evacuation system (except for the exit node):

- In the first approach, named "Selection Rule 1", an evacuee leaving a node i (except for the final exit node), selects its successor link $K(i,j), j \in S(i)$ with equal probability, so that no attention is paid to the relative speed of the links or to their congestion. The equal probability is expressed as $P(i,j) = \frac{1}{|S(i)|}$ provided that $|S(i)| > 0$.
- In the second approach, or "Selection Rule 2", an evacuee at a node (except for the final node) chooses its successor link $K(i,c)$, which is as the one that has the highest speed or service rate, i.e., the one that satisfies $\mu_{ic} \geq \mu_{ij},\ for\ j,c \in S(i)$. If there is more than one such link, then the one with the smallest value of j is chosen.
- In "Selection Rule 3", each evacuee leaving some node i (except for the final node) selects a successor link $K(i,c)$ with probability:

$$P(i,c) = \frac{\mu_{ic}}{\sum_{k \in S(i)} \mu_{ik}}. \tag{2}$$

  This selection rule results in an interesting performance result that is detailed below in Section 4.1: the average delay on each of the shared downstream links, resulting from Selection Rule 3, is identical for each of the links, and corresponds to a link whose service rate is the average of all the link service rates, and whose traffic rate is equal to $\lambda_i \times (|S(i)|)^{-1}$, i.e. an equally shared traffic rate over all of the links. Thus, Selection Rule 3 has the effect of transforming each node i into an "equivalent service center", whose service rate is the average of the service rates of all the links that exit node i, and whose incoming traffic rate is λ_i divided by the number $|S(i)|$ of outgoing links.
- Finally, with "Selection Rule 4", evacuees at all nodes (except the exit nodes) select the path to the exit that minimizes the evacuees' total time to the exit, and verifies that the specified deadline for the exit is not violated for the worst-case link delays. Dijkstra's well-known algorithm [68], or variants of this algorithm [69], can be used to find the shortest path from a given source node to every other node in a graph, or to find the shortest path to any specific destination node by stopping when it finds the shortest path to some final node f. It is of complexity $O(n^2)$ for n nodes, In the specific case of cruise ship evacuation, the worst-case delay for each link is a conservative upper

bound on the traversal time across the link, estimated based on the link length and the passenger walking speed on a cruise ship with a heel angle of 20 degrees. This walking speed is determined by the normal speed on a ship at an inclination angle of 0 degrees and movement direction regarding the inclination, and the speed reduction factor associated with a heel (or trim) angle of ± 20 degrees, where the selected deadline D is:

$$D = 0.8(T_S - \frac{2}{3}T_{EL}) - A \tag{3}$$

where 0.8 is a safety factor, T_S is the estimated survival time until capsizing for a cruise ship following an accident at sea, T_{EL} is the time required for abandonment by all passengers and crew on board, and A denotes the time taken by a passenger for all actions she takes after receiving the emergency notification, until she begins moving. According to the IMO MSC.1/Circular.1533 [58] for the Yangtze Gold 7 cruise ship, $T_S = 80$ minutes, $T_{EL} = 30$ minutes, and $A = 10$ minutes under night-time scenarios.

Note that each of these approaches uses decisions which are fixed *a priori*, and do not need a computational or communication facility to be associated with individual nodes. However, the communication facility is needed for the "Pull Policy" and the "Pull Heuristic", which are discussed below.

4.1. Key Property of Selection Rule 3

With the assumption used in Selection Rule 3, when the evacuees arrive to node i at rate λ_i, subsequently entering each link $K(i,c)$ with probability $P(i,c)$ in FIFO order, and assuming that the service time per evacuee is exponentially distributed with average value μ_{ic}^{-1}, we know [70] that the average time spent by an evacuee in each link $K(i,c),\ c \in S(i)$, is:

$$W_{ic} = \frac{1}{\mu_{ic} - \lambda_i P(i,c)}, \tag{4}$$

so that the average time spent by an evacuee arriving at node i as it travels on the set $S(i)$ of outgoing links from node i is:

$$\begin{aligned} \sum_{c \in S(i)} P(i,c) W_{ic} &= \sum_{k \in S(i)} \frac{1}{\frac{\mu_{ic}}{P(i,c)} - \lambda_i} = \sum_{k \in S(i)} \frac{1}{\sum_{k \in S(i)} \mu_{ik} - \lambda_i}, \\ &= \frac{1}{\frac{\sum_{k \in S(i)} \mu_{ik}}{|S(i)|} - \frac{\lambda_i}{|S(i)|}} . \end{aligned} \tag{5}$$

4.2. The Pull Policy

To further avoid congestion in passageways and staircases, one could also synchronize the entrance of evacuees into the passageways or staircases with the departure of preceding evacuees from the end of the passageway. To do this, one would need a sensor at the exit of the passageway that detects the departure of an evacuee, and a network-based communication system that sends a message to the entrance point of the passageway, where a visual display, e.g., a light that turns green or red, would limit or (to the contrary) encourage entrance into the passageway in a manner that offers congestion-free movement in that passageway.

Although this is feasible with enough sensors and communication and display facilities, it may become too complex to install, monitor, and maintain in a practical large-scale setting. Thus, in this paper, we consider a simpler approach, which we call the Pull Policy:

- When an evacuee leaves an exit point f of the evacuation system, a message is sent with probability $p(f,s)$ to all the waiting areas H_s at the sources, with $\sum_{s \in S} p(f,s) = 1$.
- If H_s receives a message, and if it contains at least one evacuee, then the evacuee at the head of the waiting line in First-In-First-Out (FIFO) order at H_s, immediately enters into the corresponding passageway or staircase that is selected according to one of the "Selection Rules 1–4".

- At each H_s, there is also an "impatience time" of average value $\frac{1}{\alpha_s}$, after which an evacuee would be allowed into its preferred passageway or staircase even if a message is not received from the "exit" location f.
- We also evaluate the "Pull Heuristic" whose purpose is to reduce the chances that the message from the exit node arrives at waiting areas where there are no evacuees. Thus, in this case, the message from the exit point f is sent simultaneously to *all* waiting areas H_s, and is modelled heuristically by setting $p(f,s) = 1$ for all sources s.

In the sequel, we will use the term "Baseline Model" for the mathematical model that excludes the Pull Policy, or the Pull-Heuristic, in which all nodes (except the final node) select their successor nodes with equal probability.

4.3. Analytical Solution

The analytical solution of this network of queues is a special case of the "G-Networks with triggered customer movement" introduced in [70]. Based on this analytical solution, we can obtain the following results. Define Q_s, $0 \leq Q_s < 1$, the steady-state probability that a waiting space $H_s, s \in S$, has at least one evacuee waiting in H_s to enter the evacuation system. Then:

$$Q_s = \frac{\lambda_s}{\alpha_s + \sum_{f\in F} Q_f \beta_f p(f,s)},\ for\ s \in S, \tag{6}$$

Similarly, Q_f, $0 \leq Q_f < 1$, the probability that a final or sink node $v_f \in F$ has at least one evacuee waiting to exit the evacuation system, is given by:

$$Q_f = \frac{\sum_{j\in I} q_{jf} A(j,f)\mu_{jf}}{\beta_f},\ for\ v_f \in F\ , \tag{7}$$

where for $A(i,j) = 1$, the steady-state probability that the queue $K(i,j)$ contains at least one evacuee denoted by q_{ij} for $0 \leq q_{ij} < 1$, is given by:

$$q_{ij} = \frac{A(i,j)P(i,j)[\sum_{l\in I} A(l,i) q_{li}\mu_{li} + Q_i 1[i \in S]\alpha_i]}{\mu_{ij}}\ . \tag{8}$$

Let N denote the average of the total number of evacuees in the evacuation system; it is obtained from the previously defined quantities, as:

$$N = \sum_{s\in S}(\tau_s + \frac{Q_s}{1-Q_s}) + \sum_{f\in F}\frac{Q_f}{1-Q_f} + \sum_{(i,j)\in E}\frac{q_{ij}}{1-q_{ij}}\ , \tag{9}$$

and the total average time spent by an evacuee in the evacuation system, denoted by W, can be derived using Little's Law [71,72]:

$$W = \frac{N}{\lambda},\ where\ \lambda = \sum_{s\in S}\lambda_s\ . \tag{10}$$

5. Numerical Results

The environment we use for the numerical results that are presented in this paper, encompasses the second, third, and fourth floors of the Yangtze Gold 7 cruise ship [66] shown in Figure 4 as a graph which consists of 528 edges and 347 nodes. The blue, green, and red solid lines represent the passageways on the second, third, and fourth floors, respectively, while black solid lines denote the staircases connecting the different floors. There is a single exit node which is marked with a red triangle, while the nodes representing the cabins are labelled with yellow circles, and the remaining nodes are shown as black squares. Additionally, the black numbers next to the nodes indicate their unique identifiers.

The typical delay across each edge is estimated based on its length as well as the average walking speed of evacuees on a cruise ship under normal conditions. In our

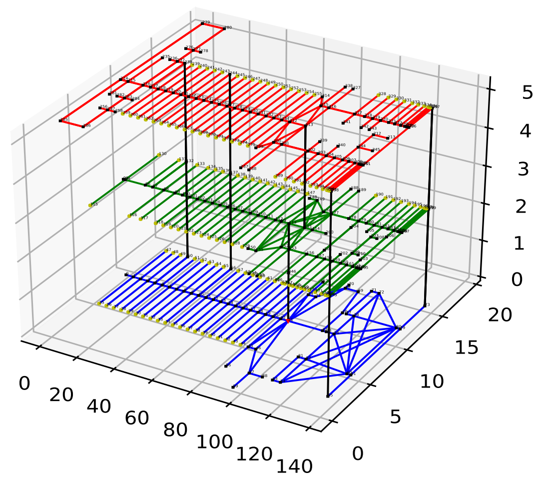

Figure 4. Graph model of the simulated environment.

simulation, according to IMO MSC.1/Circular.1533 [58], the average walking speed on flat terrain (e.g., corridors) is set to 0.56 m/s, while the speeds for going downstairs and upstairs are set to 0.45 m/s and 0.37 m/s, respectively. In Table 2, we summarize the key parameters concerning the source nodes and the exit.

Table 2. Parameters regarding the source nodes and the exit node.

Source & Exit Nodes	Corridor Length L_s	Cabins C_s	Avg. Inter-Exit Time from
Source,Exit	Meters	Number	Final Node f: β_f^{-1} secs
s_{21}	76	38	
s_{31}	80	31	
s_{32}	26	9	
s_{33}	26	9	
s_{41}	64	33	-
s_{42}	26	9	-
s_{43}	26	9	
f_{21}			1.786

5.1. Evaluation of the Pull Policy

We compare the average time spent in each waiting area using the pull algorithm against the two aforementioned algorithms, based on “Selection Rule 1”, as shown in Figure 5. The results under the other three selection rules are identical to those of “Selection Rule 1". The service rate at the waiting areas is fixed at $\frac{1}{16}\beta_f$ (i.e., 0.035). The total arrival rate at the source nodes is set to 0.02.

It can be observed that the absence of messages from the output node f leads to a deterioration of evacuation performance, as indicated by the increased average time spent by evacuees across all waiting areas. Moreover, the Pull-Heuristic algorithm results in a shorter average time spent in the waiting areas compared with the standard Pull Policy, due to the higher probability that messages from f are received by the waiting areas.

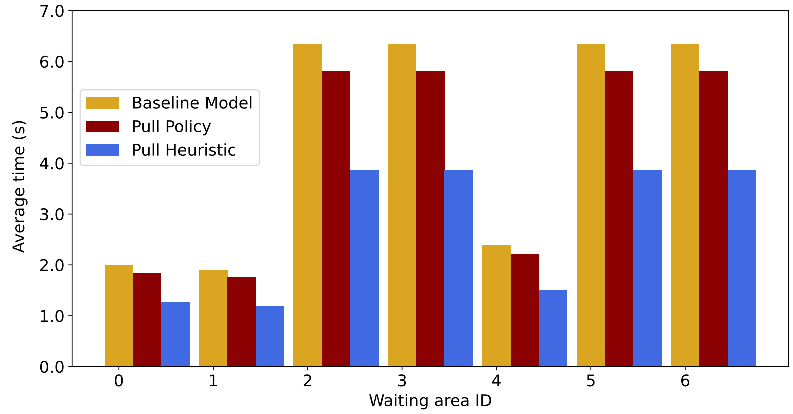

Figure 5. Comparison of the average time spent in each waiting area under "Selection Rule 1" across the three algorithms when $\alpha_s = 0.035$ and $\lambda = 0.02$.

To assess the impact of the messages transmitted from the exit to the waiting areas on overall evacuation efficiency, we compare the average total time spent in the system, calculated using the three algorithms across all four selection rules. As illustrated in Figure 6, the reception of messages by the waiting areas improves evacuation efficiency across all four selection rules. That is, both the pull algorithm and the pull-heuristic algorithm show a reduction with respect to the average total time spent by evacuees in the system. In addition, it is worth noticing that "Selection Rule 4" consistently yields a shorter average total time compared to the other three selection rules with all three algorithms, under $\alpha_s = 0.035$ and $\lambda = 0.02$. It is mainly because, in this group of simulations, evacuees are subject to a mild congestion due to the low total arrival rate at the source nodes. The successor passageway selections made by "Selection Rule 4" can achieve the shortest typical traversal time to the exit with regard to a specified deadline bound D, provided that waiting times caused by potential crowd congestion are not taken into consideration. Therefore, as illustrated in Figure 6, Selection Rule 4 minimizes the average total time under the low total arrival rate at the source nodes, among all four selection rules across the three algorithms.

5.2. Impact of the Total Arrival Rate at Source Nodes

In practical emergency evacuation scenarios aboard cruise ships, the number of evacuees that occupy different cabins can vary, which causes different arrival rates at the source nodes. Thus, in this section, we examine the influence of the total arrival rate at source nodes on evacuation efficiency measured by the average total time spent within the system. We run the three algorithms across all four selection rules with different preconfigured total arrival rates at source nodes (0.02, 0.04, 0.06, 0.08, 0.1, 0.12, 0.14, 0.16, 0.18). When $\lambda = 0.2$, the system becomes unstable across all three algorithms under each of the four selection rules. In this group of simulations, the evacuee average waiting time at the waiting areas is set to eight times the average inter-exit time, to be large enough not to influence the results, so that evacuees only very infrequently move downstream without the arrival of a message from the exit node $\alpha_s = 0.125\beta_f$.

Figure 7 presents the average total time spent by evacuees in the system, including the time at source nodes, intermediate links, and the exit, as a function of the total arrival rate λ at the source nodes, and we see that the average total exit time increases, culminating at a critical threshold beyond which the system saturates. Note that the threshold values of λ where saturation occurs will differ across the four selection rules:

- Under Selection Rule 2, the system becomes unstable when λ reaches 0.04, regardless of the algorithm employed, due to congestion on link (80, 78), where 80 and 78 denote the IDs of two intermediate nodes, as illustrated in Figure 4.

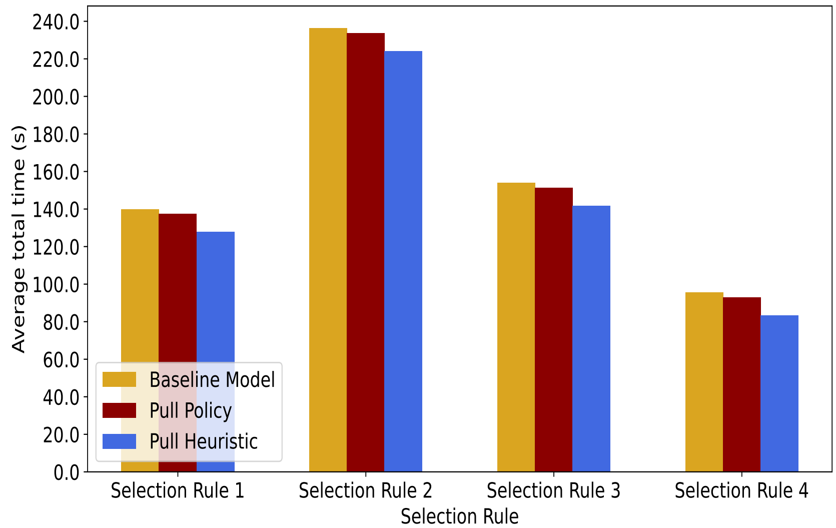

Figure 6. Comparison of the average total time spent in the system with the three algorithms under all four selection rules when $\alpha_s = 0.035$ and $\lambda = 0.02$.

- We also observe that the λ value under which the system reaches saturation under Selection Rule 4 is lower compared to the saturation level when Selection Rule 3 is used. This is because evacuees under Selection Rule 2 will choose the successor link with the highest service rate, while under Selection Rule 4, they select the successor link that yields the shortest typical travel time to the exit for a given deadline D. In contrast, under Selection Rule 3, because of the smart probabilistic traffic sharing, the system remains stable at higher total arrival rates at source nodes, compared with Selection Rule 2 and Selection rule 4.
- Moreover, we can see that when the total arrival rate at source nodes is below 0.14, the total average evacuation delay with Selection Rule 4 is consistently the smallest among all four selection rules and across all three algorithms.
- When the total arrival rate at source nodes reaches or exceeds 0.14, severe congestion is observed along the path with the shortest typical travel time for a specified deadline D across all three algorithms. This is observed in Figure 7 from the average total exit times for the four selection rules under all three algorithms. Furthermore, Selection Rule 1 consistently achieves the best performance at $\lambda = 0.14$ across the three algorithms, whereas Selection Rule 3 outperforms the other three selection rules when λ exceeds this value.

Last but not least, our results show that the Pull Policy and the Pull Heuristic reduce the average total time that the evacuees spend in the evacuation system under all of the Selection Rules for all values of λ where stability is preserved.

To compare the performance of the three algorithms with varying service rates at the waiting areas, in Figure 8, we present the average total time across various total arrival rates at source nodes, with α_s set to 0.035 (i.e., $\alpha_s = \frac{1}{16}\beta_f$). We observe that under "Selection Rule 3", the system becomes unstable when the total arrival rate at source nodes exceeds 0.16 with the Baseline Algorithm, while the other two Selection Rules preserve stability when higher values of λ are used. The waiting area, located in the second source node on the third floor (i.e., s_{32}), is the primary contributor to this transition of the system to instability under the Baseline Model, combined with Selection Rule 3. Again, we see that the use of messages sent from the exit to the waiting areas when evacuees leave the system is useful to preserve the system stability under higher total arrival rates at the source nodes.

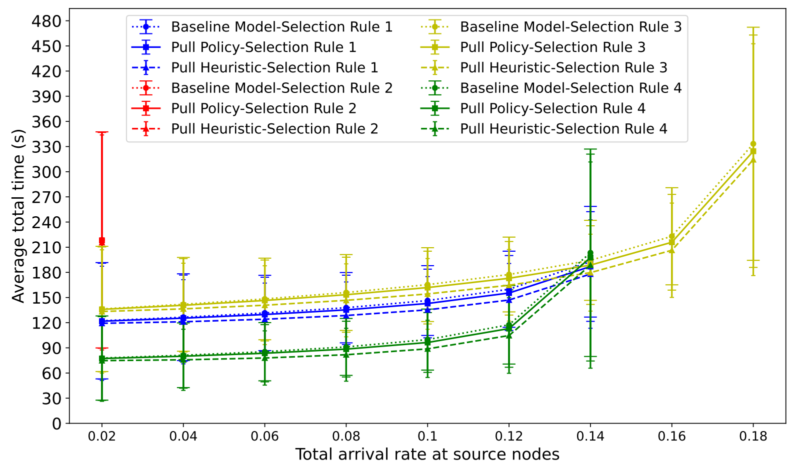

Figure 7. Average total time spent by evacuees in the system versus total arrival rate at source nodes, using the three algorithms across all four selection rules when α_s=0.07.

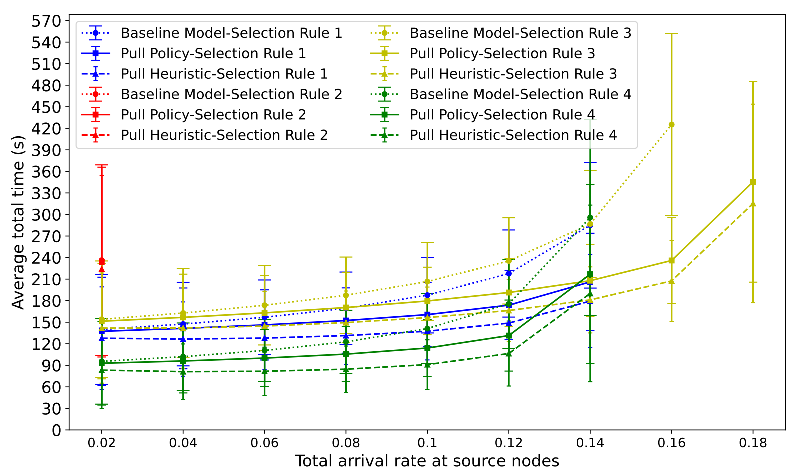

Figure 8. Average total time spent by evacuees in the system versus total arrival rate at source nodes, using all three algorithms across four selection rules when α_s=0.035.

5.3. Impact of Service Rate at Waiting Areas

In order to assess the impact of service rates at the waiting areas on evacuation efficiency, we carry out several numerical experiments to compare the average total time experienced by evacuees in the system under all four selection rules across the three algorithms for varying values of α_s. The service rate at the waiting areas, α_s, ranges from $\frac{1}{16}\beta_f$ (i.e., 0.035) to $\frac{1}{2}\beta_f$ (i.e., 0.28). In the controlled simulation, α_s is capped at $\frac{1}{2}\beta_f$, considering that excessively high values of α_s may induce congestion in intermediate links or at the exit, due to burst inflows from the waiting areas into the system.

Figures 9, 10, 11 show the average total evacuation time as a function of the service rate at the waiting areas, for three distinct total arrival rates at the source nodes: $\lambda = 0.02$, $\lambda = 0.14$, and $\lambda = 0.16$. The figures show that in all cases, the average total time decreases as α_s increases, albeit at a progressively decelerating rate.

Figure 9 shows that Selection Rule 4 achieves the best performance among all four Selection Rules across the Baseline, Pull Policy and Pull Heuristic algorithms, when $\lambda = 0.02$, mainly due to the ability of Selection Rule 4 to identify the fastest evacuation route for a given deadline D under low total arrival rates at the source nodes, when congestion does not occur on the routes that are chosen.

However, when the total arrival rate at the source nodes is 0.14, Figure 10 shows that with Selection Rule 2, the system saturates with all three algorithms. Also, the total average evacuation time with Selection Rule 1 is close to that of Selection Rule 3 and smaller than that of Selection Rule 4 with all three algorithms, primarily due to the reduced congestion due to probabilistic load sharing used by Selection Rules 1 and 2.

When the total arrival rate is $\lambda = 0.16$, Figure 11 shows the curves obtained with Selection Rule 3, while the system is unstable with the other three Selection Rules, highlighting the value of the probabilistic smart load sharing offered by Selection Rule 3. The results in Figure 11 also clearly show the effect of messages from the exit to the waiting areas. The average total exit time of the evacuees decreases significantly when the Pull Policy or the Pull Heuristic is used, confirming the results presented in Figures 9 and 10.

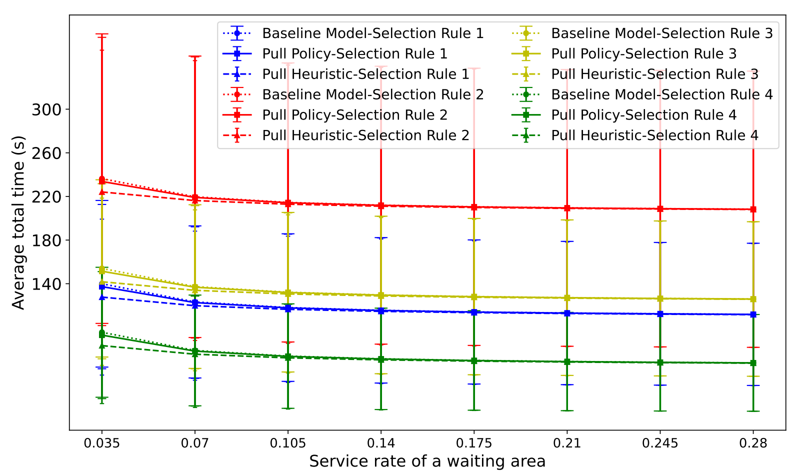

Figure 9. Average total time spent by evacuees in the system when $\lambda = 0.02$.

6. Conclusions and Further Research

In the emergency evacuation of ships, and other vehicles such as aircraft, safe and reliable methods are needed to ensure the fast movement of passengers and evacuees towards the best exits. Thus, many large vehicles, such as cruise ships rely on prior planning to instruct the evacuees on the best course of action when an emergency occurs.

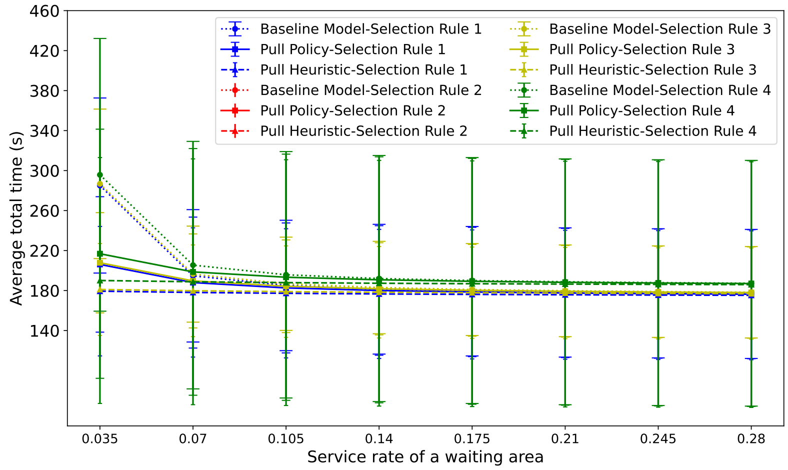

Figure 10. Average total time spent by evacuees in the system when $\lambda = 0.14$.

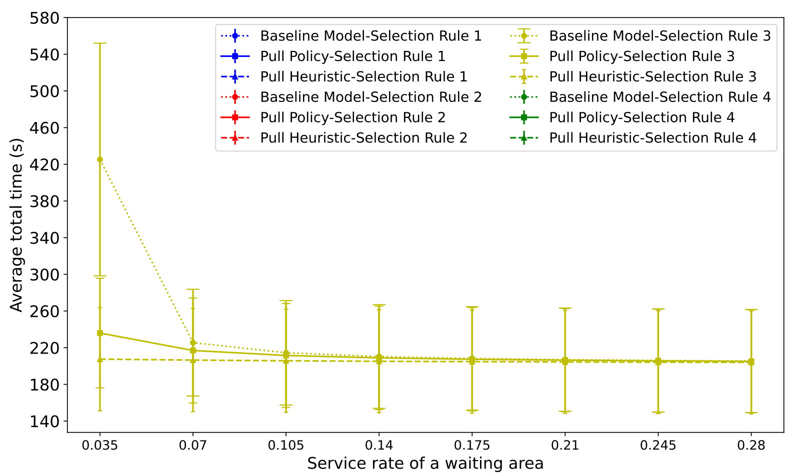

Figure 11. Average total time spent by evacuees in the system when $\lambda = 0.16$.

Thus, because of the high human consequences and costs of hazards and accidents that may require an evacuation process to be carried out, substantial research has been conducted to investigate the design of technology-assisted methods to provide evacuees with the best advice regarding evacuation procedures during emergency events. However, such systems can require expensive installations that are built into the cruise ship and vehicle, and which will require constant maintenance and updates so that they may be effective at the time when they are needed.

Thus, this paper introduces some novel algorithms that can reduce congestion and increase the speed with which evacuation can be conducted safely. To this effect, we consider two aspects of the evacuation process that can minimize the evacuation times from a built structure or vehicle. One approach involves the reduction of evacuation times through smart evacuation procedures that distribute the evacuees over multiple paths that take full advantage of the available capacity of each simultaneous path. The second approach which can be used in congestion with the previous one, is the Pull Policy, which paces the access of the evacuees to the evacuation paths, in synchrony with the safe exit of the preceding evacuees from the system, so that bottlenecks and congestion may be avoided.

This paper presents these approaches and evaluates them by using an advanced queuing network model that allows for fast computational solutions and that offers the system designer a means to compare various approaches against a baseline, and among each other, in a very rapid manner at low computational cost. The analysis we conduct compares the various relevant routing techniques for evacuees, with a modest amount of computation, providing useful output in terms of response time curves as a function of various relevant parameters, including the load of the system, in terms of evacuees per unit time, and the values of various system parameters.

In future research, we plan to examine more detailed controls that can avoid congestion, while maintaining a maximum throughput of evacuees through IoT-based signalling and control, with adaptive schemes that can react to bottlenecks before they occur. We will also investigate the possible effect of signalling and communication failures, and suggest architectures that can gracefully react by maintaining a robust level of performance in the presence of such failures.

Author Contributions: Problem definition, E.G.; relevant literature, E.G.; methodology, E.G.; software, Y.T.M.; formal analysis, E.G. and Y.T.M.; first draft preparation, E.G.; updating and correcting the manuscript, E.G.; proofreading Y.T.M.; visualization, Y.T.M.; supervision, E.G.; funding acquisition, E.G. Both authors have read and agreed to the published version of the manuscript.

Funding: This research was funded by the Institute of Theoretical & Applied Informatics (IITIS-PAN), Polish Academy of Sciences, via a Professorship for E.G. and a Research Assistantship for Yuting Ma.

Data Availability Statement: The data presented in this study are available on request from the authors. The data are not publicly available due to privacy or ethical restrictions.

Conflicts of Interest: The authors declare no conflict of interest.

References

1. Vitman-Schorr, A.; Tov, M.B.; Hagbi, L.; Freidus, L.; Shenaar-Golan, V.; Segal, M. Evacuation Experiences of Older Adults during armed conflict: Community, Place Attachment, and Well-Being. *Journal of Environmental Psychology* **2025**, p. 102754.
2. The-Sun. Fire at Westfield Stratford Shopping Centre Leads to Mass Evacuation, 2025. Accessed: 2025-09-15.
3. AP-News. Fires engulf Turkey's Mediterranean coast as government declares two disaster zones, 2025. Accessed: 2025-09-15.
4. Reuters. Thousands flee Hurricane Milton, causing traffic jams and fuel shortages, 2024. Accessed: 2025-09-15.
5. Reuters. Devastating flash floods hit northeastern Spain, killing at least 95, 2024. Accessed: 2025-09-15.
6. AP-News. Russia says 60 dead, 145 injured in concert hall raid; Islamic State group claims responsibility, 2024. Accessed: 2025-09-15.
7. The-Times. Car bomb attack in Somalia kills nine during Euro 2024 final, 2024. Accessed: 2025-09-15.
8. Wikipedia-Contributors. Kostenko mine fire, 2023. Accessed: 2025-09-15.
9. AP-News. Cave-in leaves two miners dead, one missing at Mysłowice-Wesoła coal mine in Poland, 2024. Accessed: 2025-09-15.
10. Gelenbe, E.; Gorbil, G.; Wu, F.J. Emergency cyber-physical-human systems. In Proceedings of the 2012 21st International Conference on Computer Communications and Networks (ICCCN). IEEE, 2012, pp. 1–7.
11. Gelenbe, E.; Wu, F.J. Future research on cyber-physical emergency management systems. *Future Internet* **2013**, *5*, 336–354.
12. Bi, H.; Gelenbe, E. A Survey of Algorithms and Systems for Evacuating People in Confined Spaces. *Electronics* **2019**, *8*, 711.
13. Gelenbe, E. G-networks: a unifying model for neural and queueing networks. *Annals of Operations Research* **1994**, *48*, 433–461.
14. Ören, T.I.; Numrich, S.K.; Uhrmacher, A.M.; Wilson, L.F.; Gelenbe, E. Agent-directed simulation: challenges to meet defense and civilian requirements. In Proceedings of the Proceedings of the 32nd Winter Simuation Conference, 2000, pp. 1757–1762.
15. Dimakis, N.; Filippoupolitis, A.; Gelenbe, E. Distributed building evacuation simulator for smart emergency management. *The Computer Journal* **2010**, *53*, 1384–1400.
16. Gelenbe, E.; Wu, F.J. Large-scale simulation for human evacuation and rescue. *Computers & Mathematics with Applications* **2012**, *64*, 3869–3880.
17. Desmet, A.; Gelenbe, E. Graph and analytical models for emergency evacuation. In Proceedings of the 2013 IEEE International Conference on Pervasive Computing and Communications Workshops (PERCOM Workshops). IEEE, 2013, pp. 523–527.
18. Gelenbe, E. Search in unknown random environments. *Physical Review E—Statistical, Nonlinear, and Soft Matter Physics* **2010**, *82*, 061112.
19. Filippoupolitis, A.; Gelenbe, E. A decision support system for disaster management in buildings. In Proceedings of the Proceedings of the 2009 Summer Computer Simulation Conference, 2009, pp. 141–147.

20. Filippoupolitis, A.; Gorbil, G.; Gelenbe, E. Spatial computers for emergency support. *The Computer Journal* **2013**, *56*, 1399–1416.
21. Gelenbe, E.; Liu, P.; Laine, J. Genetic algorithms for route discovery. *IEEE Transactions on Systems, Man, and Cybernetics, Part B (Cybernetics)* **2006**, *36*, 1247–1254.
22. Gorbil, G.; Filippoupolitis, A.; Gelenbe, E. Intelligent navigation systems for building evacuation. In Proceedings of the Computer and Information Sciences II: 26th International Symposium on Computer and Information Sciences. Springer, 2012, pp. 339–345.
23. Bi, H.; Desmet, A.; Gelenbe, E. Routing emergency evacuees with cognitive packet networks. In Proceedings of the Information Sciences and Systems 2013: Proceedings of the 28th International Symposium on Computer and Information Sciences. Springer International Publishing Cham, 2013, pp. 295–303.
24. Bi, H.; Gelenbe, E. A cooperative emergency navigation framework using mobile cloud computing. In Proceedings of the Information Sciences and Systems 2014: Proceedings of the 29th International Symposium on Computer and Information Sciences. Springer International Publishing Cham, 2014, pp. 41–48.
25. Gelenbe, E. Electricity Consumption by ICT: Facts, trends, and measurements. *ACM Ubiquity* **2023**, *2023*, 1–15.
26. Dobson, S.; Denazis, S.; Fernández, A.; Gaïti, D.; Gelenbe, E.; Massacci, F.; Nixon, P.; Saffre, F.; Schmidt, N.; Zambonelli, F. A survey of autonomic communications. *ACM Transactions on Autonomous and Adaptive Systems (TAAS)* **2006**, *1*, 223–259.
27. Gorbil, G.; Gelenbe, E. Disruption tolerant communications for large scale emergency evacuation. In Proceedings of the Pervasive Computing and Communications Workshops (PERCOM Workshops), 2013 IEEE International Conference on. IEEE, 2013, pp. 540–546.
28. Gorbil, G.; Gelenbe, E. Resilient emergency evacuation using opportunistic communications. In *Computer and Information Sciences III*; Springer, 2013; pp. 249–257.
29. Gelenbe, E.; Domanska, J.; Czàchorski, T.; Drosou, A.; Tzovaras, D. Security for internet of things: The SerIoT project. In Proceedings of the 2018 International Symposium on Networks, Computers and Communications (ISNCC). IEEE, 2018, pp. 1–5.
30. Gorbil, G.; Abdelrahman, O.H.; Pavloski, M.; Gelenbe, E. Modeling and analysis of RRC-based signalling storms in 3G networks. *IEEE Transactions on Emerging Topics in Computing* **2015**, *4*, 113–127.
31. Li, Q.; De Rosa, M.; Rus, D. Distributed algorithms for guiding navigation across a sensor network. In Proceedings of the 9th Annual International Conference on Mobile computing and Networking, 2003, pp. 313–325.
32. Gelenbe, E.; Wu, F.J. Large scale simulation for human evacuation and rescue. *Computers & Mathematics with Applications* **2012**, *64*, 3869–3880.
33. Birajdar, G.S.; Singh, R.; Gehlot, A.; Thakur, A.K. Development in building fire detection and evacuation system-a comprehensive review. *Int. J. Electr. Comput. Eng.(IJECE)* **2020**, *10*, 6644–6654.
34. Ma, Y.; Liu, K.; Chen, M.; Ma, J.; Zeng, X.; Wang, K.; Liu, C. ANT: Deadline-aware adaptive emergency navigation strategy for dynamic hazardous ship evacuation with wireless sensor networks. *IEEE Access* **2020**, *8*, 135758–135769.
35. Gelenbe, E.; Wu, F.J. Future research on cyber-physical emergency management systems. *Future Internet* **2013**, *5*, 336–354.
36. Singh, U.; Determe, J.F.; Horlin, F.; De Doncker, P. Crowd monitoring: State-of-the-art and future directions. *IETE Technical Review* **2021**, *38*, 578–594.
37. Bi, H.; Gelenbe, E. A Survey of Algorithms and Systems for Evacuating People in Confined Spaces. *Electronics* **2019**, *8*. https://doi.org/10.3390/electronics8060711.
38. Ibrahim, A.M.; Venkat, I.; Subramanian, K.; Khader, A.T.; Wilde, P.D. Intelligent evacuation management systems: A review. *ACM Transactions on Intelligent Systems and Technology (TIST)* **2016**, *7*, 1–27.
39. Nasso, C.; Bertagna, S.; Mauro, F.; Marinò, A.; Bucci, V. Simplified and advanced approaches for evacuation analysis of passenger ships in the early stage of design. *Brodogradnja: Teorija i praksa brodogradnje i pomorske tehnike* **2019**, *70*, 43–59.
40. Wang, X.; Liu, Z.; Loughney, S.; Yang, Z.; Wang, Y.; Wang, J. Numerical analysis and staircase layout optimisation for a Ro-Ro passenger ship during emergency evacuation. *Reliability Engineering & System Safety* **2022**, *217*, 108056.
41. Arshad, H.; Emblemsvåg, J.; Li, G.; Ostnes, R. Determinants, methods, and solutions of evacuation models for passenger ships: A systematic literature review. *Ocean Engineering* **2022**, *263*, 112371.
42. Gelenbe, E.; Mitrani, I. *Analysis and Synthesis of Xomputer Systems*; World Scientific, 2010; p. 324.
43. Möller, D.P.F. *Introduction to Transportation Analysis, Modelling and Simulation: Computational Foundations and Multimodal Applications (Simulation Foundations, Methods and Applications)*; Springer, 2014; p. 354.
44. Kleinrock, L. *Queueing Systems. Volume 1: Theory*; John Wiley & Sons, 1975.
45. Fishman, G.S. *Discrete-Event Simulation: Modeling, Programming, and Analysis*; Springer, 2001.
46. Meschini, S.; Accardo, D.; Locatelli, M.; Pellegrini, L.; Tagliabue, L.C.; Di Giuda, G.M.; et al. BIM-GIS integration and crowd simulation for fire emergency management in a large diffused university. *PROCEEDINGS OF THE... ISARC* **2023**, pp. 357–364.
47. Chu, H.; Yu, J.; Wen, J.; Huang, Y. Evacuation simulation and emergency management optimization in urban residential communities. In Proceedings of the IOP Conference Series: Earth and Environmental Science. IOP Publishing, 2019, Vol. 234, p. 012040.
48. Fang, S.; Liu, Z.; Zhang, S.; Wang, X.; Wang, Y.; Ni, S. Evacuation simulation of an Ro-Ro passenger ship considering the effects of inclination and crew's guidance. *Proceedings of the institution of mechanical engineers, part M: journal of engineering for the maritime environment* **2023**, *237*, 192–205.
49. Liu, K.; Ma, Y.; Chen, M.; Wang, K.; Zheng, K. A survey of crowd evacuation on passenger ships: Recent advances and future challenges. *Ocean Engineering* **2022**, *263*, 112403.

50. Sarvari, P.A.; Cevikcan, E.; Ustundag, A.; Celik, M. Studies on emergency evacuation management for maritime transportation. *Maritime Policy & Management* **2018**, *45*, 622–648.
51. Li, H.; Ren, X.; Yang, Z. Data-driven Bayesian network for risk analysis of global maritime accidents. *Reliability Engineering & System Safety* **2023**, *230*, 108938.
52. Choi, M.; Chi, S. Optimal route selection model for fire evacuations based on hazard prediction data. *Simulation Modelling Practice and Theory* **2019**, *94*, 321–333.
53. Luo, L.; Zhang, B.; Guo, B.; Zhong, J.; Cai, W. Why they escape: Mining prioritized fuzzy decision rule in crowd evacuation. *IEEE Transactions on Intelligent Transportation Systems* **2022**, *23*, 19456–19470.
54. Dimakis, N.; Filippoupolitis, A.; Gelenbe, E. Distributed building evacuation simulator for smart emergency management. *Computer Journal* **2010**, *53*, 1384–1400.
55. Wiandt, B.; Kokuti, A.; Simon, V. Application of Collective Movement in Real Life Scenarios: Overview of Current Flocking Solutions. *Scalable Comput. Pract. Exp.* **2015**, *16*, 233–248.
56. Wang, L.; He, Y.; Liu, W.; Jing, N.; Wang, J.; Liu, Y. On oscillation-free emergency navigation via wireless sensor networks. *IEEE Transactions on Mobile Computing* **2014**, *14*, 2086–2100.
57. Gelenbe, E.; Bi, H. Emergency Navigation without an Infrastructure. *Sensors* **2014**, *14*, 15142–15162. https://doi.org/10.3390/s140815142.
58. Organization, I.M. Guidelines for Evacuation Analysis for New and Existing Passenger Ships. *MSC. 1/Circ. 1238* **2016**.
59. Xie, Q.; Guo, S.; Zhang, Y.; Wang, C.; Ma, C.; Li, Q. An integrated method for assessing passenger evacuation performance in ship fires. *Ocean Engineering* **2022**, *262*, 112256.
60. Fang, S.; Liu, Z.; Wang, X.; Wang, J.; Yang, Z. Simulation of evacuation in an inclined passenger vessel based on an improved social force model. *Safety science* **2022**, *148*, 105675.
61. Wang, X.; Xia, G.; Zhao, J.; Wang, J.; Yang, Z.; Loughney, S.; Fang, S.; Zhang, S.; Xing, Y.; Liu, Z. A novel method for the risk assessment of human evacuation from cruise ships in maritime transportation. *Reliability Engineering & System Safety* **2023**, *230*, 108887.
62. Tseng, Y.C.; Pan, M.S.; Tsai, Y.Y. Wireless sensor networks for emergency navigation. *Computer* **2006**, *39*, 55–62.
63. Kokuti, A.; Gelenbe, E. Directional Navigation Improves Opportunistic Communication for Emergencies. *Sensors* **2014**, *14*, 15387–15399. https://doi.org/10.3390/s140815387.
64. Ma, Y.; Liu, K.; Chen, M.; Ma, J.; Zeng, X.; Wang, K.; Liu, C. ANT: Deadline-aware adaptive emergency navigation strategy for dynamic hazardous ship evacuation with wireless sensor networks. *IEEE Access* **2020**, *8*, 135758–135769.
65. Niu, C.; Wang, W.; Guo, H.; Li, K. Emergency Evacuation Simulation Study Based on Improved YOLOv5s and Anylogic. *Applied Sciences* **2023**, *13*, 5812.
66. Ma, Y.; Gelenbe, E.; Liu, K. IoT Performance for Maritime Passenger Evacuation. In Proceedings of the 2024 IEEE 10-th World Forum on the IoT, 2024, pp. 1–6.
67. Ma, Y.; Gelenbe, E.; Liu, K. Impact of IoT System Imperfections and Passenger Errors on Cruise Ship Evacuation Delay. *Sensors* **2024**, *24*, 1850.
68. Dijkstra, E.W. A note on two problems in connexion with graphs. *Numerische Mathematik* **1959**, *1*, 269–271. https://doi.org/10.1007/BF01386390.
69. Johnson, D.B. Efficient algorithms for shortest paths in sparse networks. *Journal of the ACM* **1977**, *24*, 1–13. https://doi.org/10.1145/321992.321993.
70. Gelenbe, E. G-networks with triggered customer movement. *Journal of Applied Probability* **1993**, *30*, 742–748.
71. Little, J.D.C. A Proof for the Queuing Formula: L = λ W. *Operations Research* **1961**, *9*, 383–387. https://doi.org/10.1287/opre.9.3.383.
72. Little, J.D.C.; Graves, S.C. Little's Law: Building Intuition. *International Series in Operations Research* & *Management Science* **2008**, *115*, 81–100. https://doi.org/10.1007/978-0-387-73699-0_5.